Signaling pathways as therapeutic targets in pediatric B-cell precursor acute lymphoblastic leukemia

Isabel Sophie Jerchel

ISBN 978-94-6295-845-6

Author: Isabel Sophie Jerchel

Lay-out: Isabel Sophie Jerchel

Cover design: Henning Jerchel, Isabel S. Jerchel, and Jessica Dobrig

Cover- layout, print, and publishing by: ProefschriftMaken || www.proefschriftmaken.nl

The work described in this thesis was performed at the Department of Pediatric Oncology/ Hematology of the Erasmus Medical Center Sophia Children's Hospital Rotterdam, the Netherlands and was funded by the Netherlands Organisation for Scientific Research (Nederlandse Organisatie voor Wetenschapplijk Onderzoek, NWO).

This thesis was supported by:

Signaling Pathways as Therapeutic Targets in Pediatric B-cell Precursor Acute Lymphoblastic Leukemia

Signalwegen als therapeutische doelwitten in pediatrische acute lymfatische leukemie

Proefschrift

ter verkrijging van den graad van doctor
aan de Erasmus Universiteit Rotterdam
op gezag van de rector magnificus
Prof. dr. H.A.P. Pols

en volgens besluit van het College van Promoties op

14 Maart 2018 om 9:30

door

Isabel Sophie Jerchel
geboren te Helmstedt, Bondsrepubliek Duitsland

Erasmus University Rotterdam

Erasmus

Promotiecommissie

Promoteren:	Prof. dr. Monique L. den Boer
	Prof. dr. Rob Pieters
Overige leden:	Prof. dr. C. Michel Zwaan
	Prof. dr. Ivo P. Touw
	Prof. dr. Frank C.P. Holstege

To all children with cancer and their families.

No Man Is An Island

No man is an island
Entire of itself
Every man is a piece of the continent
A part of the main
If a clod be washed away by the sea
Europe is the less
As well as if a promontory were
As well as if a manor of thy friend's
Or of thine own were
Any man's death diminishes me
Because I am involved in mankind
And therefore never send to know for whom the bell tolls
It tolls for thee.

John Donne

Table of Contents

Chapter 1

General Introduction

Leukemia, or blood cancer, occurs in children and adults, and is divided into subgroups based on cell type and presentation of the disease. It is therefore important to consider how normal blood is formed, which types of leukemia exist, and which mechanisms can cause blood cells to become malignant. This information will help developing treatment strategies.

The hematopoietic system

Blood transports nutrients, waste products, hormones, and cells throughout the body. Of the cellular components red blood cells transport oxygen, platelets form blood clots and mediate wound healing, and the immune system defends the body against pathogens with innate and adaptive immune cells. All blood cells are derived from hematopoietic stem cells (HSC), which reside in the bone marrow and ensure life-long reconstitution of the tissue (Figure 1). The progeny of HSC, so-called progenitor cells, are not yet fully mature (differentiated) and undergo further divisions and differentiation steps. They are divided into two lineages, the myeloid and the lymphoid lineage. The myeloid lineage gives rise to most cells of the innate immune system, platelet-producing megakaryoblasts, and erythrocytes. The lymphoid lineage consists of B- and T-lymphocytes, also called B- and T-cells. These constitute the adaptive immune system.

Clinical presentation of acute leukemia, risk factors, and chemotherapy

Leukemia is caused by the malignant proliferation of a white blood cell progenitor. It originates from the bone marrow, but at the time of diagnosis cells have usually spread systemically. Depending on the growth speed and whether a uniform population or a mixture of maturation stages is present, clinicians distinguish between acute and chronic leukemia. In addition, the leukemia can bear lineage markers of myeloid or lymphoid cells. These groups define the four major categories chronic or acute myeloid leukemia (CML or AML), and chronic or acute lymphoid leukemia (CLL and ALL). Very rare forms of leukemia present markers of both blood cell lineages (mixed-lineage leukemia), or are myeloid but can be neither defined as acute nor chronic (juvenile myeolomonocytic leukemia, JMML).

Acute lymphoblastic leukemia usually presents with the immunophenotype of B- or T-cell progenitors, and is therefore denominated B-cell precursor ALL (BCP-ALL) and T-cell ALL (T-ALL). Some patients present as mixed-lineage or bilineage leukemia, a more aggressive type that bears markers of both lymphoid and myeloid lineages. These can be further classified according to the genetic changes that initiate the leukemia, and provide a biologically more homogeneous classification (discussed below).

Children rarely present with chronic leukemia, while it is more common in adults. In Europe, approximately 5000 childhood leukemia cases are diagnosed every year, of which three quarters are ALL. BCP-ALL accounts for about 80 to 85% of ALL cases, and is therefore the most common leukemia in children.[1] They present with symptoms such as fatigue, dizziness, anemia, and bone or joint pain. More severe consequences of leukemia are infections due to reduced immunity, and bleeding due to deficient coagulation. The definitive diagnosis is made after a bone marrow puncture.

Causes and risk factors for children are different compared to adults. In adults, the chance

that one of the hematopoietic stem or progenitor cells transforms into a leukemic cell increases with age. This is largely explained by the fact that exposure to environmental influences (e.g. radiation and carcinogens) increases the frequency at which leukemia-causing mutations accumulate in hematopoietic stem and progenitor cells. In children, the incidence of leukemia peaks around the age of 3 to 5 years, and then declines again. While direct causes remain unknown, environmental toxins and genetic predisposition are thought to play a minor role. Instead, many studies support the hypothesis of a two-step model involving common infections: In addition to a genetic lesions in a progenitor cell, either the aberrant response to, or active infection with one or more infectious agents is thought to promote the development of ALL.[2,3]

The therapy of leukemia mainly consists of a combination of cytostatic and cytotoxic drugs. Depending on the specific treatment protocols, the exact schedule and therapy can differ. However, the backbone of all ALL treatment protocols relies on five major components: Prednisolone, a glucocorticoid which is toxic to lymphoid cells at high concentrations, vincristine, a spindle-poison which inhibits cell division, and L-asparaginase which degrades the amino acid asparagine, and the antimetabolites methotrexate and 6-mercaptopurine.[1] In the most recent Dutch treatment protocol (DCOG-ALL11), children receive up to 14 different drugs over a period of two years. In cases with high risk of relapse, the therapy is concluded by a hematopoietic stem cell transplantation.

The risks associated with intense chemotherapy and stem cell transplantation are high, and a considerable number of patients die from treatment-related toxicities. Short-term

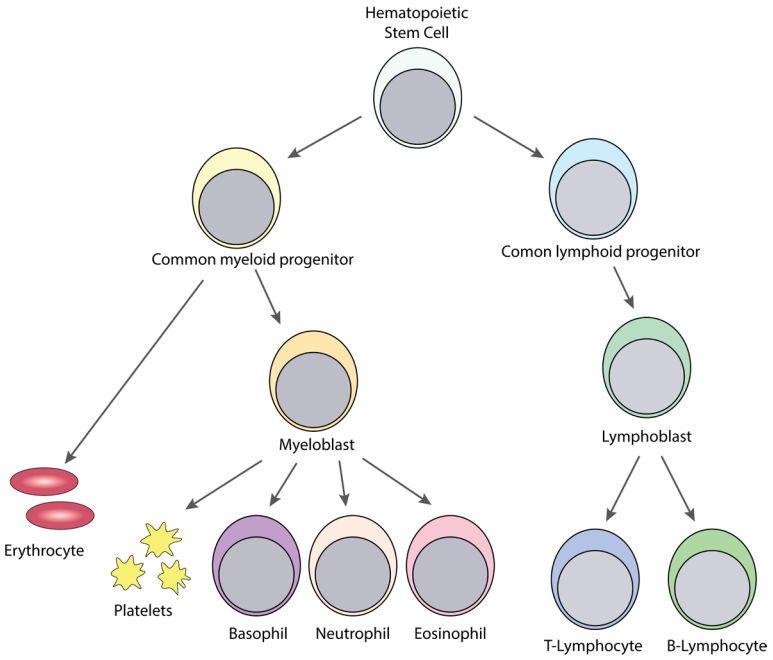

Figure 1: The developmental hierarchy of blood cells.

side effects include nausea, diarrhea, fatigue, moodiness, sleeplessness, allergic reactions, and severe infections. Possible late and long-term side effects are bone necrosis and growth retardation, heart problems, learning disabilities, infertility, and an increased chance of second cancers.

Finding cures for all children, especially those with poor response to current therapy, is a main goal for childhood cancer research.[4] However, because the current therapy achieves cure 75% of cases, a second important goal is minimizing short- and long-term side effects. Therapy is therefore adjusted depending on individual risk factors.

Many risk factors have been identified, including white blood cell count at diagnosis, age above 10 years, male sex, trisomy 21, certain cytogenetic aberrations (e.g IKZF1-deletions), T-ALL, central-nervous system involvement, and poor response to prednisone. Today, the most robust and accurate factor is the measurement of minimal residual disease (MRD).[5] MRD is determined in bone marrow aspirates during the first months of treatment, using leukemia-specific PCR or flow cytometry. Good responses with fast reduction in disease load indicate that further treatment may be safely reduced, but slow reductions are indicative for treatment failure and require treatment intensification.[5,6] The identification of risk factors is only a first step, and effective treatment alternatives are warranted to successfully treat high risk cases. Intensified chemotherapy for patients with poor treatment response largely improved the prognosis in recent protocols, but has likely reached the maximum achievable effect.[6]

In cases of relapse, treatment options are equally limited. The drugs patients receive are usually similar to those that have been given in initial therapy. However, it has been shown that leukemic cells at relapse are more drug resistant, likely due to selection during therapy.[7] In addition, relapse therapy often entails stem cell transplantation, which is associated with high rates of treatment-related death. Novel relapse therapies are urgently needed, and identification of relapse-driving aberrations for targeted therapy and immunotherapy are currently investigated in children with hematological malignancies.[8]

Pathobiology and genetic aberrations of acute lymphoblastic leukemia

Leukemogenesis is a multi-step process (Figure 2). In the case of BCP-ALL, it is initiated when a hematopoietic progenitor with B-cell capacities acquires a genetic mutation that disrupts differentiation. Initiating lesions largely determine the biology of leukemic cells, and are therefore used to distinguish the major cytogenetic subtypes. Many are chromosomal translocations that create fusion genes.

The most frequently detected fusion gene in pediatric BCP-ALL is translocation t(12;21), creating the *ETV6-RUNX1* fusion gene (~26% of cases). Another very frequent aberration is the acquisition of additional chromosomes causing high hyperdiploidy (51-67 chromosomes), which is found in approximately 24% of patients. Hypodiploidy (<45 chromosomes) and translocations causing *MLL*-, *TCF3*-, or *BCR-ABL1*-fusions are rare (1%, 7%, 5%, and 2%, respectively).[9] The remaining "B-other" group, accounting for one in every four patients, had previously included all cases lacking the aforementioned aberrations. Recent advances in genomics and transcriptomics have identified several distinct entities in this clinically and biologically heterogeneous group.

The largest group are so-called *BCR-ABL1*-like cases, which are defined by a gene expression signature similar to that of *BCR-ABL1*-positive cases.[10,11] Although definitions vary, this poor prognostic group constitutes roughly half of all B-other cases and about 15% of all BCP-ALL cases.[12,13] *BCR-ABL1*-like leukemia is, just as *BCR-ABL1*-positive leukemia, characterized by aberrant activation of signaling pathways. In many cases this is due to tyrosine kinase fusions involving receptor-associated kinases (e.g. *JAK2*, *ABL1*, or *ABL2*) or receptor-tyrosine kinases (*PDGFRB*, *EPOR*, *CSF1R*).[12,14-16] In addition, overexpression of the cytokine-receptor *CRLF2* is found in about half of *BCR-ABL1*-like. It is less frequently found among high hyperdiploid, *MLL*-rearranged, and non-*BCR-ABL1*-like B-other cases (~10% of all BCP-ALL).[12,17] In many cases, high *CRLF2* expression is caused by a deletion or translocation that juxtaposes the CRLF2 gene to a new promoter.[18,19] The prognostic impact of high *CRLF2* expression seems to depend on the treatment protocol.[17,20]

Other exclusive, recurrent aberrations within the *BCR-ABL1*-like group are internal amplification of chromosome 21 (iAMP21, ~2% of all BCP-ALL) and a dicentric chromosome containing parts of chromosomes 9 and 20 (dic(9;20), ~5% of BCP-ALL).[21-24]

Extensive genomic profiling of the remaining, non-*BCR-ABL1*-like B-other cases has recently identified so-called *ETV6-RUNX1*-like cases and recurrent fusion genes involving *MEF2D*, *ZNF384*, and *DUX4*.[25-27] Especially the latter discovery solved an important part of the puzzle around ERG-deletions, a common secondary aberration observed in BCP-ALL. A distinct gene expression profile that is associated with, but not limited to cases with *ERG*-deletions has been described in 2010.[28] Lillebjörn et al. found that this so-called ERG-cluster overlaps with *DUX4*-rearrangements, and Zhang et al. provided a mechanistic link between ERG–deletions and *DUX4*-rearrangements.[26,29] Unlike *MEF2D*- and *ZNF384*-fusions, *DUX4*-rearrangements seem to be associated with

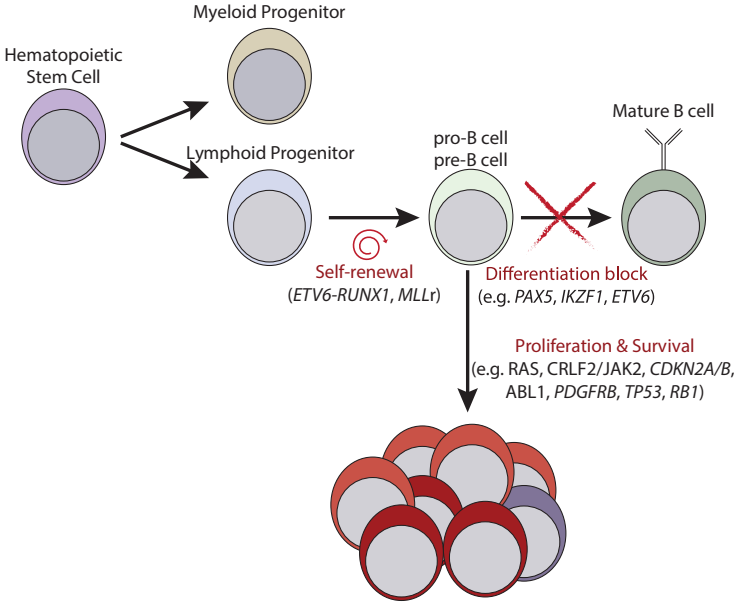

Figure 2: Genetic aberrations in the development of BCP-ALL.

a good outcome.[28,30,31]

Primary leukemogenic aberrations can often be identified in utero, but only a fraction of patients with a detectable fusion gene actually develops leukemia.[32-35] This penetrance varies: while most children with detectable *MLL*-rearrangements develop disease quickly, only about 1% of cases with an *ETV6-RUNX1*-fusion present in utero develop leukemia at a later age. This highlights the relevance of cooperative secondary events for a progression to overt leukemia. Besides the postulated infectious stimulus mentioned above, many genetic aberrations have been identified to support leukemogenesis.[27,36-42] Most aberrations are not mutually exclusive for a specific subtype, but frequencies often vary among cytogenetic groups.

B-cell transcription factors (e.g. P*AX5, IKZF1, TCF3, ETV6, EBF1, ERG,* and *RUNX1*) are frequently inactivated or functionally modified by mutations, deletions, or sequence duplications. These aberrations are thought to sustain a differentiation block in malignant cells. These biological differences have clinical impact: *IKZF1*-deletions for example, are enriched among kinase fusion-positive BCP-ALL and poor prognostic.[11,17,43,44]

Deregulation of cell cycle and DNA damage response is the result of frequently observed *CDKN2A/B* deletions and less frequent loss of RB1 or p53 function.[42] They represent important secondary aberrations that promote proliferation and survival. Mutational activation of the survival-promoting signaling pathways in BCP-ALL mostly affects JAK2/STAT5 and RAS/MAPK signaling, and is discussed below.

A third group of proteins frequently affected by aberrations are epigenetic modulators.[39,40,42,45,46] *CREBBP*, for example, is recurrently mutated or deleted and loss of function is postulated to reduce responsiveness to glucocorticoids.[45,46] Their role in leukemogenesis and suitability as treatment target is only starting to be understood.

Mutations conferring a proliferative advantage or resistance to apoptosis will give a competitive edge to expanding (pre-) leukemic cells. This concept of clonal evolution is essential for understanding disease initiation, treatment strategies, and relapse.[47,48] While leukemia-initiating aberrations are present in all cells, secondary aberrations are subject to evolutionary selection in a Darwinian model. Longitudinal genomic studies of matched sampled from diagnosis, remission, and relapse(s) have shown that considerable

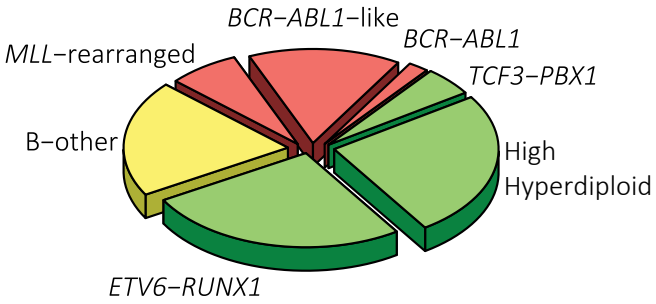

Figure 3: Estimated frequencies of cytogenetic subtypes in childhood BCP-ALL (adapted from Pui et al.[1]).

genetic heterogeneity exists at diagnosis and many relapse-forming clones are present as subpopulation.[49-52] Specific genetic mutations such as *TP53*, *CREBBP*, or those conferring resistance to chemotherapy (e.g. in *NT5C2* or *NR3C1*) are found more frequently at relapse.[45,53,54 50,52]

Inter- and intra-cellular signals: Oncogenic pathways and the microenvironment of leukemia.

Cellular signaling pathways are often affected by oncogenic hits in pediatric BCP-ALL. The aforementioned kinase fusions are an example of primary aberrations deregulating pro-survival signaling. Two major kinase pathways mediate these signals, leading to a mechanistic distinction between JAK- and ABL-type fusions.[20] ABL-type fusions result in strong activation of the MAPK pathway, JAK/STAT pathways, and PI3K/mTOR signaling.[20,55] *JAK2*-fusions as well as high *CRLF2* expression mainly act oncogenic by activating the STAT transcription factors and PI3K/mTOR signaling.[56]

The cytokine receptor CRLF2 lacks a kinase domain, and therefore relies on the associated kinase JAK2 to activate downstream signaling.[19,57] Binding of the ligand TSLP is still required and possibly limiting the oncogenic function of CRLF2. At least partial ligand-independence can be conferred by activating mutations in JAK2 which occur in about 50% of cases with high *CRLF2* expression.[18,19,58] Interestingly, although PI3K/mTOR signaling has been shown to be critical for *CRLF2*-rearranged leukemia, activating mutations in this pathway have not been described.[56,59]

A second essential oncogenic pathway is the MAPK pathway with its core components RAS, RAF, MEK and ERK. It is one of the most frequently mutated pathways in cancer.[60] The Ras GTPases (HRAS, NRAS, KRAS) mediate signals of activated receptor-tyrosine kinases (RTK). They activate the RAF kinases (ARAF, BRAF, and CRAF), which in turn activate MEK1 and MEK2. The only known targets of MEK1/2 are ERK1 and ERK2, but these can interact with and phosphorylate several hundred targets.[61,62] Cellular functions regulated by MAPK signaling include cell cycle progression, cell survival, differentiation, and motility.

In addition to the abovementioned intracellular pathways, extra-cellular signaling mediated by cytokines and growth factors have been shown to regulate normal and malignant hematopiesis.[63,64] The release of these factors from and to the microenvironment plays a crucial role for leukemia development and therapy resistance. Leukemic cells manipulate the bone marrow niche in their favor.[65] The cytokine CXCL12, expressed by stromal cells, can modulate leukemic cell egress, homing, and modulate chemotherapy resistance.[66,67] Adhesion molecules such as ITGA4 modulate leukemic cell survival and chemoresistance.[68] Tunneling nanotubes represent another, only recently identified mechanism of communication between leukemic and bone marrow stromal cells.[69]

Novel therapeutic approaches for children with acute lymphoblastic leukemia

Current treatment for children with leukemia comprises more than a dozen therapeutic agents. Decades of clinical trials have massively improved therapy outcomes by optimizing the combination of these drugs. However, survival rates are stagnating, which suggests that therapy has reached its maximum achievable effect.[1] The high cure rate of standard

therapy sets the focus on two main goals: identifying cure for those 10 to 15% of cases that relapse, and avoiding overtreatment of cases who are cured to reduce side effects and treatment-related deaths.

Further improvements are likely to come from entirely new therapy classes, such as targeted therapy or immunotherapy. Targeted therapy designates treatment strategies which abrogate the effect of oncogenic drivers and it is often linked to personalized cancer treatment.

Six cellular capacities have been initially suggested to contribute to malignancy in all cancer cells. These hallmarks of cancer are: self-sufficiency in growth signals, insensitivity to anti-growth signals, evasion of apoptosis, limitless replicative potential, tissue invasion and metastasis, and induction of angiogenesis.[70] Recently, two more principles have been added: Deregulated cellular energetics and evasion from immune destruction.[71] Many of these core capacities are driven by genetic aberrations, and usually several genetic aberrations collaborate to establish a malignant phenotype. Some aberrations can affect more than one hallmark, and as a result these aberrations may affect specific hallmarks to a varying extend in distinct tumor types and cases. These principles have to be taken into account to develop and evaluate targeted therapies.

The exploration of signaling pathways as therapeutic targets has grown with the next-generation sequencing revolution. Low costs for sequencing entire genomes facilitate molecular characterization of every tumor. Although few aberrations serve as treatment targets so far (often called "actionable aberrations"), encouraging examples exist.

All-trans retinoic acid, for example, specifically induces differentiation in *PML-RARA*-rearranged acute promyelocytic leukemia. Arsenic trioxide, which targets the PML moiety, induces apoptosis in these cell. The combination of these to drugs now achieves a 4-year overall survival of 98% in this once deadly disease.[72]

Identification and characterization of the *BCR-ABL1*-rearrangement led to the application of the first kinase inhibitor (TKI) for cancer treatment: imatinib. It has drastically improved prognosis for CML and *BCR-ABL1*-rearranged B-ALL in children and adults.[73,74] As explained above, tyrosine-kinase fusions represent primary, leukemia-driving lesions in about 5% of pediatric BCP-ALL cases.[15] So far only *BCR-ABL1*-rearranged cases receive standard TKI therapy, but preclinical and anecdotal clinical data suggest sensitivity towards inhibition of the JAK and ABL class kinases.[12,14,16,56,75-77]

Three promises are offered by kinase inhibitors for children with BCP-ALL: First, they may serve as treatment options if standard therapy fails. Second, they could be included upfront for high risk cases to prevent relapses. Third, their anticipated specificity for cancer cells could entail less short-and long-term side effects and allow reduction of chemotherapy.

Despite successful examples such as Imatinib in *BCR-ABL1*-rearranged CML, vermurafinib in *BRAF*-mutant melanoma, or ERBB2-specific antibodies in breast cancer, many other approaches have yielded minor benefits and stayed behind the expectations from pre-clinical studies. Pharmacologic hurdles such as competition with high concentrations of ATP (imatinib), or short half-lives (momelotinib) may interfere with efficacy and applicability of kinase inhibitors.[78,79]

Biologically, clonal evolution has also proven to be a major cause for disease progression on therapy. Any therapy represents a shift in selective pressures and mutations causing drug resistance, e.g. in CREBBP or ABL1 T315I, are therefore positively selected.[45] Already diagnostic patient samples contain multiple genetically distinct subclones.[80] In BCP-ALL virtually all cells retain leukemia-initiating capacity.[34,81,82] Theoretically, a mutation occurring in any of the leukemic cells present at diagnosis could therefore give rise to a resistant cell. This demonstrates the importance of a combinatorial, multi-targeted therapy.

With these advantages and possible limitations in mind, the aim of this thesis is therefore to evaluate selected signaling pathways as therapeutic targets in BCP-ALL. Five targets, JAK2, the RAS pathway, PDGFRα, FGFR, and EMP1 were selected and assessed for different treatment strategies.

Outline of this thesis

Intra- and inter-cellular signaling pathways have become promising candidates for cancer therapy, because they are frequently affected by oncogenic aberrations and specific small molecule inhibitors are available. The aim of this thesis is to identify and evaluate signaling pathways that may be targeted by novel therapeutic approaches in children with BCP-ALL.

In **chapter 2**, we determined the frequency of JAK2 mutations and translocations in a large cohort of BCP-ALL patients at diagnosis and evaluated the *ex vivo* efficiency of two clinically tested JAK inhibitors. We found selective anti-tumor activity of JAK inhibitors in cells carrying JAK2 aberrations. However, we also identified stroma mediated drug resistance, mutational activation of alternative survival pathways, and a signaling rebound effect after inhibitor release as important caveats in JAK inhibitor treatment.

A second frequently mutated signaling pathway is studied in **chapter 3**: Next generation sequencing was used to detect RAS pathway mutations. We show that clonal or subclonal RAS pathway mutations are present in 44% of BCP-ALL cases at diagnosis. Mutations were associated with poorer *ex vivo* response to chemotherapy, and clonal but not subclonal mutations associated with a poor prognosis in some treatment groups. RAS mutant BCP-ALL cells were *ex vivo* sensitive to the MEK inhibitor trametinib, which suggests that this FDA-approved drug could be used to treat BCP-ALL with RAS pathway mutations.

In **chapter 4** we study the role of high PDGFRA expression in the newly discovered ERG-deleted leukemia. No genetic aberrations within the PDGFRA locus could be identified that could explain high levels of PDGFRA transcript. Despite being translated and ligand-activated, inhibition of PDGFRα was not cytotoxic in PDGFRA-high BCP-ALL.

Two factors mediating *ex vivo* glucocorticoid resistance are discussed in the last two chapters of this thesis. In **chapter 5** we show that FGFR mutations are rare and occur outside of classical mutational hotspots. The ligand FGF2, however, can reduce the responsiveness of BCP-ALL cells to prednisolone. In **chapter 6** we identify EMP1 as a poor prognostic biomarker and regulator of glucocorticoid resistance.

Conclusions and significance of the work presented in this thesis are discussed in **chapter 7**, including future directives for targeted therapy in children with BCP-ALL. A summary of the work in English and Dutch is given in **chapter 8**, and detailed information about the author in **chapter 9**.

References

1. Pui CH, Evans WE. A 50-year journey to cure childhood acute lymphoblastic leukemia. Semin Hematol. 2013;50(3):185-196.

2. Greaves M. Infection, immune responses and the aetiology of childhood leukaemia. Nat Rev Cancer. 2006;6(3):193-203.

3. Francis SS, Wallace AD, Wendt GA, et al. In utero cytomegalovirus infection and development of childhood acute lymphoblastic leukemia. Blood. 2016.

4. Pui CH, Mullighan CG, Evans WE, Relling MV. Pediatric acute lymphoblastic leukemia: where are we going and how do we get there? Blood. 2012;120(6):1165-1174.

5. van Dongen JJ, Seriu T, Panzer-Grumayer ER, et al. Prognostic value of minimal residual disease in acute lymphoblastic leukaemia in childhood. Lancet. 1998;352(9142):1731-1738.

6. Pieters R, de Groot-Kruseman H, Van der Velden V, et al. Successful Therapy Reduction and Intensification for Childhood Acute Lymphoblastic Leukemia Based on Minimal Residual Disease Monitoring: Study ALL10 From the Dutch Childhood Oncology Group. J Clin Oncol. 2016;34(22):2591-2601.

7. Klumper E, Pieters R, Veerman AJ, et al. In vitro cellular drug resistance in children with relapsed/refractory acute lymphoblastic leukemia. Blood. 1995;86(10):3861-3868.

8. Bhojwani D, Pui CH. Relapsed childhood acute lymphoblastic leukaemia. Lancet Oncol. 2013;14(6):e205-217.

9. Mullighan CG, Downing JR. Global genomic characterization of acute lymphoblastic leukemia. Semin Hematol. 2009;46(1):3-15.

10. Den Boer ML, van Slegtenhorst M, De Menezes RX, et al. A subtype of childhood acute lymphoblastic leukaemia with poor treatment outcome: a genome-wide classification study. Lancet Oncol. 2009;10(2):125-134.

11. Mullighan CG, Su X, Zhang J, et al. Deletion of IKZF1 and prognosis in acute lymphoblastic leukemia. N Engl J Med. 2009;360(5):470-480.

12. Roberts KG, Li Y, Payne-Turner D, et al. Targetable kinase-activating lesions in Ph-like acute lymphoblastic leukemia. N Engl J Med. 2014;371(11):1005-1015.

13. Boer JM, Marchante JR, Evans WE, et al. *BCR-ABL1*-like cases in pediatric acute lymphoblastic leukemia: a comparison between DCOG/Erasmus MC and COG/St. Jude signatures. Haematologica. 2015;100(9):e354-357.

14. Roberts KG, Morin RD, Zhang J, et al. Genetic alterations activating kinase and cytokine receptor signaling in high-risk acute lymphoblastic leukemia. Cancer Cell. 2012;22(2):153-166.

15. Boer JM, Steeghs EM, Marchante JR, et al. Tyrosine kinase fusion genes in pediatric *BCR-ABL1*-like acute lymphoblastic leukemia. Oncotarget. 2016.

16. Iacobucci I, Li Y, Roberts KG, et al. Truncating Erythropoietin Receptor Rearrangements in Acute Lymphoblastic Leukemia. Cancer Cell. 2016;29(2):186-200.

17. van der Veer A, Waanders E, Pieters R, et al. Independent prognostic value of *BCR-ABL1*-like signature and IKZF1 deletion, but not high CRLF2 expression, in children with B-cell precursor ALL. Blood. 2013;122(15):2622-2629.

18. Russell LJ, Capasso M, Vater I, et al. Deregulated expression of cytokine receptor gene, CRLF2, is involved in lymphoid transformation in B-cell precursor acute lymphoblastic leukemia. Blood. 2009;114(13):2688-2698.

19. Yoda A, Yoda Y, Chiaretti S, et al. Functional screening identifies CRLF2 in precursor B-cell acute lymphoblastic leukemia. Proc Natl Acad Sci U S A. 2010;107(1):252-257.

20. Izraeli S. Beyond Philadelphia: 'Ph-like' B cell precursor acute lymphoblastic leukemias - diagnostic challenges and therapeutic promises. Curr Opin Hematol. 2014;21(4):289-296.

21. Harewood L, Robinson H, Harris R, et al. Amplification of AML1 on a duplicated chromosome 21 in acute lymphoblastic leukemia: a study of 20 cases. Leukemia. 2003;17(3):547-553.

22. Harrison CJ. Blood Spotlight on iAMP21 acute lymphoblastic leukemia (ALL), a high-risk pediatric disease. Blood. 2015;125(9):1383-1386.

23. Rieder H, Schnittger S, Bodenstein H, et al. dic(9;20): a new recurrent chromosome abnormality in adult acute lymphoblastic leukemia. Genes Chromosomes Cancer. 1995;13(1):54-61.

24. Zachariadis V, Gauffin F, Kuchinskaya E, et al. The frequency and prognostic impact of dic(9;20)(p13.2;q11.2) in childhood B-cell precursor acute lymphoblastic leukemia: results from the NOPHO ALL-2000 trial. Leukemia. 2011;25(4):622-628.

25. Yasuda T, Tsuzuki S, Kawazu M, et al. Recurrent DUX4 fusions in B cell acute lymphoblastic leukemia of adolescents and young adults. Nat Genet. 2016;48(5):569-574.

26. Lilljebjorn H, Henningsson R, Hyrenius-Wittsten A, et al. Identification of *ETV6-RUNX1*-like and DUX4-rearranged subtypes in paediatric B-cell precursor acute lymphoblastic leukaemia. Nat Commun. 2016;7:11790.

27. Liu YF, Wang BY, Zhang WN, et al. Genomic Profiling of Adult and Pediatric B-cell Acute Lymphoblastic Leukemia. EBioMedicine. 2016;8:173-183.

28. Harvey RC, Mullighan CG, Wang X, et al. Identification of novel cluster groups in pediatric high-risk B-precursor acute lymphoblastic leukemia with gene expression profiling: correlation with genome-wide DNA copy number alterations, clinical characteristics, and outcome. Blood. 2010;116(23):4874-4884.

29. Zhang J, McCastlain K, Yoshihara H, et al. Deregulation of DUX4 and ERG in acute lymphoblastic leukemia. Nat Genet. 2016;48(12):1481-1489.

30. Clappier E, Auclerc MF, Rapion J, et al. An intragenic ERG deletion is a marker of an oncogenic subtype of B-cell precursor acute lymphoblastic leukemia with a favorable outcome despite frequent IKZF1 deletions. Leukemia. 2014;28(1):70-77.

31. Zaliova M, Zimmermannova O, Dorge P, et al. ERG deletion is associated with CD2 and attenuates the negative impact of IKZF1 deletion in childhood acute lymphoblastic leukemia. Leukemia. 2014;28(1):182-185.

32. Taub JW, Konrad MA, Ge Y, et al. High frequency of leukemic clones in newborn screening blood samples of children with B-precursor acute lymphoblastic leukemia. Blood. 2002;99(8):2992-2996.

33. Greaves MF, Wiemels J. Origins of chromosome translocations in childhood leukaemia. Nat Rev Cancer. 2003;3(9):639-649.

34. Greaves M. Molecular genetics, natural history and the demise of childhood leukaemia. Eur J Cancer. 1999;35(14):1941-1953.

35. Mori H, Colman SM, Xiao Z, et al. Chromosome translocations and covert leukemic clones are generated during normal fetal development. Proc Natl Acad Sci U S A. 2002;99(12):8242-8247.

36. Andersson AK, Ma J, Wang J, et al. The landscape of somatic mutations in infant MLL-rearranged acute lymphoblastic leukemias. Nat Genet. 2015;47(4):330-337.

37. Fischer U, Forster M, Rinaldi A, et al. Genomics and drug profiling of fatal TCF3-HLF-positive acute lymphoblastic leukemia identifies recurrent mutation patterns and therapeutic options. Nat Genet. 2015;47(9):1020-1029.

38. Holmfeldt L, Wei L, Diaz-Flores E, et al. The genomic landscape of hypodiploid acute lymphoblastic leukemia. Nat Genet. 2013;45(3):242-252.

39. Huether R, Dong L, Chen X, et al. The landscape of somatic mutations in epigenetic regulators across 1,000 paediatric cancer genomes. Nat Commun. 2014;5:3630.

40. Paulsson K, Lilljebjorn H, Biloglav A, et al. The genomic landscape of high hyperdiploid childhood acute lymphoblastic leukemia. Nat Genet. 2015;47(6):672-676.

41. Pui CH. Genomic and pharmacogenetic studies of childhood acute lymphoblastic leukemia. Front Med. 2015;9(1):1-9.

42. Zhang J, Mullighan CG, Harvey RC, et al. Key pathways are frequently mutated in high-risk childhood acute lymphoblastic leukemia: a report from the Children's Oncology Group. Blood. 2011;118(11):3080-3087.

43. van der Veer A, Zaliova M, Mottadelli F, et al. IKZF1 status as a prognostic feature in *BCR-ABL1*-positive childhood ALL. Blood. 2014;123(11):1691-1698.

44. Boer JM, van der Veer A, Rizopoulos D, et al. Prognostic value of rare IKZF1 deletion in childhood B-cell precursor acute lymphoblastic leukemia: an international collaborative study. Leukemia. 2016;30(1):32-38.

45. Mullighan CG, Zhang J, Kasper LH, et al. CREBBP mutations in relapsed acute lymphoblastic leukaemia. Nature. 2011;471(7337):235-239.

46. Malinowska-Ozdowy K, Frech C, Schonegger A, et al. KRAS and CREBBP mutations: a relapse-linked malicious liaison in childhood high hyperdiploid acute lymphoblastic leukemia. Leukemia. 2015;29(8):1656-1667.

47. Greaves M, Maley CC. Clonal evolution in cancer. Nature. 2012;481(7381):306-313.

48. Shlush LI, Hershkovitz D. Clonal evolution models of tumor heterogeneity. Am Soc Clin Oncol Educ Book. 2015:e662-665.

49. Mullighan CG, Phillips LA, Su X, et al. Genomic analysis of the clonal origins of relapsed acute lymphoblastic leukemia. Science. 2008;322(5906):1377-1380.

50. Oshima K, Khiabanian H, da Silva-Almeida AC, et al. Mutational landscape, clonal evolution patterns, and role of RAS mutations in relapsed acute lymphoblastic leukemia. Proc Natl Acad Sci U S A. 2016.

51. Ma X, Edmonson M, Yergeau D, et al. Rise and fall of subclones from diagnosis to relapse in pediatric B-acute lymphoblastic leukaemia. Nat Commun. 2015;6:6604.

52. Kuster L, Grausenburger R, Fuka G, et al. ETV6/RUNX1-positive relapses evolve from an ancestral clone and frequently acquire deletions of genes implicated in glucocorticoid signaling. Blood. 2011;117(9):2658-2667.

53. Stengel A, Schnittger S, Weissmann S, et al. TP53 mutations occur in 15.7% of ALL and are associated with MYC-rearrangement, low hypodiploidy, and a poor prognosis. Blood. 2014;124(2):251-258.

54. Tzoneva G, Perez-Garcia A, Carpenter Z, et al. Activating mutations in the NT5C2 nucleotidase gene drive chemotherapy resistance in relapsed ALL. Nat Med. 2013;19(3):368-371.

55. Cilloni D, Saglio G. Molecular pathways: BCR-ABL. Clin Cancer Res. 2012;18(4):930-937.

56. Tasian SK, Doral MY, Borowitz MJ, et al. Aberrant STAT5 and PI3K/mTOR pathway signaling occurs in human CRLF2-rearranged B-precursor acute lymphoblastic leukemia. Blood. 2012;120(4):833-842.

57. Hertzberg L, Vendramini E, Ganmore I, et al.

Down syndrome acute lymphoblastic leukemia, a highly heterogeneous disease in which aberrant expression of CRLF2 is associated with mutated JAK2: a report from the International BFM Study Group. Blood. 2010;115(5):1006-1017.

58. Harvey RC, Mullighan CG, Chen IM, et al. Rearrangement of CRLF2 is associated with mutation of JAK kinases, alteration of IKZF1, Hispanic/Latino ethnicity, and a poor outcome in pediatric B-progenitor acute lymphoblastic leukemia. Blood. 2010;115(26):5312-5321.

59. Francis OL, Milford TA, Martinez SR, et al. A novel xenograft model to study the role of TSLP-induced CRLF2 signals in normal and malignant human B lymphopoiesis. Haematologica. 2016;101(4):417-426.

60. Ciriello G, Miller ML, Aksoy BA, Senbabaoglu Y, Schultz N, Sander C. Emerging landscape of oncogenic signatures across human cancers. Nat Genet. 2013;45(10):1127-1133.

61. Caunt CJ, Sale MJ, Smith PD, Cook SJ. MEK1 and MEK2 inhibitors and cancer therapy: the long and winding road. Nat Rev Cancer. 2015;15(10):577-592.

62. Yoon S, Seger R. The extracellular signal-regulated kinase: multiple substrates regulate diverse cellular functions. Growth Factors. 2006;24(1):21-44.

63. Morrison SJ, Scadden DT. The bone marrow niche for haematopoietic stem cells. Nature. 2014;505(7483):327-334.

64. Sison EA, Brown P. The bone marrow microenvironment and leukemia: biology and therapeutic targeting. Expert Rev Hematol. 2011;4(3):271-283.

65. Colmone A, Amorim M, Pontier AL, Wang S, Jablonski E, Sipkins DA. Leukemic cells create bone marrow niches that disrupt the behavior of normal hematopoietic progenitor cells. Science. 2008;322(5909):1861-1865.

66. Jin L, Tabe Y, Konoplev S, et al. CXCR4 up-regulation by imatinib induces chronic myelogenous leukemia (CML) cell migration to bone marrow stroma and promotes survival of quiescent CML cells. Mol Cancer Ther. 2008;7(1):48-58.

67. Hoellenriegel J, Zboralski D, Maasch C, et al. The Spiegelmer NOX-A12, a novel CXCL12 inhibitor, interferes with chronic lymphocytic leukemia cell motility and causes chemosensitization. Blood. 2014;123(7):1032-1039.

68. Hsieh YT, Gang EJ, Geng H, et al. Integrin alpha4 blockade sensitizes drug resistant pre-B acute lymphoblastic leukemia to chemotherapy. Blood. 2013;121(10):1814-1818.

69. Polak R, de Rooij B, Pieters R, den Boer ML. B-cell precursor acute lymphoblastic leukemia cells use tunneling nanotubes to orchestrate their microenvironment. Blood. 2015;126(21):2404-2414.

70. Hanahan D, Weinberg RA. The hallmarks of cancer. Cell. 2000;100(1):57-70.

71. Hanahan D, Weinberg RA. Hallmarks of cancer: the next generation. Cell. 2011;144(5):646-674.

72. Tallman MS, Altman JK. Curative strategies in acute promyelocytic leukemia. Hematology Am Soc Hematol Educ Program. 2008:391-399.

73. Biondi A, Schrappe M, De Lorenzo P, et al. Imatinib after induction for treatment of children and adolescents with Philadelphia-chromosome-positive acute lymphoblastic leukaemia (EsPhALL): a randomised, open-label, intergroup study. Lancet Oncol. 2012;13(9):936-945.

74. O'Brien SG, Guilhot F, Larson RA, et al. Imatinib compared with interferon and low-dose cytarabine for newly diagnosed chronic-phase chronic myeloid leukemia. N Engl J Med. 2003;348(11):994-1004.

75. David M, Cross NC, Burgstaller S, et al. Durable responses to imatinib in patients with PDGFRB fusion gene-positive and BCR-ABL-negative chronic myeloproliferative disorders. Blood. 2007;109(1):61-64.

76. Lengline E, Beldjord K, Dombret H, Soulier J, Boissel N, Clappier E. Successful tyrosine kinase inhibitor therapy in a refractory B-cell precursor acute lymphoblastic leukemia with EBF1-PDGFRB fusion. Haematologica. 2013;98(11):e146-148.

77. Weston BW, Hayden MA, Roberts KG, et al. Tyrosine kinase inhibitor therapy induces remission in a patient with refractory EBF1-PDGFRB-positive acute lymphoblastic leukemia. J Clin Oncol. 2013;31(25):e413-416.

78. Tyner JW, Bumm TG, Deininger J, et al. CYT387, a novel JAK2 inhibitor, induces hematologic responses and normalizes inflammatory cytokines in murine myeloproliferative neoplasms. Blood. 2010;115(25):5232-5240.

79. Cortes JE, Kim DW, Pinilla-Ibarz J, et al. A phase 2 trial of ponatinib in Philadelphia chromosome-positive leukemias. N Engl J Med. 2013;369(19):1783-1796.

80. Notta F, Mullighan CG, Wang JC, et al. Evolution of human *BCR-ABL1* lymphoblastic leukaemia-initiating cells. Nature. 2011;469(7330):362-367.

81. Rehe K, Wilson K, Bomken S, et al. Acute B lymphoblastic leukaemia-propagating cells are present at high frequency in diverse lymphoblast populations. EMBO Mol Med. 2013;5(1):38-51.

82. Ebinger S, Ozdemir EZ, Ziegenhain C, et al. Characterization of Rare, Dormant, and Therapy-Resistant Cells in Acute Lymphoblastic Leukemia. Cancer Cell. 2016;30(6):849-862.

Chapter 2

JAK2 aberrations in childhood B-cell precursor acute lymphoblastic leukemia

Elisabeth M.P. Steeghs*, Isabel S. Jerchel*, Willemieke de Goffau-Nobel, Alex Q. Hoogkamer, Judith M. Boer, Aurélie Boeree, Cesca van de Ven, Marco J. Koudijs, Nicolle J.M. Besselink, Hester A. de Groot-Kruseman, C. Michel Zwaan, Martin A. Horstmann, Rob Pieters, and Monique L. den Boer

*E.M.P. Steeghs and I.S. Jerchel contributed equally to this work

Oncotarget. 2017 Sep 16;8(52):89923-89938.

Summary

JAK2 abnormalities may serve as target for precision medicines in pediatric B-cell precursor acute lymphoblastic leukemia (BCP-ALL). In the current study we performed a screening for JAK2 mutations and translocations, analyzed the clinical outcome and studied the efficacy of two JAK inhibitors in primary BCP-ALL cells. Importantly, we identify a number of limitations of JAK inhibitor therapy.

JAK2 mutations mainly occurred in the poor prognostic subtypes *BCR-ABL1*-like and non-*BCR-ABL1*-like B-other (negative for sentinel cytogenetic lesions). JAK2 translocations were restricted to *BCR-ABL1*-like cases. Momelotinib and ruxolitinib were cytotoxic in both JAK2 translocated and JAK2 mutated cells, although efficacy in JAK2 mutated cells highly depended on cytokine receptor activation by TSLP. However, our data also suggest that the effect of JAK inhibition may be compromised by mutations in alternative survival pathways and microenvironment-induced resistance. Furthermore, inhibitors induced accumulation of phosphorylated JAK2 Y1007, which resulted in a profound re-activation of JAK2 signaling upon release of the inhibitors. This preclinical evidence implies that further optimization and evaluation of JAK inhibitor treatment is necessary prior to its clinical integration in pediatric BCP-ALL.

Introduction

Janus kinase 2 (JAK2) is a member of the non-receptor tyrosine kinase family and mediates intracellular signaling upon activation of cytokine receptors, which lack an intrinsic tyrosine kinase domain, such as cytokine receptor-like factor 2 (CRLF2). Ligand binding (e.g. TSLP for CLRF2) induces dimerization of cytokine receptors chains, resulting in activation of JAK proteins via cross-phosphorylation. JAKs activate signal transducers of transcription (STATs), which, upon dimerization, migrate to the nucleus and induce transcription of genes involved in differentiation and proliferation of hematopoietic cells.[1]

JAK2 has seven homologous domains (JH1-JH7). The JH1 and JH2 domains are C-terminally located and comprise the catalytic kinase (JH1) and pseudokinase (JH2) domain. The JH2 domain has a dual regulatory function: exerting a negative regulatory effect on the kinase domain, and facilitating JAK2 activation upon receptor activation by ligand binding.[2] The JH3-JH4 domains share homology with Src homology 2 (SH2) domains and mediate protein-protein interactions. The N-terminal located JH6 and JH7 domains, also known as the FERM domain, are required for binding of JAK2 to cytokine receptors.[1]

In pediatric BCP-ALL patients, gain of function mutations and translocations affecting *JAK2* have been identified.[3-15] Genomic translocations of *JAK2* have been observed in high-risk *BCR-ABL1*-like patients. For several of these fusion genes, constitutive JAK2 kinase activation has been demonstrated.[12-14, 16] Point mutations often occur in Down Syndrome ALL, mainly affect exon 16 (located in the pseudokinase domain), and functionally cooperate with overexpression of the type I cytokine receptor CRLF2.[6, 9, 10] Indeed, requirement for the interaction of mutant JAK2 with a cytokine receptor was shown in cell lines models by several groups.[6, 8, 9]

Mutations and translocations represent biologically distinct entities, but both are potential targets for precision medicines. JAK inhibitors were shown to be effective against mutant and translocated JAK2 in vitro.[3, 5, 7, 8, 12, 13, 16, 17] However, in vivo mouse studies show conflicting data and none has been reported to be curative.[13, 17-21] To date, clinical data with JAK inhibitors are scarce. The Children's Oncology Group performed a phase 1 dosing study of the JAK inhibitor ruxolitinib, but no cases harboring JAK2 activating mutations or translocations were included.[22]

Several papers have reported data with a focus on either fusion genes or mutations of *JAK2*, although often with small sample size or only in specific subtypes of BCP-ALL. Furthermore, most reports lack *ex vivo* efficacy data of JAK inhibitors in primary leukemic cells. To assess the clinical potential of JAK inhibitors in pediatric BCP-ALL, we performed a comprehensive study to determine the frequency and prognosis of *JAK2* mutations and translocations among different subtypes of childhood BCP-ALL. Furthermore, the biological efficacy of the JAK inhibitors momelotinib and ruxolitinib was studied in primary leukemic cells harboring JAK2 aberrations, and the clonal stability of *JAK2* mutations was investigated in ALL patient derived xenograft models. We show that JAK inhibitors are overall effective towards BCP-ALL cells, but also identified a number of limitations of JAK inhibitor therapy.

Results

Frequency and type of JAK2 aberrations in BCP-ALL patients

JAK2 mutation status was analyzed in 461 newly diagnosed BCP-ALL cases representing all major subtypes seen in children, with a distribution that is comparable to the general pediatric BCP-ALL population. *JAK2* exons 16, 20, 21 and 23 were examined by targeted amplicon sequencing at a median read depth of 673, 577, 711 and 944, respectively. Analyses revealed that 3.5 % (16/461) of these BCP ALL cases harbored *JAK2* mutations, which were detected in 7.6 % (6/79) of *BCR-ABL1*-like cases, 11.9 % (8/67) of non-*BCR-ABL1*-like B-other cases, and 1.6 % (2/124) of high hyperdiploid cases. No JAK2 mutations were detected in *MLL-AF4* (0/15), *BCR-ABL1* (0/26), *ETV6-RUNX1* (0/124) or *TCF3-PBX1* (0/26) cases. The variant allele frequency (VAF) ranged from 1.0 % to 56 % (Figure 1A). Seven patients carried two different *JAK2* mutations, and one patient even harbored three different *JAK2* mutations. Mutations involved amino acid residue R683 in 13 of 16 mutated cases, which is an important amino acid for the JH2 domain mediated negative auto-regulation of JAK2 activity [23]. CRLF2 overexpression was detected in 87.5 % (14/16) of these cases (Figure 1A, Supplementary Figure 1). One *CRLF2* low expressing case harbored a subclonal JAK2 mutation, suggesting that *CRLF2* overexpression might be subclonal as well. The other case harbored a JAK2 R923H with a VAF of 50 %, suggesting that this mutation in the kinase domain is not associated with *CRLF2* overexpression.

The screen for *JAK2* fusion genes was confined to 153 BCP-ALL cases, negative for sentinel BCP-ALL associated lesions (*MLL*-rearranged, *BCR-ABL1*, *ETV6-RUNX1*, *TCF3-PBX1*, high hyperdiploid), as *JAK2* translocations were previously reported in this group of patients.[12, 13, 24] No *JAK2* translocations were detected in 76 non-*BCR-ABL1*-like B-other cases, whereas in five of the 77 (6.5%) *BCR-ABL1*-like cases JAK2 tyrosine kinase

A

	Patient	Protocol	Risk group	Age (years)	WBC (x10⁹/L)	Down Syndrome	MRD (d29/d33)	Subtype	Translocation	Mutation 1 (VAF)	Mutation 2 (VAF)	Mutation 3 (VAF)	*CRLF2* status
JAK2 Mutation	A20	ALL9	HR	14	75		<10^-3	*BCR-ABL1*-like		p.R873N 40%	p.R683S 2%	p.R683G 2%	High
	A35	ALL9	NHR	1	44		NA	*BCR-ABL1*-like		p.R683T 56%	p.R683G 13%		High
	A38	ALL9	HR	6	128,8		NA	*BCR-ABL1*-like		p.R683G 32%	p.T875N 10%		High
	A129	COALL03	HR-S	4	450	Yes	NA	B-other		p.R683G 2%	p.K914E 1%		High
	A159	COALL03	HR-S	4	39		NA	High Hyperdiploid		p.R683G 1%			Low
	A160	COALL03	LR-S	3	4,3		NA	B-Other		p.R683G 24%			High
	A167	COALL03	HR-S	9	30		NA	B-other		p.D873N 10%	p.R683G 8%		High
	A178	COALL03	LR-R	7	10		≥10^-3	B-other		p.R683T 30%	p.R683G 4%		High
	A186	COALL97	HR-S	11	9,9		≥10^-3	*BCR-ABL1*-like		p.T875N 37%			High
	A251	COALL97	HR-S	7	115		NA	*BCR-ABL1*-like		p.R683G 63%			High
	A282	ALL10	SR	3	21		<10^-3	B-Other		p.R683S 25%	p.R683G 7%		High
	A315	ALL10	MR	3	3,6	Yes	<10^-3	B-Other		p.R683G 41%			High
	A359	ALL10	MR	8	390	Yes	≥10^-3	B-other		p.R683G 27%	p.R683S 25%		High
	A404	ALL10	MR	8	222,6		<10^-3	*BCR-ABL1*-like		p.R683G 26%			High
	A433	ALL10	MR	2	1,9	Yes	≥10^-3	High Hyperdiploid		p.R683G 25%			High
	A521	ALL10	MR	11	12,1		<10^-3	B-Other		p.R923H 50%			Low
JAK2 Translocation	A31	ALL9	HR	1	53,8		<10^-3	*BCR-ABL1*-like	*PAX5-JAK2*				Low
	A204	COALL03	HR-S	14	4,5		<10^-3	*BCR-ABL1*-like	*PAX5-JAK2*				Low
	A286	ALL10	SR	1	3,4		<10^-3	*BCR-ABL1*-like	*PAX5-JAK2*				Low
	A214	COALL03	HR-S	11	19,5		≥10^-3	*BCR-ABL1*-like	*TERF2-JAK2*				Low
	A216	COALL03	HR-S	5	204		<10^-3	*BCR-ABL1*-like	*BCR-JAK2*				Low

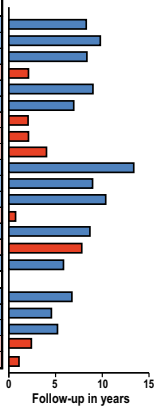

B

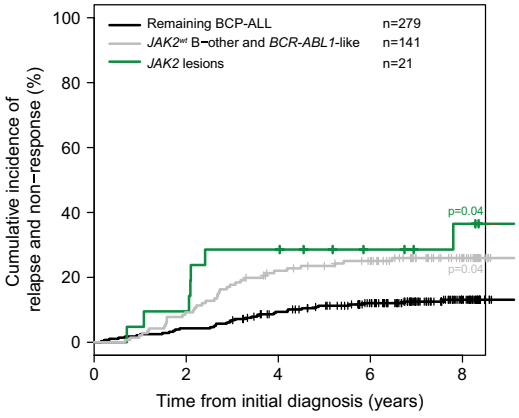

Figure 1: *JAK2* aberrations in BCP-ALL patients

(A) Type of lesions, clinical characteristics and follow-up of *JAK2* lesion positive patients. Treatment protocol and risk group assigned to each patient per protocol have been listed (HR-S: High Risk Standard. HR: High Risk. MR: Median Risk. SR: Standard Risk. LR-S: Low Risk Standard. LR-R: Low Risk Reduced. NHR: Non-High Risk). WBC indicates white blood cell count. Minimal residual disease (MRD) levels at day 29/33 of treatment of COALL and DCOG protocol, respectively. Type of translocation or mutation is listed. VAF indicates the variant allele frequency (%). CRLF2 status indicates gene expression below (low) or above (high) the 90th percentile levels. Right panel: Bar plot represents years from diagnosis to event or last contact. In blue: cases in complete clinical remission. In red: cases with an event (relapse or death). **(B)** Cumulative incidence of relapse curves for patients with *JAK2* lesions (green line), *JAK2* wildtype *BCR-ABL1*-like and B-other cases (grey line), and *JAK2* wildtype remaining BCP-ALL cases (black line; *ETV6-RUNX1*, high hyperdiploid, *TCF3-PBX1*). Patients were treated according to ALL8, ALL9, ALL10, COALL97 or COALL03 protocol. Cumulative incidence of relapse (CIR) was estimated using a competing risk model. Relapse and non-response were considered as event, and death as competing event. Non-response was counted as event at day 79. The Gray's test was applied to test for equality of CIRs (*JAK2* lesion versus remaining BCP-ALL p=0.04; *JAK2* wildtype B-other/*BCR-ABL1*-like versus remaining BCP-ALL p=0.04).

activating fusion genes were identified. The cases involved three *PAX5-JAK2* cases, one *BCR-JAK2* case and one *TERF2-JAK2* case (Figure 1A). The *PAX5-JAK2* and *BCR-JAK2* fusions contained identical exons as reported before [12, 13]. The *TERF2-JAK2* case displayed an in frame fusion of *TERF2* exon 10 to *JAK2* exon 19. All *JAK2* fusion genes harbored an intact JH1 kinase domain (Supplementary Figure 2). Gene expression data revealed high expression levels of *JAK2* in these cases (Supplementary Figure 3). Absence of the cytokine receptor-binding FERM domain in *JAK2* fusion protein suggests that they signal independent of a cytokine receptor.

Clinical characteristics and prognosis of patients harboring JAK2 lesions

Ten out of sixteen (62.5%) *JAK2*-mutated patients remained in continuous complete remission at more than 5 years of follow up. The median time to relapse in the six other patients was 2.1 years [range 0.71-7.8 years]. Minimal residual disease (MRD) data were available for nine out of fourteen patients. The four patients with high MRD levels (≥10-3) at day 29/33 of treatment (time point 1 of COALL and DCOG protocol, respectively) relapsed, whereas the remaining five mutated patients with low MRD levels remained in continuous complete remission (p=0.008, Fisher exact test).

Three out of the five cases harboring *JAK2* fusion genes remained in continuous complete remission at more than 5 years of follow up, whereas two cases suffered from a relapse within 2.4 years of diagnosis (Figure 1A). Both patients who relapsed were assigned to the High Risk arm of the COALL-03 study protocol because of unfavorable age (>10 years) or high white blood cell count at diagnosis (>50 WBC/nl).

Cumulative incidence of relapse in these *JAK2* aberrant patients did not differ from *JAK2* wildtype *BCR-ABL1*-like and B-other cases. Both displayed an unfavorable outcome compared to remaining BCP-ALL cases (p=0.04; Figure 1B). These findings underline the clinical relevance of *JAK2* lesions. Mutations and translocations represent biologically distinct entities, but both may be targetable by JAK-inhibitors.

Leukemic cells with JAK2 lesions can be targeted by JAK inhibitors

Primary leukemic and patient-derived-xenograft (PDX) cells (Supplementary Figure 4, reference 25) were exposed to momelotinib and ruxolitinib. *JAK2* translocated cells were more sensitive to both momelotinib and ruxolitinib compared to *JAK2* wildtype cases ($P<0.05$; Figure 2A-B, Supplementary Figure 5). *JAK2* mutated cells were less sensitive to these inhibitors than *JAK2* fusion positive cells, and were only marginally more sensitive than wildtype cells ($P<0.05$). Leukemic cells without genetic *JAK2* aberrations were resistant to ruxolitinib, but showed some sensitivity to momelotinib. Importantly, normal bone marrow mononuclear cells were resistant to both inhibitors (Supplementary Figure 5). Both JAK inhibitors effectively reduced levels of phosphorylated STAT5 Y694 and/or STAT1 Y701 (Figure 2C-D, Supplementary Figure 6).

The marginal sensitivity for both inhibitors and the low levels of phosphorylated STAT5 in *JAK2* mutated cells may be explained by lack of human TSLP ligand to activate the CRLF2 pathway in our culture conditions. Addition of human TSLP sensitized *JAK2* mutated cells to ruxolitinib, but not to momelotinib ($P<0.01$, Figure 3A-B, Supplementary Figure

7A-B). TSLP exposure did not further sensitize JAK2-fusion positive cells, confirming cytokine-independent signaling (Figure 3C D, Supplementary Figure 7C-D). These results confirm that JAK2 signaling triggered by JAK2 fusion proteins is independent of cytokine receptor activation. JAK2 wildtype leukemic cells were not sensitized to JAK inhibitors by TSLP treatment (Figure 3E-F, Supplementary Figure 7E F). In the presence of TSLP both JAK2 translocated and JAK2 mutated cells were sensitive to JAK inhibitors (Figure 3G-H). At the protein level, TSLP exposure upregulated the levels of phosphorylated STAT1 Y701 and STAT5 Y694 in JAK2 R683S mutated cells, whereas no effect was observed in JAK2 fusion positive and JAK2-wildtype leukemic cells (Figure 3I-K). Notably, TSLP triggered the phosphorylation and hence activation of the MEK/ERK pathway in JAK2 R683S mutated cells, but not in JAK2 R683G mutated cells (Figure 3I, 3L), suggesting that this activation is context-dependent. Phosphorylation of STAT1 Y701 and STAT5 Y694 was inhibited by momelotinib and ruxolitinib (Figure 3L).

JAK2 inhibition results in accumulation of phosphorylated JAK2

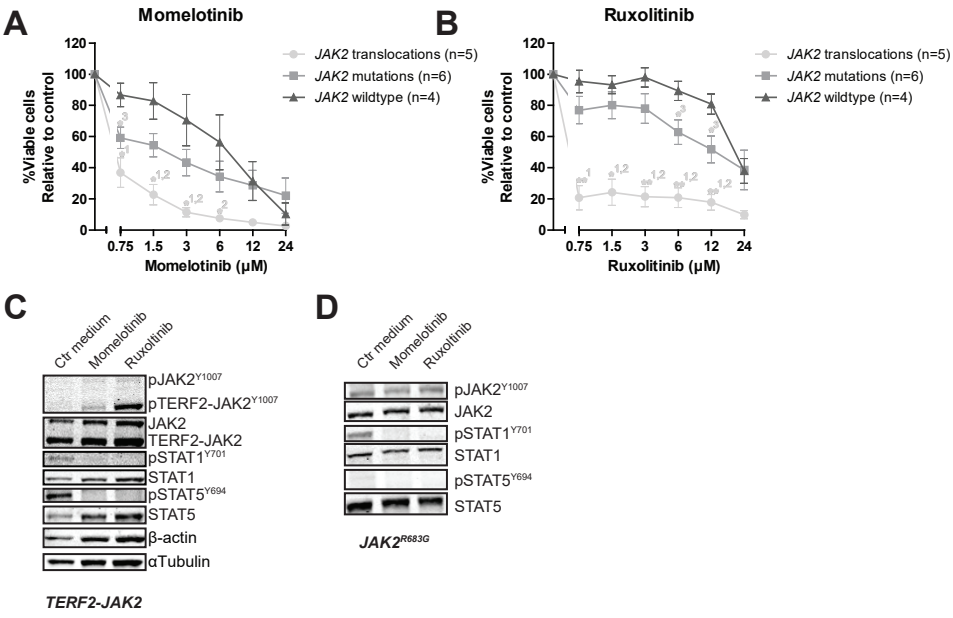

Figure 2: The efficacy of JAK inhibitors on JAK2 translocated and mutated cells

(A-B) Leukemic (PDX or primary patient) cells were incubated for four days with to an increasing concentration range of momelotinib or ruxolitinib, after which cell viability was measured using an MTT assay. Sensitivity of exposed cells was calculated relative to vehicle treated controls. Individual samples were tested in duplicate. Mean±SEM of five *JAK2* translocated cases, six JAK2 mutated cases and four JAK2 wildtype cases is shown. Cell viability of samples was compared using independent sample T-test. **p≤0.01, *p≤0.05, [1]JAK2 translocations versus *JAK2* wildtype, [2] JAK2 translocations versus *JAK2* mutations, [3]*JAK2* mutations versus *JAK2* wildtype. **(C-D)** TERF2-JAK2 and JAK2 R683G PDX cells were exposed for four hours to vehicle control medium, 1.5 μM momelotinib or 0.75 μM ruxolitinib, after which (phosphorylated) TERF2-JAK2, JAK2, STAT1 and STAT5 levels were analysed using western blot (25 μg lysate).

Exposure of primary leukemic cells, harboring TERF2-JAK2 or PAX5-JAK2, to momelotinib and ruxolitinib resulted in accumulation of phosphorylated JAK2 Y1007 fusion proteins (Figure 2C, Supplementary Figure 6). Wash out of both inhibitors induced a slight rebound effect with upregulation of pSTAT1 Y701 and pSTAT5 Y694 in TERF2-JAK2 cells (Figure 4A).

This rebound effect was also observed in the JAK2 V617F -positive leukemic cell line HEL (Supplemental Figure 7). Phosphorylated JAK2 Y1007 accumulated upon exposure to ruxolitinib. Removal of the inhibitor resulted in reactivation of JAK2 signaling, observed by a clear increase in phosphorylated STAT 5Y694 levels within 4 hours (time point 100 hours; Supplementary Figure 7A-B). The inhibitory effect of momelotinib was more transient compared to ruxolitinib, resulting in an earlier reactivation of JAK2, observed by high levels of phosphorylated STAT5 Y694 after 48 hours of momelotinib exposure (Supplemental Figure 7A).

Mesenchymal stromal cells protect against JAK inhibitors

Leukemic cells reside in the bone marrow microenvironment, where they disrupt normal hematopoietic stem cell niches.[26] This abnormal niche protects ALL cells against chemotherapy.[27,28] To study whether the bone marrow microenvironment protects against JAK inhibitors, we mimicked this niche by co-culturing PDX cells with bone marrow mesenchymal stromal cells (MSCs) derived from a leukemia patient. Survival of leukemic cells was improved in co-cultures together with MSCs compared to leukemic cells cultured without MSCs (Figure 5A). In these PDX/MSC co-cultures, JAK inhibitors decreased leukemic cell survival (Supplementary Figure 9A-G). However, leukemic cells were more resistant to ruxolitinib in PDX/MSC co-culture compared to culture without MSCs ($P<0.05$). A similar trend was observed for momelotinib (Figure 5B-C, Supplementary Figure 9H-I).

Different outgrowth pattern in xenografts

The outgrowth patterns of primary leukemic cells (>90% blast purity) in three NSG mice

Figure 3 (opposite page): The effect of TSLP stimulation on the efficacy of JAK inhibitors

Cells (PDX or primary ALL) were pre-incubated for 1 hour with or without 25 ng/ml TSLP, after which cells were exposed for four days to indicated concentrations of momelotinib or ruxolitinib. Cell viability was measured using an MTT assay. Sensitivity was calculated relative to vehicle treated controls. Individual samples were tested in duplicate. **(A-B)** Efficacy of momelotinib and ruxolitinib on *JAK2* mutated cells with or without TSLP pre-incubation. Mean±SEM of six independent samples is shown. **(C-D)** Efficacy of momelotinib and ruxolitinib on cells with *JAK2* translocations. Mean±SEM of two independent samples is shown. **(E-F)** Efficacy of momelotinib and ruxolitinib on *JAK2* wildtype PDX cells. Mean±SEM of three independent samples is shown. **(G-H)** Combined graph of the efficacy of momelotinib (G) and ruxolitinib (H) on TSLP stimulated cells with *JAK2* mutations (n=6), *JAK2* translocations (n=2), or *JAK2* wildtype cells (n=3). Mean±SEM of independent samples is shown. Cell viability of samples was compared using the independent sample T-test. **p≤0.01, *p≤0.05. [1]*JAK2* translocations versus *JAK2* wildtype, [2]*JAK2* wildtype versus *JAK2* mutations. **(I-K)** Western blot of JAK2 R683S, TERF2-JAK2 and JAK2wt PDX cells with or without TSLP stimulation (25 ng/ml for 1 hour). **(L)** JAK2 R683G cells were pre-incubated for 1 hour with or without 25 ng/ml TSLP, after which cells were exposed for four hours to vehicle control medium, 1.5 μM momelotinib or 0.75 μM ruxolitinib. Levels of (phosphorylated) JAK2, STAT1, STAT5, MEK1/2 and ERK1/2 were analysed using western blot.

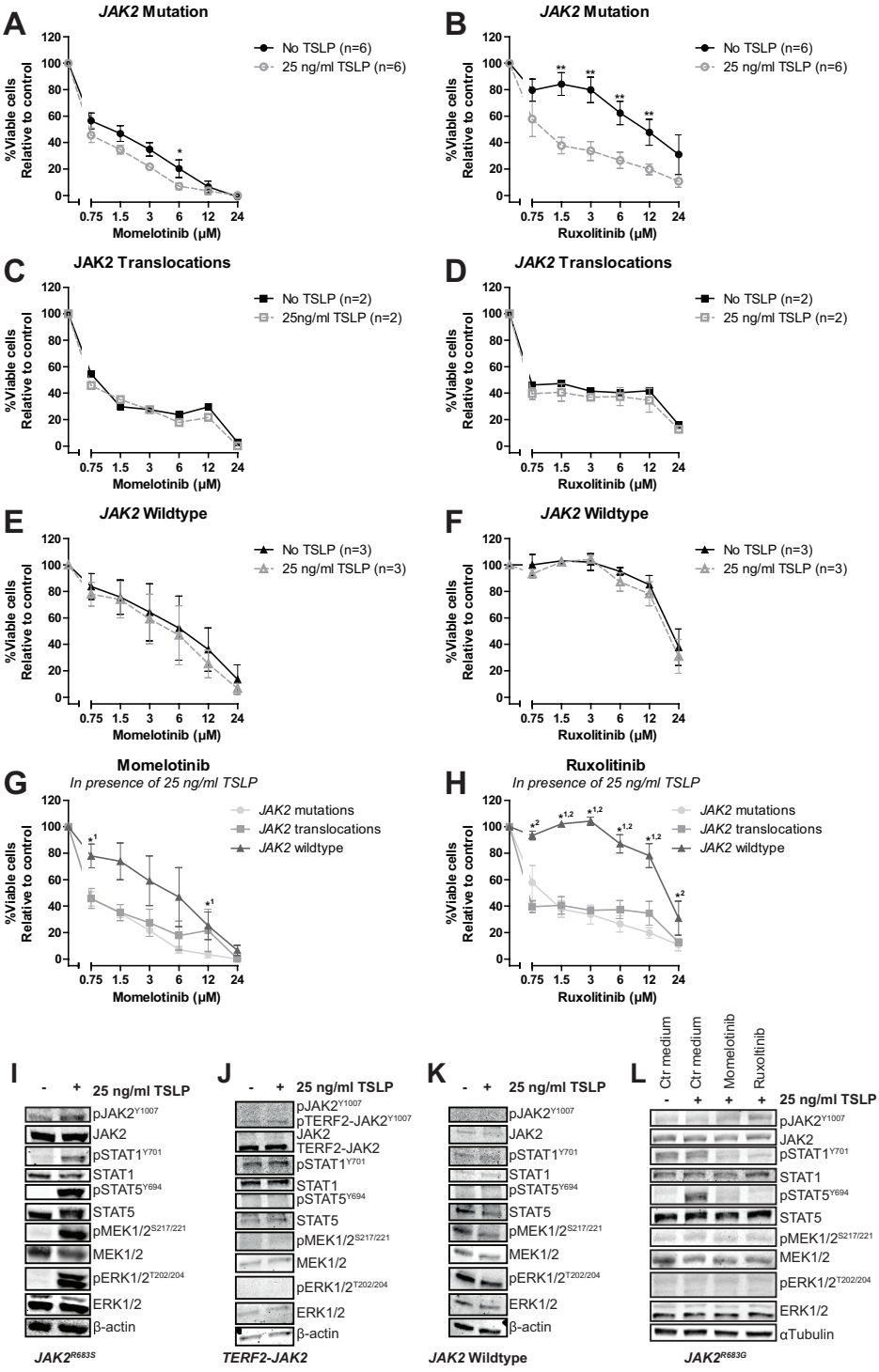
A
JAK2 Mutation
No TSLP (n=6)
25 ng/ml TSLP (n=6)
%Viable cells Relative to control
Momelotinib (μM)
B
JAK2 Mutation
No TSLP (n=6)
25 ng/ml TSLP (n=6)
%Viable cells Relative to control
Ruxolitinib (μM)
C
JAK2 Translocations
No TSLP (n=2)
25ng/ml TSLP (n=2)
%Viable cells Relative to control
Momelotinib (μM)
D
JAK2 Translocations
No TSLP (n=2)
25 ng/ml TSLP (n=2)
%Viable cells Relative to control
Ruxolitinib (μM)
E
JAK2 Wildtype
No TSLP (n=3)
25 ng/ml TSLP (n=3)
%Viable cells Relative to control
Momelotinib (μM)
F
JAK2 Wildtype
No TSLP (n=3)
25 ng/ml TSLP (n=3)
%Viable cells Relative to control
Ruxolitinib (μM)
G
Momelotinib
In presence of 25 ng/ml TSLP
JAK2 mutations
JAK2 translocations
JAK2 wildtype
%Viable cells Relative to control
Momelotinib (μM)
H
Ruxolitinib
In presence of 25 ng/ml TSLP
JAK2 mutations
JAK2 translocations
JAK2 wildtype
%Viable cells Relative to control
Ruxolitinib (μM)
I
- + 25 ng/ml TSLP
pJAK2Y1007
JAK2
pSTAT1Y701
STAT1
pSTAT5Y694
STAT5
pMEK1/2S217/221
MEK1/2
pERK1/2T202/204
ERK1/2
β-actin
JAK2R683S
J
- + 25 ng/ml TSLP
pJAK2Y1007
pTERF2-JAK2Y1007
JAK2
TERF2-JAK2
pSTAT1Y701
STAT1
pSTAT5Y694
STAT5
pMEK1/2S217/221
MEK1/2
pERK1/2T202/204
ERK1/2
β-actin
TERF2-JAK2
K
- + 25 ng/ml TSLP
pJAK2Y1007
JAK2
pSTAT1Y701
STAT1
pSTAT5Y694
STAT5
pMEK1/2S217/221
MEK1/2
pERK1/2T202/204
ERK1/2
β-actin
JAK2 Wildtype
L
Ctr medium
Ctr medium
Momelotinib
Ruxoltinib
- + + + 25 ng/ml TSLP
pJAK2Y1007
JAK2
pSTAT1Y701
STAT1
pSTAT5Y694
STAT5
pMEK1/2S217/221
MEK1/2
pERK1/2T202/204
ERK1/2
αTubulin
JAK2R683G

per patient was determined by paired-end deep-sequencing of *JAK2* hot spot regions (exon 16, 20, 21 and 23; median read depth 554, 465, 411 and 593, respectively). PDX cells originating from a JAK2 R863G mutated case had a different VAF profile compared to the original patient sample (Figure 6A, Supplementary Figure 10A). The primary sample contained a major JAK2 R683G clone at a VAF of 63% and a minor KRAS G12D clone at VAF 14%. In two out of three PDX samples generated, the VAF of the JAK2 R683G mutation increased to 98% (PDX1) and 99% (PDX3), whereas in the remaining PDX sample the VAF decreased to 49% (PDX2). In contrast, the KRAS G12D mutation increased to a VAF 23% in this PDX2 sample, whereas this mutation was not detected in PDX1 and PDX3. The reduced VAF of the JAK2 clone in PDX2 did not result in a decreased efficacy of momelotinib or ruxolitinib (Figure 6B). However, levels of pMEK1/2 S217/221 and pERK1/2 T202/Y204 in this sample were increased compared to the other two PDX samples (Figure 6C). Exposure to both JAK inhibitors did not decrease the levels of phosphorylated MEK and ERK.

Sanger sequencing of JAK2 R683S and JAK2 R683T PDX models also indicated a change in the VAF of PDX cells compared to the primary sample. In PDX cells from three NSG mice injected with JAK2 R683S cells, the A/T peak ratio at nucleotide position 2049 differed, suggesting heterogeneity in frequency of *JAK2* mutations between samples (Supplementary Figure 10B). Strikingly, two mice injected with JAK2 R683T mutated leukemic cells developed JAK2 wildtype leukemia (Supplementary Figure 10C). Although the *JAK2* mutation was lost, *CRLF2* expression levels remained high (Supplementary Figure 10D-E). TSLP stimulation activated the JAK2 pathway signaling (Supplementary Figure 10F), but cells were not sensitive for JAK2 inhibition (Supplementary Figure 10G-H).

Discussion

This study aimed to evaluate the clinical need (frequency of lesions and prognostic value) and potential of JAK inhibitors in pediatric BCP-ALL. For this purpose pediatric BCP-ALL patients were screened for *JAK2* lesions. *JAK2* point mutations were found in 3.6% of our BCP-ALL patients, of which the majority were JAK2 R683 mutations. These mutations were solely detected in *BCR-ABL1*-like, B-other and high hyperdiploid patients, but not in *MLL-AF4*, *BCR-ABL1*, *ETV6-RUNX1* or *TCF3-PBX1* patients. *JAK2* translocations were detected in the poor prognostic *BCR-ABL1*-like group, but not in non-*BCR-ABL1*-like B-other cases. The prognosis of patients with *JAK2* aberrations was as poor as *JAK2* wildtype *BCR-ABL1*-like and non-*BCR-ABL1*-like B-other patients.

JAK2 mutations were not detected as frequently in our DCOG/COALL sequencing cohort as reported for COG high-risk cohorts.[5, 10] Two independent classifiers are used to describe *BCR-ABL1*-like BCP-ALL.[29-31] Differences in genetic ancestry between the American COG and European DCOG/COALL cohorts likely affected the signatures to classify patients as *BCR-ABL1*-like. Hence, genetic differences, or more specifically the lack of Hispanic/Latino cases[10, 32] might explain the lower frequencies of JAK2 mutations, as well as the difference in treatment outcome.

A targeted approach was used to detect *JAK2* translocations. All cases with high *JAK2* expression levels harbored one of the known fusion genes, making it therefore unlikely

that novel fusion genes were missed.

The poor outcome of cases harboring JAK2 lesions underline the clinical relevance of activated JAK2, which can be targeted by precision medicines. The therapeutic potential of JAK2 was demonstrated by the efficacy of JAK inhibitors in JAK2 mutated and JAK2 translocated primary BCP-ALL cells. JAK2 translocated cells were sensitive to both JAK inhibitors, independent of CRLF2 activation.

The strong association between *CRLF2* overexpression and *JAK2* mutations suggests that these genetic lesions cooperate.[3, 6] As *JAK2* aberrations might be targeted with precision medicines, we studied the clinical relevance and the efficacy of JAK inhibitors in these cases. In contrast to *JAK2* translocations, JAK2 R683 mutated leukemic cells only became sensitive to ruxolitinib upon activation of CRLF2 by TSLP, confirming the requirement for type I cytokine receptor activation as reported before.[3, 5, 7, 8, 17] Besides emphasizing differences between the genomic context of *JAK2* translocations and mutations, these

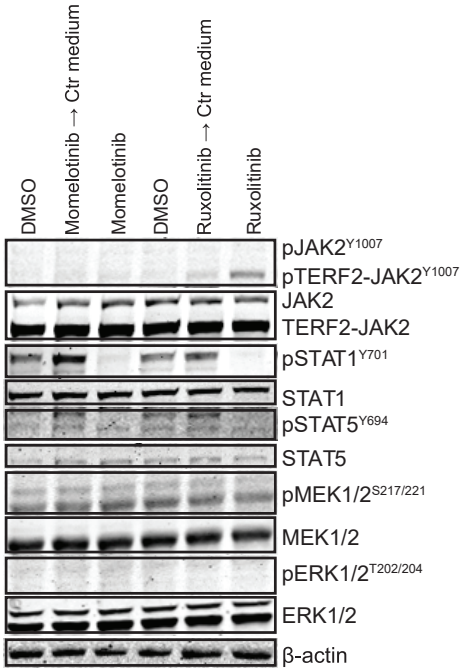

Figure 4: Accumulation of pJAK2 Y1007 results in a rebound effect of JAK2

(A) TERF2-JAK2 PDX cells were incubated for four hours with or without 1.5 μM momelotinib or 0.75 μM ruxolitinib, after which cells were washed to remove the JAK inhibitors. Half of the cells were exposed for another 1.5 hours to 1.5 μM momelotinib or 0.75 μM ruxolitinib, whereas the other cells were incubated in vehicle control (Ctr) medium. Protein expression levels were examined by western blot (25 μg lysate). **(B)** HEL cells were incubated with or without 1.5 μM momelotinib or 0.75 μM ruxolitinib for 4 hours, 24 hours, 48 hours, 72 hours and 96 hours, after which cells were lysed and protein expression levels were examined using western blot (25 μg lysate). **(C)** After 96 hours of exposure to JAK inhibitors (indicated by * in panel B), cells were washed in normal culture medium, to remove momelotinib and ruxolitinib. Subsequently, half of the cells were incubated with 1.5 μM momelotinib or 0.75 μM ruxolitinib for another 4 hours, 24 hours or 48 hours, whereas the remaining cells were incubated in vehicle control (Ctr) medium. Protein expression levels were examined using western blot (25 μg lysate).

results highlight the importance of TSLP in in vitro and in vivo studies involving *JAK2* mutations. Since human CRLF2 cannot be activated by mouse TSLP, conventional mouse xenograft models are not suitable to test the efficacy of ruxolitinib and other JAK inhibitors on *JAK2* mutated cells. Absence of human TSLP in ALL xenograft mouse models might therefore explain the disappointing efficacy of JAK inhibitors in in vivo models.[18-21] The recently engineered xenograft model which synthesizes human TSLP may overcome this limitation.[33]

Despite the need for human TSLP, we and others observed engraftment of primary *JAK2* mutated cells in NSG mice, giving rise to leukemia within months after intra-femoral injection.[18, 19, 21] This implies that the proliferation of *JAK2* mutated leukemic cells in the mouse bone marrow does not (solely) depend on CRLF2 signaling, but may be supported by activation of alternative pathways.[34, 35] This argues against targeted monotherapy, as cells might escape via an alternative pathway, such as the RAS pathway.[35, 36] This is further strengthened by a study in Down syndrome ALL, in which a switch was observed from

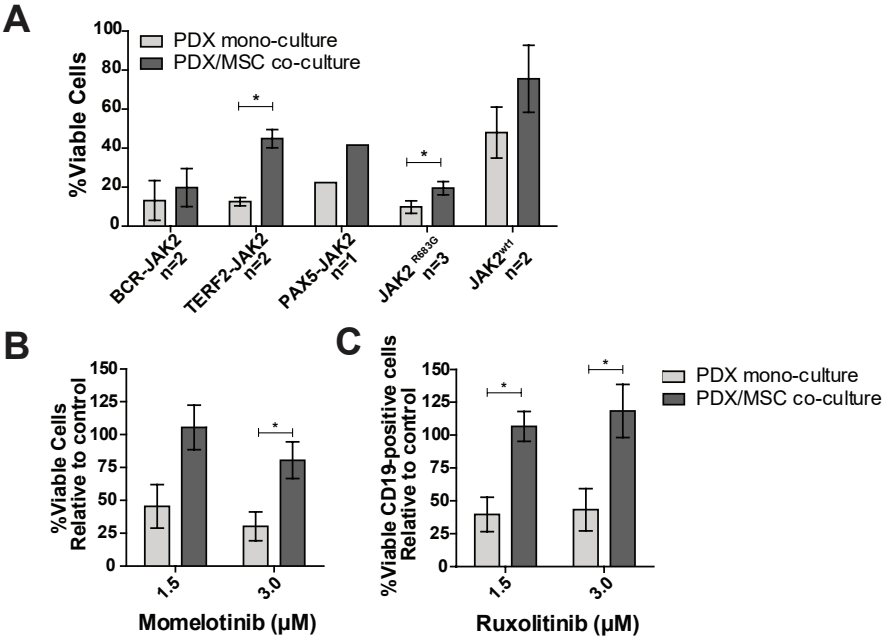

Figure 5: Efficacy of JAK inhibitors in co-culture

The response of CD19+ PDX cells, co-cultured with MSCs (hCD19-), to increasing concentrations of momelotinib and ruxolitinib, was assessed after four days of culture using flow cytometry. Cells were stained with Brilliant Violet 421 anti-human CD19 antibody, FITC Annexin V, and PI. Viability was calculated relative to vehicle controls. **(A)** Survival of PDX cells in mono-culture, or PDX/MSC co-culture. Individual samples were tested in duplicate. Bars represent the mean±SEM of two *BCR-JAK2*, two *TERF2-JAK2*, one *PAX5-JAK2*, three JAK2 R683G and two *JAK2* wildtype samples. Cell viability of samples in mono-culture versus co-culture was compared using the independent sample T-test. *p≤0.05. **(B-C)** The effect of 1.5 μM and 3.0 μM momelotinib or ruxolitinib on the viability of PDX cells with *JAK2* translocations in mono-culture, or in co-culture with primary MSCs. Mean±SEM of three *JAK2* translocated samples is shown. Cell viability of samples was compared using independent sample T-test. *p≤0.05.

a *JAK2* mutation at initial diagnosis to a RAS-mutation at relapse.[37] In the current study, we also observed co-occurrence of *JAK2* and *KRAS* lesions in non-Down syndrome BCP-ALL cells. More importantly, these *JAK2* and *KRAS* mutations showed different outgrowth patterns in NSG xenograft models. Co-occurrence of these mutations suggests that a combination of JAK and RAS pathway inhibitors may be more effective for *JAK2*-aberrant cases. Moreover our results indicate that *JAK2* mutations by itself might not be drivers of leukemic outgrowth, which is also corroborated by the outgrowth of *JAK2* wildtype leukemic cells in mice injected with JAK2 R683T cells. Taken together, these data imply that 1) the expansion properties of *JAK2* mutated leukemic cells vary, 2) other subclones (e.g. KRAS G12D) can grow out at the expense of the major JAK2 mutated

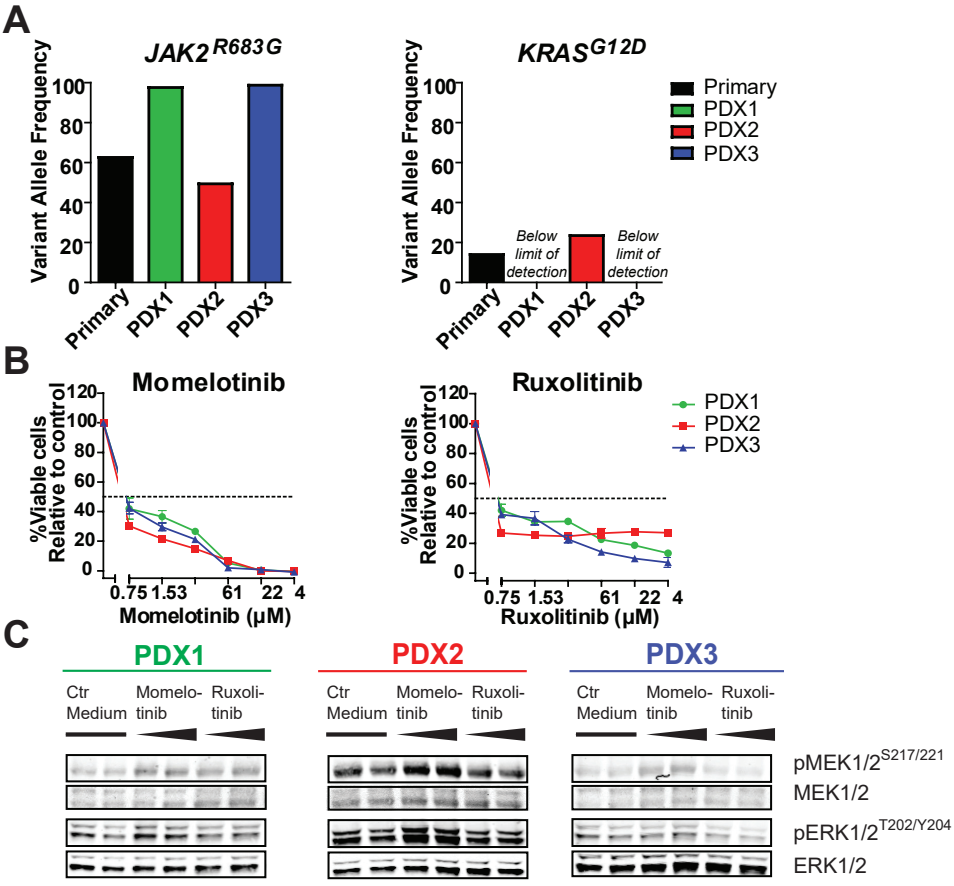

Figure 6: Outgrowth pattern of *JAK2* mutated samples in xenografts

(A) VAF of JAK2 R683G and KRAS G12D in primary leukemic cells and three PDX samples of the same patient was determined using targeted amplicon sequencing. **(B)** PDX cells were pre-incubated for 1 hour with 25 ng/ml TSLP, after which they were exposed for four days to indicated concentrations of momelotinib or ruxolitinib in the presence of TSLP. Cell viability was measured using an MTT assay. Cell survival was calculated relative to vehicle treated controls. Samples were tested in duplicate. Mean±SD of each sample is shown. **(C)** Protein expression levels of PDX samples, exposed to 1.5 μM momelotinib or 0.75 μM ruxolitinib for four hours.

clone, 3) *JAK2* mutations can get lost while leukemia progresses. Therefore, *JAK2* mutations are most likely secondary lesions, in contrast to *JAK2* translocation, which are primary lesions. The selection of alternative pathways indicates a potential risk for use of JAK inhibitors in *JAK2* mutated cases without detailed monitoring of the mutational status of leukemic cells in time.

Interestingly, we observed a difference in the cytotoxicity of momelotinib and ruxolitinib. Both agents fully inhibited JAK/STAT signaling by downregulation of phosphorylation levels of STAT1 and STAT5. However, only momelotinib affected *JAK2* wildtype and non-TSLP stimulated *JAK2* mutated cells, regardless of activation of STAT5. Therefore, it is likely that momelotinib also affects alternative targets.[38, 39] In addition, our data revealed that exposure to JAK inhibitors, especially ruxolitinib, resulted into accumulation of phosphorylated JAK2 Y1007, which consequently induced a profound re-activation of downstream STAT signaling. Accumulation of phosphorylated JAK2 Y1007 is in concordance with other reports.[20, 40-42] The rebound effect observed in the present study identifies an important limitation of these agents. As type I inhibitors bind JAK2 in its active conformation, reactivation of JAK2 may be overcome by type II inhibitors, which bind JAK2 in its inactive conformation.[17, 43] Preclinical in vitro and in vivo data indicate high efficacy of the type II inhibitor CHZ868. Clinical data of this inhibitor and other novel inhibitors are warranted.

Besides studying the mechanism of action, we showed influences of the bone marrow microenvironment on the efficacy of JAK inhibitors. Microenvironment-induced resistance of leukemic cells has been reported for conventional drugs, e.g. prednisolone and asparaginase, for imatinib in *BCR-ABL1*-positive cells, and for JAK inhibitors in the present study.[44-46] These data imply that the local tumor environment can stimulate a survival program, which may provide leukemic cells a way to escape from JAK inhibitors.

Taken together, *JAK2* lesions are infrequently found in children with newly diagnosed BCP-ALL and are mainly restricted to *BCR-ABL1*-like and non-*BCR-ABL1*-like B-other cases (negative for sentinel cytogenetic lesions). Although mutations and translocations represent biologically distinct entities, both may be targetable by JAK-inhibitors, demonstrated the efficacy of momelotinib and ruxolitinib in *JAK2* translocated and *JAK2* mutated primary leukemic cells. As both inhibitors have a short half-life (less than half a day), the observed rebound effect may be therapeutically of risk.[47, 48] Although it should be confirmed by functional in vivo studies, our data suggest that the effect of JAK inhibition may be compromised by microenvironment-induced resistance and induction of alternative survival pathways. In conclusion, JAK inhibitors may be considered to be added to, but not substitute, chemotherapy for patients with *JAK2* aberrations, especially for those at high risk of relapse due to high MRD levels upon induction therapy. Therapeutic monitoring for activation of alternative pathways (e.g. RAS) is highly recommended.

Methods

Primary patient-derived material

Bone marrow and/or peripheral blood samples were obtained from children (1-18

years) with newly diagnosed ALL. Written informed consent was obtained from parents or guardians to use excess diagnostic material for research purposes, as approved by the institutional review board. These studies were conducted in accordance with the Declaration of Helsinki. Mononuclear cells were isolated and processed as described previously.[49] Samples were enriched towards > 90% leukemic cells by depletion of non-leukemic cells using immunomagnetic beads. The major cytogenetic subtypes were determined using fluorescent in situ hybridization, (RT-)PCR, and the 110-probeset gene expression classifier.[30] Patients were treated according to the DCOG ALL8, ALL9 or ALL10 protocol, or the COALL-06-97 and COALL-07-03 study protocols.[50-54] Patient characteristics were provided by the central study centers of DCOG (The Hague, the Netherlands) and COALL (Hamburg, Germany).

Mesenchymal stromal cells (MSCs) were isolated from the bone marrow aspirate of a *BCR-ABL1*-like patient as described previously.[55] Purity of MSCs was assessed by negativity for the hematopoietic markers CD34, CD45, and CD19, and positivity for the mesenchymal markers CD13, CD29, CD44, CD54, CD73, CD90, CD105, CD146 and CD166, as detected by flow cytometry (MACS Quant). Expression was measured using the human mesenchymal stem cell marker antibody panel (R&D Systems, Minneapolis, Minnesota, USA), and CD13-APC, CD29-APC, CD34-PE, CD54-PE, CD73-PE, IgG1-PE, and IgG1-APC (BD Biosciences, San Jose, California, USA).

Cell lines

The human erythroleukemia cell line HEL was obtained from the German Collection of Microorganisms and Cell lines (DSMZ, Braunschweig, Germany) and cultured in RPMI-1640 medium, supplemented with 10% fetal calf serum (Bodinco BV, Alkmaar, Netherlands), 100 units/ml penicillin, 100 µg/ml streptomycin and 0.125 µg/mL fungizone (Life Technologies, Bleiswijk, Netherlands). The identity of the cell line was routinely verified by DNA fingerprinting. Additionally, presence of Mycoplasma was excluded every 25 passages by PCR.

Patient-derived-xenograft cells

Primary leukemic cells were transplanted by intra-femoral injection in 7-12 weeks old female NOD.Cg-*Prkdc*^{scid}*Il2rg*^{tm1Wjl}/SzJ (NSG) mice (Charles River, Wilmington, Massachusetts, USA; three NSG mice per patient), as approved by the animal ethics committee (EMC 2863). Mice were sacrificed upon overt leukemia or 6 months after injection. Leukemic cells were isolated from bone marrow and spleen. The percentage of human leukemic cells was analyzed by flow cytometry (APC anti-human CD19, PE anti-human CD45 and FITC anti-mouse CD45; Biolegend, London, UK) and May-Grünwald-Giemsa staining. Patient-derived-xenograft cells (PDX) were enriched for > 90% human leukemic cells using anti-human-CD19 immunomagnetic beads (MACS Miltenyi, Leiden, Netherlands).

JAK2 mutations

JAK2 mutations status was analyzed in 461 BCP-ALL cases, representing the major cytogenetic subtypes (6% *BCR-ABL1*, 17% *BCR-ABL1*-like, 15% non-*BCR-ABL1*-like B-other, 27% *ETV6-RUNX1*, 27% high hyperdiploid, 3% *MLL-AF4*, 6% *TCF3-PBX1*). Genomic DNA was isolated using Trizol reagent (Life Technologies), or in some cases

using the DNeasy blood and tissue kit (Qiagen) according to manufacturer's instructions, and quantified using the Qubit dsDNA Broad Range Assay Kit (Life Technologies). 100-250ng genomic DNA was used to prepare sequencing libraries according to manufacturer's instructions. Successful library preparation, correct amplicon length and concentration were assessed using the Labchip GX genomic analyzer (Caliper Life Sciences Benelux N.V.) with the HT DNA 12K Reagent Kit, Version 2. Samples were pooled equi-molarly and sequenced on an Illumina MiSeq in paired-end reads of 250bp each. The custom amplicons covered the exons 16, 20, 21 and 23 and represent the mutational hotspot region of JAK2.

Sequence reads were exported in fastq format and, aligned to the standard 1000 genomes human reference sequences (version b37, from the GATK resource bundle provided by the Broad institute, USA), using BWA version 0.7.10 and the GATK indel realigner version 3.3-0. Freebayes version 0.9.18-24, Varscan version 2.3.7, Bcftools version 1.0, and GATK version 3.3-0 were used to call single nucleotide variants. The resulting variant call format files were annotated using snpEff and snpSift version 4.1a and the dbNSFP version 2.7 database. Variants were combined and filtered based on several criteria using an in-house developed pipeline: variants were excluded if they were not located in targeted regions, were reported by only one caller, had coverage of < 100 reads, or had < 10 reads supporting the variant allele. Furthermore, variants had to occur at least once with a VAF above 2% in any sample and to be distributed equally between runs according to a chi-square test. Additionally only variants were taken into account if they were reported in the COSMIC V73 GRCh37 database, lead to an amino acid change, were unlikely to be a germline variant and not a known SNP. SNPs were defined as having a mean population frequency of ≥ 5% across the 1000Gp1 complete human population, 1000Gp1 population of European decent, and the ESP-6500 population of European decent allele frequency databases. Variants found in ≥ 10 samples with a mean and median VAF > 40% were labelled as possible germline. Sufficient coverage was crucial to detect subclonal mutations, which could be reliably detected ≥ 5% VAF in on average 91% of the cases. Detection of variants with a frequency of 1% was limited to a smaller group (26%), and is therefore a conservative estimate in the present study.

Genomic DNA of PDX cells was used to identify JAK2 mutations in exon 16. Samples were analyzed by Baseclear B.V. using Sanger sequencing (forward primer 5'-ATGCCTCCAAATTATTATACTATCA-3', reverse primer 5'-ATCACCTCACAGTCCATGGTTAT-3').

JAK2 translocations

Presence of ten recurrently reported *JAK2* translocations was examined by RT-PCR in 153 BCP-ALL cases, negative for sentinel BCP-ALL associated lesions (n=77 *BCR-ABL1*-like, n=76 non-*BCR-ABL1*-like B-other). Total RNA was extracted from leukemic cells using Trizol reagents (Life Technologies). cDNA was synthesized using random hexamers and oligodT primers, and M-MLV reverse transcriptase (Promega, Leiden, Netherlands). RT-PCR was performed in a final volume of 25 µl, containing 0.3 µM forward primer, 0.3 µM reverse primer, 200 µM dNTPs, 1x PCR buffer II, 4 mM MgCl2, 0.125 µl AmpliTaq DNA polymerase (Promega) and 2.5 µl cDNA. Primer sequences are shown in Supplementary Table 1. PCR products were Sanger sequenced by Baseclear B.V. (Leiden, Netherlands).

CRLF2 status

As *P2RY8-CRLF2* and *IGH-CRLF2* are linked to high *CRLF2* mRNA expression levels in different studies.[10, 56-58] CRLF2 status was determined by Affymetrix gene expression microarrays (U133 Plus 2.0; Santa Clara, California, USA), of a previously published cohort of pediatric BCP-ALL patients at initial diagnosis.[56] Of 406 cases, both CRLF2 gene expression data and JAK2 mutation status was available. Signal intensity of probeset 208303_s_at above the 90th percentile levels was classified as CRLF2 high, as described previously.[56]

In addition, CRLF2 expression in primary leukemic and PDX samples was determined using RT-qPCR and SYBR green. CRLF2 expression (forward primer 5'-ACGGGGATCTCCTCTATG-3', reverse primer: 5'-GAGGCGTTGG TGTCTCT-3') was calculated relative to RSP20 expression (forward primer 5'-AAGGGCTGAGGATTTT TG-3', reverse primer 5'-CGTTGCGGCTTGTTAG-3'), using the comparative cycle time (C_t) method; 2 ΔC_t x 100%, whereby $\Delta C_t = C_t$CRLF2 – C_tRPS20. RT-qPCR expression values were correlated to Affymetrix microarray data of probeset 208303_s_at.

JAK2 expression levels

JAK2 expression levels were analyzed using Affymetrix gene expression microarrays, in a previously published pediatric BCP-ALL cohort.[56] Signal intensity of probeset 205841_at was used to quantify JAK2 gene expression.

Ex vivo drug cytotoxicity assays

Cell-intrinsic resistance towards momelotinib and ruxolitinib (Selleck Chemicals, Kirby Drive, Houston, USA) was evaluated as described previously.[49] Briefly, leukemic cells were exposed to a concentration range (24μM to 750nM) of these compounds for four days and cytotoxicity was quantified using 3-(4,5-dimethylthiazol-2-yl)-2,5-diphenyltetrazolium bromide (MTT). For TSLP stimulation, cells were pre-incubated for 1 hour with 25 ng/ml TSLP (R&D systems, Oxon, UK). In addition to single cell cultures, leukemic cells (1×10^6 cells) were co-cultured with primary MSCs (5×10^4 cells) for four days in a 24 well plate in the presence of a dilution series of momelotinib and ruxolitinib. Cell survival was quantified using flow cytometry (MACSQuant, FlowJo 10.0.8r1), and cells were stained with Brilliant Violet 421 anti-human CD19 antibody (Biolegend), FITC Annexin V (Biolegend), and Propidium Iodide (PI; Invitrogen, Bleiswijk, Netherlands), as described previously.[44]

Western blotting

Leukemic cells were lysed in lysis buffer supplemented with freshly added protease and phosphatase inhibitors. 25μg (BCA method; Thermo Scientific) lysate was loaded on 10% mini protean precast gels (BioRad, Veenendaal, Netherlands), and transferred to a nitrocellulose membrane (Biorad). Primary antibody incubation was performed according to manufacturer's protocol. Anti-JAK2 (#3230), anti-phospho-JAK2-Y1007 (#4406), anti-phospho-STAT5-Tyr694 (#9351), anti-phospho-STAT1-Tyr701 (#9167), anti-Stat1 (#9175), anti-phospho-MEK1/2-Ser217/221 (#9154), anti-MEK1/2 (#4694), anti-phospho-Erk1/2-T202/Y204 (#4370), anti-Erk1/2 (#91078), and anti-αTubulin (#2144) were obtained from Cell Signaling Technology (Danvers, Massachusetts, USA).

Anti-β-actin (ab6276) was obtained from Abcam (Cambridge, UK), and anti-STAT5 (sc-835) from Santa Cruz (Heidelberg, Germany). Blots were stained with secondary antibodies (IRDye 680RD- or 800CW-labelled anti-rabbit and IRDye 680RD- or 800CW-labelled anti-mouse; Li-Cor Biosciences, Leusden, Netherlands) and scanned using the Odyssey infrared imaging system (Li-Cor Biosciences). To reprobe membranes, they were stripped in NewBlot Nitrocellulose stripping buffer (Li-Cor Biosciences) according to manufacturer's protocol. BCR-JAK2, PAX5-JAK2 and TERF2-JAK2 proteins were separated from wildtype JAK2 based on size (~94, 57, 95 and 125 kDa, respectively).

Statistics

Cumulative incidence of relapse (CIR) was estimated using a competing risk model. Relapse and non-response (counted at day 79) were considered as event, and death as competing event. The Gray's test was applied to test for equality of CIRs.[59] Outcome analyses were performed in R 3.0.1, using the packages cmprsk version 2.2-7[60], mstate version 0.2.7[61], and survival version 2.37-4[62].

Acknowledgements

We thank Ies Nijman, Annelies Smouters and Edwin Cuppen (University Medical Centre Utrecht) for their help in setting up the sequencing experiments and analysis pipeline.

This work was supported by the VICI program grant 016.126.612 from Netherlands Organization for Scientific Research (NWO), the Dutch Cancer Society grants AMC 2008-4265 and EMCR 2014-6998, the Kika Foundation (grant 132 and 161), the Pediatric Oncology Foundation Rotterdam (KOCR), and by the Centre for Personalized Cancer Treatment, which is a collaboration between all University Medical Cancer Centres and the Netherlands Cancer Institute Amsterdam and is supported by grants from KWF/Alpe d'Huzes and Nuts/Ohra.

Authorship Contributions

EMPS and ISJ designed and performed experiments, and analyzed and interpreted data. MJK designed deep sequencing primers. ISJ and NJMB performed deep sequencing. ISJ, AQH and JMB analyzed and interpreted deep sequence data. EMPS and WGN performed *ex vivo* experiments and analyzed data. EMPS, AB and CvdV collected PDX samples. EMPS and AB performed PCR reactions for Sanger sequencing analyses. RP, HAdGK, CMZ and MH provided clinical characteristics and clinical outcome data, and interpreted data. MLdB designed the study and interpreted data. EMPS, ISJ and MLdB drafted the manuscript. The manuscript was revised and approved by all authors.

Disclosure of Conflicts of Interest

The authors declare no conflicts of interest.

Literature

1. Smith CA and Fan G. The saga of JAK2 mutations and translocations in hematologic disorders: pathogenesis, diagnostic and therapeutic prospects, and revised World Health Organization diagnostic criteria for myeloproliferative neoplasms. Hum Pathol. 2008; 39(6):795-810.

2. Saharinen P and Silvennoinen O. The pseudokinase domain is required for suppression of basal activity of Jak2 and Jak3 tyrosine kinases and for cytokine-inducible activation of signal transduction. J Biol Chem. 2002; 277(49):47954-47963.

3. Bercovich D, Ganmore I, Scott LM, Wainreb G, Birger Y, Elimelech A, Shochat C, Cazzaniga G, Biondi A, Basso G, Cario G, Schrappe M, Stanulla M, Strehl S, Haas OA, Mann G, et al. Mutations of JAK2 in acute lymphoblastic leukaemias associated with Down's syndrome. Lancet. 2008; 372(9648):1484-1492.

4. Russell LJ, Capasso M, Vater I, Akasaka T, Bernard OA, Calasanz MJ, Chandrasekaran T, Chapiro E, Gesk S, Griffiths M, Guttery DS, Haferlach C, Harder L, Heidenreich O, Irving J, Kearney L, et al. Deregulated expression of cytokine receptor gene, CRLF2, is involved in lymphoid transformation in B-cell precursor acute lymphoblastic leukemia. Blood. 2009; 114(13):2688-2698.

5. Mullighan CG, Zhang J, Harvey RC, Collins-Underwood JR, Schulman BA, Phillips LA, Tasian SK, Loh ML, Su X, Liu W, Devidas M, Atlas SR, Chen IM, Clifford RJ, Gerhard DS, Carroll WL, et al. JAK mutations in high-risk childhood acute lymphoblastic leukemia. Proc Natl Acad Sci U S A. 2009; 106(23):9414-9418.

6. Mullighan CG, Collins-Underwood JR, Phillips LA, Loudin MG, Liu W, Zhang J, Ma J, Coustan-Smith E, Harvey RC, Willman CL, Mikhail FM, Meyer J, Carroll AJ, Williams RT, Cheng J, Heerema NA, et al. Rearrangement of CRLF2 in B-progenitor- and Down syndrome-associated acute lymphoblastic leukemia. Nat Genet. 2009; 41(11):1243-1246.

7. Kearney L, Gonzalez De Castro D, Yeung J, Procter J, Horsley SW, Eguchi-Ishimae M, Bateman CM, Anderson K, Chaplin T, Young BD, Harrison CJ, Kempski H, So CW, Ford AM and Greaves M. Specific JAK2 mutation (JAK2R683) and multiple gene deletions in Down syndrome acute lymphoblastic leukemia. Blood. 2009; 113(3):646-648.

8. Yoda A, Yoda Y, Chiaretti S, Bar-Natan M, Mani K, Rodig SJ, West N, Xiao Y, Brown JR, Mitsiades C, Sattler M, Kutok JL, DeAngelo DJ, Wadleigh M, Piciocchi A, Dal Cin P, et al. Functional screening identifies CRLF2 in precursor B-cell acute lymphoblastic leukemia. Proc Natl Acad Sci U S A. 2010; 107(1):252-257.

9. Hertzberg L, Vendramini E, Ganmore I, Cazzaniga G, Schmitz M, Chalker J, Shiloh R, Iacobucci I, Shochat C, Zeligson S, Cario G, Stanulla M, Strehl S, Russell LJ, Harrison CJ, Bornhauser B, et al. Down syndrome acute lymphoblastic leukemia, a highly heterogeneous disease in which aberrant expression of CRLF2 is associated with mutated JAK2: a report from the International BFM Study Group. Blood. 2010; 115(5):1006-1017.

10. Harvey RC, Mullighan CG, Chen IM, Wharton W, Mikhail FM, Carroll AJ, Kang H, Liu W, Dobbin KK, Smith MA, Carroll WL, Devidas M, Bowman WP, Camitta BM, Reaman GH, Hunger SP, et al. Rearrangement of CRLF2 is associated with mutation of JAK kinases, alteration of IKZF1, Hispanic/Latino ethnicity, and a poor outcome in pediatric B-progenitor acute lymphoblastic leukemia. Blood. 2010; 115(26):5312-5321.

11. Tirado CA, Chen W, Huang LJ, Laborde C, Hiemenz MC, Valdez F, Ho K, Winick N, Lou Z and Koduru P. Novel JAK2 rearrangement resulting from a t(9;22)(p24;q11.2) in B-acute lymphoblastic leukemia. Leuk Res. 2010; 34(12):1674-1676.

12. Roberts KG, Li Y, Payne-Turner D, Harvey RC, Yang YL, Pei D, McCastlain K, Ding L, Lu C, Song G, Ma J, Becksfort J, Rusch M, Chen SC, Easton J, Cheng J, et al. Targetable kinase-activating lesions in Ph-like acute lymphoblastic leukemia. N Engl J Med. 2014; 371(11):1005-1015.

13. Roberts KG, Morin RD, Zhang J, Hirst M, Zhao Y, Su X, Chen SC, Payne-Turner D, Churchman ML, Harvey RC, Chen X, Kasap C, Yan C, Becksfort J, Finney RP, Teachey DT, et al. Genetic alterations activating kinase and cytokine receptor signaling in high-risk acute lymphoblastic leukemia. Cancer Cell. 2012; 22(2):153-166.

14. Cuesta-Dominguez A, Ortega M, Ormazabal C, Santos-Roncero M, Galan-Diez M, Steegmann JL, Figuera A, Arranz E, Vizmanos JL, Bueren JA, Rio P and Fernandez-Ruiz E. Transforming and tumorigenic activity of JAK2 by fusion to BCR: molecular mechanisms of action of a novel BCR-JAK2 tyrosine-kinase. PLoS One. 2012; 7(2):e32451.

15. Boer JM, Steeghs EM, Marchante JR, Boeree A, Beaudoin JJ, Beverloo HB, Kuiper RP, Escherich G, van der Velden VH, van der Schoot CE, de Groot-Kruseman HA, Pieters R and den Boer ML. Tyrosine kinase fusion genes in pediatric BCR-ABL1-like acute lymphoblastic leukemia. Oncotarget. 2017; 8(3):4618-4628.

16. Schinnerl D, Fortschegger K, Kauer M, Marchante JR, Kofler R, Den Boer ML and Strehl S. The role of the Janus-faced transcription factor PAX5-JAK2 in acute lymphoblastic leukemia. Blood. 2015; 125(8):1282-1291.

17. Wu SC, Li LS, Kopp N, Montero J, Chapuy B, Yoda A, Christie AL, Liu H, Christodoulou A, van Bodegom D, van der Zwet J, Layer JV, Tivey T, Lane AA, Ryan JA, Ng SY, et al. Activity of the Type II JAK2 Inhibitor CHZ868 in B Cell Acute Lymphoblastic Leukemia. Cancer Cell. 2015; 28(1):29-41.

18. Suryani S, Bracken LS, Harvey RC, Sia KC, Carol H, Chen IM, Evans K, Dietrich PA, Roberts KG, Kurmasheva RT, Billups CA, Mullighan CG, Willman CL, Loh ML, Hunger SP, Houghton PJ, et al. Evaluation of the in vitro and in vivo efficacy of the JAK inhibitor AZD1480 against JAK-mutated acute lymphoblastic leukemia. Mol Cancer Ther. 2015; 14(2):364-374.

19. Maude SL, Tasian SK, Vincent T, Hall JW, Sheen C, Roberts KG, Seif AE, Barrett DM, Chen IM, Collins JR, Mullighan CG, Hunger SP, Harvey RC, Willman CL, Fridman JS, Loh ML, et al. Targeting JAK1/2 and mTOR in murine xenograft models of Ph-like acute lymphoblastic leukemia. Blood. 2012; 120(17):3510-3518.

20. Weigert O, Lane AA, Bird L, Kopp N, Chapuy B,

van Bodegom D, Toms AV, Marubayashi S, Christie AL, McKeown M, Paranal RM, Bradner JE, Yoda A, Gaul C, Vangrevelinghe E, Romanet V, et al. Genetic resistance to JAK2 enzymatic inhibitors is overcome by HSP90 inhibition. J Exp Med. 2012; 209(2):259-273.

21. Tasian SK, Teachey DT, Li Y, Shen F, Harvey RC, Chen IM, Ryan T, Vincent TL, Willman CL, Perl AE, Hunger SP, Loh ML, Carroll M and Grupp SA. Potent efficacy of combined PI3K/mTOR and JAK or ABL inhibition in murine xenograft models of Ph-like acute lymphoblastic leukemia. Blood. 2017; 129(2):177-187.

22. Loh ML, Tasian SK, Rabin KR, Brown P, Magoon D, Reid JM, Chen X, Ahern CH, Weigel BJ and Blaney SM. A phase 1 dosing study of ruxolitinib in children with relapsed or refractory solid tumors, leukemias, or myeloproliferative neoplasms: A Children's Oncology Group phase 1 consortium study (ADVL1011). Pediatr Blood Cancer. 2015; 62(10):1717-1724.

23. Li F, Guo HY, Wang M, Geng HL, Bian MR, Cao J, Chen C, Zeng LY, Wang XY and Wu QY. The effects of R683S (G) genetic mutations on the JAK2 activity, structure and stability. Int J Biol Macromol. 2013; 60:186-195.

24. Imamura T, Kiyokawa N, Kato M, Imai C, Okamoto Y, Yano M, Ohki K, Yamashita Y, Kodama Y, Saito A, Mori M, Ishimaru S, Deguchi T, Hashii Y, Shimomura Y, Hori T, et al. Characterization of pediatric Philadelphia-negative B-cell precursor acute lymphoblastic leukemia with kinase fusions in Japan. Blood Cancer J. 2016; 6:e419.

25. Schmitz M, Breithaupt P, Scheidegger N, Cario G, Bonapace L, Meissner B, Mirkowska P, Tchinda J, Niggli FK, Stanulla M, Schrappe M, Schrauder A, Bornhauser BC and Bourquin JP. Xenografts of highly resistant leukemia recapitulate the clonal composition of the leukemogenic compartment. Blood. 2011; 118(7):1854-1864.

26. Colmone A, Amorim M, Pontier AL, Wang S, Jablonski E and Sipkins DA. Leukemic cells create bone marrow niches that disrupt the behavior of normal hematopoietic progenitor cells. Science. 2008; 322(5909):1861-1865.

27. McMillin DW, Delmore J, Weisberg E, Negri JM, Geer DC, Klippel S, Mitsiades N, Schlossman RL, Munshi NC, Kung AL, Griffin JD, Richardson PG, Anderson KC and Mitsiades CS. Tumor cell-specific bioluminescence platform to identify stroma-induced changes to anticancer drug activity. Nat Med. 2010; 16(4):483-489.

28. Lane SW, Scadden DT and Gilliland DG. The leukemic stem cell niche: current concepts and therapeutic opportunities. Blood. 2009; 114(6):1150-1157.

29. Boer JM, Marchante JR, Evans WE, Horstmann MA, Escherich G, Pieters R and Den Boer ML. BCR-ABL1-like cases in pediatric acute lymphoblastic leukemia: a comparison between DCOG/Erasmus MC and COG/St. Jude signatures. Haematologica. 2015; 100(9):e354-357.

30. Den Boer ML, van Slegtenhorst M, De Menezes RX, Cheok MH, Buijs-Gladdines JG, Peters ST, Van Zutven LJ, Beverloo HB, Van der Spek PJ, Escherich G, Horstmann MA, Janka-Schaub GE, Kamps WA, Evans WE and Pieters R. A subtype of childhood acute lymphoblastic leukaemia with poor treatment outcome: a genome-wide classification study. Lancet Oncol. 2009; 10(2):125-134.

31. Mullighan CG, Su X, Zhang J, Radtke I, Phillips LA, Miller CB, Ma J, Liu W, Cheng C, Schulman BA, Harvey RC, Chen IM, Clifford RJ, Carroll WL, Reaman G, Bowman WP, et al. Deletion of IKZF1 and prognosis in acute lymphoblastic leukemia. N Engl J Med. 2009; 360(5):470-480.

32. Hicks C, Miele L, Koganti T, Young-Gaylor L, Rogers D, Vijayakumar V and Megason G. Analysis of Patterns of Gene Expression Variation within and between Ethnic Populations in Pediatric B-ALL. Cancer informatics. 2013; 12:155-173.

33. Francis OL, Milford TA, Martinez SR, Baez I, Coats JS, Mayagoitia K, Concepcion KR, Ginelli E, Beldiman C, Benitez A, Weldon AJ, Arogyaswamy K, Shiraz P, Fisher R, Morris CL, Zhang XB, et al. A novel xenograft model to study the role of TSLP-induced CRLF2 signals in normal and malignant human B lymphopoiesis. Haematologica. 2016; 101(4):417-426.

34. Ma X, Edmonson M, Yergeau D, Muzny DM, Hampton OA, Rusch M, Song G, Easton J, Harvey RC, Wheeler DA, Ma J, Doddapaneni H, Vadodaria B, Wu G, Nagahawatte P, Carroll WL, et al. Rise and fall of subclones from diagnosis to relapse in pediatric B-acute lymphoblastic leukaemia. Nat Commun. 2015; 6:6604.

35. Vesely C, Frech C, Eckert C, Cario G, Mecklenbrauker A, Zur Stadt U, Nebral K, Kraler F, Fischer S, Attarbaschi A, Schuster M, Bock C, Cave H, von Stackelberg A, Schrappe M, Horstmann MA, et al. Genomic and transcriptional landscape of P2RY8-CRLF2-positive childhood acute lymphoblastic leukemia. Leukemia. 2017.

36. Winter PS, Sarosiek KA, Lin KH, Meggendorfer M, Schnittger S, Letai A and Wood KC. RAS signaling promotes resistance to JAK inhibitors by suppressing BAD-mediated apoptosis. Science signaling. 2014; 7(357):ra122.

37. Nikolaev SI, Garieri M, Santoni F, Falconnet E, Ribaux P, Guipponi M, Murray A, Groet J, Giarin E, Basso G, Nizetic D and Antonarakis SE. Frequent cases of RAS-mutated Down syndrome acute lymphoblastic leukaemia lack JAK2 mutations. Nat Commun. 2014; 5:4654.

38. Zhu Z, Aref AR, Cohoon TJ, Barbie TU, Imamura Y, Yang S, Moody SE, Shen RR, Schinzel AC, Thai TC, Reibel JB, Tamayo P, Godfrey JT, Qian ZR, Page AN, Maciag K, et al. Inhibition of KRAS-driven tumorigenicity by interruption of an autocrine cytokine circuit. Cancer discovery. 2014; 4(4):452-465.

39. Asshoff M, Petzer V, Warr MR, Haschka D, Tymoszuk P, Demetz E, Seifert M, Posch W, Nairz M, Maciejewski P, Fowles P, Burns CJ, Smith G, Wagner KU, Weiss G, Whitney JA, et al. Momelotinib inhibits ACVR1/ALK2, decreases hepcidin production, and ameliorates anemia of chronic disease in rodents. Blood. 2017; 129(13):1823-1830.

40. Haan S, Wuller S, Kaczor J, Rolvering C, Nocker T, Behrmann I and Haan C. SOCS-mediated downregulation of mutant Jak2 (V617F, T875N and K539L) counteracts cytokine-independent signaling. Oncogene. 2009; 28(34):3069-3080.

41. Hart S, Goh KC, Novotny-Diermayr V, Hu CY, Hentze H, Tan YC, Madan B, Amalini C, Loh YK, Ong LC, William AD, Lee A, Poulsen A, Jayaraman R, Ong KH, Ethirajulu K, et al. SB1518, a novel macrocyclic pyrimidine-based JAK2 inhibitor for the treatment of myeloid and lymphoid malignancies. Leukemia. 2011; 25(11):1751-1759.

42. Grandage VL, Everington T, Linch DC and Khwaja A. Go6976 is a potent inhibitor of the JAK 2 and FLT3 tyrosine kinases with significant activity in primary acute myeloid leukaemia cells. Br J Haematol. 2006; 135(3):303-316.

43. Meyer SC and Levine RL. Molecular pathways: molecular basis for sensitivity and resistance to JAK kinase inhibitors. Clin Cancer Res. 2014; 20(8):2051-2059.

44. Polak R, de Rooij B, Pieters R and den Boer ML. B-cell precursor acute lymphoblastic leukemia cells use tunneling nanotubes to orchestrate their microenvironment. Blood. 2015; 126(21):2404-2414.

45. Iwamoto S, Mihara K, Downing JR, Pui CH and Campana D. Mesenchymal cells regulate the response of acute lymphoblastic leukemia cells to asparaginase. J Clin Invest. 2007; 117(4):1049-1057.

46. Vianello F, Villanova F, Tisato V, Lymperi S, Ho KK, Gomes AR, Marin D, Bonnet D, Apperley J, Lam EW and Dazzi F. Bone marrow mesenchymal stromal cells non-selectively protect chronic myeloid leukemia cells from imatinib-induced apoptosis via the CXCR4/CXCL12 axis. Haematologica. 2010; 95(7):1081-1089.

47. Shilling AD, Nedza FM, Emm T, Diamond S, McKeever E, Punwani N, Williams W, Arvanitis A, Galya LG, Li M, Shepard S, Rodgers J, Yue TY and Yeleswaram S. Metabolism, excretion, and pharmacokinetics of [14C]INCB018424, a selective Janus tyrosine kinase 1/2 inhibitor, in humans. Drug Metab Dispos. 2010; 38(11):2023-2031.

48. Tyner JW, Bumm TG, Deininger J, Wood L, Aichberger KJ, Loriaux MM, Druker BJ, Burns CJ, Fantino E and Deininger MW. CYT387, a novel JAK2 inhibitor, induces hematologic responses and normalizes inflammatory cytokines in murine myeloproliferative neoplasms. Blood. 2010; 115(25):5232-5240.

49. Den Boer ML, Harms DO, Pieters R, Kazemier KM, Gobel U, Korholz D, Graubner U, Haas RJ, Jorch N, Spaar HJ, Kaspers GJ, Kamps WA, Van der Does-Van den Berg A, Van Wering ER, Veerman AJ and Janka-Schaub GE. Patient stratification based on prednisolone-vincristine-asparaginase resistance profiles in children with acute lymphoblastic leukemia. J Clin Oncol. 2003; 21(17):3262-3268.

50. Escherich G, Zimmermann M, Janka-Schaub G and CoALL study group. Doxorubicin or daunorubicin given upfront in a therapeutic window are equally effective in children with newly diagnosed acute lymphoblastic leukemia. A randomized comparison in trial CoALL 07-03. Pediatr Blood Cancer. 2013; 60(2):254-257.

51. Veerman AJ, Kamps WA, van den Berg H, van den Berg E, Bokkerink JP, Bruin MC, van den Heuvel-Eibrink MM, Korbijn CM, Korthof ET, van der Pal K, Stijnen T, van Weel Sipman MH, van Weerden JF, van Wering ER, van der Does-van den Berg A and Dutch Childhood Oncology G. Dexamethasone-based therapy for childhood acute lymphoblastic leukaemia: results of the prospective Dutch Childhood Oncology Group (DCOG) protocol ALL-9 (1997-2004). Lancet Oncol. 2009; 10(10):957-966.

52. Escherich G, Troger A, Gobel U, Graubner U, Pekrun A, Jorch N, Kaspers G, Zimmermann M, zur Stadt U, Kazemier K, Pieters R, Den Boer ML, Horstmann M, Janka GE and CoALL study group. The long-term impact of in vitro drug sensitivity on risk stratification and treatment outcome in acute lymphoblastic leukemia of childhood (CoALL 06-97). Haematologica. 2011; 96(6):854-862.

53. Kamps WA, Bokkerink JP, Hakvoort-Cammel FG, Veerman AJ, Weening RS, van Wering ER, van Weerden JF, Hermans J, Slater R, van den Berg E, Kroes WG and van der Does-van den Berg A. BFM-oriented treatment for children with acute lymphoblastic leukemia without cranial irradiation and treatment reduction for standard risk patients: results of DCLSG protocol ALL-8 (1991-1996). Leukemia. 2002; 16(6):1099-1111.

54. Pieters R, de Groot-Kruseman H, Van der Velden V, Fiocco M, van den Berg H, de Bont E, Egeler RM, Hoogerbrugge P, Kaspers G, Van der Schoot E, De Haas V and Van Dongen J. Successful Therapy Reduction and Intensification for Childhood Acute Lymphoblastic Leukemia Based on Minimal Residual Disease Monitoring: Study ALL10 From the Dutch Childhood Oncology Group. J Clin Oncol. 2016; 34(22):2591-2601.

55. van den Berk LC, van der Veer A, Willemse ME, Theeuwes MJ, Luijendijk MW, Tong WH, van der Sluis IM, Pieters R and den Boer ML. Disturbed CXCR4/CXCL12 axis in paediatric precursor B-cell acute lymphoblastic leukaemia. Br J Haematol. 2014; 166(2):240-249.

56. van der Veer A, Waanders E, Pieters R, Willemse ME, Van Reijmersdal SV, Russell LJ, Harrison CJ, Evans WE, van der Velden VH, Hoogerbrugge PM, Van Leeuwen F, Escherich G, Horstmann MA, Mohammadi Khankahdani L, Rizopoulos D, De Groot-Kruseman HA, et al. Independent prognostic value of BCR-ABL1-like signature and IKZF1 deletion, but not high CRLF2 expression, in children with B-cell precursor ALL. Blood. 2013; 122(15):2622-2629.

57. Cario G, Zimmermann M, Romey R, Gesk S, Vater I, Harbott J, Schrauder A, Moericke A, Izraeli S, Akasaka T, Dyer MJ, Siebert R, Schrappe M and Stanulla M. Presence of the P2RY8-CRLF2 rearrangement is associated with a poor prognosis in non-high-risk precursor B-cell acute lymphoblastic leukemia in children treated according to the ALL-BFM 2000 protocol. Blood. 2010; 115(26):5393-5397.

58. Chen IM, Harvey RC, Mullighan CG, Gastier-Foster J, Wharton W, Kang H, Borowitz MJ, Camitta BM, Carroll AJ, Devidas M, Pullen DJ, Payne-Turner D, Tasian SK, Reshmi S, Cottrell CE, Reaman GH, et al. Outcome modeling with CRLF2, IKZF1, JAK, and minimal residual disease in pediatric acute lymphoblastic leukemia: a Children's Oncology Group study. Blood. 2012; 119(15):3512-3522.

59. Fine JP and R.J. G. A Proportional Hazards Model for the Subdistribution of a Competing Risk. Journal of the American Statistical Association. 1999; 94(446):496-509.

60. Gray RJ. cmprsk: Subdistribution Analysis of Competing Risks. R package version 22-6 2013; http://CRAN.R-project.org/package=cmprsk.

61. De Wreede LC, Fiocco M and Putter H. mstate: An R Package for the Analysis of Competing Risks and Multi-State Models. J Stat Softw. 2011; 38(7):1-30.

62. Therneau T. A Package for Survival Analysis in S. R package version 236-12. 2012.

Supplemental Data

Supplementary Table 1: RT-PCR primers used for the detection of JAK2 translocations

Gene fusion	Forward Primer ID	Forward sequence 5' to 3'	Reverse Primer ID	Reverse sequence 5' to 3'
ATF7IP-JAK2	ATF7IP_ exon12_F2	aacccatacaaccagcaccgcctct	JAK2_ exon20_R4	tgttgtcatgctgtagggatttcagga
BCR-JAK2	BCR_ exon1_F1	gtgccataagcggcaccggcact	JAK2_ exon18_R1	aggcctgaaatctggttcata
EBF1-JAK2	EBF_ exon14_F2	cacgagcatgaacggatacggctct	JAK2_ exon20_R4	tgttgtcatgctgtagggatttcagga
ETV6-JAK2	ETV6_ exon3_F1	atggcaaagctctcctgctgctgac	JAK2_ exon20_R4	tgttgtcatgctgtagggatttcagga
PAX5-JAK2	PAX5_ exon3_F2	acaatgacaccgtgcctagcgtcag	JAK2_ exon19_	tcaaaggcaccagaaaac
PPFIBP1-JAK2	PPFIBP1_ exon10_F1	tgcaagatgaaaggagaaggggttga	JAK2_ exon20_R4	tgttgtcatgctgtagggatttcagga
SSBP2-JAK2	SSBP2_ exon7_F1	ggcacttggaggtgtcccaggaagt	JAK2_ exon20_R4	tgttgtcatgctgtagggatttcagga
STRN3-JAK2	STRN3_ exon7_F3	tgaaggagctggagaagcacggagt	JAK2_ exon20_R4	tgttgtcatgctgtagggatttcagga
TPR-JAK2	TPR_ exon38_F1	tggaaatgcctcttccaaagaagttga	JAK2_ exon20_R4	tgttgtcatgctgtagggatttcagga
TERF2-JAK2	TERF2_ exon10_F1	tggggaaggaaactgg	JAK2_ exon20_R4	tgttgtcatgctgtagggatttcagga

PCR program

50°C	2 minutes	
95°C	10 minutes	
95°C	15 seconds	
60°C	1 minute	8 cycles
72°C	30 seconds	
95°C	15 seconds	
57°C	1 minute	8 cycles
72°C	30 seconds	
95°C	15 seconds	
54°C	1 minute	8 cycles
72°C	30 seconds	
95°C	15 seconds	
51°C	1 minute	8 cycles
72°C	30 seconds	
95°C	15 seconds	
48°C	1 minute	8 cycles
72°C	30 seconds	

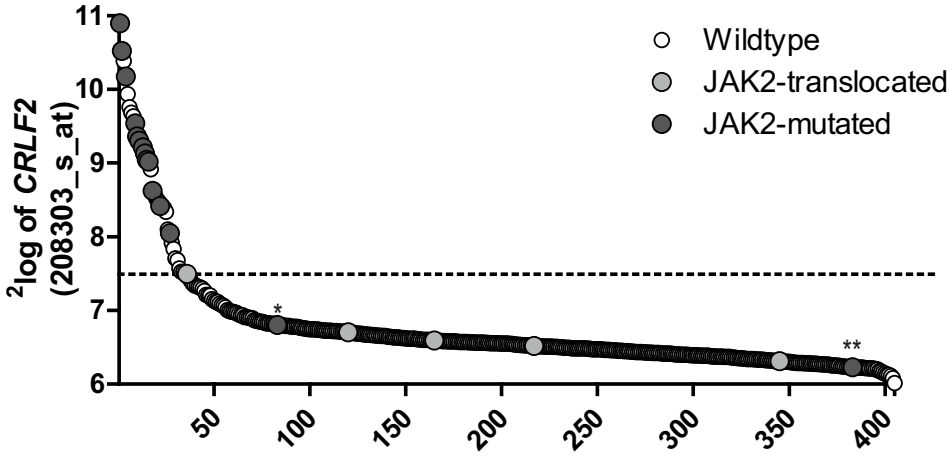

Supplementary Figure 1: *CRLF2* expression values

2log expression levels of Affymetrix probeset 205841_at in 405 pediatric BCP-ALL cases, which were tested for *JAK2* aberrations. * represents patient A159. ** represents patient A521.

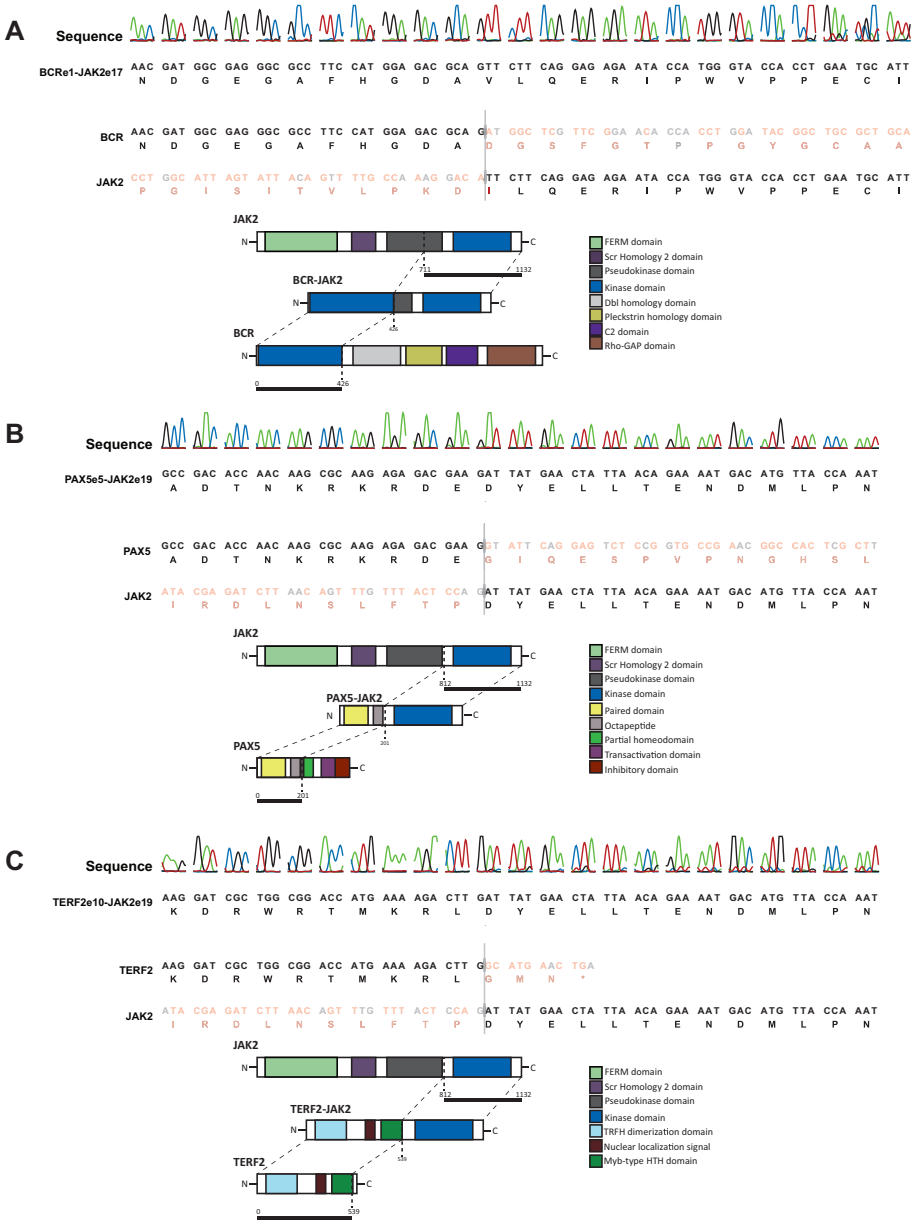

Supplementary Figure 2: Sequencing results of *JAK2* translocations

(A-C) Presence of fusion genes was examined on cDNA level using RT-PCR, followed by Sanger sequencing to detect *BCR-JAK2*, *PAX5-JAK2* and *TERF2-JAK2* translocations.

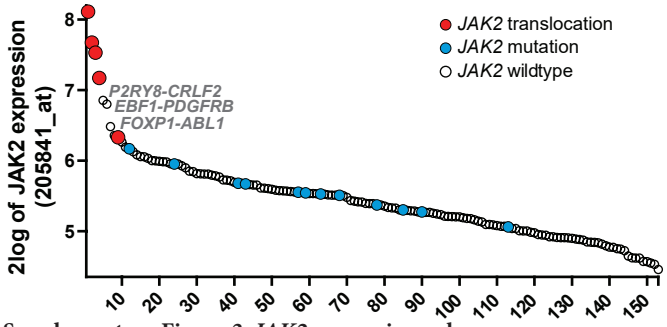

Supplementary Figure 3: *JAK2* expression values

2log expression levels of Affymetrix probeset 205841_at in 77 *BCR-ABL1*-like and 76 B-other cases, which were tested for *JAK2* translocations. JAK2 mutation status is also indicated. (Information was added to the three cases with high *JAK2* expression levels, without *JAK2* translocations.)

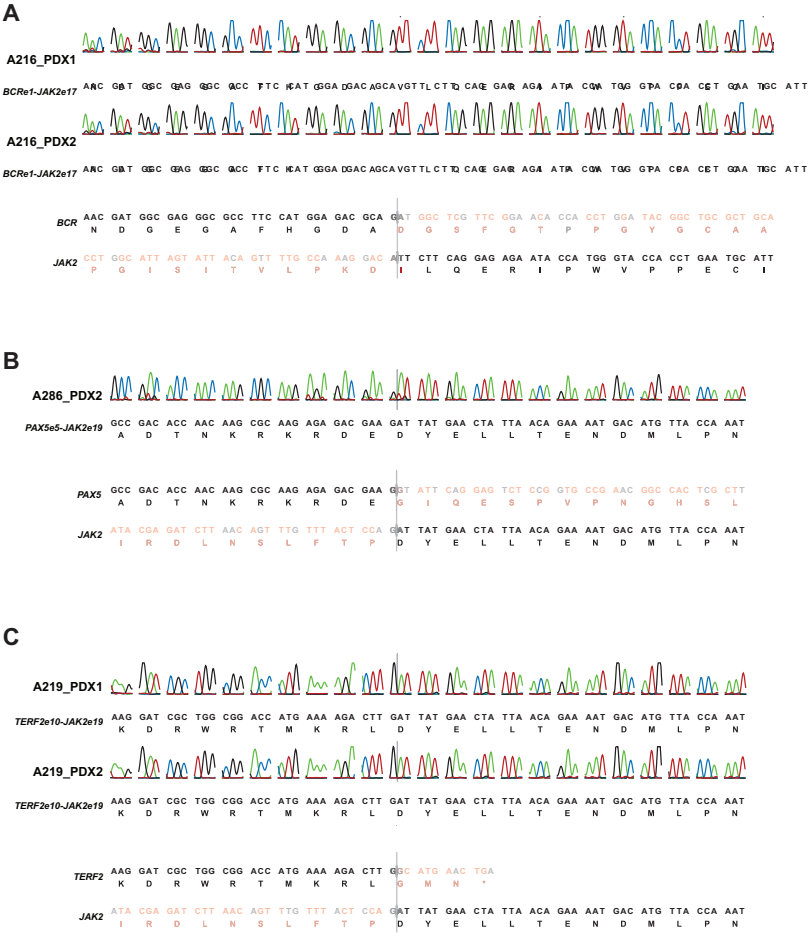

Supplementary Figure 4: *JAK2* aberrations in PDX cells

(A-C) Presence of *JAK2* translocation in PDX cells was validated on cDNA level using Sanger sequencing of cDNA.

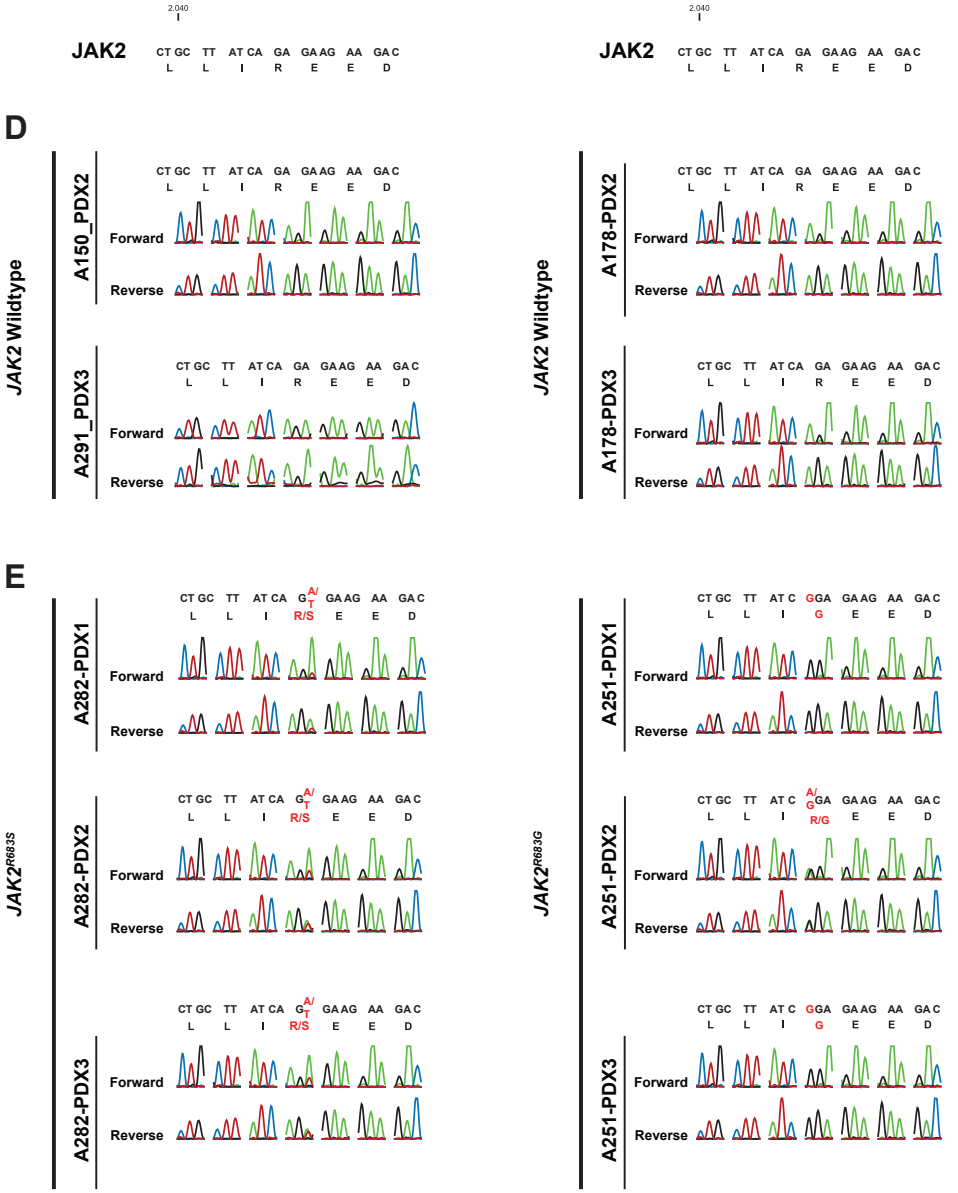

Supplementary Figure 4: *JAK2* aberrations in PDX cells (continued)

(**D-E**) Genomic DNA of PDX cells was used to identify the absence (**D**) or presence (**E**) of *JAK2* mutations in exon 16.

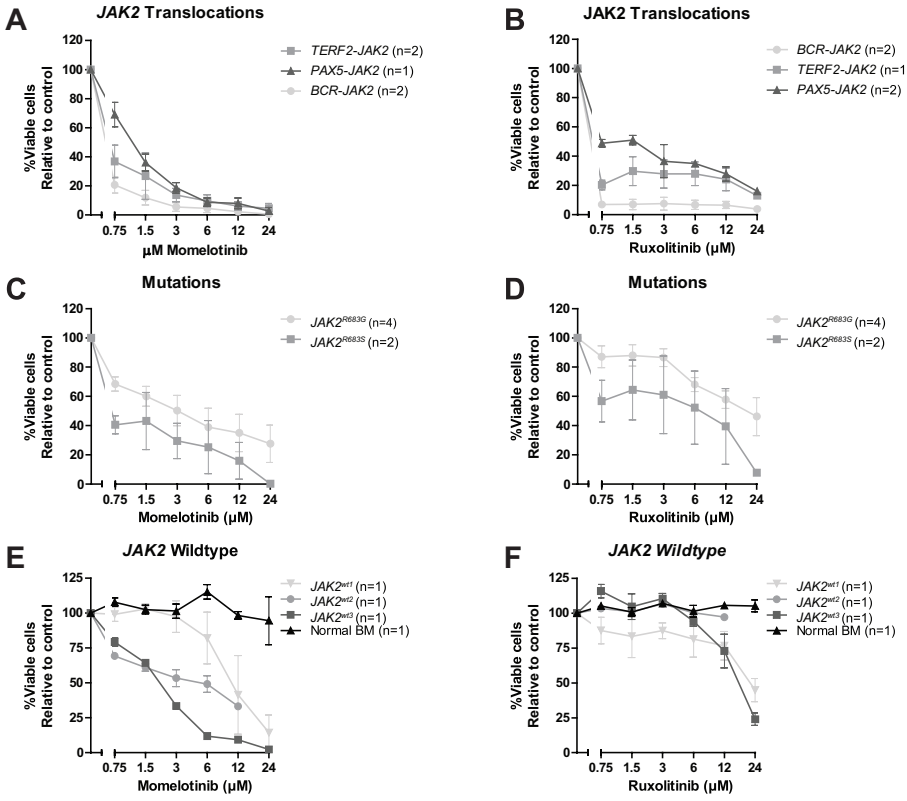

Supplementary Figure 5: The efficacy of JAK inhibitors on *JAK2* translocated and mutated cells per type of aberration

Leukemic (PDX or primary patient) cells were incubated for four days to indicated concentrations of momelotinib or ruxolitinib, after which viability was measured using an MTT assay. Sensitivity of exposed cells was calculated relative to vehicle treated controls. Individual samples were tested in duplicate. Data derived from samples with identical JAK2 lesions were grouped for analyses. **(A-B)** Efficacy of momelotinib and ruxolitinib on PDX cells with *JAK2* translocations: *BCR-JAK2* (n=2), *TERF2-JAK2* (n=2) and *PAX5-JAK2* (n=1). Mean±SD of individual samples (in duplicate) are shown. **(C-D)** Efficacy of momelotinib and ruxolitinib on *JAK2* mutated cells: JAK2 R683G (n=4) and JAK2 R683S (n=2) Mean±SEM of individual samples is depicted. **(E-F)** Efficacy of momelotinib and ruxolitinib on *JAK2* wildtype PDX cells and normal bone marrow cells. Mean±SD of individual samples (in duplicate) are shown. **(H-I)** Efficacy of momelotinib and ruxolitinib on Down syndrome and non-Down syndrome JAK2 R683G cells. Mean±SD of individual samples (in duplicate) are shown.

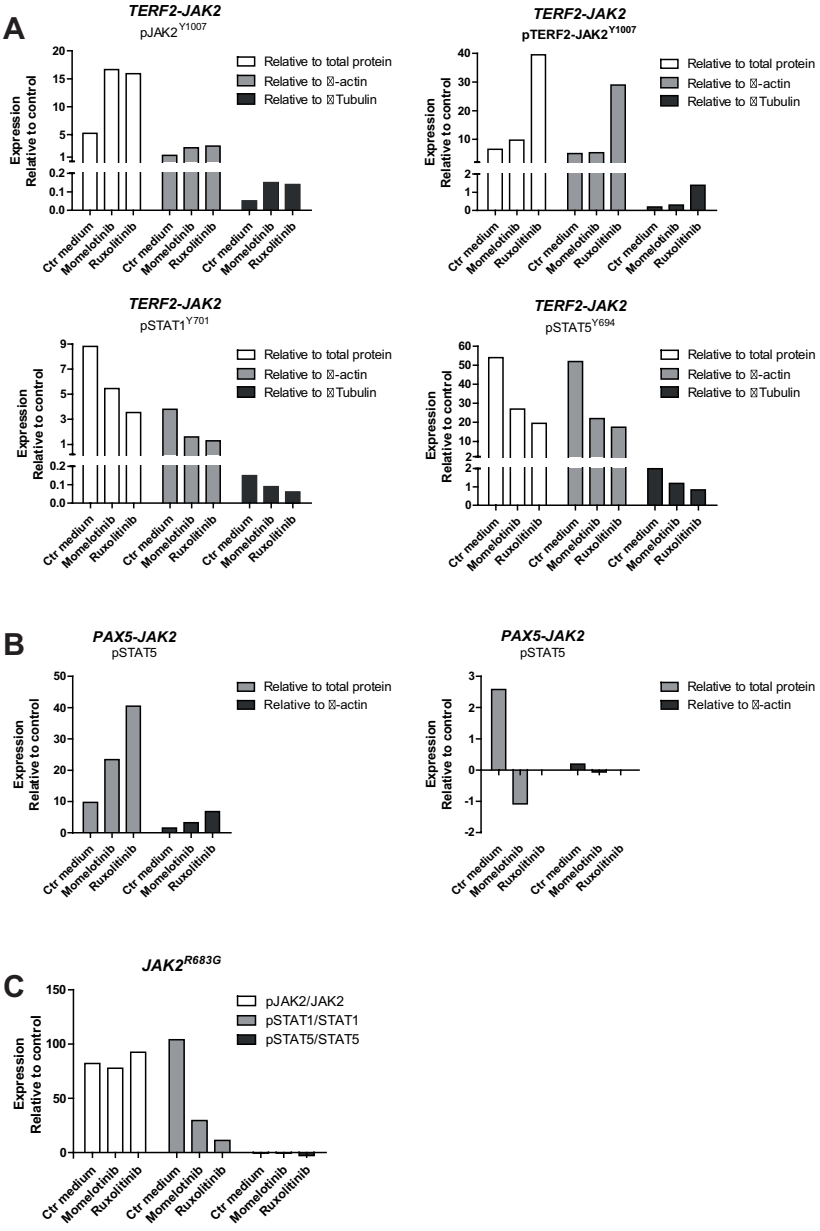

Supplementary Figure 6: Quantified expression levels western blots Figure 2

(A-C) TERF2-JAK2, PAX5-JAK2 and JAK2 R683G PDX cells were exposed for four hours to vehicle control medium, 1.5 μM momelotinib or 0.75 μM ruxolitinib, after which (phosphorylated) TERF2-JAK2, PAX5-JAK2, JAK2, STAT1 and STAT5 levels were analyzed using western blot (25 μg lysate). Expression levels of phospho-proteins were quantified relative to total protein or loading control.

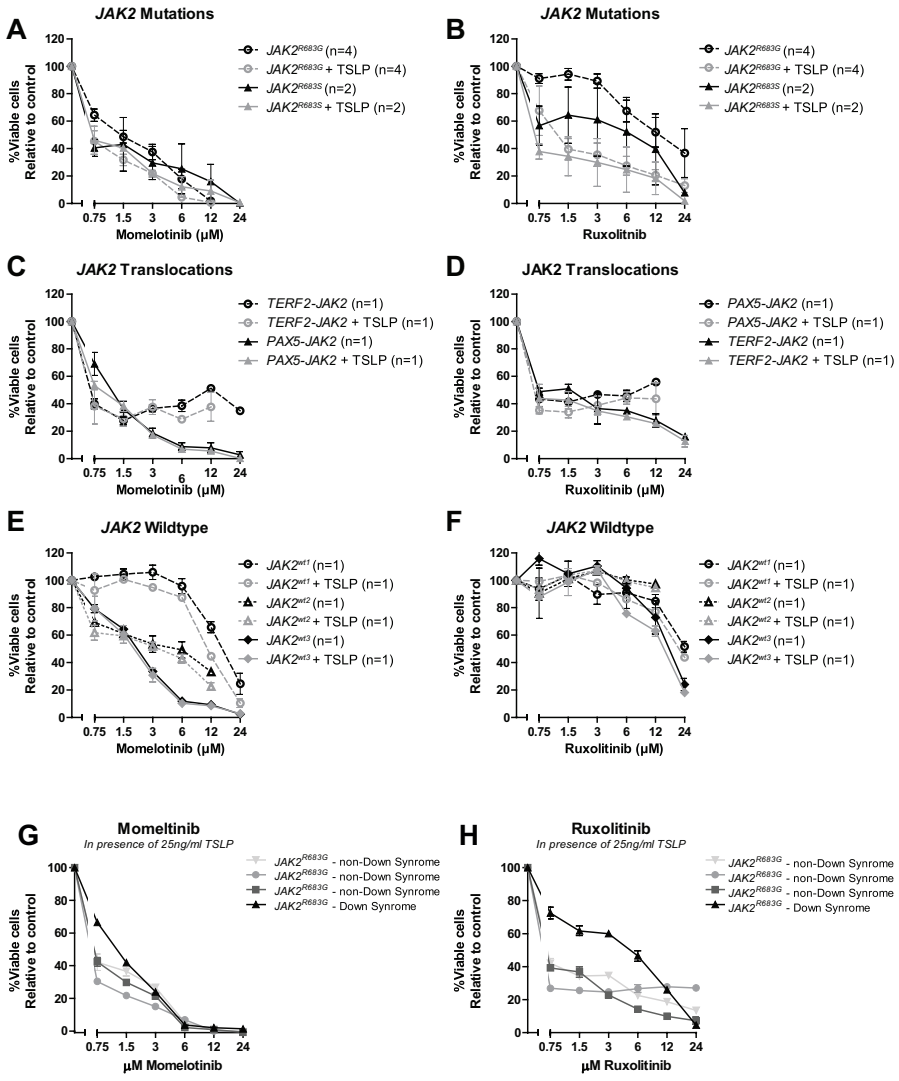

Supplementary Figure 7: The effect of TSLP stimulation on the efficacy of JAK inhibitors per type of aberration

Leukemic (PDX or primary patient) cells were pre-incubated for 1 hour without or with 25 ng/ml TSLP, after which they were exposed for four days to indicated concentrations of momelotinib or ruxolitinib. Viability was measured using an MTT assay. Sensitivity was calculated relative to vehicle treated controls. Individual samples were tested in duplicate. **(A-B)** Efficacy of momelotinib and ruxolitinib on *JAK2* mutated samples with or without TSLP pre-incubation: Mean±SEM four JAK2 R683G and two JAK2 R683S samples is shown. **(C-D)** Efficacy of momelotinib and ruxolitinib on cells with JAK2 translocations (n=2). Mean±SD of sample duplicates from a *TERF2-JAK2* and *PAX5-JAK2* sample are shown. **(E-F)** Efficacy of momelotinib and ruxolitinib on *JAK2* wildtype PDX cells (n=3). Mean±SD of sample duplicates are shown.

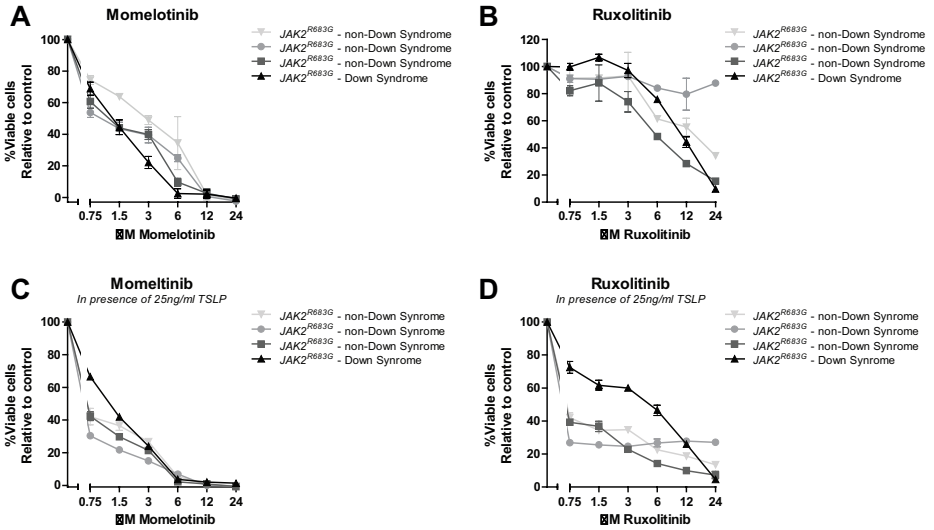

Supplementary Figure 8: Down syndrome and the efficacy of JAK inhibitors on *JAK2* mutated cells

Cells were exposed for four days to indicated concentrations of momelotinib or ruxolitinib. Viability was measured using an MTT assay. Sensitivity of exposed cells was calculated relative to vehicle treated controls. Individual samples were tested in duplicate. Mean±SD of sample duplicates is shown.

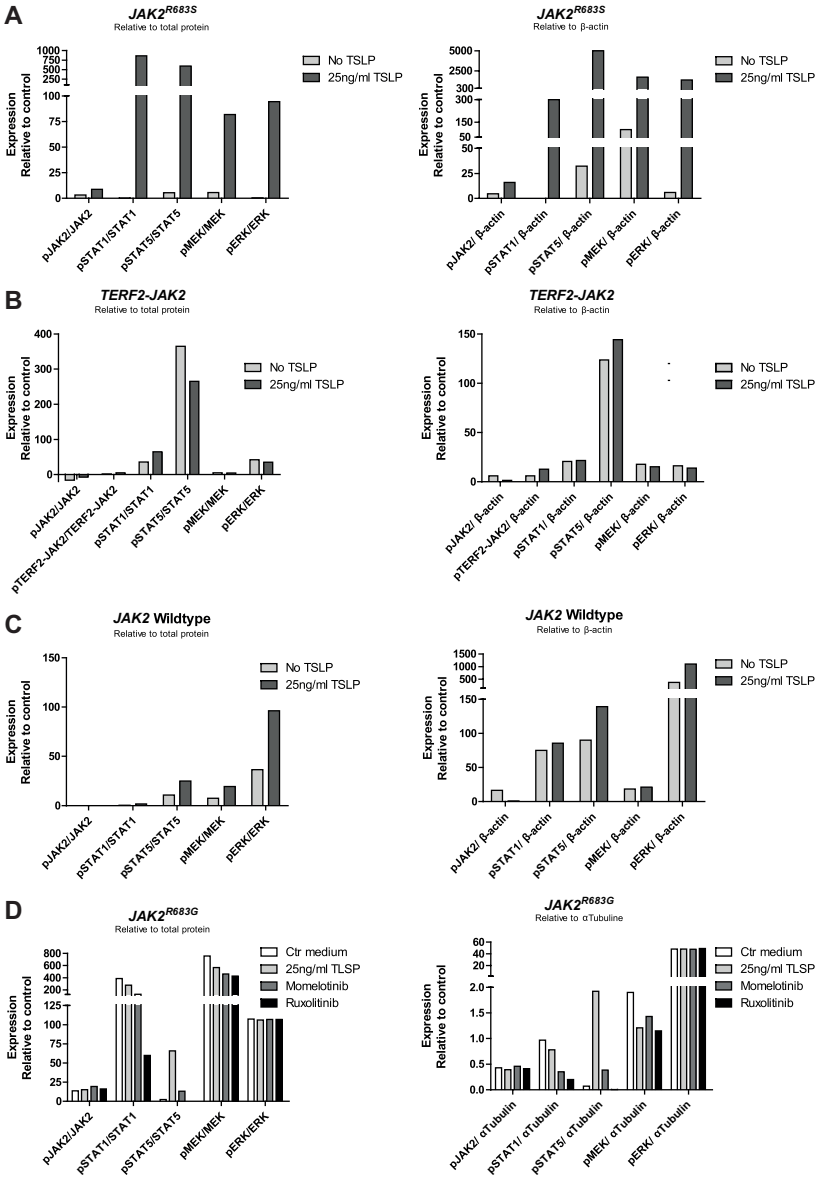

Supplementary Figure 9: Quantified expression levels western blots Figure 3

(A-C) Western blot of JAK2 R683S, TERF2-JAK2 and JAK2wt PDX cells with or without TSLP stimulation (25 ng/ml for 1 hour). Expression levels of phospho-proteins were quantified relative to total protein or loading control (β-actin).

(D) JAK2 R683G cells were pre-incubated for 1 hour with or without 25 ng/ml TSLP, after which cells were exposed for four hours to vehicle control medium, 1.5 μM momelotinib or 0.75 μM ruxolitinib. Levels of (phosphorylated) JAK2, STAT1, STAT5, MEK1/2 and ERK1/2 were analyzed using western blot. Expression levels of phospho-proteins were quantified relative to total protein or loading control (α-Tubulin).

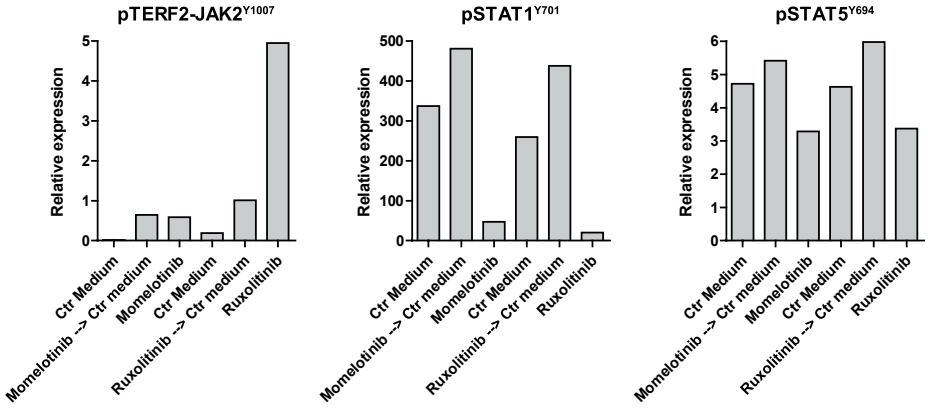

Supplementary Figure 10: Quantified expression levels western blots Figure 4

TERF2-JAK2 PDX cells were incubated for four hours with or without 1.5 μM momelotinib or 0.75 μM ruxolitinib, after which cells were washed to remove the JAK inhibitors. Half of the cells were exposed for another 1.5 hours to 1.5 μM momelotinib or 0.75 μM ruxolitinib, whereas the other cells were incubated in vehicle control (Ctr) medium. Protein expression levels were examined by western blot (25 μg lysate). Expression levels of phospho-proteins were quantified relative to total protein.

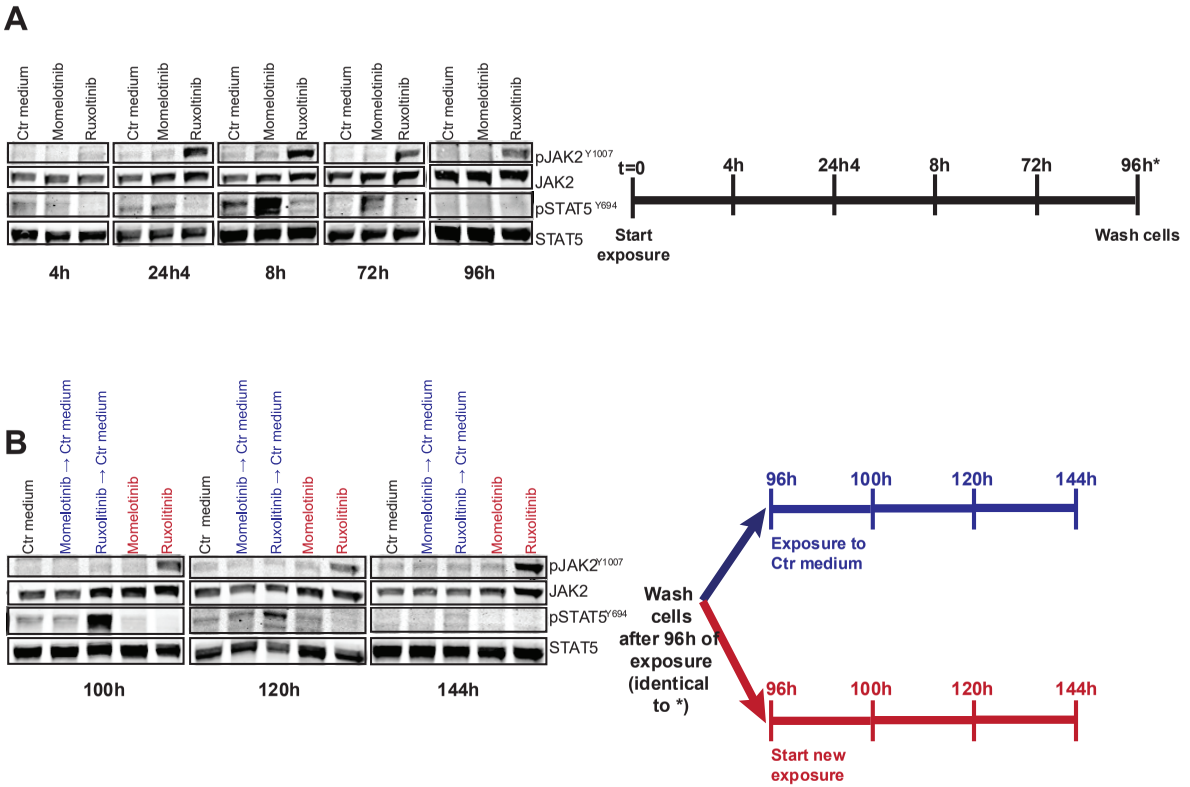

Supplementary Figure 11: Accumulation of pJAK2 Y1007 results in a rebound effect of JAK2

(A) HEL cells were incubated with or without 1.5 μM momelotinib or 0.75 μM ruxolitinib for 4 hours, 24 hours, 48 hours, 72 hours and 96 hours, after which cells were lysed and protein expression levels were examined using western blot (25 μg lysate). **(B)** After 96 hours of exposure to JAK inhibitors (indicated by * in panel A), cells were washed in normal culture medium, to remove momelotinib and ruxolitinib. Subsequently, half of the cells were incubated with 1.5 μM momelotinib or 0.75 μM ruxolitinib for another 4 hours, or 24 hours, whereas the remaining cells were incubated in vehicle control (Ctr) medium. Protein expression levels were examined using western blot (25 μg lysate).

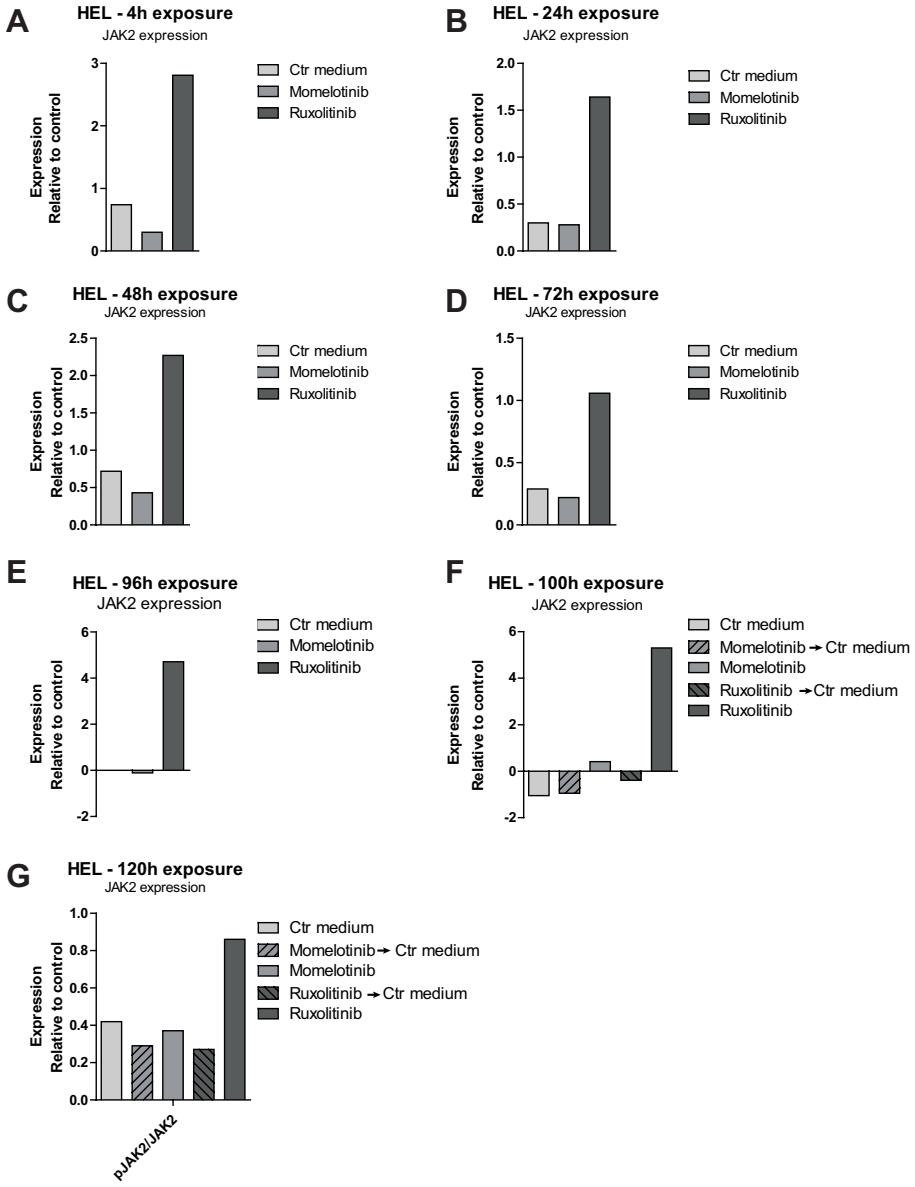

Supplementary Figure 12: Quantified expression levels western blots Supplementary Figure 8 (continued on next page)

(A-N) HEL cells were incubated with or without 1.5 μM momelotinib or 0.75 μM ruxolitinib for 4 hours, 24 hours, 48 hours, 72 hours and 96 hours. After 96 hours of exposure to JAK inhibitors, cells were washed in normal culture medium, to remove momelotinib and ruxolitinib. Subsequently, half of the cells were incubated with 1.5 μM momelotinib or 0.75 μM ruxolitinib for another 4 hours, or 24 hours, whereas the remaining cells were incubated in vehicle control (Ctr) medium. Protein expression levels were examined using western blot (25 μg lysate). Expression levels of phospho-proteins were quantified relative to total protein.

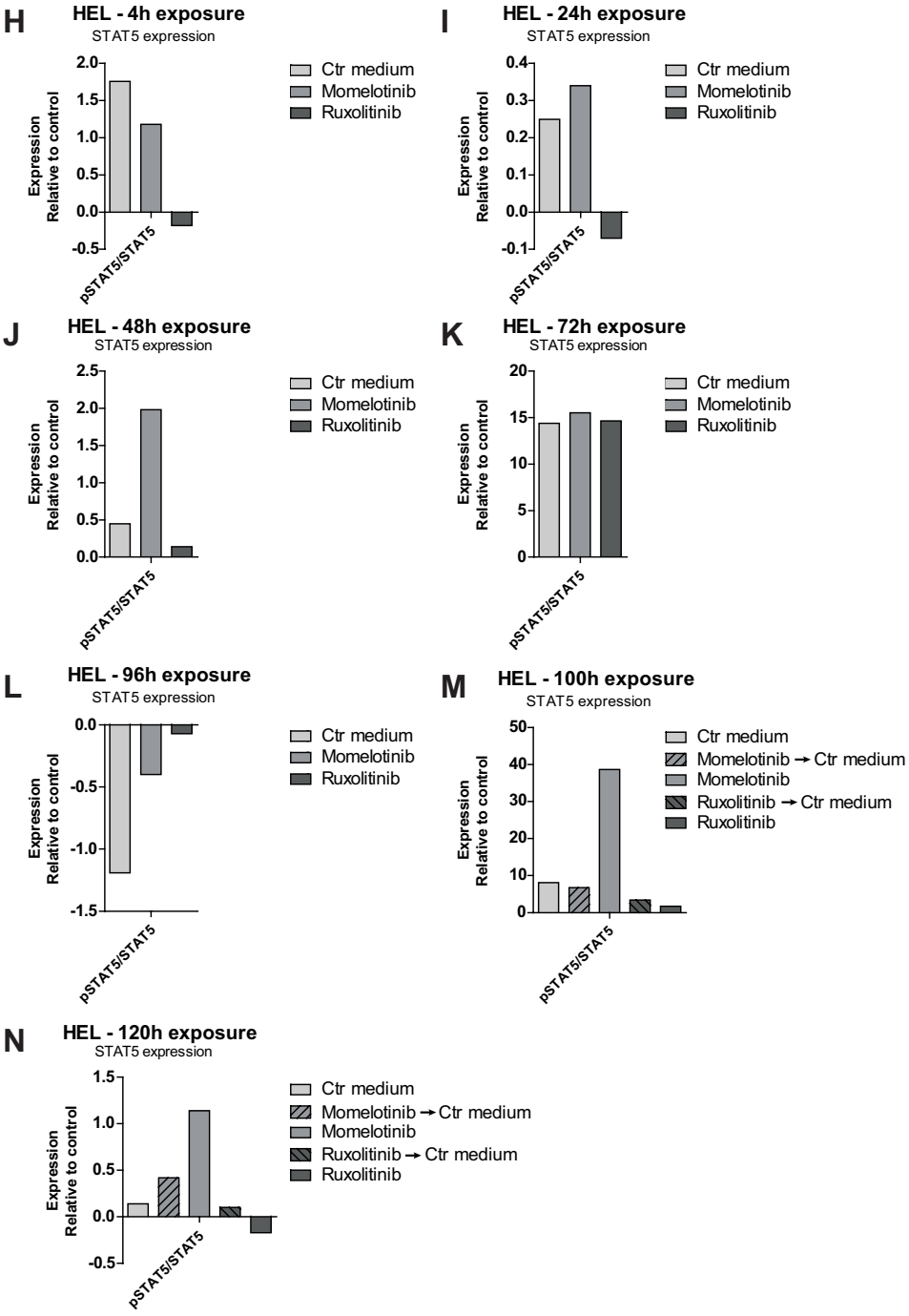

Supplementary Figure 12: Quantified expression levels western blots Supplementary Figure 8 (continued)

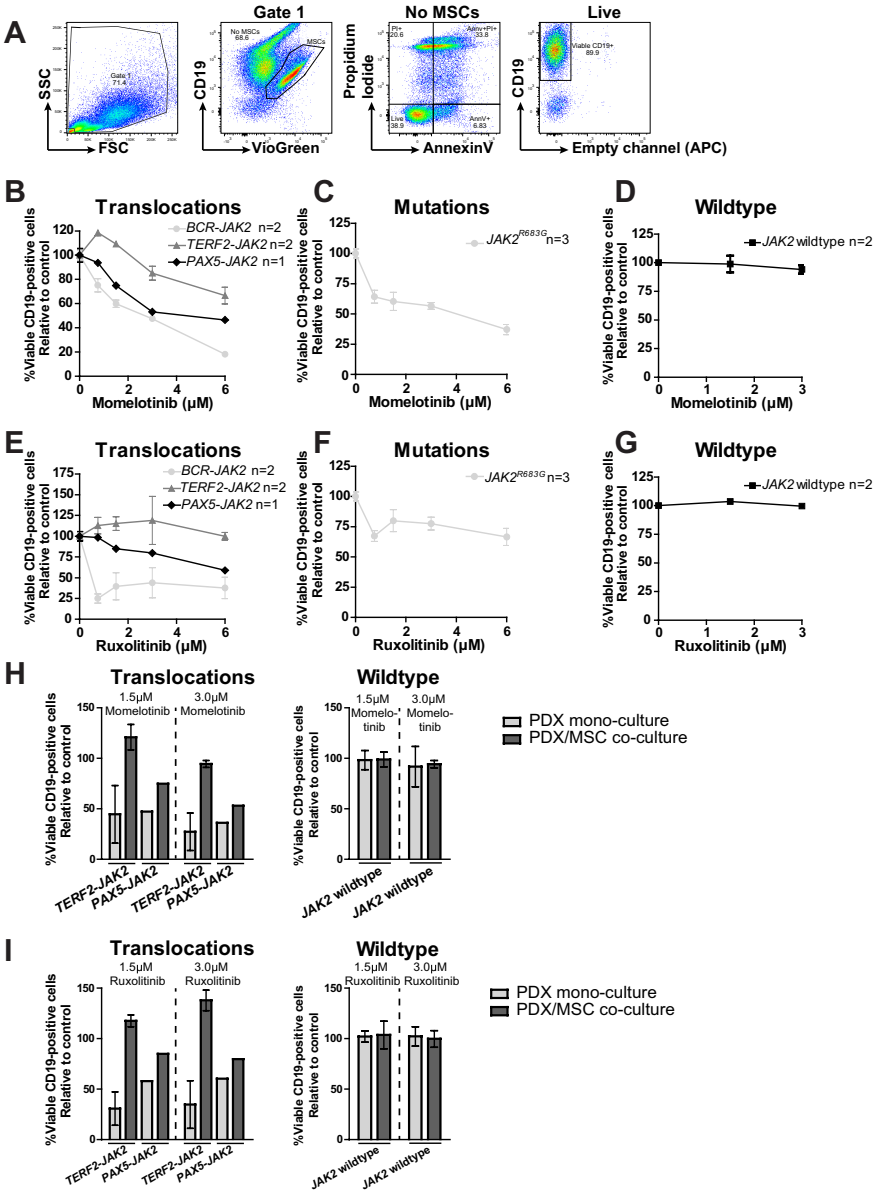

Supplementary Figure 13: The efficacy of JAK inhibitors in PDX/MSC co-cultures

The response of PDX cells (CD19+) co-cultured with MSCs (CD19-) to increasing concentrations of momelotinib and ruxolitinib was assessed after four days of culture using flow cytometry. Viability was calculated relative to untreated controls. Mean±SEM is shown. **(A)** Gating strategy. **(B-G)** Percentage of viable PDX cells being *JAK2* translocated (*BCR-JAK2* n=2; *TERF2-JAK2* n=2; *PAX5-JAK2* n=1), JAK2 mutated (JAK2 R683G n=3), or *JAK2* wildtype cells (*JAK2* wildtype n=2), co-cultured with patient MSCs, after four days exposure to momelotinib and ruxolitinib. **(H-I)** The effect of 1.5 μM and 3.0 μM momelotinib or ruxolitinib on the viability of *JAK2* translocated PDX cells in mono-culture, or in co-culture with patient MSCs. *TERF2-JAK2* n=2; *PAX5-JAK2* n=1, *JAK2* wildtype n=2.

Chapter 3

RAS pathway mutations as predictive biomarker for treatment adaptation in pediatric B-cell precursor acute lymphoblastic leukemia

Isabel S. Jerchel, Alex Q. Hoogkamer, Ingrid M. Ariës, Elisabeth M.P. Steeghs, Judith M. Boer, Nicolle J.M. Besselink, Aurélie Boeree, Cesca van de Ven, Hester A. de Groot-Kruseman, Valerie de Haas, Martin A. Horstmann, Gabriele Escherich, C. Michel Zwaan, Edwin Cuppen, Marco J. Koudijs, R. Pieters, and Monique L. den Boer

Leukemia. 2017 Oct 3 (Epub ahead of print)

Abstract

RAS pathway mutations have been linked to relapse and chemotherapy resistance in pediatric B-cell precursor acute lymphoblastic leukemia (BCP-ALL). However, comprehensive data on the frequency and prognostic value of subclonal mutations in well-defined subgroups using highly sensitive and quantitative methods is lacking. Targeted deep sequencing of 13 RAS-pathway genes was performed in 461 pediatric BCP-ALL cases at initial diagnosis and in 19 diagnosis-relapse pairs. Mutations were present in 44.2% of patients, with 24.1% carrying a clonal mutation. Mutation frequencies were highest in high hyperdiploid, infant t(4;11)-rearranged, *BCR-ABL1*-like, and B-other cases (50-70%), whereas mutations were less frequent in *ETV6-RUNX1*-rearranged, and rare in *TCF3-PBX1*- and *BCR-ABL1*-rearranged cases (27 to 4%). RAS-pathway mutated cells were more resistant to prednisolone and vincristine *ex vivo*. Clonal, but not subclonal mutations were linked to unfavorable outcome in standard and high risk-treated patients. At relapse, most RAS pathway mutations were clonal (9 of 10). RAS-mutant cells were sensitive to the MEK-inhibitor trametinib *ex vivo*, and trametinib sensitized resistant cells to prednisolone. We conclude that RAS pathway mutations are frequent, and that clonal, but not subclonal mutations are associated with unfavorable risk parameters in newly diagnosed pediatric BCP-ALL. These mutations may designate patients eligible for MEK-inhibitor treatment.

Introduction

The prognosis of children with B-cell precursor acute lymphoblastic leukemia (BCP-ALL) has improved considerably over the past decades, and nowadays about 80% of the patients are cured.[1] However, especially medium and high risk cases still show dissatisfying rates of relapse despite intense chemotherapy.[2-4] Relapsed ALL is treated with the same drugs as the initial leukemia, but cells of relapsed cases are more resistant.[5] New, targeted approaches are therefore warranted.

Activating mutations in *KRAS*, *NRAS*, and *HRAS* are among the most frequent mutations in cancer.[6-9] The RAS GTPases are convert extracellular growth signals into a complex intracellular response. Upon activation of a growth factor receptor, RAS-guanidine exchange factors (e.g. SHP2 encoded by *PTPN11*) activate RAS by enabling binding of GTP, which activates the RAF and PI3 kinases and RALGDS. The RAF-MEK-ERK kinase axis is crucial for mediating the oncogenic effects of RAS, demonstrated by the efficacy of MEK-inhibitors in RAS-mutated cancers.[10-12] Clinical trials are ongoing, and benefits were reported for RAF-mutated melanomas, ovarian cancer, and thyroid cancer.[13-18]

RAS mutations have been initially reported in about 15% of pediatric BCP-ALL.[19-21] However, these studies were often restricted to N- and KRAS, certain subtypes or high risk groups, or were technically limited in sensitivity (therefore overlooking subclonal mutations), and did not compare mutation frequencies between cytogenetic subtypes.[22-26] Mutations were reported in the context of recent genomic studies but not studied for their prognostic impact in isolation. Therefore, the clinical significance of RAS mutations is still debated, and it is unknown whether the recent inclusion of minimal residual disease levels as risk criterion influences the prognostic effect of RAS pathway mutations in

contemporary protocols. Recent studies found that mutations in *NRAS, KRAS, FLT3,* and *PTPN11* are more frequently observed at relapse (34-38%), and in part confer a poor prognosis.[26-29] We previously observed in a small cohort of 26 patients that RAS-pathway mutations are more frequent in *ex vivo* prednisolone-resistant cases, which are sensitized to prednisolone by RAS-pathway inhibition.[30] Backtracking has shown that RAS-mutant relapse-forming clones may exist as small subclones at initial diagnosis.[27, 31, 32] However, these retrospective analyses rely on selected cases, and the predictive value of (sub) clonal RAS pathway mutations at initial diagnosis of BCP-ALL treated in contemporary protocols is unknown.

Here we report deep next-generation sequencing of thirteen RAS pathway genes together with a risk-stratified survival analysis in a clinically and biologically well-characterized cohort of 461 initial diagnosis patients with BCP-ALL, treated according to a contemporary, MRD-based ALL treatment protocol (DCOG ALL10). In addition, we report links between RAS mutation status, clonality, *ex vivo* cellular drug resistance and *ex vivo* response to MEK inhibition.

Material and Methods

A detailed description of all methods can be found in the online supplement.

Patient material and patient-derived xenografts (PDX)

This study comprised children with newly diagnosed BCP-ALL with an age range of 0 to 18 years. These studies were conducted in accordance with the Declaration of Helsinki; written informed consent was obtained from parents or guardians and approval given by institutional review boards. Mononuclear cells were isolated using density gradient centrifugation with Lymphoprep (Axis Shield, Norway) as described previously.[33] Animal experiments were approved by the animal ethics committee (EMC 2863 (103-12-08)). In some cases, xenografts of primary patient material were established in three 7-12 week-old female NOD.Cg-*Prkdc*^{scid}*Il2rg*^{tm1Wjl}/SzJ (NSG) mice per patient (Charles River, France). Leukemic cells were isolated and subsequently used for sequencing, western blot, and trametinib (GSK1120212) cytotoxicity assays. For all samples leukemic blast percentage was at least 90%, in relapse samples blast percentage was at least 80%. Subtypes were determined by karyotype, fluorescence in-situ hybridization (FISH) and/or fusion-gene specific PCR. *BCR-ABL1*-like cases were identified using microarray gene expression profiling by means of a 110 probe set classifier.[34, 35] The composition of analyzed groups is described in a flow diagram (Figure S1).

Ex vivo cytotoxicity assays

Sensitivity towards chemotherapeutics was evaluated as previously described.36 In brief, freshly isolated primary ALL cells were incubated with a concentration range of prednisolone, vincristine, daunorubicin, L-asparaginase, 6-mercaptopurine, and 6-thioguanine. After four days, cell viability was evaluated by adding MTT and measuring formazan-conversion with optical density measurement. LC50-values were calculated (concentration at which 50% conversion activity was measured relative to no-drug control cells) and compared between groups using Mann-Whitney U tests. *Ex vivo* sensitivity towards trametinib was measured similarly (5μM-0.6nM).

Sequencing and code availability

DNA and RNA were isolated using Trizol reagent (Life Technologies), or using DNeasy (Qiagen) in two cases (used only for trametinib sensitivity assay) and the cell line 697. For TruSeq Custom Amplicon sequencing (Illumina, USA), sequencing libraries were prepared from 100-250ng genomic DNA. Successful library preparation was confirmed using the Labchip GX genomic analyzer (Caliper Life Sciences Benelux N.V., the Netherlands). Samples were then pooled equimolarly and sequenced on an Illumina MiSeq in paired-end reads of 250bp each. 49 amplicons of 425bp covered mutational hotspot regions in thirteen RAS pathway genes (Table S1). The analysis script will be provided upon request.

Sequence reads were aligned to the 1000 genomes human reference sequences (version b37, GATK resource bundle, Broad Institute, USA) using BWA v0.7.10[37] and GATK indel realigner v.3.3-0. Single nucleotide variants were called with Freebayes v0.9.18-24[38], Varscan v.2.3.7[39], Bcftools v1.0[40], and GATK v3.3-0[41]. The resulting variant call format files were annotated using snpEff and snpSift v.4.1a[42] and dbNSFP v.2.7[43]. For reliable detection of high-confidence mutations, variants were filtered based on several criteria: For each sample, variants were excluded if they were reported by only one caller, coverage was <100 reads, or <20 reads supported the variant allele. Overall, variants were excluded if variant allele frequency (VAF) never exceeded 2% or distribution was unequal between runs. Furthermore, variants were only considered if they were reported in the COSMIC V73 GRCh37 database[44], non-synonymous, unlikely to be germline variants and not known SNPs (see Supplemental Methods for detail). Read depth per amplicon is summarized in Table S1. An estimate of cases missed due to insufficient coverage is given in Table S2. In a comparison with 25 samples that were sequenced previously (Ariës et al.[30]), all variants could be identified by both platforms, indicating a low false-positive rate. Only Exon 3 of *NRAS* was sequenced using Sanger sequencing in 248 ALL10 samples since primer design for this exon in a multiplex amplicon setting failed. Chromatograms were visually inspected for presence of mutations in codons 59 to 63 as well as analyzed by the R package sangerseqR in combination with the tools above to call and annotate detected variants.

Clinical characteristics and statistics

Clinical characteristics were compared using Fisher's exact test in R (version 3.2.1). We analyzed cases from the Dutch Childhood Oncology Group (DCOG) and Cooperative Study Group for Children with ALL (COALL) (n=432). We restricted the RAS pathway mutated group to those carrying a verified MAPK pathway activating mutation (codons 12, 13, and 146 of NRAS or KRAS and FLT3 or PTPN11). Event-free survival (EFS) and cumulative incidence of relapse and non-response after induction therapy (CIR) were evaluated in 244 eligible cases treated within one protocol (DCOG ALL10), stratified for risk group. The COALL97/03 cohort consisted of patients treated in the consecutive COALL 06-97 and COALL 07-03 protocols (n=131). For details see Escherich et al.[45] Treatment intensity in arms LR-R and LR-S is comparable to DCOG ALL10 standard risk treatment; LR-I, HR-R, and HR-S treatment is comparable to DCOG ALL10 medium risk treatment. In the COALL97/03 cohort, no patient was treated with an intensity comparable to that of the DCOG ALL10 high risk arm. CIR was estimated using a

competing risks model and compared using Gray's test. EFS probabilities were estimated using the actuarial Kaplan-Meier method and compared using the log-rank test. Hazard ratios were calculated in SPSS v21 using Cox's proportional hazard model. Outcome analyses were performed in R 3.2.1, using the packages cmprsk46 version 2.2-7, mstate version 0.2.7[47], and survival version 2.38-3[48].

Results

Frequency and clonality of RAS pathway mutations in newly diagnosed pediatric BCP-ALL

Targeted amplicon deep-sequencing was used to identify RAS pathway mutations in samples from 461 children with BCP-ALL at initial diagnosis. Mutational hotspots in 13 key members of the RAS pathway were analyzed with 49 amplicons. The median read depth per amplicon was 1085 reads per sample (IQR: 527-2647) (Table S1 and Figure S2).

Most recurrent lesions were activating mutations in NRAS and KRAS (79%), followed by mutations in PTPN11 and FLT3 (9.3% and 10.1% respectively, Figure 1A and Figure S3). Mutations in BRAF, NF1, CBL, and other genes occurred sporadically. Overall, variants in RAS pathway genes were observed in 44.2% of pediatric BCP-ALL cases. Clonal mutations (VAF ≥25%) were found in 24.1% of all patients (median: 40.5% VAF Figure S4), and subclonal mutations (VAF<25%) were exclusively found in 20.1% of patients (median: 4.3% VAF).

Most cases with RAS pathway mutations were high hyperdiploid or those with rare or negative for *BCR-ABL1*, *ETV6-RUNX1*, *TCF3-PBX1*, *MLL*-rearrangement, and high hyperdiploidy (51-67 chromosomes), including non-*BCR-ABL1*-like "B-other" and *BCR-ABL1*-like cases (Figure 1B, Table S3). Mutation frequencies were high in *BCR-ABL1*-like (49.4%), B-other (41.8%), high hyperdiploid (72.6%), and t(4;11)-rearranged (*MLL-AF4*, 73.3%) cases, with clonal mutations observed in 31.6%, 25.4%, 41.9%, and 20%, respectively (Figure 1B). Comparison of each subtype to the remaining BCP-ALL cases showed significantly more mutations in cases with *MLL*-rearrangement and high hyperdiploid karyotype (Odds ratio 3.8 and 5.7, respectively), and significantly less mutations in cases with *ETV6-RUNX1*-, *TCF3*-, and *BCR-ABL1*- rearrangement (Odds ratios <0.3, Table S4). Interestingly, within the *BCR-ABL1*-like group RAS pathway mutations were mutually exclusive with ABL/JAK class tyrosine kinase fusions, but not with high *CRLF2* expression (Figure S5). *ETV6-RUNX1*-rearranged cases showed an intermediate frequency (26.6%, 10.5% clonal), and *TCF3-PBX1*- or *BCR-ABL1*-rearranged cases had the lowest frequencies with 8% (0% clonal) and 4% (4% clonal) of cases being affected, respectively.

Frequent secondary aberrations in clonal RAS pathway mutant cases were chromosome 21 aberrations, dic(9;20) chromosomes, 9p-deletion, *PAX5* amplifications, and *CDKN2A/B* deletions. Opposed to that, significantly less *BTG1* deletions and *ETV6* deletions were detected in cases with clonal RAS pathway mutations. Cases with subclonal RAS pathway mutations also more frequently carried chromosome 21 aberrations and additionally more often expressed high *CRLF2* and harbored less mutations in *IKZF1* and *PAX5* (Table S5).

Table 1. Incidence of clonal RAS pathway mutations among BCP-ALL patients with clinical risk factors

Risk parameter	Incidence of clonal mutations among		Statistics (clonal vs. wildtype)			
	Risk parameter: Yes	Risk parameter: No	Fisher's p=[a]	Odds ratio[b]	95%-CI	
Age ≥10	22/75 (29%)	90/357 (25%)	0.88			
Male	55/227 (24%)	57/205 (24%)	0.56			
High WBC (>50/nL)	34/99 (34%)	78/331 (24%)	0.24			
Down Syndrome	2/16 (13%)	105/305 (27%)	0.10	0.3	0.03	1.38
CNS+	0/1 (0%)	24/248 (10%)	1			
PPR	7/17 (41%)	51/181 (21%)	0.15	2.220	0.649	7.418
MRD high d33 ALL10	16/48 (33%)	35/147 (18%)	0.01	2.99	1.27	7.05
MRD high d79 ALL10	2/8 (25%)	47/171 (20%)	1			

WBC: White blood cell count; CNS+: non-traumatic puncture and >5 WBC/µl CSF with identifiable leukemic cells; patients with a traumatic lumbar puncture were not included; PPR: Prednisone poor responder, i.e. ≥1000 leukemic blasts/µl in peripheral blood on day 8 of induction therapy; MRD high: Minimal residual disease $\geq 10^{-3}$; d33: at the end of induction therapy (day 33); d79: at the end of consolidation therapy (day 79); [a] Fisher's Exact test p-values <0.05 are printed in bold font; [b] Odds ratios are only given if p-values in Fisher's Exact test were <0.2.

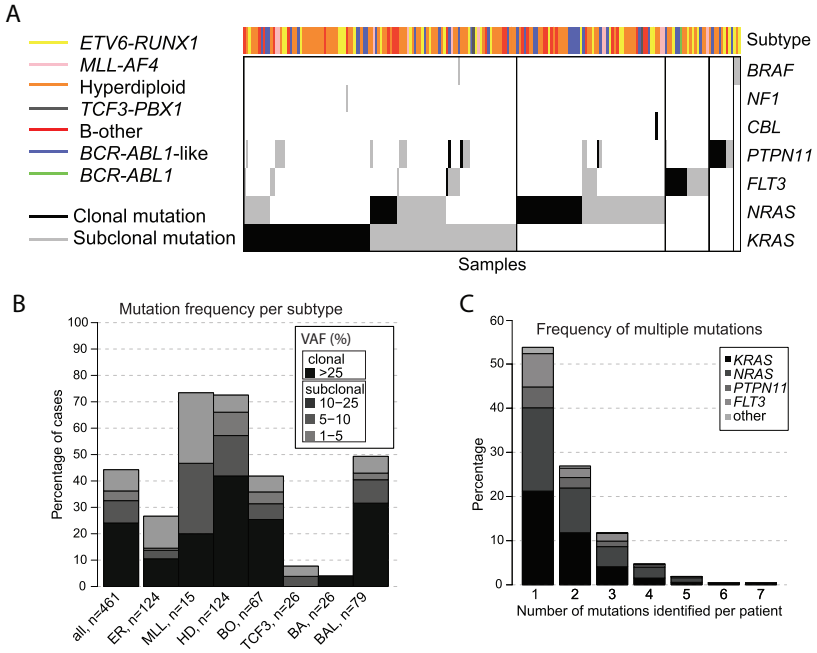

Figure 1. Frequency and distribution of RAS pathway mutations in pediatric BCP-ALL.

(A) Overview of all clonal or subclonal mutations found in pediatric BCP-ALL cases at initial diagnosis. Top bar represents the cytogenetic subtype. Black boxes represent clonal mutations (variant allele frequency (VAF) ≥25%), grey boxes represent subclonal mutations (VAF <25%). **(B)** Frequency of clonal and subclonal RAS pathway mutations overall and within the cytogenetic subtypes. ER: *ETV6-RUNX1*-rearranged, MLL: t(4;11)-rearranged, HD: High hyperdiploid, BO: B-other, TCF3: *TCF3-PBX1*-rearranged, BA: *BCR-ABL1*-rearranged, BAL: *BCR-ABL1*-like. **(C)** Co-occurrence of RAS pathway mutations: Bar heights indicate the frequency of mutated cases carrying the number of RAS pathway mutations indicated on the x-axis. Segmentation of each bar indicates the distribution of mutated genes.

All except three *NRAS* mutations and three quarters of the *KRAS* mutations affected the codons 12 and 13 (Figure S6).

Although clonal RAS pathway mutations were mutually exclusive (Figure 1A), additional subclonal mutations were present in 41% of cases with a clonal mutation and in 49% of cases with a subclonal mutation (46.2% of all mutated patients, Figure 1C). Most of these additional RAS pathway mutations were present at a VAF <10% (Figure S4).

Clinical characteristics and outcome

Clinical characteristics were compared between BCP-ALL cases with clonal RAS pathway mutations (n = 110, *KRAS, NRAS, PTPN11,* or *FLT3*) and wildtype cases (n = 235). Age, white blood cell count, gender, Down syndrome, CNS status at diagnosis, and prednisone window response at day 8 of therapy did not differ significantly (Table 1). In DCOG ALL10 patients clonal mutations were enriched among cases with high minimal residual disease (MRD) levels (≥10-3) after 4 weeks of induction treatment (33% in of MRD-high versus 18% in MRD-low cases, p = 0.01). This had an impact on mutation frequencies in the actual treatment arms: 13.5% of cases in the standard risk arm carried a clonal RAS pathway mutation, compared to 21.9% in medium risk and 40.9% in the high risk treatment arm (Table S6, p=0.02).

In contrast, subclonal mutations were not associated with poor risk features. These mutations were significantly more common among younger children (p=0.04), those with low white blood cell counts (<50 cells/nL, p=0.02), and those in the medium risk treatment arm (p=0.01, Table S7).

The prognostic value of RAS pathway mutations was analyzed in 244 newly diagnosed BCP-ALL patients treated according to the DCOG ALL10 protocol (for baseline characteristics and cohort composition see Table S8 and Figure S1). In the total cohort, clonal and subclonal RAS pathway mutations did not associate with an inferior clinical outcome (Table 2 and Figure 2A). In the DCOG ALL10 study, patients are risk-stratified by minimal residual disease response on day 33 and day 79 into standard risk, medium risk, and high risk treatment arms. In standard and high risk treated cases clonal RAS pathway mutations were associated with a significantly worse event-free survival compared to wildtype cases, caused in part by a higher incidence of relapse and non-response (Table 2 and Figure 2B, red lines). Significantly fewer relapses occurred in medium risk-treated patients harboring clonal mutations compared to wildtype cases, which resulted in a trend for better event-free survival. Subclonal mutations were not predictive for outcome (Figure 2B, blue lines).

Univariate analysis of RAS pathway status in these 3 risk arms revealed that clonal but not subclonal mutations in RAS pathway genes were predictive for an unfavorable outcome in the standard risk treated group (Hazard Ratio 4.6, p=0.047), which remained prognostic in a multivariate analysis including WBC and age (Hazard Ratio 5.4, p=0.032, Table S9). Univariate analysis of RAS pathway mutations in the medium risk and high risk group did not reveal statistical significant associations with event-free survival in this DCOG ALL10 study cohort.

The impact of RAS pathway mutations on clinical outcome was also evaluated in the COALL97/03 cohort (Figure S7). These patients had been stratified into treatment arms

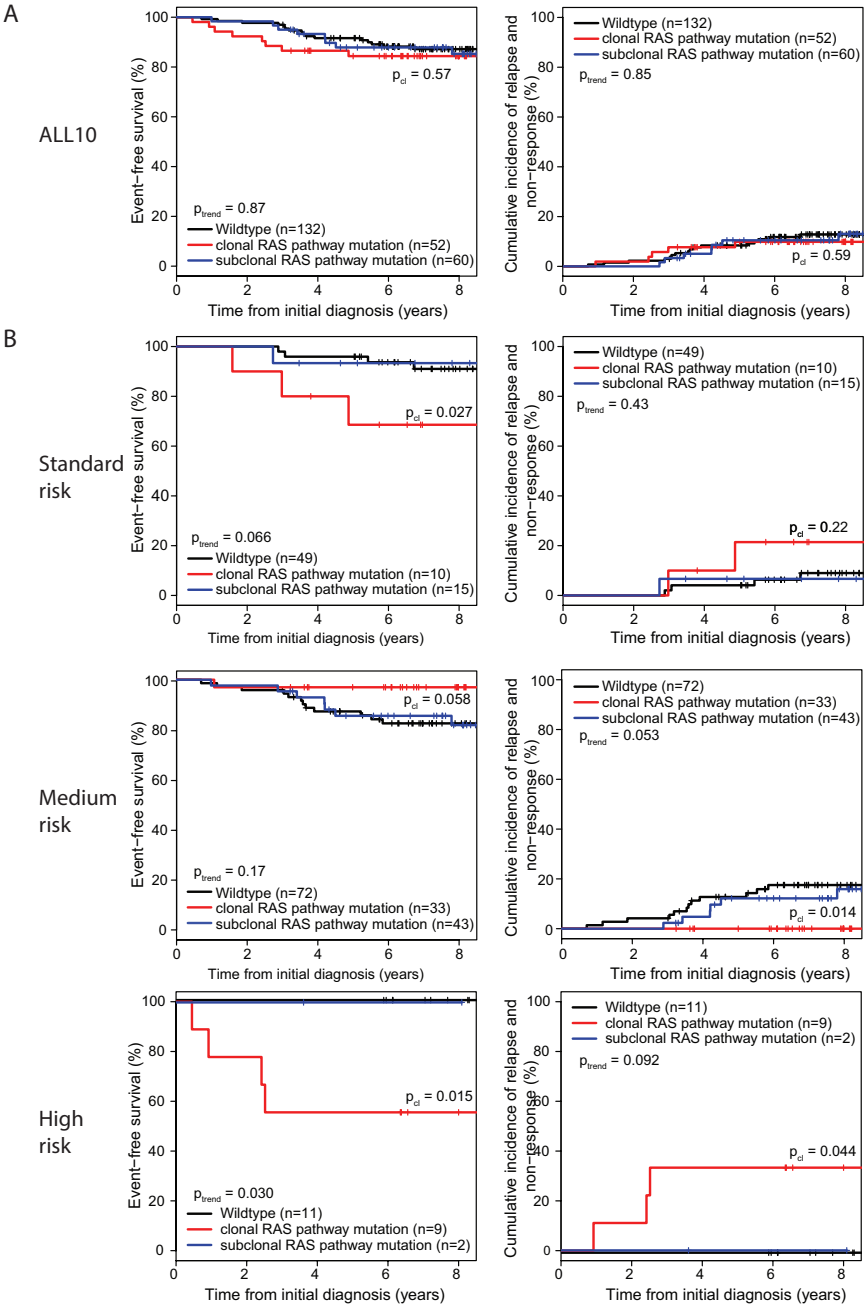

Figure 2. Clinical outcome of patients carrying clonal or subclonal RAS pathway mutations. Event-free survival (left panel) and cumulative incidence of relapse and non-response (CIR, right panel) **(A)** within the ALL10 cohort (n=244) and **(B)** divided by the three risk arms of ALL10. SR: Standard-risk group, MR: Medium-risk group, HR: High-risk group. ptrend represents the p-value in a log-rank (EFS) or Gray-test (CIR) across all three groups, p_{cl} represents the p-value in a log-rank or Gray-test comparing wildtype patients and those with a clonal RAS pathway mutation.

Table 2. Clinical outcome of patients with clonal or subclonal RAS pathway mutations.

		Mutation Status	n=	EFS			CIR	
				5-year EFS in % (s.e.)	Cox's hazard ratio[a]	Log-rank p[cl]=	5-year CIR in % (s.e.)	Gray's test p[cl]=
ALL10[b]		Wildtype	135	92 (2)			8 (2)	
		Mutated	109	86 (3)			11 (3)	
ALL10[b]		Wildtype	135	92 (2)			8 (2)	
		Subclonal	59	88 (4)			11 (4)	
		Clonal	50	84 (5)			10 (4)	
	SR	Wildtype	49	96 (3)			4 (3)	
		Subclonal	15	93 (6)			7 (7)	
		Clonal	10	69 (15)	4.57 (CI: 1.02-20.5)	0.027	21 (14)	
	MR	Wildtype	75	88 (4)			12 (4)	
		Subclonal	42	85 (6)			12 (5)	
		Clonal	31	97 (3)		0.058	0	0.01
	HR	Wildtype	11	100			0	
		Subclonal	2	n/a[c]			n/a[c]	
		Clonal	9	56 (16.6)		0.015	33 (17)	0.044

Only p-values <0.1 are shown. EFS: Event-free survival; CIR: Cumulative incidence of relapse and non-response; pcl: p-value for comparison clonal vs. wildtype cases; SR: Standard risk; MR: Medium risk; HR: High risk; [a] Only shown if significantly different, reference group: wildtype cases; [b] all tests stratified for risk arms of this protocol (SR, MR, and HR). [c] 5-year follow-up only reached by one patient.

according to white blood cell count, age, immunophenotype, and *ex vivo* drug response. Small group sizes are limiting this analysis and differences were not statistically significant, but the trends support our results of the DCOG ALL10 study. In standard risk-treated cases, those with clonal but not subclonal mutations more often suffered from a relapse than did non-mutated cases, whereas this prognostic impact was absent in the medium risk-treated group (Figure S7).

Ex vivo RESISTANCE TO CHEMOTHERAPEUTIC AGENTS

Ex vivo cytotoxicity data of prednisolone, L-asparaginase, vincristine, daunorubicin, 6-mercaptopurine, and 6-thiopurine was available for 211 cases. RAS pathway mutated cells were median 3-fold more resistant to prednisolone compared to wildtype cases (Figure 3A; p=0.024). Leukemic cells harboring clonal or subclonal KRAS G13 mutations were most resistant to prednisolone: these cells were median >2000-fold more resistant compared to wildtype cells (p=0.001 and p=0.006, respectively, Table S9, Figure 3A and Figure S8). Clonal NRAS G13 mutations showed a trend, but the difference was not significant (p=0.18). NRAS and KRAS G12 mutations did not significantly affect resistance towards prednisolone, although several cases were highly resistant. Mutations in *PTPN11* and *FLT3* were not associated with cellular prednisolone resistance (Table S10 and Figure S8A).

Ex vivo cytotoxicity of the tubulin-inhibitor vincristine was also reduced in RAS pathway mutated cells (Figure 3B): Cases with a clonal *KRAS* or *PTPN11* mutations were significantly more resistant to vincristine compared to wildtype cases (15-fold, p=0.005 and 5-fold, p=0.041, respectively). A trend was observed for clonal NRAS G13 mutations (3-fold, p=0.074). No significant difference was observed for KRAS G12 mutations, and an inverse trend was found in cases carrying an NRAS G12 mutation (5-fold decrease, p=0.057, see also Figure S8B).

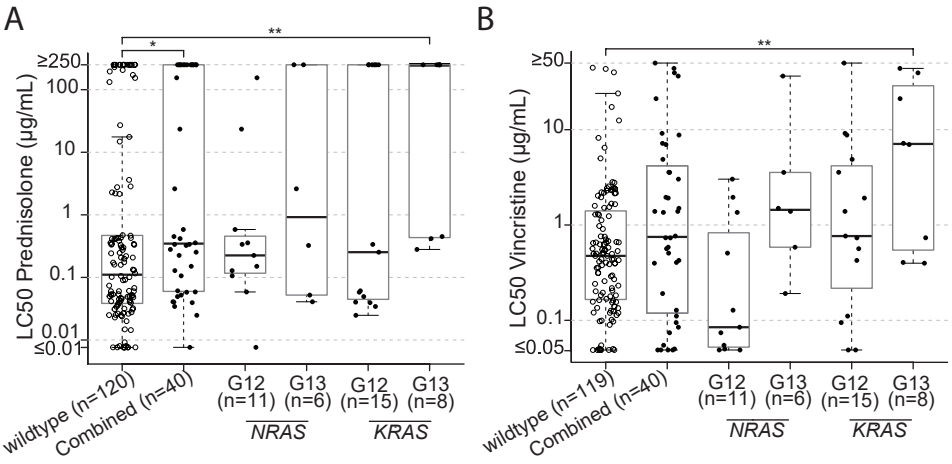

Figure 3. RAS pathway mutations and ex vivo cytotoxicity of chemotherapeutic agents.

Ex vivo sensitivity of 211 primary patient samples towards **(A)** prednisolone and **(B)** vincristine, distinguished by RAS mutation status. Only clonally mutated cases are considered. Only KRAS and NRAS mutated groups are shown due to low recurrence of other mutations (see also supplement). Combined: All cases with a clonal mutation in NRAS, KRAS, PTPN11, FLT3. Groups were compared by Mann-Whitney U test, * $p<0.05$, ** $p<0.01$. LC50-values were evaluated by MTT assays as reported previously.

In K/NRAS G13 mutated cases the glycine (G) was replaced by an aspartic acid (D) in 13 of 15 cases. In contrast, the type of amino acid being substituted at the G12 position was more variable (see also Figure S6). As visualized in Figure S9 the substituting amino acid was not predictive for *ex vivo* prednisolone or vincristine resistance.

In contrast, wildtype cases tended to be more resistant towards L-asparaginase *ex vivo* than RAS pathway mutated cases, however, this trend was not significant (Table S10). No consistent association of mutation status with *ex vivo* drug response was observed for daunorubicin, 6-thioguanine, and 6-mercaptopurine (Figure S10).

RAS pathway mutations at relapse

RAS pathway mutations were detected in 13 out of 19 cases with matched initial diagnosis and relapse samples (Figure 4). Ten mutations were found at diagnosis, and ten at relapse (53%). From diagnosis onwards, the evolution of RAS pathway mutations followed three distinct patterns: In three cases, a clonal RAS pathway mutation was detected at initial diagnosis and at relapse ("Retained"). In seven cases, a subclonal mutation (four patients) or no mutation (three patients) was observed at diagnosis, but at relapse a RAS pathway mutation was detected with higher VAF ("Gained"). In six of these relapses the mutation was clonal, in one it was subclonal. One of these cases was remarkable in that five different subclones were observed at diagnosis but only one of these mutations (NRAS G12S) was found at relapse. Loss of one and selection of a second clone was observed in two cases, where they constituted the major clone in all subsequent relapses. In three cases, the initially observed RAS pathway mutation was not detected at relapse ("Lost"). For all "lost"mutations VAF at initial diagnosis was lower than 10%. Remarkably, in nine out of

ten relapse cases a single, clonal mutation was observed (VAF of 27% or higher).

MEK-inhibitors as therapeutic option

The MEK-inhibitor trametinib was cytotoxic to RAS mutant but not wildtype leukemic cells in a range of concentrations (Figure 5A and Figure S11A). This effect is also illustrated by individual data points at a fixed concentration of 0.14μM (Figure 5B, p=0.001). High levels of MEK1/2 and ERK1/2 phosphorylation indicated an activated RAS pathway in mutant but not in wildtype cells (Figure 5C). The cytotoxicity of increasing trametinib concentrations corresponded with effective reduction of ERK1/2 phosphorylation (Figure S11B). In addition, we found that intrinsic resistance to prednisolone could be reversed by trametinib irrespective of RAS mutation status (Figure 5D), which corroborates our previous findings.[30]

Discussion

The RAS pathway is the most frequently mutated pathway in cancer, and may serve as treatment target.[7, 8, 49] Recent reports suggest that RAS pathway mutations are recurrent in pediatric BCP-ALL.[20, 27, 30, 31, 50] However, frequency and prognostic value of subclonal mutations at initial presentation was unknown. In this study we addressed the clinical value of mutations in thirteen key members of the RAS pathway using deep targeted sequencing, which allowed detection of subclones down to 1% VAF. Our study cohort contained 461 newly diagnosed cases and represents all subtypes and risk groups of BCP-ALL, with a distribution comparable to the general pediatric BCP-ALL population.

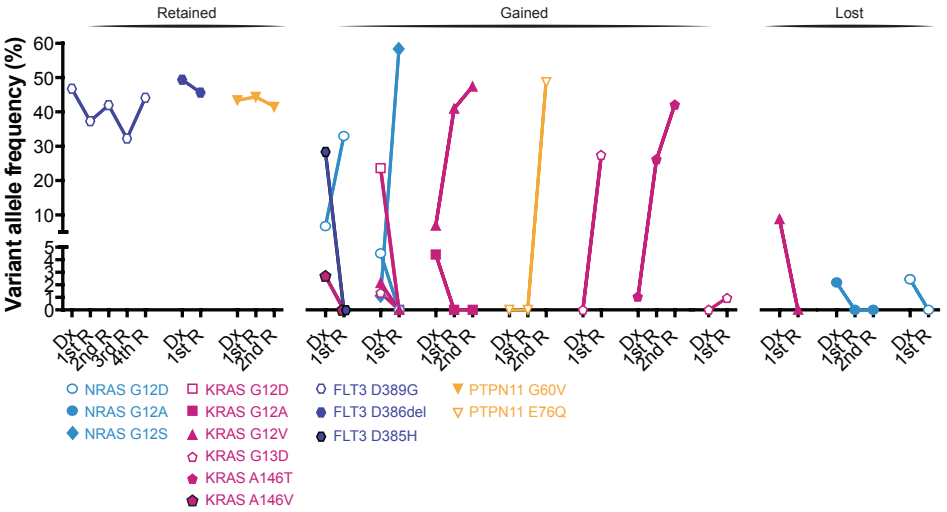

Figure 4. Evolution of clonal and subclonal RAS pathway mutations between initial diagnosis and subsequent relapse in thirteen BCP-ALL cases.

Variant allele frequency of all RAS pathway mutations found at initial diagnosis and/or relapse(s) is shown for cases with RAS pathway mutations detected at either time point (13 of 19). Colours distinguish affected genes, symbols distinguish observed variants. Dx: Initial diagnosis sample; R: relapse sample.

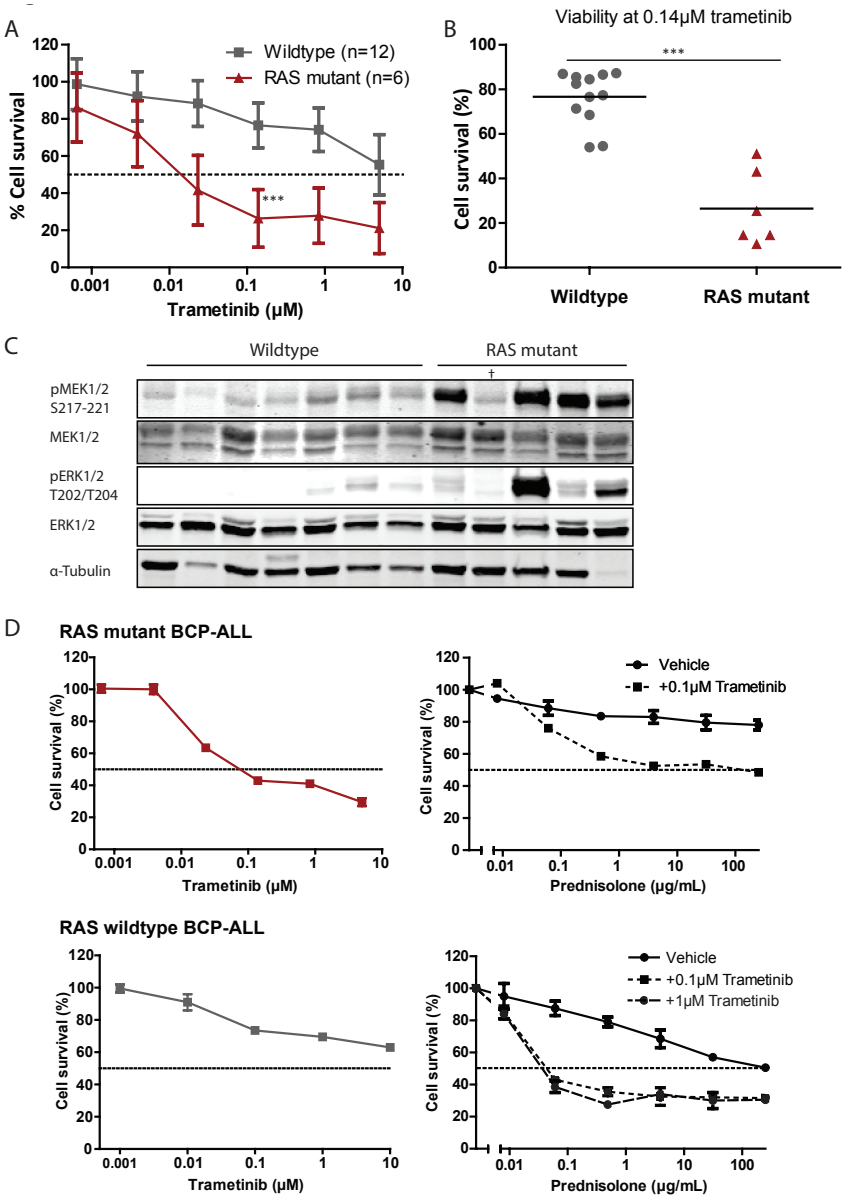

Figure 5. The MEK-inhibitor trametinib effectively kills RAS mutant primary BCP-ALL cells.

(A) Sensitivity towards the MEK-inhibitor trametinib in primary or xenograft-derived BCP-ALL cells. Mean and standard deviation are shown. **(B)** Relative cell survival at 0.14μM trametinib split up per case. Grey circles represent wildtype cases, red triangles represent RAS pathway mutant cases. Bars represent group mean. Groups were compared by Mann-Whitney U test, ***p=0.001. **(C)** Western blot analysis of phospho-ERK (T202/Y204) and phospho-MEK (S217/S221) in a subset of samples tested in panel A. †Sample isolated after thawing, cells previously tested positive. **(D)** *Ex vivo* response to trametinib (left panels) and sensitization towards prednisolone (right panels) in one NRAS G12D-mutant and one RAS pathway wildtype case.

We identified clonal RAS pathway mutations (≥25% VAF) in 24.1% and subclonal mutations (<25% VAF) in 20.1% of patients at initial diagnosis. This total of 44.2% is considerably higher than the 15% mutation frequency previously detected by Sanger sequencing, and shows that RAS pathway activation cooperates with several primary oncogenic lesions.[20, 31] The vast majority of mutations (98%) occurred in *NRAS, KRAS*, *FLT3*, and *PTPN11*, revealing a central role of these genes in pediatric BCP-ALL.

We observed high mutation frequencies among high hyperdiploid, *MLL-AF4*-rearranged, *BCR-ABL1*-like, and B-other cases, moderate frequencies among *ETV6-RUNX1* cases, and rarely observed them in *TCF3-PBX1* and *BCR-ABL1*-rearranged cases, confirming reports of smaller sample sets.[23, 27, 32, 51]

The BCR-ABL1 fusion is known to require MAPK signaling, but the low mutation frequency suggests independent RAS pathway activation is not required for this aggressive disease.[52-56] *BCR-ABL1*-like cases, who bare strong similarities with *BCR-ABL1*-positive leukemia, frequently carry RAS pathway mutations. These were mutually exclusive with tyrosine kinase-fusions, suggesting divergent pathogenic mechanisms. Our data further show that RAS pathway activating mutations play a role in about half of all B-other patients. The largest group of RAS pathway mutated cases was observed within high hyperdiploid cases. Our extensive screen extends the existing knowledge by revealing frequent subclonal events.[27, 32, 57, 58] Our data advocate MEK inhibitors as treatment option in high hyperdiploid cases with poor therapy response. We further identified several secondary aberrations that co-occurred less or more frequently with RAS pathway mutations. Interestingly, RAS pathway mutant cases infrequently carried BTG1 deletions, which have recently been linked to glucocorticoid resistance and may represent a distinct resistance mechanism in RAS pathway wildtype cases.[59]

In the largest dataset analyzed so far (n=211), we confirmed the association of RAS pathway mutations with prednisolone resistance.[30, 60, 61] Additionally, RAS pathway mutant cells were *ex vivo* resistant to vincristine, but not to L-asparaginase, daunorubicin, and thiopurines. This suggests that patients with RAS pathway mutations could profit from intensification of these drugs.

Patients with high MRD levels ($\geq 10^{-3}$ after induction or consolidation) are at higher risk for relapse and treated more intensely, also in DCOG ALL10.[4, 62] Patients with clonal RAS pathway mutations treated in the DCOG standard risk arm had an unfavorable clinical outcome despite negative MRD levels. Since the prognosis of clonally mutated patients is highly favorable in the medium risk group (5-year EFS 97%, CIR 0%; Figure 2B), MRD-low risk patients with clonal RAS pathway mutations may benefit from medium risk treatment which includes intensive PEG-asparaginase and dexamethasone/vincristine pulses during maintenance therapy.[4] This is further supported by RAS mutated patients being relatively sensitive to asparaginase *ex vivo*. The prognosis of those 20.1% of patients with subclonal mutations was similar to wildtype cases, and they generally presented with good risk features. Therefore, subclonal mutations in RAS pathway genes should not be used to assign patients to a higher risk group or treatment with a MEK-inhibitor.

Evaluation of 19 cases with matched diagnosis and relapse material gave an important insight into the evolution of RAS pathway mutations: 1) Clonal mutations at diagnosis were preserved at relapse, 2) subclonal mutations detected at initial diagnosis were

often found at relapse, and 3) a single, clonal mutation was found in nine out of ten relapses. These observations confirm that RAS pathway mutations are frequent at relapse in pediatric BCP-ALL.[28, 29, 63, 64] The reduced mutational diversity at relapse suggests outgrowth of a single clone with stronger dependence on MAPK signaling, which may increase the chance of success for RAS-targeted therapy.

NRAS and *KRAS* mutations increase the risk for therapy failure at relapse, demanding alternative treatment options.[27, 28] These patients may be eligible for MEK-inhibitors such as trametinib. Leukemic cells with RAS pathway mutations were sensitive to trametinib, while wildtype cells were not. We further confirm our previous finding that MEK-inhibition can synergize with prednisolone.[30] Interestingly, nine of eleven RAS mutated cases allocated to the high risk arm had a poor in vivo response to prednisone after one week of therapy. This provides a rationale to combine MEK-inhibitors with glucocorticoids. Notably, within our data no correlation was observed between the response to prednisolone and the response to trametinib.

In conclusion, clonal mutations in *NRAS, KRAS, PTPN11*, and *FLT3* are associated with therapy resistance. Given that clonal mutations at initial diagnosis were retained at relapse and that subclonal mutations often expanded at relapse, RAS pathway mutations may serve as a biomarker to identify patients eligible for MEK/ERK targeted therapy. The synergistic effect between MEK-inhibition and prednisolone may be of additional advantage. While our results and supremacy of MEK inhibitors require confirmation in independent cohorts, our data suggests screening a) all cases that are eligible for treatment reduction based on MRD, and b) patients for whom treatment intensification is advised and who may benefit from adjuvant MEK inhibitor treatment. Methodically, accurate detection of any clonal RAS pathway mutation should be ensured, but detection of subclonal mutations is not required.

Authorship

I.S.J, M.L.d.B. designed/performed experiments, analyzed/interpreted data, and wrote the manuscript, A.Q.H and J.M.B. analyzed/interpreted data, I.M.A., N.J.M.B., M.J.K., and E.C. designed sequencing experiments, E.M.P.S. designed/performed experiments and obtained xenograft material, A.B. and C.v.d.V. obtained xenograft samples, H.A.d.G.-K., M.A.H., and G.E., provided samples and clinical information, M.L.d.B. and R.P. conceptualized the study and interpreted results. All authors read, revised, and approved the manuscript. Correspondence: Monique den Boer, E-Mail: m.l.denboer@erasmusmc.nl.

Acknowledgement

This work was supported by the NWO VICI program (grant 016.126.612), the Dutch Cancer Society (grants AMC 2008-4265 and EMCR 2014-6998), and the KIKA Foundation (grants 132 and 161) and the Pediatric Oncology Foundation Rotterdam. The CPCT is supported by the NutsOhra Foundation (grant 1102-062). We thank Ies Nijman and Annelies Smouters for their help in setting up the analysis pipeline.

Conflict of interest

The authors declare no conflict of interest.

References

1. Pui CH. Genomic and pharmacogenetic studies of childhood acute lymphoblastic leukemia. Front Med 2015 Mar; 9(1): 1-9.

2. Pui CH, Evans WE. A 50-year journey to cure childhood acute lymphoblastic leukemia. Semin Hematol 2013 Jul; 50(3): 185-196.

3. Marshall GM, Dalla Pozza L, Sutton R, Ng A, de Groot-Kruseman HA, van der Velden VH, et al. High-risk childhood acute lymphoblastic leukemia in first remission treated with novel intensive chemotherapy and allogeneic transplantation. Leukemia : official journal of the Leukemia Society of America, Leukemia Research Fund, UK 2013 Jul; 27(7): 1497-1503.

4. Pieters R, de Groot-Kruseman H, Van der Velden V, Fiocco M, van den Berg H, de Bont E, et al. Successful Therapy Reduction and Intensification for Childhood Acute Lymphoblastic Leukemia Based on Minimal Residual Disease Monitoring: Study ALL10 From the Dutch Childhood Oncology Group. J Clin Oncol 2016 Aug 01; 34(22): 2591-2601.

5. Klumper E, Pieters R, Veerman AJ, Huismans DR, Loonen AH, Hahlen K, et al. In vitro cellular drug resistance in children with relapsed/refractory acute lymphoblastic leukemia. Blood 1995 Nov 15; 86(10): 3861-3868.

6. Knight T, Irving JA. Ras/Raf/MEK/ERK Pathway Activation in Childhood Acute Lymphoblastic Leukemia and Its Therapeutic Targeting. Front Oncol 2014; 4: 160.

7. Pylayeva-Gupta Y, Grabocka E, Bar-Sagi D. RAS oncogenes: weaving a tumorigenic web. Nature reviews Cancer 2011 Nov; 11(11): 761-774.

8. Ledford H. Cancer: The Ras renaissance. Nature 2015 Apr 16; 520(7547): 278-280.

9. Prior IA, Lewis PD, Mattos C. A comprehensive survey of Ras mutations in cancer. Cancer research 2012 May 15; 72(10): 2457-2467.

10. Burgess MR, Hwang E, Firestone AJ, Huang T, Xu J, Zuber J, et al. Preclinical efficacy of MEK inhibition in Nras-mutant AML. Blood 2014 Dec 18; 124(26): 3947-3955.

11. Caunt CJ, Sale MJ, Smith PD, Cook SJ. MEK1 and MEK2 inhibitors and cancer therapy: the long and winding road. Nature reviews Cancer 2015 Sep 24; 15(10): 577-592.

12. Hatzivassiliou G, Haling JR, Chen H, Song K, Price S, Heald R, et al. Mechanism of MEK inhibition determines efficacy in mutant KRAS- versus BRAF-driven cancers. Nature 2013 Sep 12; 501(7466): 232-236.

13. Sullivan R, LoRusso P, Boerner S, Dummer R. Achievements and challenges of molecular targeted therapy in melanoma. American Society of Clinical Oncology educational book / ASCO American Society of Clinical Oncology Meeting 2015; 35: 177-186.

14. Robert C, Karaszewska B, Schachter J, Rutkowski P, Mackiewicz A, Stroiakovski D, et al. Improved overall survival in melanoma with combined dabrafenib and trametinib. N Engl J Med 2015 Jan; 372(1): 30-39.

15. Farley J, Brady WE, Vathipadiekal V, Lankes HA, Coleman R, Morgan MA, et al. Selumetinib in women with recurrent low-grade serous carcinoma of the ovary or peritoneum: an open-label, single-arm, phase 2 study. Lancet Oncol 2013 Feb; 14(2): 134-140.

16. Ho AL, Grewal RK, Leboeuf R, Sherman EJ, Pfister DG, Deandreis D, et al. Selumetinib-enhanced radioiodine uptake in advanced thyroid cancer. N Engl J Med 2013 Feb 14; 368(7): 623-632.

17. Borthakur G, Popplewell L, Kirschbaum MH, Foran JM, Kadia TM, Jabbour E, et al. Phase I/II trial of the MEK1/2 inhibitor GSK1120212 (GSK212) in patients (pts) with relapsed/refractory myeloid malignancies: Evidence of activity in pts with RAS mutation. Journal of Clinical Oncology 2011 May 20; 29(15).

18. Long GV, Stroyakovskiy D, Gogas H, Levchenko E, de Braud F, Larkin J, et al. Combined BRAF and MEK inhibition versus BRAF inhibition alone in melanoma. N Engl J Med 2014 Nov 13; 371(20): 1877-1888.

19. Ward AF, Braun BS, Shannon KM. Targeting oncogenic Ras signaling in hematologic malignancies. Blood 2012 Oct 25; 120(17): 3397-3406.

20. Perentesis JP, Bhatia S, Boyle E, Shao Y, Shu XO, Steinbuch M, et al. RAS oncogene mutations and outcome of therapy for childhood acute lymphoblastic leukemia. Leukemia : official journal of the Leukemia Society of America, Leukemia Research Fund, UK 2004 Apr; 18(4): 685-692.

21. Neri A, Knowles DM, Greco A, McCormick F, Dalla-Favera R. Analysis of RAS oncogene mutations in human lymphoid malignancies. Proceedings of the National Academy of Sciences of the United States of America 1988 Dec; 85(23): 9268-9272.

22. Zhang J, Mullighan CG, Harvey RC, Wu G, Chen X, Edmonson M, et al. Key pathways are frequently mutated in high-risk childhood acute lymphoblastic leukemia: a report from the Children's Oncology Group. Blood 2011 Sep 15; 118(11): 3080-3087.

23. Paulsson K, Lilljebjorn H, Biloglav A, Olsson L, Rissler M, Castor A, et al. The genomic landscape of high hyperdiploid childhood acute lymphoblastic leukemia. Nature genetics 2015 Jun; 47(6): 672-676.

24. Holmfeldt L, Wei L, Diaz-Flores E, Walsh M, Zhang J, Ding L, et al. The genomic landscape of hypodiploid acute lymphoblastic leukemia. Nature genetics 2013 Mar; 45(3): 242-252.

25. Andersson AK, Ma J, Wang J, Chen X, Gedman AL, Dang J, et al. The landscape of somatic mutations in infant MLL-rearranged acute lymphoblastic leukemias. Nature genetics 2015 Apr; 47(4): 330-337.

26. Ma X, Edmonson M, Yergeau D, Muzny DM, Hampton OA, Rusch M, et al. Rise and fall of subclones from diagnosis to relapse in pediatric B-acute lymphoblastic leukaemia. Nat Commun 2015;

6: 6604.

27. Irving J, Matheson E, Minto L, Blair H, Case M, Halsey C, et al. Ras pathway mutations are prevalent in relapsed childhood acute lymphoblastic leukemia and confer sensitivity to MEK inhibition. Blood 2014 Nov 27; 124(23): 3420-3430.

28. Irving JA, Enshaei A, Parker CA, Sutton R, Kuiper RP, Erhorn A, et al. Integration of genetic and clinical risk factors improves prognostication in relapsed childhood B-cell precursor acute lymphoblastic leukemia. Blood 2016 Aug 18; 128(7): 911-922.

29. Oshima K, Khiabanian H, da Silva-Almeida AC, Tzoneva G, Abate F, Ambesi-Impiombato A, et al. Mutational landscape, clonal evolution patterns, and role of RAS mutations in relapsed acute lymphoblastic leukemia. Proceedings of the National Academy of Sciences of the United States of America 2016 Sep 21.

30. Aries IM, van den Dungen RE, Koudijs MJ, Cuppen E, Voest E, Molenaar JJ, et al. Towards personalized therapy in pediatric acute lymphoblastic leukemia: RAS mutations and prednisolone resistance. Haematologica 2015 Apr; 100(4): e132-136.

31. Case M, Matheson E, Minto L, Hassan R, Harrison CJ, Bown N, et al. Mutation of genes affecting the RAS pathway is common in childhood acute lymphoblastic leukemia. Cancer research 2008 Aug 15; 68(16): 6803-6809.

32. Malinowska-Ozdowy K, Frech C, Schonegger A, Eckert C, Cazzaniga G, Stanulla M, et al. KRAS and CREBBP mutations: a relapse-linked malicious liaison in childhood high hyperdiploid acute lymphoblastic leukemia. Leukemia : official journal of the Leukemia Society of America, Leukemia Research Fund, UK 2015 Aug; 29(8): 1656-1667.

33. Den Boer ML, Harms DO, Pieters R, Kazemier KM, Gobel U, Korholz D, et al. Patient stratification based on prednisolone-vincristine-asparaginase resistance profiles in children with acute lymphoblastic leukemia. J Clin Oncol 2003 Sep 1; 21(17): 3262-3268.

34. Den Boer ML, van Slegtenhorst M, De Menezes RX, Cheok MH, Buijs-Gladdines JG, Peters ST, et al. A subtype of childhood acute lymphoblastic leukaemia with poor treatment outcome: a genome-wide classification study. Lancet Oncol 2009 Feb; 10(2): 125-134.

35. van der Veer A, Waanders E, Pieters R, Willemse ME, Van Reijmersdal SV, Russell LJ, et al. Independent prognostic value of *BCR-ABL1*-like signature and IKZF1 deletion, but not high CRLF2 expression, in children with B-cell precursor ALL. Blood 2013 Oct 10; 122(15): 2622-2629.

36. Kaspers GJ, Veerman AJ, Pieters R, Van Zantwijk CH, Smets LA, Van Wering ER, et al. In vitro cellular drug resistance and prognosis in newly diagnosed childhood acute lymphoblastic leukemia. Blood 1997 Oct 1; 90(7): 2723-2729.

37. Li H. Aligning sequence reads, clone sequences and assembly contigs with BWA-MEM. arXiv preprint arXiv:13033997 2013.

38. Garrison E, Marth G. Haplotype-based variant detection from short-read sequencing. arXiv preprint arXiv:12073907 2012.

39. Koboldt DC, Zhang Q, Larson DE, Shen D, McLellan MD, Lin L, et al. VarScan 2: somatic mutation and copy number alteration discovery in cancer by exome sequencing. Genome Res 2012 Mar; 22(3): 568-576.

40. Li H. A statistical framework for SNP calling, mutation discovery, association mapping and population genetical parameter estimation from sequencing data. Bioinformatics 2011 Nov 1; 27(21): 2987-2993.

41. DePristo MA, Banks E, Poplin R, Garimella KV, Maguire JR, Hartl C, et al. A framework for variation discovery and genotyping using next-generation DNA sequencing data. Nature genetics 2011 May; 43(5): 491-498.

42. Cingolani P, Platts A, Wang le L, Coon M, Nguyen T, Wang L, et al. A program for annotating and predicting the effects of single nucleotide polymorphisms, SnpEff: SNPs in the genome of Drosophila melanogaster strain w1118; iso-2; iso-3. Fly 2012 Apr-Jun; 6(2): 80-92.

43. Liu X, Wu C, Li C, Boerwinkle E. dbNSFP v3.0: A One-Stop Database of Functional Predictions and Annotations for Human Nonsynonymous and Splice-Site SNVs. Hum Mutat 2016 Mar; 37(3): 235-241.

44. Forbes SA, Beare D, Gunasekaran P, Leung K, Bindal N, Boutselakis H, et al. COSMIC: exploring the world's knowledge of somatic mutations in human cancer. Nucleic Acids Res 2015 Jan; 43(Database issue): D805-811.

45. Escherich G, Troger A, Gobel U, Graubner U, Pekrun A, Jorch N, et al. The long-term impact of in vitro drug sensitivity on risk stratification and treatment outcome in acute lymphoblastic leukemia of childhood (CoALL 06-97). Haematologica 2011 Jun; 96(6): 854-862.

46. Gray RJ. cmprsk: Subdistribution Analysis of Competing Risks. 2013; R package version 2.2-7 http://CRAN.R-project.org/package=cmprsk.

47. de Wreede LC, Fiocco M, Putter H. mstate: An R Package for the Analysis of Competing Risks and Multi-State Models. J Stat Softw 2011 Jan; 38(7): 1-30.

48. Therneau T. A Package for Survival Analysis in S. 2012; R Package version 2.38-3.

49. Stephen AG, Esposito D, Bagni RK, McCormick F. Dragging ras back in the ring. Cancer cell 2014 Mar 17; 25(3): 272-281.

50. Driessen EM, van Roon EH, Spijkers-Hagelstein JA, Schneider P, de Lorenzo P, Valsecchi MG, et al. Frequencies and prognostic impact of RAS mutations in MLL-rearranged acute lymphoblastic leukemia in infants. Haematologica 2013 Jun; 98(6): 937-944.

51. Fischer U, Forster M, Rinaldi A, Risch T, Sungalee S, Warnatz HJ, et al. Genomics and drug profiling of fatal TCF3-HLF-positive acute lymphoblastic leukemia identifies recurrent mutation patterns and therapeutic options. Nature genetics 2015 Sep; 47(9): 1020-1029.

52. Cilloni D, Saglio G. Molecular pathways: BCR-ABL. Clinical cancer research : an official journal of the American Association for Cancer Research 2012 Feb 15; 18(4): 930-937.

53. Deininger MW, Goldman JM, Melo JV. The molecular biology of chronic myeloid leukemia. Blood 2000 Nov 15; 96(10): 3343-3356.

54. Shojaee S, Caeser R, Buchner M, Park E,

Swaminathan S, Hurtz C, et al. Erk Negative Feedback Control Enables Pre-B Cell Transformation and Represents a Therapeutic Target in Acute Lymphoblastic Leukemia. Cancer cell 2015 Jul 13; 28(1): 114-128.

55. Sawyers CL, McLaughlin J, Witte ON. Genetic requirement for Ras in the transformation of fibroblasts and hematopoietic cells by the Bcr-Abl oncogene. The Journal of experimental medicine 1995 Jan 1; 181(1): 307-313.

56. Reichert A, Heisterkamp N, Daley GQ, Groffen J. Treatment of Bcr/Abl-positive acute lymphoblastic leukemia in P190 transgenic mice with the farnesyl transferase inhibitor SCH66336. Blood 2001 Mar 1; 97(5): 1399-1403.

57. Chen C, Bartenhagen C, Gombert M, Okpanyi V, Binder V, Rottgers S, et al. Next-generation-sequencing of recurrent childhood high hyperdiploid acute lymphoblastic leukemia reveals mutations typically associated with high risk patients. Leukemia research 2015 Sep; 39(9): 990-1001.

58. Davidsson J, Paulsson K, Lindgren D, Lilljebjorn H, Chaplin T, Forestier E, et al. Relapsed childhood high hyperdiploid acute lymphoblastic leukemia: presence of preleukemic ancestral clones and the secondary nature of microdeletions and RTK-RAS mutations. Leukemia : official journal of the Leukemia Society of America, Leukemia Research Fund, UK 2010 May; 24(5): 924-931.

59. Scheijen B, Boer JM, Marke R, Tijchon E, van Ingen Schenau D, Waanders E, et al. Tumor suppressors BTG1 and IKZF1 cooperate during mouse leukemia development and increase relapse risk in B-cell precursor acute lymphoblastic leukemia patients. Haematologica 2017 Mar; 102(3): 541-551.

60. Jones CL, Gearheart CM, Fosmire S, Delgado-Martin C, Evensen NA, Bride K, et al. MAPK signaling cascades mediate distinct glucocorticoid resistance mechanisms in pediatric leukemia. Blood 2015 Nov 5; 126(19): 2202-2212.

61. Rambal AA, Panaguiton ZL, Kramer L, Grant S, Harada H. MEK inhibitors potentiate dexamethasone lethality in acute lymphoblastic leukemia cells through the pro-apoptotic molecule BIM. Leukemia : official journal of the Leukemia Society of America, Leukemia Research Fund, UK 2009 Oct; 23(10): 1744-1754.

62. van Dongen JJ, Seriu T, Panzer-Grumayer ER, Biondi A, Pongers-Willemse MJ, Corral L, et al. Prognostic value of minimal residual disease in acute lymphoblastic leukaemia in childhood. Lancet 1998 Nov 28; 352(9142): 1731-1738.

63. Irving J, Matheson E, Minto L, Blair H, Case M, Halsey C, et al. Ras pathway mutations are highly prevalent in relapsed childhood acute lymphoblastic leukaemia, may act as relapse-drivers and confer sensitivity to MEK inhibition. Blood 2014; 124(23): 3420-3430.

64. Vesely C, Frech C, Eckert C, Cario G, Mecklenbrauker A, Zur Stadt U, et al. Genomic and transcriptional landscape of P2RY8-CRLF2-positive childhood acute lymphoblastic leukemia. Leukemia : official journal of the Leukemia Society of America, Leukemia Research Fund, UK 2017 Jan 06.

Full online Material and Methods

Patient material, patient-derived xenografts (PDX), cell lines, and subtype classification

This study comprised children with newly diagnosed BCP-ALL enrolled in consecutive Dutch Childhood Oncology Group trials (DCOG ALL-8, ALL-9 and ALL-10) and German Cooperative ALL trials (COALL 06-97 and 07-03). Written informed consent was obtained from parents or guardians and institutional review boards approved the use of excess of diagnostic material for research purposes. These studies were conducted in accordance with the Declaration of Helsinki. Mononuclear cells were isolated using density gradient centrifugation with Lymphoprep (Axis Shield, Norway) as described previously.[1] If not indicated otherwise, samples contained at least 90% leukemic blasts evaluated by morphological examination. In some cases this was achieved by negative selection using immunomagnetic beads. Animal experiments were approved by the animal ethics committee (EMC 2863 (103-12-08)). Xenografts of primary patient material were established in three 7-12 week-old female NOD.Cg-*Prkdc*^{scid}*Il2rg*^{tm1Wjl}/SzJ (NSG) mice (Charles River, France) per patient, using intra-femoral injection. Animals were randomly assigned to receive leukemia cell injections.Mice were sacrificed upon signs of overt leukemia or 180 days after transplantation. Leukemic cells were isolated from bone marrow and spleen, and subsequently used for sequencing, western blot, and trametinib cytotoxicity assays. Blast percentage was above >90% by morphological evaluation in all samples, in one case achieved by positive selection using immunomagnetic beads directed

to human CD19 (Miltenyi Biotec, Germany). The leukemic cell line 697 was obtained from the German Collection of Microorganisms and Cell Cultures, regularly checked for mycoplasma contamination, and its identity verified using DNA fingerprinting (DSMZ, Germany).

Subtypes were determined by karyotype, fluorescence in-situ hybridization (FISH) and/or fusion-gene specific PCR, subdividing patients into *ETV6-RUNX1*-rearranged, *BCR-ABL1*-rearranged, high hyperdiploid karyotype (51-65 chromosomes and/or DNA index ≥1.16 and <1.5), *MLL*-rearranged (t(4;11)), *TCF3-PBX1*-rearranged, and B-lineage other (B-other). *BCR-ABL1*-like cases were identified using microarray gene expression profiling by the means of a 110 probeset classifier with proven independent prognostic relevance.[2,3] In 11 cases all subtypes have been excluded, except the extremely rare *TCF3-HLF* fusion. As this is extremely rare, we consider it safe to allocate these cases to the B-other group.

Cell culture

Primary cells were cultured in RPMI-1640 Dutch modified supplemented with 20% FCS, Penicillin, Streptomycin, Fungizone, gentamicin, insulin, selenite, transferrine, and L-Glutamine (all Life Technologies Europe BV, the Netherlands). Cell line 697 was cultured in RPMI-1640 +GlutaMAX, supplemented with 10% FCS, Penicillin, Streptomycin, and Fungizone.

Ex vivo drug cytotoxicity assays

Cell-intrinsic resistance towards common chemotherapeutics was evaluated as previously described.[4] In brief, freshly isolated primary leukemic cells were incubated with a range of concentrations of prednisolone (0.076 - 250µg/mL), vincristine (0.05 – 50µg/mL), daunorubicin (0.002 – 1.2µg/mL), L-asparaginase (0.003 – 10IU/mL), 6-mercaptopurine (0.002 – 0.05µg/mL) and 6-thioguanine (0.02 – 0.5µg/mL). After four days, cell viability was evaluated by adding 3-(4,5-dimethylthiazolyl-2)-2,5-diphenyltetrazolium bromide (MTT) and measuring formazan-conversion with optical density measurement. LC50-values were calculated (concentration at which 50% conversion activity was measured relative to untreated control) and compared between groups using a Mann-Whitney U test. *Ex vivo* sensitivity towards trametinib was measured similarly (range 5µM to 0.6nM and four days incubation). Both primary material and patient-derived xenograft samples were used to evaluate trametinib sensitivity.

Protein isolation and western blot

Leukemic cells were lysed either using radioimmunoprecipitation buffer (Thermo Fisher Scientific) with fresh phosphatase and protease inhibitors (Sigma Aldrich) or in protein lysis buffer pH 7.4 containing 25mM Tris base, 150mM NaCl, 5mM EDTA pH 8.0, 1% Triton X-100, 10% glycerol, 10mM sodium pyrophosphate, 1mM sodium orthovanadate, 10mM glycerolphosphate, dithiothreitol, phenylmethylsulfonyl fluoride, Aprotinin, and Sodium-Fluoride (all Sigma Aldrich). Samples were blotted on nitrocellulose membranes using the BioRad Trans-blot Turbo system and membranes probed with anti-MEK1/2 (#4694), anti-phospho-MEK1/2 S217/221 (#9154), anti-ERK1/2 (#9107), anti-phospho-ERK1/2 T202/Y204 (#4370), and anti-alpha-tubulin (#2144) according to manufacturer's instructions (all Cell Signaling Technologies).

DNA isolation and sequencing

Genomic DNA and RNA were isolated using Trizol reagent according to manufacturer's protocol (Life Technologies), or in some cases using the DNeasy blood and tissue kit (Qiagen). Genomic DNA concentration was determined using the Qubit dsDNA Broad Range Assay Kit (Life Technologies). For TruSeq Custom Amplicon sequencing (Illumina, USA), 100-250ng genomic DNA was used to prepare sequencing libraries according to manufacturer's instructions. Successful library preparation, correct amplicon length, and concentration was assessed using the Labchip GX genomic analyzer (Caliper Life Sciences Benelux N.V., the Netherlands) with the HT DNA 12K Reagent Kit, Version 2. Samples were then pooled equimolarly sequenced on an Illumina MiSeq in paired-end reads of 250bp each. In total, 49 amplicons of mutational hotspot regions in 13 RAS pathway genes were sequenced (Supplemental Table S1). Detailed information on the design and analysis script will be provided upon request.

Sequence reads were exported in fastq format and aligned to the standard 1000 genomes human reference sequences (version b37, from the GATK resource bundle, the Broad institute, USA) using BWA version 0.7.10[5]. We applied the GATK indel realigner version 3.3-0 to remove artefacts caused by indels. Reads mapping outside targeted regions (e.g. due to false priming or poor quality) were excluded. Single nucleotide variants were called with Freebayes version 0.9.18-24[6], Varscan version 2.3.7[7], Bcftools version 1.0[8], and GATK version 3.3-0[9]. The resulting variant call format files were annotated using snpEff and snpSift version 4.1a[10] and dbNSFP version 2.7 database[11]. All variants were combined into a single table and filtered based on several criteria using an in-house developed pipeline: For each sample, variants were excluded if they were reported by only one caller, had coverage of less than 100 reads, or had less than 20 reads supporting the variant allele. Overall, variants were excluded if they did not occur at least once with a variant allele frequency (VAF) >2% or were not distributed equally between runs according to a chi-square test. Furthermore only variants were taken into account that were reported in the COSMIC V73 GRCh37 database (cancer.sanger.ac.uk)[12], lead to an amino acid change, were unlikely to be a germline variant (see below), and not a known SNP. A variant was considered to be a SNP if it had a mean population frequency of 5% or higher across the 1000Gp1 complete human population, 1000Gp1 population of European decent, and the ESP-6500 population of European decent allele frequency database. Variants were labelled as a possible germline variant if they were found in more than 10 samples with a mean and median VAF of more than 40%.

Clonal and subclonal mutations were distinguished based on VAF: assuming heterozygosity, a mutation was considered to be clonal if VAF exceeded 25% (representing 50% of the cells) and subclonal if VAF was <25%. Since a minimum number of 20 variant reads was required for variant calling, sufficient coverage was crucial to detect subclonal mutations. In the 7 most frequently mutated amplicons, coverage allowed detection of clonal mutations in on average 99% of the samples (Supplemental Tables S1 and S2). Subclonal mutations could be reliably detected up to 3% VAF in most cases and amplicons (average 87% of cases). Because detection of variants with a frequency of 1% was limited to a smaller group, the frequency of subclonal mutations is a conservative estimate. However, based on the observed frequencies we calculated that only a small number

of 9 subclonal mutations might be missed in our study (Supplemental Table S2B). In a comparison with 25 samples that were sequenced previously (Ariës et al.13), all variants could be identified by both platforms, indicating a low false-positive rate.

Exon 3 of *NRAS* was sequenced using Sanger sequencing in 253 ALL10 samples, which were part of the clinical outcome analyses. 248 yielded good quality chromatograms. Samples were analyzed by visual inspection of codons 59 to 63 as well as the R package sangerseqR in combination with the tools above to call and annotate detected variants. Primer sequences are available upon request.

Clinical characteristics and statistics

Clinical characteristics were compared using Fisher's exact test in R (version 3.2.1). We analyzed cases from the DCOG and COALL diagnosed between 1992 and 2013 with diagnostic data available (n=432). We restricted the RAS pathway mutated group to those carrying a verified activating mutation in amino acid positions 12, 13, and 146 of NRAS or KRAS or carrying a variant in FLT3 or PTPN11. Event-free survival (EFS) and cumulative incidence of relapse and non-response after induction therapy (CIR) were evaluated in 244 eligible cases treated within one protocol (DCOG ALL10), and analyses were stratified for risk group. Non-eligible were cases who had resided less than 3 months in the Netherlands or who were not treated in a childhood oncology center. Since induction death precludes risk-group allocation these cases (n=5) were excluded. The COALL97/03 cohort consisted of patients treated in the consecutive COALL 06-97 and the COALL 07-03 protocols (n=131). For details see Escherich et al.14 Treatment intensity in arms LR-R and LR-S was considered comparable to DCOG ALL10 standard risk treatment; LR-I, HR-R, and HR-S treatment is comparable to the DCOG ALL10 medium risk treatment. In the COALL97/03 study, no high risk treatment is given that is comparable to the intensity given in the DCOG ALL10 high risk arm. Mean follow-up for patients at risk was 7.7 years (±1.86 years) in ALL10 and 8.6 years (±2.63 years) for COALL97/03. CIR was estimated using a competing risks model and compared using Gray's test. EFS probabilities were estimated using the actuarial Kaplan-Meier method and compared using the log-rank test. Hazard ratios were calculated in SPSS v21 using Cox's proportional hazard model. All reported tests are two-sided, adjustments for multiple testing were deemed expendable due to low numbers of comparisons. Outcome analyses were performed in R 3.2.1, using the packages cmprsk[15] version 2.2-7, mstate version 0.2.7[16], and survival version 2.38-3[17].

Supplemental Tables and Figures

Supplemental Table S1: Median coverage per sample itemized by amplicon. Amplicons are indicated by chromosome and start/end coordinates according to GRCh37. Amplicon ID consists of gene name and a consecutive number, + or – indicate targeted strand. ULSO: Upstream Locus-Specific Oligo, DLSO: Downstream Locus-Specific Oligo

Chromosome	Start	End	Amplicon ID	Targetexon	Median read depth per sample	ULSO	DLSO
1	115258677	115259080	NRAS_1_+	2	1912	GAGGTAGAATTGCGTAA-CAGCTCTCT	AACTTCCGGTCTG-GACGCGCAGTGC
2	39249582	39249982	SOS1_1_+	11	3405	GAGTCCTGAGACCA-GAAAGTTACAAGA	CTTCAATTATATACCC-GAAAAGTCTGC
2	39249854	39250256	SOS1_2_+	11	4303	GTCAGCTGAAGAGAAAAA-CAATTGGATG	CAACCAAAGACCTCTTTTC-TTTGACTAAA
2	39250176	39250579	SOS1_3_+	11	3126	CACTAGGCAGCCTCATCT-GCTCCTCTTT	CTTCCATTATAAATTCATTA-CAACACTGTC
2	39278250	39278665	SOS1_4_+	7	908	AACATTAGCACAATCAGAC-TGGAAGAA	CAAATCACAAGTGTGACT-TAAAACAGG
3	12625886	12626290	RAF1_1_+	17	3037	CTCTAGAGGAAGCAGGAGA-CAGGG	CAAACCCACAGCGGTCC-CTGGG
3	12626160	12626560	RAF1_2_+	16	3993	GCAATATAAGGTGG-GAGTGTTTTGTTTTGT	AGAAGCTGCTGCTAAGGAC-CTTCTAG
3	12626432	12626835	RAF1_3_+	15+16	5824	AACAAAGCCCAAGAATGCT-CTCATTAG	ACAAGTCCTAACCCTC-TAGCTGCTTA
3	12626708	12627112	RAF1_4_+	15	8246	AAAGGGACAGCCTGGCCCC-TAGATGTC	GGATATGCCTCCCCAGATC-TTAGTAAG
3	12627036	12627437	RAF1_5_+	14	5165	AAACTGAATGGGTTGT-TATCCTGCATTC	GAAATGTACAGAAACGCTT-TAAGTTTGC
3	12629037	12629445	RAF1_6_+	13	628	TGAACTGATGGCCCAGT-GAACTAATG	GACCCAG-GCATCAAATTTGTCCCTAA
3	12632242	12632688	RAF1_7_+	12	1282	CAGAGGGACTGGACCGC-CAGCTTTCTA	AGGTTAACTGCTATCGCTA-CAGTTAGG
3	12633174	12633623	RAF1_8_+	11	54	AGAAAAACCTCGTTG-GAAATTAGAATAC	TTGGGGCCCTCCCTTTAC-TAACTGCA
3	12641157	12641607	RAF1_9_+	10	604	CTGCATGATCACAGGTCCT-CTAAACAT	ATCTAAGAGGCCTGCC-CACATCCCTCAT
7	140453074	140453511	BRAF_1_+	16	2800	GGAGGAAAGAAGAAATTAC-CAGAGGTC	CCATTACCATCTTGGACC-TGGAAGAAG
11	533746	534150	HRAS_1_+	3	636	CAAGAGAATATCTGGGCC-TACATTGCT	CAGTTGTCTGGATC-CATTTTGTGGATG
11	534080	534480	HRAS_2_+	2	343	AGGATAGGGCTGGCT-GCAGCCCCTGG	AGTACAGGTGAACCCCGT-GAGGCTGG
11	119148789	119149238	CBL_1_+	8	1529	TTCTGAGTGGAATCCCTGC-CACAAATCC	GAGGCACTCCGCTCAATC-TTGG
11	119149169	119149569	CBL_2_+	9	597	AGCCCTGACCTTCTGATT-CCTGC	GTTAACAGAAAAAGTGAA-GACTTGTTTCC
12	25378499	25378910	KRAS_1_+	4	1413	GAAACCTTAGGAAGTT-CAGTGCAGAGA	TAGTGACAGCCAGCCT-CAGGGCAATTGT
12	25380234	25380683	KRAS_2_+	3	926	CCTGAGAACATCAGAACC-TTTCTGCAT	TCTGGATGGTTTTGGGAA-CGTCAATAT
12	25398208	25398635	KRAS_3_+	2	2064	CCAGCAATGCACAAA-GATTTCAGTGTC	AATGAGGGACCAGTACAT-GAGGACTG
12	112888116	112888551	PTPN11_1_+	3	2576	TAGAGCTGAGAAGCCTT-CGGGGAGTAA	CCACTTTGTAGATGAATAT-GATCCCAC
12	112926839	112927258	PTPN11_2_+	13	1053	ATGCAACCCCTATAGGAT-GAGTGTAAG	GTGGGTGACAGCTCCATTT-CTTCTAAA
13	28592577	28593002	FLT3_1_+	20	1381	GCAGAACAGCAGTCTG-GCTATTTAGAT	TGTGGACGAATATGATC-CAACAATAGA
13	28608193	28608596	FLT3_2_+	13+14	1051	CTTTTGCTCGGAATCT-GCAAAAGATCT	TGTGAGGCTGCTATTTCC-TACTTATTT
13	28610091	28610494	FLT3_3_+	11	172	AATGTCACACAGGAATTC-TGTTTCATC	TGGTAAGAATGGAATGT-GCCAAATGTT

Chromosome	Start	End	Amplicon ID	Targetexon	Median read depth per sample	ULSO	DLSO
15	38545247	38545694	SPRED1_1_+	1	529	GCAATCATTGTGCTTTT-TAGAACACTGAA	GCCAAACATGAGAGA-CACATATTTCTCTTT
15	38591535	38591950	SPRED1_2_+	2	1906	CTTCCATCCATC-CACATTATTCCCTCT	ACAGGGGCCTCAC-CATGGTGGATGC
15	38614381	38614826	SPRED1_3_+	3	293	CCCATCCCCCAA-CAAATGTGTATCAAT	GCAAAGATCAGGAAT-TAGCTTTTCCAT
15	38643086	38643489	SPRED1_4_+	7	3114	CATGCAATTGACATAGAC-TATGATGTG	ACATATATCAAATGCATC-TAATGTAGCTC
15	38643358	38643759	SPRED1_5_+	7	3957	ATTTTTAATGAGGAAGGCT-GCGTCTTA	TTCTGGACATTTCTATGA-TATGTTTTTGG
15	38643684	38644084	SPRED1_6_+	7	1655	GATTCCAGTATTCAGTTTT-CTAAACCAGAC	CTTGCGATGGTTAGCCC-TGGTAGCTTT
15	66727334	66727751	MAP2K1_1_+	2	434	CTGCAAATACTCTACAACC-TGTAACAAAAC	GTCACACGAACAGG-GATCAGAAAAATCT
15	66729037	66729486	MAP2K1_2_+	3	529	TATTGACTTGTGCTCCC-CACTTTGGA	TTGCCCAGGCTGGTGT-GCAACCTCCAT
17	29528006	29528443	NF1_1_+	10	1085	TTCCCTAAATTTAGAACC-GAGCAGTCA	CTCCCAGTAGCCGGGAC-CACAGGCAT
17	29652753	29653190	NF1_2_+	37	2647	CTGAGCCAGGCAGATCTA-TAGAAAAAG	ACAAAAGCCTTTAAATACC-CATGCAGT
17	29654472	29654917	NF1_3_+	38	4061	CATAAAATAAAATTGAT-TAGTGGCATCTGT	GAACAACAGAAACTACCT-GCTGCCA
17	29677138	29677547	NF1_4_+	50	2071	GGTCTCATTTTAAAAGCAA-CAAACCCC	CGGGGTGAAGTGGAGAA-GAATTAAACT
19	4099156	4099558	MAP2K2_1_+	7	179	TGAGCACTTGGGA-CACGTTTCTGTGTG	AACAGAGCATGTTGGGGA-GAAGGAAG
19	4110438	4110845	MAP2K2_2_+	3	775	GGATCCTTTCCTTCTACAC-CATGAACC	AGTGGTGGGGAAGGTCCC-CCTGGAAA
19	4117360	4117773	MAP2K2_3_+	2	1255	AACTATGAGAGGTGCTC-TAGGTACACC	AGAGAGGTTTTATGAAA-GAAAGAGGGA
X	47426580	47427029	ARAF_1_+	10	454	CTGCATGATCACAGGTCCT-CTAAACAT	ATCTAAGAGGCCTGCC-CACATCCCTCAT
X	47428072	47428517	ARAF_2_+	11+12	61	CTTTTGAGAGAGATA-CAAGGTTTCTGT	ACAGATCTGTTTTCT-GCAAAATCATAA
X	47428811	47429228	ARAF_3_+	13	420	TTGTAATTCCCAGAACCCC-CACAAGAG	AGTGTCAGAGGTGGGGAG-GAAAAATAG
X	47429159	47429559	ARAF_4_+	14	287	AGATCCCACTGGC-CACACAGGGTAC	ATCCTGACCAGGAGCCCC-TTAATATCA
X	47430152	47430552	ARAF_5_+	15	220	GTCTGGACTCCTCATGTC-CCACCT	AACCTAAAATTTTCTAGGA-TAAGGACTCCC
X	47430424	47430824	ARAF_6_+	16	527	CTCATGGTGAAA-CACACACACACACA	AGCTGGGGTACTGTCAG-TATCAAGG
X	47430758	47431158	ARAF_7_+	16	360	GGGGCTGGACACC-TTGGGTGGGTGACT	CCCAGGCCGATGAGTTGC-CTGCCT

Supplemental Table S2: Estimate of false negative cases missed due to low coverage in the 8 most frequently mutated regions.

The frequency of 1-3%VAF mutations, 3-5% VAF mutations, and 5-10%VAF mutations was calculated in a set of samples with sufficient coverage (>2000rds). This frequency was used to estimate the number of cases that would be expected in the group of cases where coverage was below the required minimum. All missed cases in these three groups were summed up. WT: Wildtype for RAS pathway mutations.

Estimated number of <3%VAF mutations missed in cases with coverage <666, based on the frequency of 1-3%VAF mutations observed in a group that did reach the coverage of >2000

Amplicon	cases with enough coverage	mutation frequency VAF 1-3%	WT cases with coverage <666	Estimate missed cases
NRAS_1_+	210	10.5	20	2
KRAS_1_+	118	2.5	57	1
KRAS_2_+	10	0.0	59	0
KRAS_3_+	248	4.8	20	1
PTPN11_1_+	327	2.4	9	0
PTPN11_2_+	32	0.0	41	0
FLT3_1_+	95	4.2	24	1
FLT3_2_+	40	0.0	46	0
ΣMissed cases				6

Estimated number of 5-10%VAF mutations missed in cases with coverage <200, based on the frequency of 5-10%VAF mutations observed in a group that did reach the coverage of >2000

Amplicon	cases with enough coverage	mutation frequency VAF 5-10%	WT cases with coverage <666	Estimate missed cases
NRAS_1_+	446	4.7	8	0
KRAS_1_+	396	0.3	28	0
KRAS_2_+	437	0.0	5	0
KRAS_3_+	448	4.5	7	0
PTPN11_1_+	454	0.4	2	0
PTPN11_2_+	427	0.0	3	0
FLT3_1_+	443	0.5	11	0
FLT3_2_+	432	0.5	16	0
ΣMissed cases				1

Estimated number of 3-5%VAF mutations missed in cases with coverage <400, based on the frequency of 3-5%VAF mutations observed in a group that did reach the coverage of >2000

Amplicon	cases with enough coverage	mutation frequency VAF 3-5%	WT cases with coverage <400	Estimate missed cases
NRAS_1_+	210	3.8	12	0
KRAS_1_+	118	1.7	35	1
KRAS_2_+	10	0.0	16	0
KRAS_3_+	248	2.0	10	0
PTPN11_1_+	327	0.6	6	0
PTPN11_2_+	32	0.0	18	0
FLT3_1_+	95	0.0	13	0
FLT3_2_+	40	0.0	21	0
ΣMissed cases				2

Supplemental Table S3: Frequency and total number of clonal and subclonal RAS pathway mutations per subtype and gene.

WT: Wildtype, n: number of cases, 1-10: mutations with 1 to 10% VAF, 50+: 50 to 100% VAF, all: all mutations summed up. ER: *ETV6-RUNX1*-rearranged; MLL: t(4;11)-rearranged, HD: high hyperdiploid, BO: B-other, TCF3: *TCF3*-rearranged, BA: *BCR-ABL1*-rearranged, BAL: *BCR-ABL1*-like.

		total n tested	Wildtype		1-10%		10-20%		20-30%		30-40%		40-50%		>50%		all	
			n	% of total	n	% of total	n	% of total	n	% of total	n	% of total	n	% of total	n	% of total	n	% of total
ER	KRAS	124	107	86.3	6	4.8	3	2.4	1	0.8	5	4.0	2	1.6	0	0.0	17	13.7
	NRAS	124	110	88.7	10	8.1	0	0.0	1	0.8	2	1.6	0	0.0	1	0.8	13	10.5
	FLT3	124	119	96.0	4	3.2	0	0.0	0	0.0	0	0.0	1	0.8	0	0.0	5	4.0
	PTPN11	124	120	96.8	3	2.4	0	0.0	0	0.0	1	0.8	0	0.0	0	0.0	4	3.2
	other	124	122	98.4	2	1.6	0	0.0	0	0.0	0	0.0	0	0.0	0	0.0	2	1.6
t(4;11)	KRAS	15	9	60.0	3	20.0	1	6.7	0	0.0	2	13.3	0	0.0	0	0.0	6	40.0
	NRAS	15	9	60.0	2	13.3	3	20.0	1	6.7	0	0.0	0	0.0	0	0.0	6	40.0
	FLT3	15	13	86.7	1	6.7	0	0.0	1	6.7	0	0.0	0	0.0	0	0.0	2	13.3
	PTPN11	15	13	86.7	2	13.3	0	0.0	0	0.0	0	0.0	0	0.0	0	0.0	2	13.3
	other	15	15	100.0	0	0.0	0	0.0	0	0.0	0	0.0	0	0.0	0	0.0	0	0.0
HD	KRAS	124	69	55.6	19	15.3	7	5.6	10	8.1	7	5.6	12	9.7	0	0.0	55	44.4
	NRAS	124	82	66.1	18	14.5	5	4.0	8	6.5	4	3.2	6	4.8	1	0.8	41	33.1
	FLT3	124	110	88.7	5	4.0	4	3.2	1	0.8	0	0.0	2	1.6	2	1.6	12	9.7
	PTPN11	124	110	88.7	4	3.2	4	3.2	1	0.8	1	0.8	4	3.2	0	0.0	14	11.3
	other	124	122	98.4	0	0.0	0	0.0	1	0.8	0	0.0	0	0.0	1	0.8	1	0.8
BO	KRAS	67	52	77.6	6	9.0	2	3.0	1	1.5	2	3.0	3	4.5	1	1.5	14	20.9
	NRAS	67	48	71.6	7	10.4	3	4.5	1	1.5	4	6.0	3	4.5	1	1.5	18	26.9
	FLT3	67	62	92.5	4	6.0	0	0.0	0	0.0	1	1.5	0	0.0	0	0.0	5	7.5
	PTPN11	67	65	97.0	2	3.0	0	0.0	0	0.0	0	0.0	0	0.0	0	0.0	2	3.0
	other	67	66	98.5	1	1.5	0	0.0	0	0.0	0	0.0	0	0.0	0	0.0	1	1.5
TCF3	KRAS	26	25	96.2	0	0.0	1	3.8	0	0.0	0	0.0	0	0.0	0	0.0	1	3.8
	NRAS	26	25	96.2	1	3.8	0	0.0	0	0.0	0	0.0	0	0.0	0	0.0	1	3.8
	FLT3	26	26	100.0	0	0.0	0	0.0	0	0.0	0	0.0	0	0.0	0	0.0	0	0.0
	PTPN11	26	26	100.0	0	0.0	0	0.0	0	0.0	0	0.0	0	0.0	0	0.0	0	0.0
	other	26	26	100.0	0	0.0	0	0.0	0	0.0	0	0.0	0	0.0	0	0.0	0	0.0
BA	KRAS	26	26	100.0	0	0.0	0	0.0	0	0.0	0	0.0	0	0.0	0	0.0	0	0.0
	NRAS	26	26	100.0	0	0.0	0	0.0	0	0.0	0	0.0	0	0.0	0	0.0	0	0.0
	FLT3	26	25	96.2	0	0.0	0	0.0	0	0.0	0	0.0	1	3.8	0	0.0	1	3.8
	PTPN11	26	26	100.0	0	0.0	0	0.0	0	0.0	0	0.0	0	0.0	0	0.0	0	0.0
	other	26	26	100.0	0	0.0	0	0.0	0	0.0	0	0.0	0	0.0	0	0.0	0	0.0
BAL	KRAS	79	61	77.2	7	8.9	1	1.3	3	3.8	3	3.8	3	3.8	1	1.3	17	21.5
	NRAS	79	58	73.4	9	11.4	2	2.5	0	0.0	2	2.5	7	8.9	1	1.3	20	25.3
	FLT3	79	72	91.1	2	2.5	1	1.3	2	2.5	0	0.0	1	1.3	1	1.3	6	7.6
	PTPN11	79	72	91.1	3	3.8	0	0.0	1	1.3	0	0.0	3	3.8	0	0.0	7	8.9
	other	79	78	98.7	1	1.3	0	0.0	0	0.0	0	0.0	0	0.0	0	0.0	1	1.3

Supplemental Table S4: Frequencies of RAS pathway mutations among cytogenetic subtypes of BCP-ALL.

Fisher's Exact test comparing the frequency of each cytogenetic subtype to the remaining BCP-ALL subtypes. ER: *ETV6-RUNX1*-rearranged, MLL: t(4;11)-rearranged, HD: high hyperdiploid karyotype, BO: B-other, TCF3: *TCF3*-rearranged, BA: *BCR-ABL1*-rearranged, BAL: *BCR-ABL1*-like gene expression profile. OR: Odds ratio. P-values < 0.05 are printed in bold. CI: confidence interval.

	Wildtype	**Mutated**	**Total**	**Frequency**	**Fisher's Exact p-value**	**OR**	**95% CI of OR**	
ER	96	28	124	22.6%	8.2E-08	0.3	0.2	0.5
MLL	4	11	15	73.3%	1.8E-02	3.8	1.1	16.8
HD	34	90	124	72.6%	4.7E-15	5.7	3.5	9.3
BO	39	28	67	41.8%	0. 90	1.0	0.5	1.7
TCF3	26	0	26	0.0%	3.6E-07	0.0	0.0	0.2
BA	25	1	26	4.0%	7.5E-06	0.0	0.0	0.3
BAL	40	39	79	49.4%	0.21	1.4	0.8	2.3
total	264	197	461					

Supplemental Table S5: Frequency of common secondary aberrations in RAS pathway wildtype, clonal and subclonal mutation cases. Genomic data obtained by MLPA and array comparative genomic hybridization (aCGH) were available for a subset of patients analysed in this study. The overlap with RAS pathway mutations is shown. total: Total number of cases in the analysis and per group. Cases: Cases positive for the respective feature OR: Odds ratio. p: p-value

	Total			RAS pathway wildtype			clonal RAS pathway mutation							subclonal RAS pathway mutation						
Feature	total	freq.	cases	total	freq.	cases	total	freq.	cases	p =	OR	CI (95%)		total	freq.	cases	p =	OR	CI (95%)	
ERG deletion or break	272	3%	8	156	3%	5	70	1%	1	0.669	0.44	0.01	4.03	46	4%	2	0.659	1.37	0.13	8.73
JAK2 mutation	419	4%	15	239	4%	9	103	1%	1	0.293	0.25	0.01	1.85	77	6%	5	0.341	1.77	0.45	6.11
high *CRLF2* expression	407	11%	45	231	9%	20	102	9%	9	1.000	1.02	0.39	2.45	75	21%	16	0.006	2.85	1.29	6.20
chromosome 21 abnormality	392	42%	164	224	32%	72	99	56%	55	0.000	2.63	1.58	4.42	69	54%	37	0.002	2.43	1.36	4.39
Morbus Down	392	4%	14	224	5%	11	99	2%	2	0.358	0.40	0.04	1.89	69	1%	1	0.306	0.29	0.01	2.03
iAMP21	390	4%	15	222	4%	8	99	1%	1	0.284	0.27	0.01	2.09	69	9%	6	0.106	2.54	0.70	8.70
dic(9;20)	390	5%	19	222	2%	5	99	11%	11	0.002	5.39	1.67	20.39	69	4%	3	0.399	1.97	0.30	10.42
9p deletion	390	9%	34	222	4%	9	99	21%	21	0.000	6.33	2.64	16.40	69	6%	4	0.515	1.45	0.32	5.42
PAX5 amplification	401	1%	6	231	0%	1	95	4%	4	0.027	10.03	0.98	499	75	1%	1	0.431	3.09	0.04	244
PAX5 del	401	26%	105	231	31%	71	95	27%	26	0.595	0.85	0.48	1.48	75	11%	8	0.000	0.27	0.11	0.60
CDKN2A deletion	404	33%	134	232	29%	68	97	46%	45	0.003	2.08	1.24	3.50	75	28%	21	0.884	0.94	0.50	1.72
CDKN2B deletion	403	32%	127	231	27%	63	97	44%	43	0.003	2.12	1.25	3.58	75	28%	21	0.883	1.04	0.55	1.91
CDKN2A and *CDKN2B* wildtype	403	65%	260	231	69%	159	97	52%	50	0.004	0.48	0.29	0.81	75	68%	51	0.887	0.96	0.53	1.77
IKZF1 deletion	400	21%	84	230	25%	57	95	19%	18	0.311	0.71	0.37	1.32	75	12%	9	0.023	0.41	0.17	0.91
BTG1 deletion	400	10%	38	229	14%	32	96	1%	1	0.000	0.07	0.00	0.40	75	7%	5	0.106	0.44	0.13	1.20
EBF1 deletion	402	7%	28	231	8%	19	96	4%	4	0.240	0.49	0.12	1.52	75	7%	5	0.807	0.80	0.22	2.32
ETV6 deletion	399	25%	101	227	30%	68	97	14%	14	0.003	0.40	0.19	0.76	75	25%	19	0.467	0.79	0.41	1.48
TCF3 deletion	121	26%	32	63	29%	18	37	24%	9	0.816	0.81	0.28	2.21	21	24%	5	0.782	0.78	0.19	2.69

Supplemental Table S6: Distribution of clonal and subclonal RAS pathway mutations among the treatment arms of DCOG ALL10.

SR: Standard risk treatment arm; MR: medium risk treatment arm; HR: high risk treatment arm.

Within	Mutated, clonal	Mutated, subclonal
ALL10 SR	10/75 (13%)	15/75 (20%)
ALL10 MR	33/151 (22%)	46/151 (30%)
ALL10 HR	9/22 (41%)	2/22 (9%)
Fisher test, p=	0.024	0.047

Supplemental Table S7: Clinical characteristics of BCP-ALL patients with subclonal RAS pathway mutations.

WBC: White blood cell count; CNS+: non-traumatic puncture and >5 WBC/µl CSF with identifiable leukemic cells; patients with a traumatic lumbar puncture were not included; PPR: Prednisone poor responder, i.e. ≥1000 leukemic blasts/µl in peripheral blood on day 8 of induction therapy; MRD high: Minimal residual disease $\geq 10^{-3}$; d33: at the end of induction therapy (day 33); d79: at the end of consolidation therapy (day 79); [a]Fisher's Exact test p-values <0.05 are printed in bold font; [b]Odds ratios are only given if p-values in Fisher's Exact test were <0.2.

Risk parameter	Incidence of subclonal mutations among		Statistics			
	Risk parameter: Yes	Risk parameter: No	Fisher's p=[a]	Odds ratio[b]	95%-CI	
Age ≥10	8/75 (15%)	80/357 (30%)	0.04	0.43	0.17	0.97
Male	49/227 (28%)	39/205 (38%)	0.53			
High WBC (>50/nL)	10/99 (15%)	77/331 (30%)	0.02	0.42	0.18	0.88
Down Syndrome	1/16 (7%)	86/391 (28%)	0.12	0.18	0	1.26
CNS+	0/1 (0%)	38/248 (15%)	1			
PPR	2/17 (20%)	63/244 (32%)	0.73			
MRD high d33 ALL10	15/48 (45%)	44/191 (23%)	0.06	2.24	0.95	5.23
MRD high d79 ALL10	0/8 (0%)	60/231 (32%)	0.18	0	0	1.82

Supplemental Table S8: Baseline characteristics of the ALL10 and COALL97/03 cohorts.

WBC: white blood cell count; MRD: Minimal residual disease, MRD positive: MRD ≥ 10^{-3}; PPR: poor prednisone window response. Color intensities are used to indicate the treatment intensity. Treatment intensity: COALL treatment arms LR-R and LR-S are comparable to ALL10 standard risk treatment (labeled standard); LR-I, HR-R and HR-R are comparable to ALL10 medium risk treatment (labeled medium, see method section for details).

ALL10						COALL97/03					
	n	%	Median	25th	75th		n	%	Median	25th	75th
Total	244	100%				Total	131	100%			
Treatment intensity											
Standard	22	9%				Stanard	31	24%			
Medium	148	61%				Medium	100	76%			
High	74	30%						-			
Risk characteristics											
Age			5	3	8	Age			4	2	9
WBC			11	4.9	32.2	WBC			24.1	9.5	55
MRD positive d33	48/239	20%				MRD positive d29	20/61	33%			
MRD positive d79	8/239	3%				MRD positive d79	N/A				
PPR	15	6%				PPR	N/A				
Down S.	8	3%				Down S.	3/110	3%			
Events	32	13%				Events	29	22%			
Relapse	28	11%				Relapse	26	20%			

Supplemental Table S9: Univariate and multivariate analysis of Cox's proportional hazard ratio in Standard-risk treated DCOG ALL10 cases.

WBC: White blood cell count; Clonal mutation: VAF ≥ 25%; subclonal VAF < 25%; 95% CI: 95% confidence interval.

	Univariate		Multivariate	
Variable	**HR (95% CI)**	**p-value**	**HR (95% CI)**	**p-value**
Age (≥10 years)	0.05 (0 - >1000)	0.66	0 (0-∞)	0.99
WBC (≥ 50/nL)	1.1 (0.1-9.2)	0.91	0.7 (0.08 – 5.9)	0.73
RAS pathway status		0.11		0.074
Clonal	4.6 (1.0 – 21)	0.047	5.4 (1.2 - 25)	0.032
subclonal	0.9 (0.1 – 7.8)	0.9	0.9 (0.1 – 7.7)	0.9

Supplemental Table S10: Median ex vivo LC50-values per RAS pathway mutations.

The allocated group is determined by the largest clone. LC50-values are given in IU/mL for L-asparaginase and in µg/mL for all other chemotherapeutic agents. p-value is determined with a Mann-Whitney U test. Significant p-values are printed in bold. wt: wildtype, Combined: all RAS pathway mutations taken together. PRED: Prednisolone, VCR: Vincristine, ASP: L-asparaginase, DNR: Daunorubicine, 6TG: 6-Thioguanine, 6MP: 6-Mercaptopurine. Values containing ≥ or ≤ represent the highest or lowest concentration in the range, which was used as IC50 if limits were exceeded.

	Clonal						Subclonal					
	n =	Median LC50	Min. (µg/mL)	Max. (µg/mL)	Fold change	p-Value	n =	Median LC50	Min. (µg/mL)	Max. (µg/mL)	Fold change	p-Value
PRED wildtype	111	0.10	≤0.0076	≥250	.	.	111	0.10	≤0.0076	≥250	.	.
PRED combined	49	0.32	≤0.0076	≥250	3.2	**0.02**	34	0.17	≤0.0076	≥250	1.7	0.34
PRED KRAS G13	8	>250	0.280	≥250	>2000	**0.00**	7	>250	0.06	≥250	>2000	**0.01**
PRED KRAS G12	15	0.25	0.025	≥250	2.5	0.19	6	0.35	0.04	≥250	3.4	0.37
PRED NRAS G13	6	1.47	0.041	≥250	14.4	0.18	0	NA			.	.
PRED NRAS G12	11	0.23	≤0.0076	154.89	2.2	0.37	13	0.06	0.01	≥250	0.6	0.98
PRED FLT3	3	0.10	0.028	14.84	1	1	5	0.55	0.16	≥250	5.4	0.06
PRED PTPN11	4	0.10	≤0.0076	≥250	1	0.66	2	159.24	68.48	≥250	1566	0.06
PRED KRAS other	2	0.03	0.015	0.05	0.3	0.22	1	0.36	0.36	0.36	3.5	0.54
VCR wildtype	110	0.49	≤0.049	44.68	.	.	110	0.49	≤0.049	44.68	.	.
VCR combined	49	0.73	≤0.049	≥50	1.5	0.15	35	0.50	≤0.049	>50	1	0.91
VCR KRAS G13	8	7.09	0.397	43.95	14.6	**0.01**	7	0.67	0.12	>50	1.4	0.33
VCR KRAS G12	15	0.77	≤0.049	≥50	1.6	0.21	6	0.51	≤0.049	2.26	1	0.77
VCR NRAS G13	6	1.44	0.191	36.50	3	0.07	0	NA			.	.
VCR NRAS G12	11	0.09	≤0.049	3.03	0.2	0.06	14	0.45	≤0.049	2.66	0.9	0.86
VCR FLT3	3	0.05	≤0.049	2.03	0.1	0.21	5	0.41	≤0.049	1.65	0.8	0.95
VCR PTPN11	4	2.48	0.488	43.38	5.1	**0.04**	2	3.41	0.10	6.72	7	0.94
VCR KRAS other	2	0.32	0.157	0.48	0.7	0.50	1	1.51	1.51	1.51	3.1	0.37
ASP wildtype	109	0.22	≤0.003	≥10	.	.	109	0.22	≤0.003	≥10	.	.
ASP combined	49	0.04	≤0.003	≥10	0.2	0.18	35	0.07	≤0.003	≥10	0.3	0.48
ASP KRAS G13	8	0.06	≤0.003	1.58	0.3	0.55	7	0.13	≤0.003	≥10	0.6	0.86
ASP KRAS G12	15	0.03	≤0.003	≥10	0.1	0.56	6	0.05	≤0.003	1.68	0.2	0.51
ASP NRAS G13	6	0.87	0.009	1.98	3.9	0.52	0	NA			.	.
ASP NRAS G12	11	0.02	≤0.003	1.58	0.1	0.21	14	0.01	≤0.003	≥10	0.1	0.09
ASP FLT3	3	0.10	≤0.003	0.13	0.4	0.36	5	0.03	0.01	0.27	0.1	0.33
ASP PTPN11	4	0.56	≤0.003	1.31	2.5	0.72	2	0.01	0.01	0.02	0.1	0.23
ASP KRAS other	2	0.01	0.010	0.01	0.1	0.14	1	0.01	0.01	0.01	0.1	0.31
DNR wildtype	109	0.05	≤0.002	0.32	.	.	109	0.05	≤0.002	0.32	.	.
DNR combined	48	0.03	≤0.002	1.13	0.5	0.64	34	0.05	≤0.002	1.18	1	0.79
DNR KRAS G13	8	0.09	0.018	0.25	1.7	0.15	7	0.03	0.02	0.42	0.6	0.66
DNR KRAS G12	15	0.03	≤0.002	1.13	0.6	0.87	6	0.05	0.01	0.15	0.9	0.82
DNR NRAS G13	6	0.03	0.020	0.10	0.5	0.36	0	NA			.	.
DNR NRAS G12	11	0.02	0.007	0.12	0.4	0.14	14	0.04	≤0.002	0.22	0.8	0.67
DNR FLT3	3	0.02	0.006	0.27	0.4	0.59	5	0.05	0.02	0.08	1	0.84
DNR PTPN11	3	0.19	≤0.002	0.23	3.7	0.44	1	1.18	1.18	1.18	22.9	0.09
DNR KRAS other	2	0.02	0.022	0.02	0.4	0.23	1	0.12	0.12	0.12	2.4	0.21
6TG wildtype	83	0.00	≤0.002	0.02	.	.	83	0.00	≤0.002	0.02	.	.
6TG combined	37	0.00	≤0.002	≥0.05	1.1	0.89	25	0.00	≤0.002	0.02	0.9	0.73
6TG KRAS G13	5	0.00	≤0.002	0.02	1.4	0.31	4	0.00	0.00	0.02	0.8	0.58
6TG KRAS G12	9	0.00	≤0.002	≥0.05	1.3	0.40	5	0.00	0.00	0.00	0.8	0.08
6TG NRAS G13	5	0.01	≤0.002	0.01	1.8	0.80	0	NA			.	.
6TG NRAS G12	11	0.00	≤0.002	0.01	0.7	0.25	12	0.00	≤0.002	0.01	0.9	0.45
6TG FLT3	3	0.01	≤0.002	0.01	1.5	0.85	2	0.01	0.01	0.01	2.8	**0.03**
6TG PTPN11	2	0.00	0.003	0.00	1	0.81	1	0.01	0.01	0.01	2.3	0.25
6TG KRAS other	2	0.00	≤0.002	0.00	0.6	0.08	1	0.00	≤0.002	0.00	0.4	0.11
6MP wildtype	82	0.09	≤0.016	≥0.5	.	.	82	0.09	≤0.016	≥0.5	.	.

	Clonal						Subclonal					
	n =	Median LC50	Min. (µg/mL)	Max. (µg/mL)	Fold change	p-Value	n =	Median LC50	Min. (µg/mL)	Max. (µg/mL)	Fold change	p-Value
6MP combined	32	0.06	≤0.016	≥0.5	0.7	0.07	25	0.08	≤0.016	≥0.5	0.9	0.39
6MP KRAS G13	4	0.14	0.044	≥0.5	1.6	0.43	4	0.04	0.02	0.09	0.4	0.07
6MP KRAS G12	8	0.05	≤0.016	≥0.5	0.5	0.15	5	0.10	0.02	0.10	1.1	0.41
6MP NRAS G13	5	0.07	≤0.016	≥0.5	0.8	0.70	0	NA				.
6MP NRAS G12	10	0.09	≤0.016	0.36	1	0.57	12	0.03	≤0.016	0.27	0.3	**0.01**
6MP FLT3	1	0.04	0.038	0.04	0.4	0.22	2	0.38	0.27	≥0.5	4.3	0.05
6MP PTPN11	2	0.02	≤0.016	0.03	0.2	**0.03**	1	0.12	0.12	0.12	1.4	0.52
6MP KRAS other	2	0.05	0.034	0.06	0.5	0.15	1	0.02	0.02	0.02	0.2	0.14

Supplemental Figure S1: Diagram with detailed information about the patient cohorts.

(A) Subtype distribution among patients with complete subtype information, used to determine RAS pathway mutation frequency among genetic subtypes of BCP-ALL (red) and subtype distribution among cases used to compare clinical characteristics in wildtype or RAS pathway mutated patients (green). **(B)** Treatment protocols of cases used for analysis of clinical characteristics (green) and those used for analysis of event-free survival and cumulative incidence of relapse (blue). Cases with ex vivo drug sensitivity (yellow frame) data were treated in the COALL97/03 and DCOG ALL10 cohorts, but only a subset of these cases had data available (n=211). Observation patient: not eligible for follow-up, only baseline characteristics analyzed

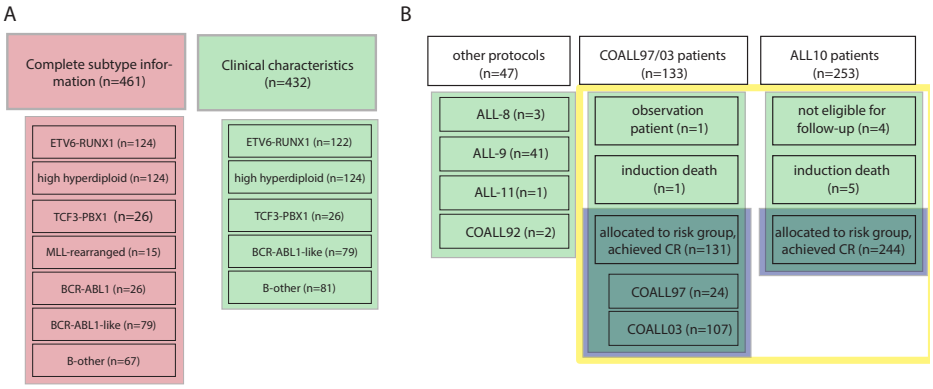

Supplemental Figure S2: Amplicon coverage across samples.

Coverage was calculated from the number of reads mapped for each sample. Amplicons are identified by their amplicon ID (see also Supplemental Table S1). Boxes represent first and third quartile, whiskers represent outer two quartiles (max. 1.5-times the inner quartile range), and bar represents group median.

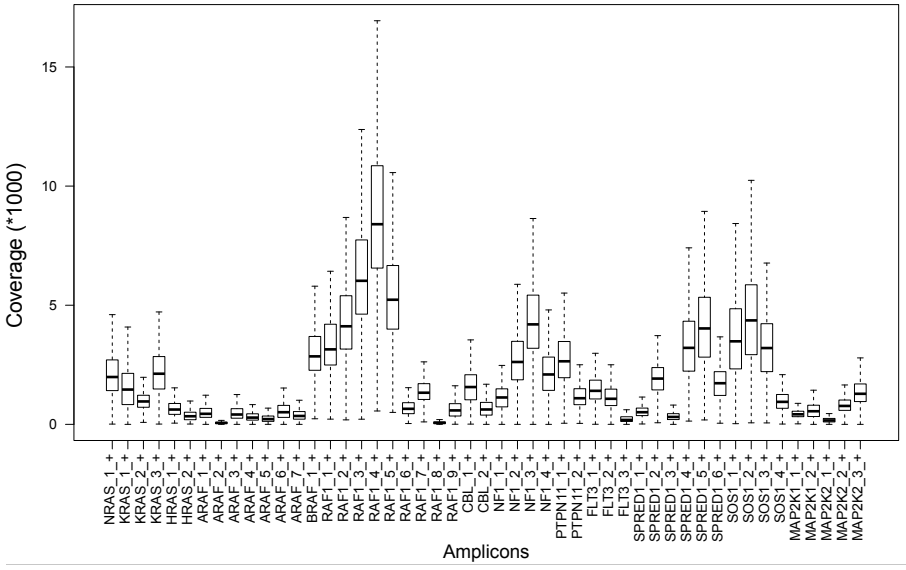

Supplemental Figure S3: Relative frequency of *NRAS, KRAS, PTPN11, FLT3* and other RAS pathway mutations.

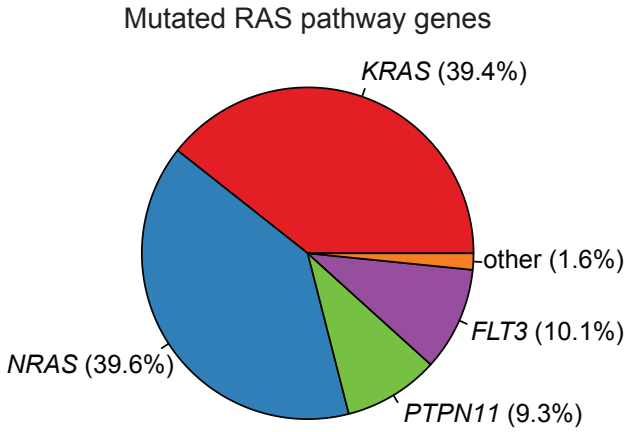

Supplemental Figure S4: Histogram of observed variant allele-frequencies.

Histogram of the VAF of all mutations in RAS pathway genes identified in our dataset. Dashed lines depict median VAF of all clonal or subclonal mutations. Background shading represents subclonal (light) and (dark) clonal mutations.

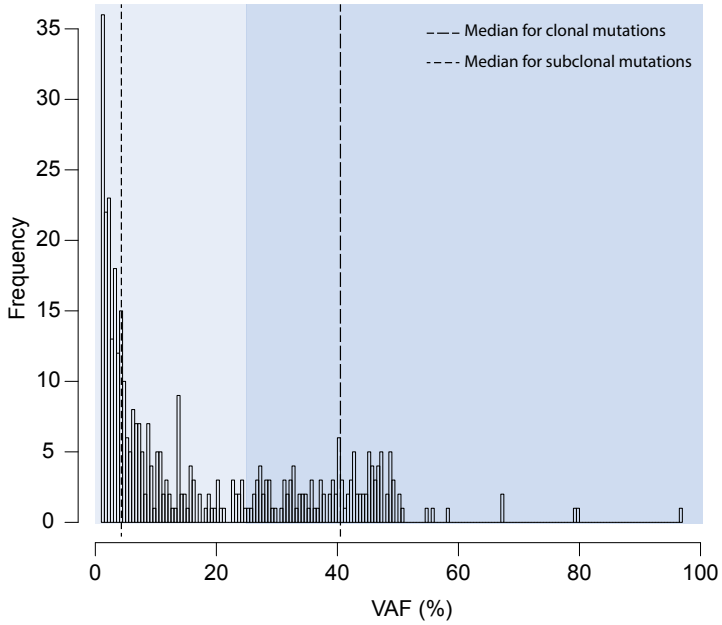

Supplemental Figure S5: Frequency of clonal and subclonal RAS pathway mutations among tyrosine kinase (TK) fusion positive *BCR-ABL1*-like cases, *CRLF2*-high *BCR-ABL1*-like cases, and TK fusion negative *BCR-ABL1*-like cases with low *CRLF2* expression.

TK fusions were identified as described by Boer et al. (manuscript submitted) and included the following fusions: *EBF1-PDGFRB* (3 cases), *PAX5-JAK2* (3), *BCR-JAK2* (1), *FOXP1-ABL1* (1), *SSBP-CSFR* (1), *TERF2-JAK2* (1), and *ZMIZ1-ABL1* (1). High *CRLF2* expression was, as previously, defined as the 90th percentile of the entire BCP-ALL cohort.

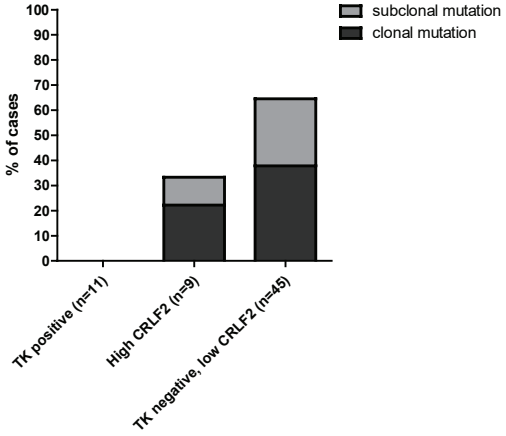

Supplemental Figure S6: Overview of amino acid changes in RAS mutated cases.

(A) Relative frequency of different *KRAS* and *NRAS* variants observed in pediatric BCP-ALL. **(B)** Histogram of amino acid substitutions in *KRAS, NRAS, FLT3* and *PTPN11* variants.

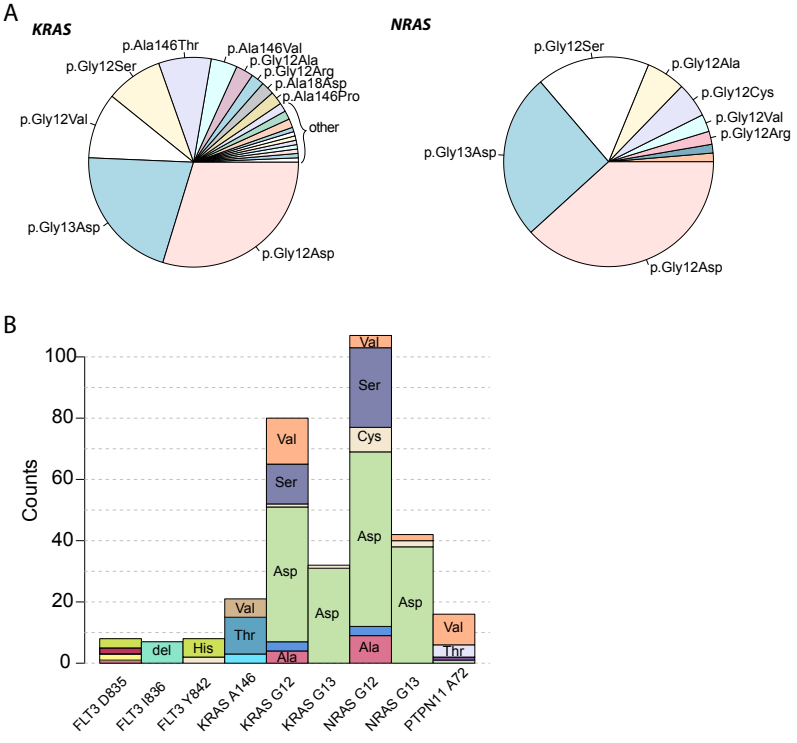

Supplemental Figure S7: Event-free survival and cumulative incidence of relapse in the COALL97/03 cohort.

p_{trend} = p-value for the analysis comparing wildtype, subclonal, and clonal mutation cases; p_{cl} = p-value for the analysis comparing wildtype to cases with clonal RAS pathway mutations.

Standard risk

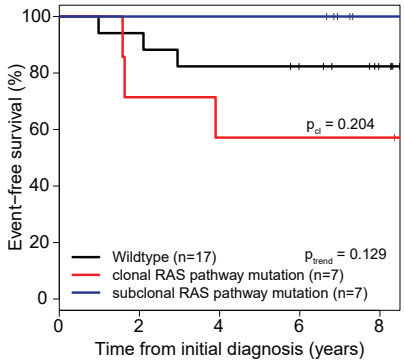

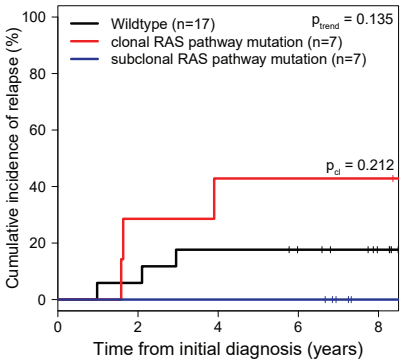

Medium risk

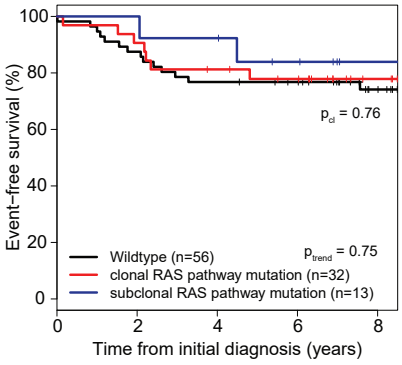

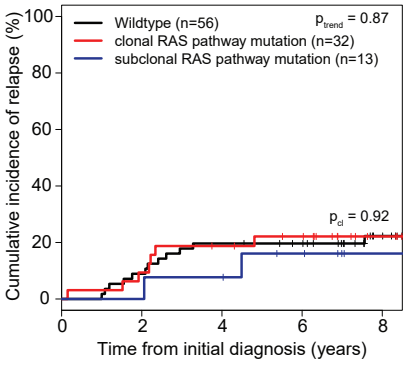

Supplemental Figure S8: *Ex vivo* sensitivity to prednisolone (A) and vincristine (B) in BCP-ALL cases carrying subclonal or clonal RAS pathway mutations including *FLT3* and *PTPN11*.

Sensitivity of primary patient cells towards prednisolone and vincristine, distinguished by RAS mutation status. LC50-values of cases with clonal and subclonal mutations are depicted. "All": All cases with a mutation in *NRAS, KRAS, PTPN11,* or *FLT3*. In cases with multiple mutations, the mutation with the highest VAF (largest clone) was used to classify cases.

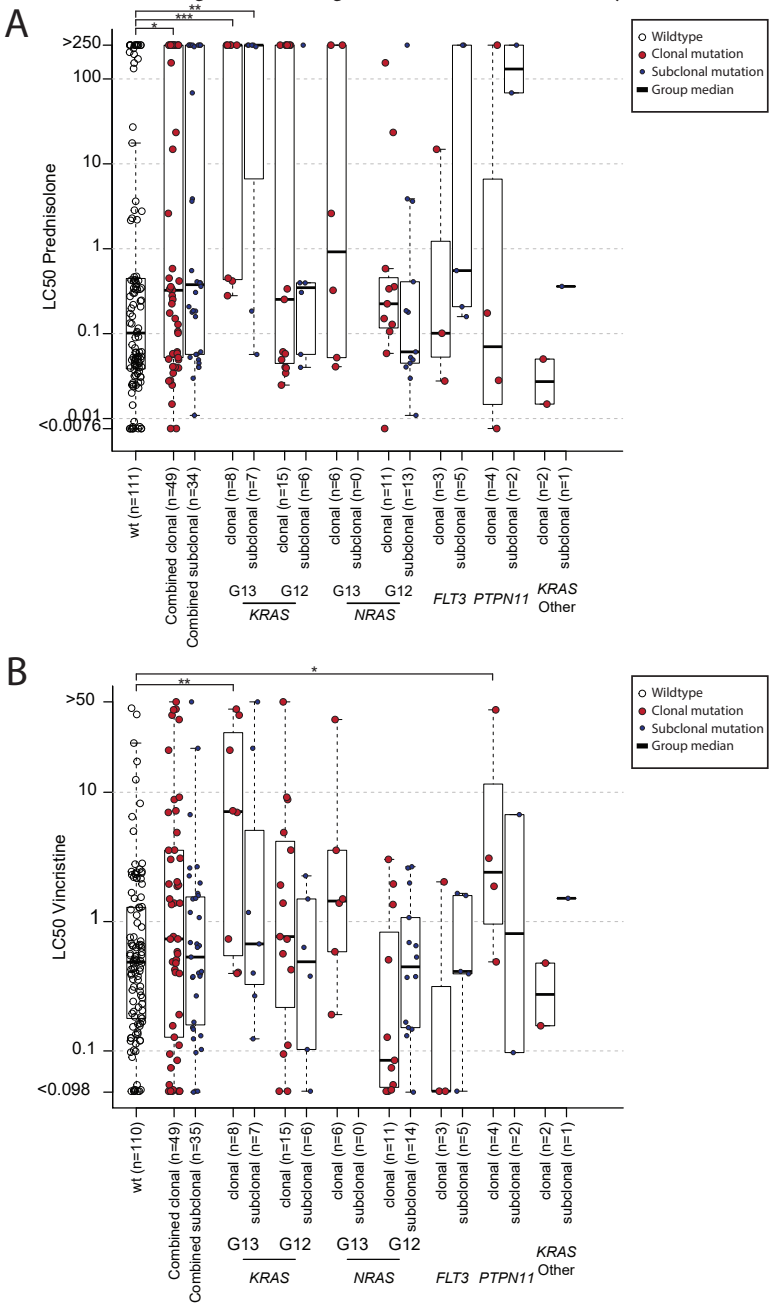

Supplemental Figure S9: *Ex vivo* chemotherapeutic sensitivity of RAS mutated BCP-ALL cases distinguished by the amino acid variant in the *NRAS* or *KRAS* gene.

In cases with multiple mutations, the mutation with the highest VAF (largest clone) was used to classify cases. (**A**) Prednisolone sensitivity. (**B**) Vincristine sensitivity.

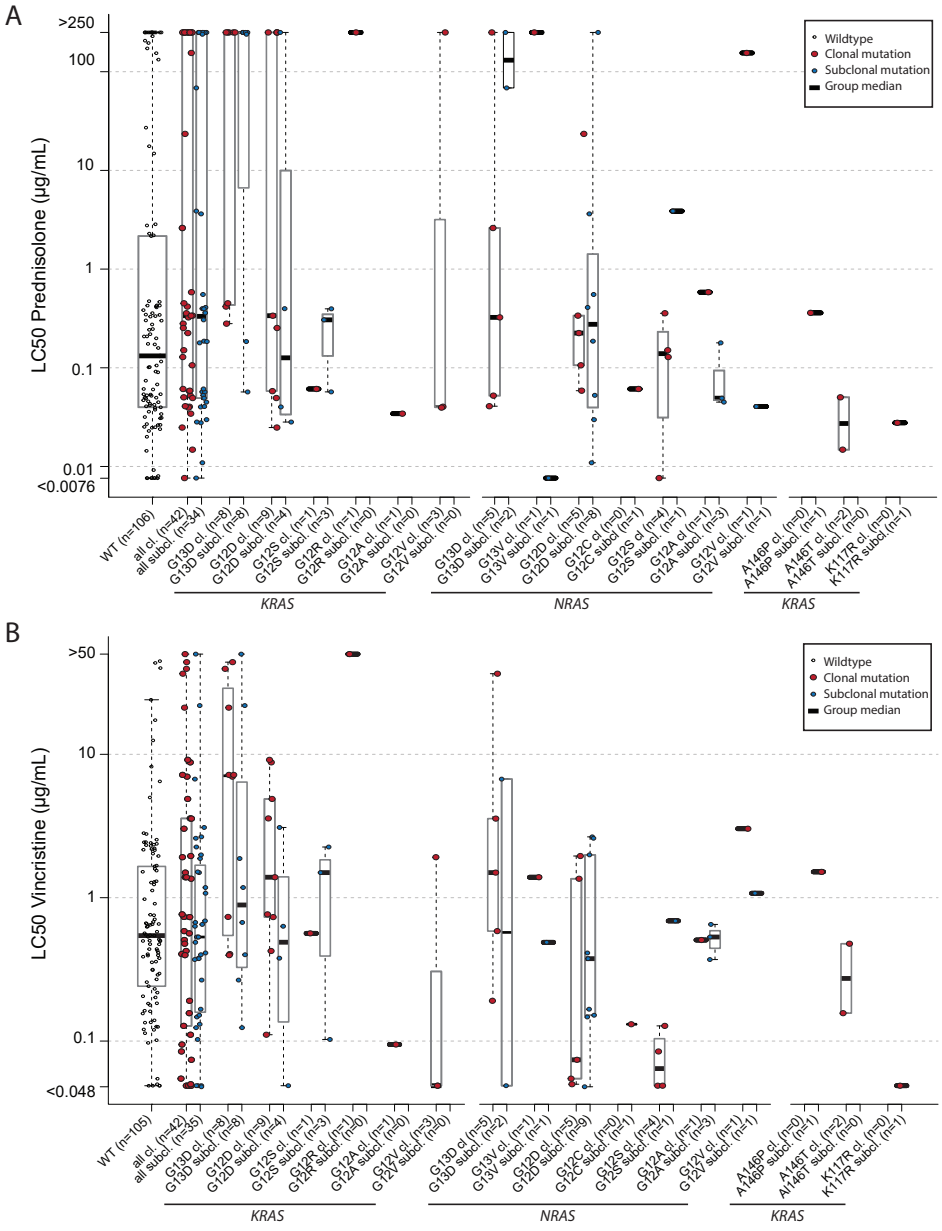

Supplemental Figure S10: RAS pathway mutations and *ex vivo* cytotoxicity of chemotherapeutic agents.

Ex vivo sensitivity of 211 primary patient samples towards **(A)** L-asparaginase, **(B)** daunorubicin, **(C)** 6-thioguanine, and **(D)** 6-mercaptopurinol, distinguished by RAS mutation status. Only clonally mutated cases are depicted. Only *KRAS* and *NRAS* mutated groups are shown due to low recurrence of other mutations (see also supplement). Combined: All cases with a clonal mutation in *NRAS, KRAS, PTPN11, FLT3.* Groups were compared by Mann-Whitney U test, * p<0.05, ** p<0.01. LC50-values were evaluated by MTT assays as reported previously.

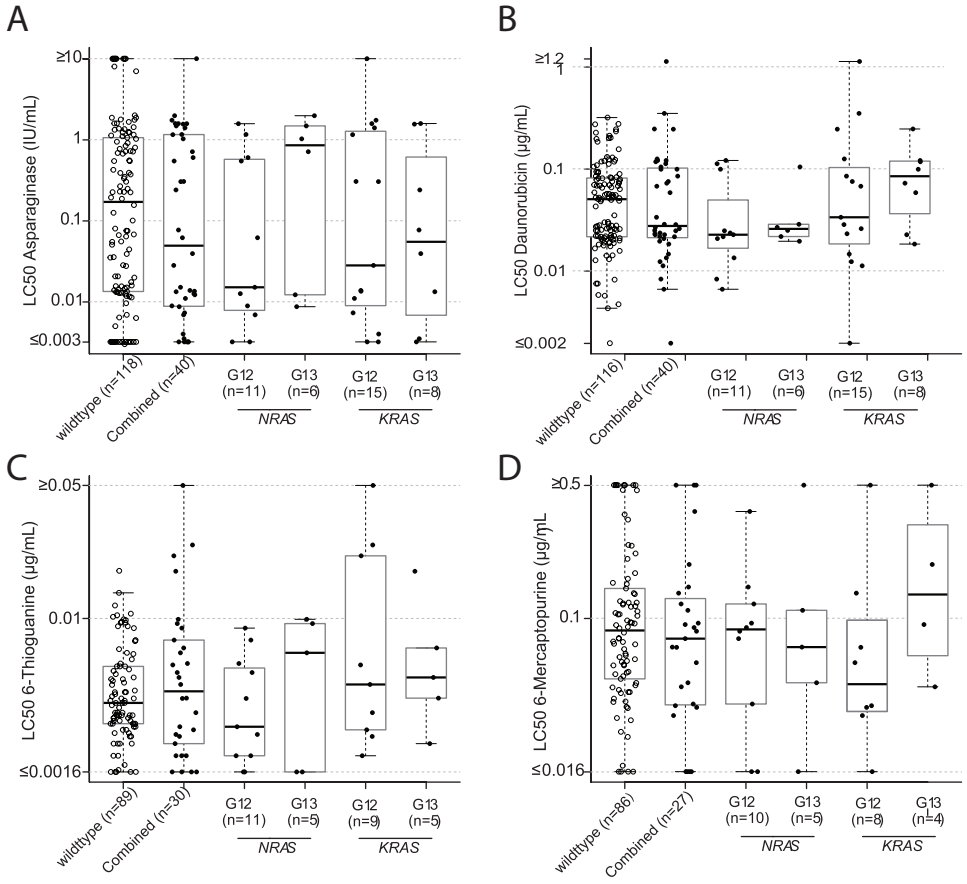

Supplemental Figure S11: Efficacy of the MEK-inhibitor trametinib in RAS pathway mutant BCP-ALL.

(A) *Ex vivo* sensitivity of primary BCP-ALL cases towards trametinib. Red lines represent RAS pathway mutated cases, black lines represent RAS pathway wildtype cases. **(B)** Western blot of phosphorylated ERK1/2 to confirm effective MEK-inhibition by a range of trametinib concentrations.

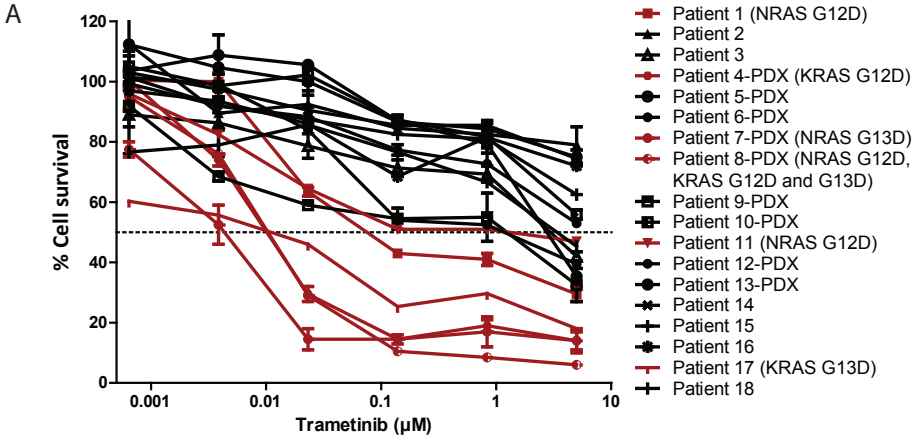

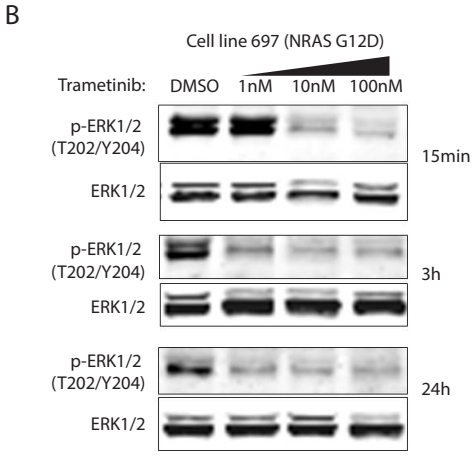

References

1. Den Boer ML, Harms DO, Pieters R, Kazemier KM, Gobel U, Korholz D, et al. Patient stratification based on prednisolone-vincristine-asparaginase resistance profiles in children with acute lymphoblastic leukemia. J Clin Oncol 2003 Sep 1; 21(17): 3262-3268.

2. Den Boer ML, van Slegtenhorst M, De Menezes RX, Cheok MH, Buijs-Gladdines JG, Peters ST, et al. A subtype of childhood acute lymphoblastic leukaemia with poor treatment outcome: a genome-wide classification study. Lancet Oncol 2009 Feb; 10(2): 125-134.

3. van der Veer A, Waanders E, Pieters R, Willemse ME, Van Reijmersdal SV, Russell LJ, et al. Independent prognostic value of *BCR-ABL1*-like signature and IKZF1 deletion, but not high CRLF2 expression, in children with B-cell precursor ALL. Blood 2013 Oct 10; 122(15): 2622-2629.

4. Kaspers GJ, Veerman AJ, Pieters R, Van Zantwijk CH, Smets LA, Van Wering ER, et al. In vitro cellular drug resistance and prognosis in newly diagnosed childhood acute lymphoblastic leukemia. Blood 1997 Oct 1; 90(7): 2723-2729.

5. Li H. Aligning sequence reads, clone sequences and assembly contigs with BWA-MEM. arXiv preprint arXiv:13033997 2013.

6. Garrison E, Marth G. Haplotype-based variant detection from short-read sequencing. arXiv preprint arXiv:12073907 2012.

7. Koboldt DC, Zhang Q, Larson DE, Shen D, McLellan MD, Lin L, et al. VarScan 2: somatic mutation and copy number alteration discovery in cancer by exome sequencing. Genome Res 2012 Mar; 22(3): 568-576.

8. Li H. A statistical framework for SNP calling, mutation discovery, association mapping and population genetical parameter estimation from sequencing data. Bioinformatics 2011 Nov 1; 27(21): 2987-2993.

9. DePristo MA, Banks E, Poplin R, Garimella KV, Maguire JR, Hartl C, et al. A framework for variation discovery and genotyping using next-generation DNA sequencing data. Nature genetics 2011 May; 43(5): 491-498.

10. Cingolani P, Platts A, Wang le L, Coon M, Nguyen T, Wang L, et al. A program for annotating and predicting the effects of single nucleotide polymorphisms, SnpEff: SNPs in the genome of Drosophila melanogaster strain w1118; iso-2; iso-3. Fly 2012 Apr-Jun; 6(2): 80-92.

11. Liu X, Wu C, Li C, Boerwinkle E. dbNSFP v3.0: A One-Stop Database of Functional Predictions and Annotations for Human Nonsynonymous and Splice-Site SNVs. Hum Mutat 2016 Mar; 37(3): 235-241.

12. Forbes SA, Beare D, Gunasekaran P, Leung K, Bindal N, Boutselakis H, et al. COSMIC: exploring the world's knowledge of somatic mutations in human cancer. Nucleic Acids Res 2015 Jan; 43(Database issue): D805-811.

13. Aries IM, van den Dungen RE, Koudijs MJ, Cuppen E, Voest E, Molenaar JJ, et al. Towards personalized therapy in pediatric acute lymphoblastic leukemia: RAS mutations and prednisolone resistance. Haematologica 2015 Apr; 100(4): e132-136.

14. Escherich G, Troger A, Gobel U, Graubner U, Pekrun A, Jorch N, et al. The long-term impact of in vitro drug sensitivity on risk stratification and treatment outcome in acute lymphoblastic leukemia of childhood (CoALL 06-97). Haematologica 2011 Jun; 96(6): 854-862.

15. Gray RJ. cmprsk: Subdistribution Analysis of Competing Risks. 2013; R package version 2.2-7 http://CRAN.R-project.org/package=cmprsk.

16. de Wreede LC, Fiocco M, Putter H. mstate: An R Package for the Analysis of Competing Risks and Multi-State Models. J Stat Softw 2011 Jan; 38(7): 1-30.

17. Therneau T. A Package for Survival Analysis in S. 2012; R Package version 2.38-3.

Chapter 4

High PDGFRA expression does not serve as effective therapeutic target in ERG-deleted B-cell precursor acute lymphoblastic leukemia

Isabel S. Jerchel; Danai Chatzivasileiou; Alex Q. Hoogkamer, Judith M. Boer, H. Berna Beverloo, Rob Pieters, and Monique L. den Boer

Hemtatologica. 2017 Nov 23 (Epub ahead of print)

Abstract

Several oncogenic aberrations of receptor tyrosine kinases have been reported in pediatric B-cell precursor acute lymphoblastic leukemia. Here we describe a subgroup of patients lacking sentinel chromosomal aberrations with high expression of *PDGFRA*. Given the implications of *PDGFRA* rearrangements in myeloid malignancies, we tested for genetic aberrations in *PDGFRA* and evaluated the inhibition of PDGFRα as treatment option. By means of fusion gene-specific RT-PCR, fluorescence in situ hybridization (FISH), and targeted locus amplification (TLA), we confirmed absence of genetic aberrations affecting *PDGFRA*. Instead, array-based comparative genomic hybridization data revealed ERG deletions in 63% of cases (10 of 16), compared to 0% in *PDGFRA* low BCP-ALL cases (n=71). Expression and activation of PDGFRα were confirmed by western blot in a cell line and primary BCP-ALL cells. *Ex vivo* drug sensitivity assays with and without bone marrow-derived mesenchymal stromal cells (MSC) revealed no sensitivity of *PDGFRA* high BCP-ALL cells towards two PDGFR inhibitors (imatinib and CP673451). We therefore conclude that high expression of wildtype *PDGFRA* is characteristic for ERG-deleted leukemia and might serve as a biomarker, but not as treatment target.

Introduction

Current event-free survival rates of pediatric B-cell precursor acute lymphoblastic leukemia (BCP-ALL) have reached approximately 85%.[1] A large part of relapses occurs in the genetically heterogeneous group that lacks sentinel chromosomal aberrations, a group which is widely referred to as "B-other" cases. Even after identification of the *BCR-ABL1*¬-like subtype, B-other cases still constitute a considerable proportion (about 18%) of BCP-ALL patients.[1-3] Genetic aberrations that define distinct subtypes are essential for diagnosis and risk evaluation. The primary oncogenic aberration driving the leukemia is also likely to be the most effective treatment target, and revealing these aberrations is crucial to identifying novel treatment targets and improving the prognosis for B-other cases.

Gene expression profiling and extensive sequencing has been performed to further classify B-other ALL, and several characteristic but not mutually exclusive aberrations have been found. Among the genes that are recurrently affected by aberrations are B-cell transcription factors (*PAX5, IKZF1, ETV6, ERG*) and components of signaling pathways (*NRAS, KRAS, JAK2, CRLF2*).

Patients carrying intragenic deletions of the ERG gene on chromosome 21 have a favorable outcome, but the severe side effects and risks associated with chemotherapy still call for new therapeutic approaches.[4-6] A distinct gene expression profile (referred to as R6 cluster) has been identified to be characteristic of, but not limited to *ERG*-deleted cases.[7] In a recent report, Lilljebjörn et al. found a strong overlap of *DUX4*-rearrangements and ERG deletions, and provide evidence that the *DUX4*-rearrangement is the origin of this exclusive gene expression profile.[8] In this newly described subtype of BCP-ALL, a truncated copy of the usually silenced germline transcription factor *DUX4* is inserted into an actively transcribed region and aberrantly expressed.[8, 9] Zhang et al. showed that aberrant *DUX4* induces the expression of an alternative isoform of *ERG*, thereby directly

linking the function of these two transcription factors.[10]

Transcription factors are difficult to target with small molecule inhibitors and other targets such as kinases should therefore be investigated. We here describe high expression of the receptor tyrosine kinase PDGFRα in cases with ERG deletions. Given its implication in other hematological malignancies we evaluated possible genetic aberrations and assessed the response of primary BCP-ALL cells with high *PDGFRA* expression to two PDGFR inhibitors.

Methods

Primary leukemic cells, cell lines, and mesenchymal stromal cells

The study comprised children with newly diagnosed BCP-ALL with age at diagnosis ranging from 0 to 18 years. Written informed consent was obtained from parents or guardians, and institutional review boards approved the use of excess diagnostic material for research purposes. Clinical characteristics were kindly provided by the Dutch Childhood Oncology Group (the Hague, Netherlands). These studies were conducted in accordance with the Declaration of Helsinki. Mononuclear cells were isolated using density gradient centrifugation with Lymphoprep (Axis Shield, Norway) as previously described.[11] All samples contained at least 90% leukemic blasts. Cytogenetic subtypes were determined by karyotype, fluorescence in-situ hybridization (FISH), and/or fusion-gene specific PCR. *BCR-ABL1*-like cases were identified using microarray gene expression profiling by the means of a 110 probeset classifier.[4] Animal experiments were approved by the animal ethics committee (EMC 2863 (103-12-08)). Xenografts of BCP-ALL cells from patient D were established as previously reported (Steeghs et al., submitted manuscript) in NOD.Cg-*Prkdc*^{scid}*Il2rg*^{tm1Wjl}/SzJ (NSG) mice (Charles River, France) using intra-femoral injection. Leukemic cells were isolated from the spleen, frozen as viable cells, and subsequently thawed for protein isolation and *ex vivo* co-culture assays. Leukemic cell lines were obtained from the German Collection of Microorganisms and Cell Cultures (DSMZ, Germany) and routinely validated by DNA fingerprinting. Mesenchymal stromal cells (MSCs) were isolated from the bone marrow aspirate taken from a BCP-ALL patient after consolidation therapy as previously described.[12] MSCs were negative for hematopoietic markers and positive for mesenchymal markers.[12, 13]

Gene expression profiling and RT-qPCR

RNA and DNA was isolated using Trizol reagent (Life technologies) according to manufacturer's instructions and RNA subsequently used for gene expression profiling and RT-qPCR. Gene expression profiling was performed using Affymetrix U133 plus 2.0 GeneChips. Detailed methods have been reported previously[14], and data is deposited at NCBI's Gene Expression Omnibus with accession numbers GSE13351 and GSE13425. High *PDGFRA* expression was defined based on the probe set 203131_at, with a cut-off at log2 expression value 5.9 (see also Figure 1A). cDNA was generated using the SensiFAST cDNA synthesis kit (Bioline), and RT-qPCR was performed in a standard SYBR green-based assay (ThermoFisher) on the ABI-PRISM 9700HT Fast Real-Time PCR System. Primer sequences were as follows: exon 3 forward: 5' TTGGGGAGAGTGAAGTGA-3', exon 3/4 reverse: 5' TGGGTCTGGCACATAGAT-3',

exon 12 forward: 5' GCTGCCTTATGACTCAAG-3', exon 14 reverse: 5' GCTCCCAGCAAGTTTACA-3', exon 17 forward: 5' CCGAGGAATGGAGTTTTT-3', exon 18 reverse: 5' TGCCTTTCGACACATAGTT-3'.

Genetic aberrations of B-other cases

Genetic aberrations were determined by array-based comparative genomic hybridization and multiplex-ligated probe assays as previously reported.[2, 15] As previously, cases with a signal intensity of the probe set 208303_s_at above the 90th percentile of the total BCP-ALL group were classified as CRLF2-high.[4]

RT-PCR for detection of known fusion genes

RT-PCR was performed on cDNA of 49 BCP-ALL cases from the B-other and *BCR-ABL1*-like subtype, including 24 of the 26 patients with high *PDGFRA* expression identified by microarray profiling. Primer sequences are reported in Supplemental Table 1. Forward primers were used as previously reported, except for an adaptation in BCR-ex7 forward (new sequence: 5' TACAAGCCTGTGGACCGTGT-3').[16-20] Forward primers for known fusion partners of *PDGFRA* were confirmed to be functional in an RT-PCR using a reverse primer located within the partner gene. All forward primers were combined with *PDGFRA* exon 14 reverse (see above), but an additional PCR run with *FIP1L1*-forward combined with *PDGFRA*-R2 as published by Cools et al.[18] PCR products were amplified as follows: 2min 50°C, 10min 95°C, five times 8 cycles of 15s 95°C and 1min at 60°C, 57°C, 54°C, 51°C, or 48°C, followed by 30s at 72°C. PCR products were separated on agarose gel and evaluated for bands by visual inspection under UV light.

Fluorescence in situ hybridization (FISH)

FISH was performed using the *FIP1L1/CHIC2/PDGFRA* deletion probes by Cytocell (Cambridge, UK). Cytospins were made from freshly isolated cells or from viable frozen cells after thawing. They were dried and stored at -80°C until used. Prior to hybridization, samples were treated with 20 µg/mL pepsin in 0.01 M HCl at 37°C for 10 min and fixated in PBS containing 1% formaldehyde and 200 g/L MgCl2 for 10 min. Denaturation was performed for 5 min at 75°C and probes hybridized at 37°C overnight. Nuclei were stained with DAPI antifade and results evaluated and recorded with a Leica AF6000 workstation and Leica LAF LS imaging software version 2.0.0 build 1929 (Wetzlar, Germany). Visibility of blue DAPI signals in Figure 2A were enhanced using Adobe Photoshop CS6.

Targeted locus-amplification (TLA)

The precise methods for targeted locus amplification have been published previously.[21] In brief, viable frozen cells of BCP-ALL cases were thawed and directly used for the procedure. Crosslinking and DNA isolation were performed according to manufacturer's instruction. Custom primers were designed by Cergentis (Utrecht, Netherlands) to amplify regions of *PDGFRA* that were previously reported to be involved in structural aberrations, and PCR products sequenced by Illumina paired-end sequencing. Raw reads in FASTQ format were aligned to GRCh37 using BWA mem. Whole genome coverage in a sliding window of 10 kb was calculated using Samtools view, and per base pair coverage near the *PDGFRA* gene using the GATKs DepthOfCoverage tool. Coverage plots in a sliding window of 10 kb and 100 bp were then generated using R language.

Protein isolation and western blot

Primary BCP-ALL cells and cell lines were treated with recombinant human PDGF-BB (#8912, Cell Signaling, Danvers, USA) and inhibitors imatinib (10 μM) and CP673451 (1 μM, both Selleckchem, Munich, Germany) for the indicated time span and lysed using caspase lysis buffer (150 mM NaCl, 50 mM Tris, 10 mM EDTA, 1% Triton-X, 1mM DTT, 1mM PMSF, 2μg/ml Aprotinin, 1mM Sodium-Pervanadate, and 10mM Sodium-Fluoride, all Sigma Aldrich, St. Louis, USA). Nalm6 cells were serum starved for 2 hours, which was omitted in primary BCP-ALL cells to avoid massive cell death. Protein concentrations were quantified using a BCA assay (Thermo Fisher Scientific, Waltham, USA), and 25μg loaded and separated on precast polyacrylamide gels (BioRad, Hercules, USA). Proteins were transferred to nitrocellulose membranes using 1.3 A and 25 V for 13 minutes in the Bio-Rad Trans-blot Turbo system. Membranes were blocked with 5% BSA (w/v) in TBS containing 0.1% Tween-20 (TBST) for 2 h and probed with anti-PDGFRα #3174, anti-phospho-PDGFRα (Y762) #12022, (both Cell Signaling) or anti-β-actin ab6276 (Abcam, Cambridge, UK). Fluorescent-labeled secondary antibodies were obtained from Li-COR (Lincoln, USA), and blots were scanned using the Odyssey system (Li-COR). Odyssey software version 3.0 was used for image acquisition and signal quantification.

Cell culture, ex vivo drug sensitivity and co-culture model

Cell lines were cultured in RPMI-1640 GlutaMAX supplemented with penicillin, streptomycin, and fungizone (all Life technologies, Bleiswijk, Netherlands) and 10% (Nalm6) or 20% (EOL1) FCS. Primary BCP-ALL cells were cultured in RPMI-1640 Dutch modified supplemented with glutamine, insulin, transferrin, selenium, penicillin, streptomycin, fungizone, gentamycin, and 20% FCS. For MTT-based *ex vivo* cytotoxicity assays, cells were exposed to a range of Imatinib (100 μM – 0.003 μM) or CP673451 (10 μM – 0.0003μM) for four days and survival analyzed using 3-(4,5-Dimethylthiazol-2-yl)-2,5-diphenyltetrazolium (MTT). For *ex vivo* co-culture assays, MSC were seeded one day prior to start. Leukemic cells were cultured at a concentration of $2*10^6$/mL in presence or absence of MSC, in presence or absence of 50 ng/mL recombinant human PDGF-BB, and with three different concentrations of Imatinib (12.5 μM, 1.6 μM, 0.2 μM) or CP673451 (1.25 μM, 0.16 μM, 0.02 μM). After four days, cells were harvested and analyzed by flow cytometry. Viable leukemic cells were quantified within a fixed volume by combined staining for CD19-APC (positive), Annexin-V-FITC (negative, both BioLegend, San Diego, USA), and propidium iodide (negative, Sigma Aldrich). The gating strategy was as previously reported.[13]

Results

PDGFRA expression in pediatric BCP-ALL

Gene expression microarray analysis of 654 pediatric ALL cases of all cytogenetic subtypes identified elevated *PDGFRA* expression in 26 BCP-ALL cases by two different probe sets (Figure 1A). The high PGFRA expression levels was confirmed by RT-qPCR in 23 of 25 tested cases (Figure 1B and Figure S1). All cases belonged to the B-other (n=22) or *BCR-ABL1*-like (n=4) subtype. High *PDGFRA* was also maintained in xenograft-derived cells of a *PDGFRA* high case, and found in the BCP-ALL cell line Nalm6 (Figure S1).

The *FIP1L1-PDGFRA*-positive chronic eosinophilic leukemia cell line EOL1 served as a positive control in all experiments.[22]

Clinical characteristics of *PDGFRA* expressing BCP-ALL cases

Since high *PDGFRA* expression was mainly found in the B-other subtype, we restricted our analysis of clinical characteristics to this group. Age, white blood cell count (WBC), gender, risk stratification arm, and the frequency of relapse, death, and events were not significantly different between *PDGFRA* high and low B-other cases (Table 1). However, patients with high *PDGFRA* expression were more sensitive to prednisolone *ex vivo* ($p = 0.03$, see also Figure S2). Differences in sensitivity towards L-asparaginase and vincristine were not statistically significant.

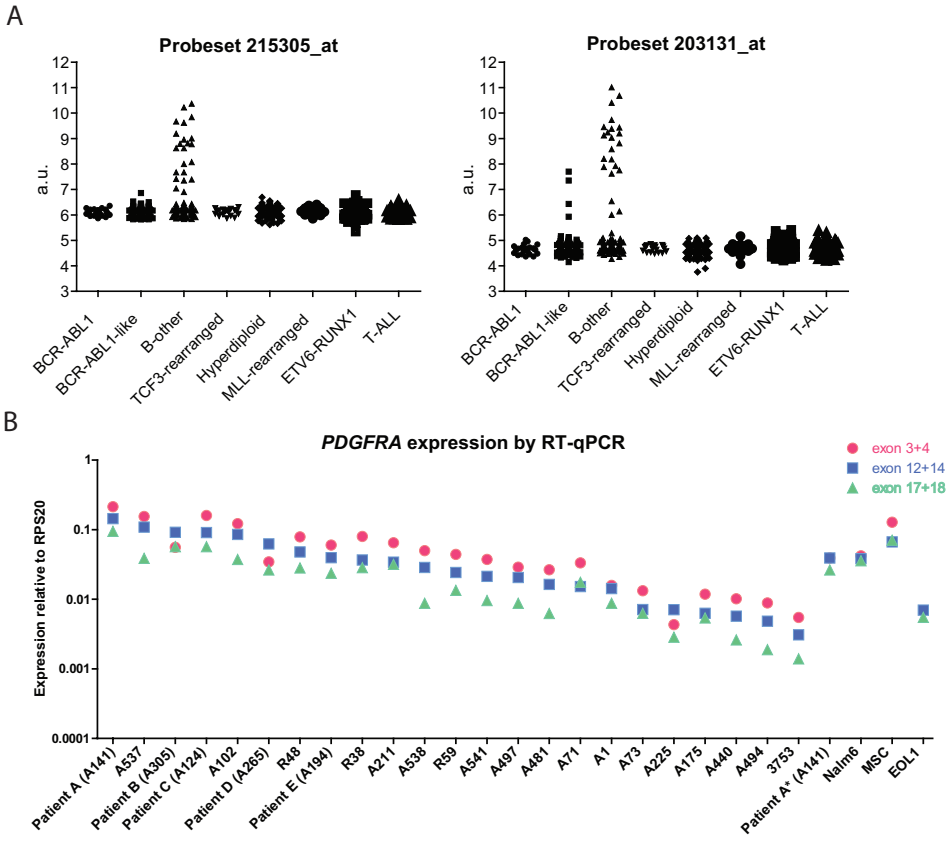

Figure 1: Gene expression of *PDGFRA*.
(A) Gene expression of *PDGFRA* in the genetic subtypes of pediatric BCP-ALL. Expression was measured on Affymetrix U133 plus 2.0 GeneChips using two different probe sets. **(B)** Confirmation of *PDGFRA* mRNA levels by RT-qPCR using primer pairs located in three regions of the transcript. Expression values are given relative to *RPS20* housekeeping gene. Numbers on x-axis represent patient identifiers with reference to the samples used in in vitro experiments. *identifies the xenograft-derived sample of patient A.

Table 1. Clinical characteristics of B-other patients with high *PDGFRA* expression.

"Total" designates number of cases for whom data is available, "cases" designates the number of patients carrying presenting the clinical characteristic. Frequencies are calculated from these numbers. Fisher's Exact test p-value is given, significant p-values are printed in bold. Odds ratio is given for cases with $p \leq 0.1$. WBC: white blood cell count; HR: high risk; Event: Relapse, non-response after consolidation phase, or death. LC50: 50% lethal concentration of in vitro drug sensitivity testing as described previously, PRED: Prednisolone, VCR: Vincristine, ASP: Asparaginase.

Clinical feature	PDGFRA high			PDGFRA low				
	Total (n)	Cases (n)	Frequency (%)	Total (n)	Cases (n)	Frequency (%)	p=	Odds ratio (95%-CI)
Age ≥10	22	9	41%	90	30	33%	0,62	
WBC ≥50	22	4	18%	90	25	28%	0,43	
Male	22	15	68%	90	50	56%	0,34	
Treatment group HR	22	6	27%	87	39	45%	0,15	
Relapse	22	2	9%	90	19	21%	0,24	
Event	22	3	14%	90	26	29%	0,18	
Death	22	2	9%	90	21	23%	0,24	
PRED LC50 ≥ 0.1 µg/mL	7	1	14%	26	18	69%	0,03	0.08 (0.002 -0.83)
VCR LC50 ≥ 0.39 µg/mL	7	4	57%	25	15	60%	1	
ASP LC50 ≥ 0.033 µg/mL	7	6	86%	25	18	72%	0,64	

Absence of genetic aberrations in the *PDGFRA* locus

Oncogenic fusions involving the tyrosine kinase domain of *PDGFRA* are recurrent in adult myeloproliferative neoplasms, but have not been reported in pediatric BCP-ALL. Using fusion gene specific RT-PCRs, we did not detect any of the six *PDGFRA* fusions reported to date, including *PDGFRA* fused to *FIP1L1, STRN, BCR, CDK5RAP2, ETV6,* and *KIF5B* (Table S1).[16-20]

Novel translocations and other large structural aberrations affecting the *PDGFRA* locus may also be responsible for *PDGFRA* gene expression. We therefore performed FISH with three probes targeting regions upstream of *FIP1L1* (green), between *FIP1L1* and *PDGFRA* (red) and downstream of *PDGFRA* (green, see also scheme in Figure 2A). The cell line EOL1 served as a positive control, and showed the previously reported pattern of one wildtype allele and two alleles with an interstitial deletion (Figure S5). None of the tested primary BCP-ALL samples and cell lines with high or low *PDGFRA* expression showed interstitial deletions between *FIP1L1* and *PDGFRA* or split FISH signals (Figure 2A). The complete set of tested patients with high or low *PDGFRA* is available in the supplemental data published online (Figure S5).

For a higher resolution of the genomic sequence within and outside of the *PDGFRA* gene, we applied targeted locus amplification to 17 cases for which viable cells were available. This technique allows amplification and sequencing of genomic regions that are in close proximity to a region of interest.[21] Following cross-linking, digestion, and proximity-based re-ligation, targeted amplification was performed from a so-called anchor or viewpoint in the *PDGFRA* gene. Reads obtained in the following sequencing step therefore mapped to the genomic regions close to the viewpoint. With increasing distance from the viewpoint, genomic regions are less likely to be captured by proximity ligation and will yield a lower

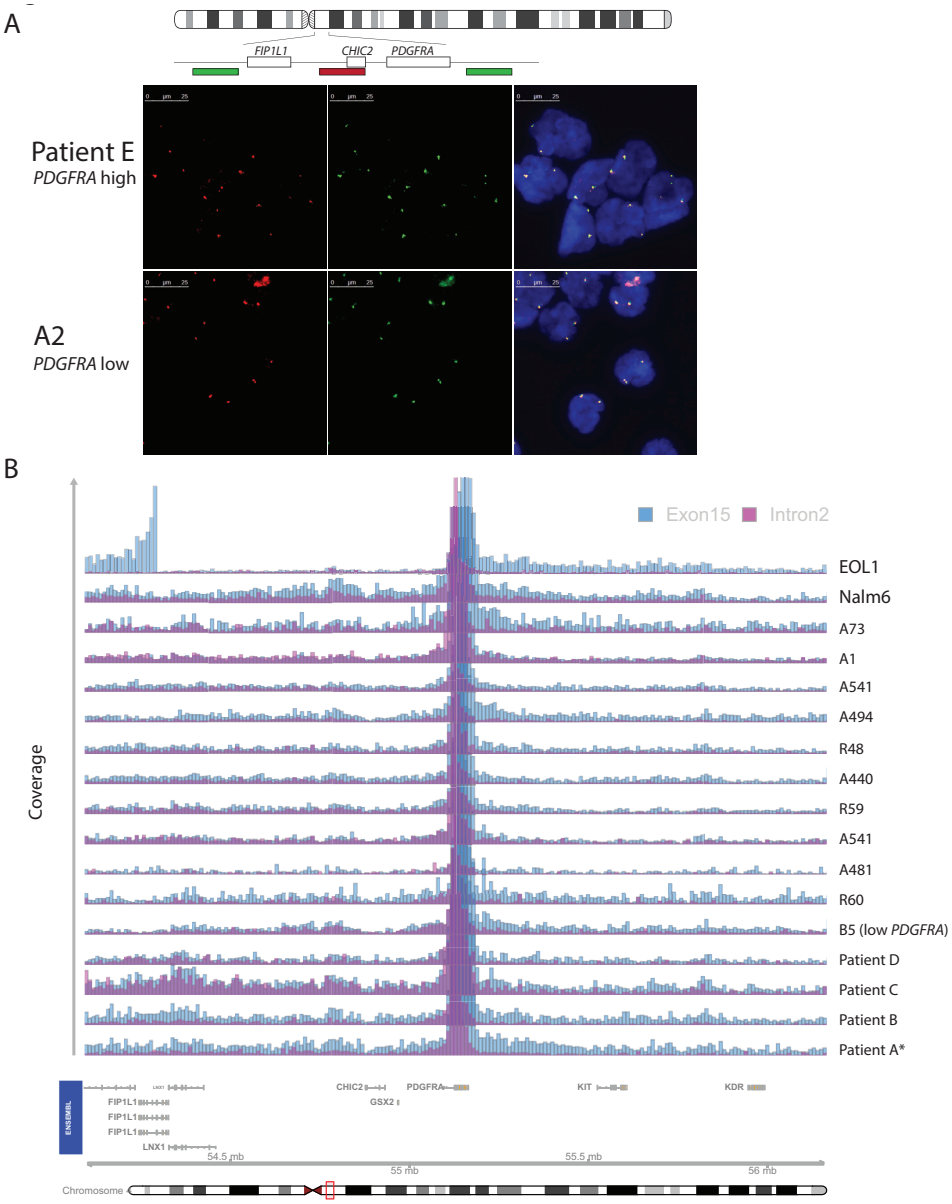

Figure 2: Genomics of *PDGFRA* high cases and Nalm6.

(A) Schematic overview and representative results of interphase FISH probing the *FIP1L1-PDGFRA* locus in a case with high and a case with low *PDGFRA* expression. Red (left panel): probe spanning the *CHIC2* gene; green (middle panel): probes upstream of *FIP1L1* and downstream of *PDGFRA*, respectively. Merge (right panel): Overlay of red and green signal, blue: DNA stained by DAPI. **(B)** Targeted locus amplification performed from two viewpoints within the *PDGFRA* locus. Bars represent the mean coverage over a 10 kb bin plotted on the y-axis, while chromosomal position is indicated on the x-axis. Coverage around the viewpoint is capped for data visualization. 14 cases with high *PDGFRA*, one case with low *PDGFRA*, and two cell lines were tested.

Table 2. Molecular characteristics of B-other patients with high *PDGFRA* expression.

The frequency of aberrations in known B-cell differentiation factors and other genes associated with BCP-ALL was evaluated by array CGH data and/or MLPA and compared between *PDGFRA* high and low expressing B-other patients. The p-value calculated by a Fisher's exact test is given. chr21 aberration: partial or complete amplification of chromosome 21, including germline trisomy. *IKZF1* Δ4-7: deletion of exons 4 to 7 in *IKZF1*. Odds ratio is only given for significant associations.

	***PDGFRA* high**			***PDGFRA* low**				
Biological feature	**Total (n)**	**Cases (n)**	**Frequency (%)**	**Total (n)**	**Cases (n)**	**Frequency (%)**	**p=**	**Odds ratio (95%-CI)**
ERG intragenic deletion	16	10	63%	71	0	0%	<0.001	∞ (19.1 - ∞)
chr21 amplification	19	0	0%	84	23	27%	0.006	0 (0 - 0.63)
High *CRLF2*	22	0	0%	90	16	18%	0.038	0 (0 – 0.97)
9p-deletion	19	0	0%	83	19	23%	0.02	0 (0 – 0.82)
ETV6 deletion	22	0	0%	87	23	26%	0.003	0 (0 – 0.57)
PAX5 deletion	22	3	14%	85	36	42%	0.013	0.22 (0.04 – 0.82)
CDKN2A or *B* deletion	22	5	23%	87	43	49%	0.031	0.30 (0.08 – 0.96)
IKZF1 deletion	22	2	9%	85	25	29%	0.057	
IKZF1 Δ4-7	22	2	9%	85	5	6%	0.63	
EBF1 deletion	22	0	0%	85	4	5%	0.58	
RB1 deletion	22	1	5%	86	6	7%	1	
BTG1 deletion	22	1	5%	86	8	9%s	0.683	
TCF3 deletion	16	1	6%	71	19	27%	0.1	

coverage. In case of translocations with breakpoints close to the viewpoint, coverage would increase on another chromosome. In case of interstitial deletions (e.g. causing the *FIP1L1-PDGFRA* fusion gene), sequencing coverage will drop steeply first and then rise again on a distant site. Two viewpoints were selected in intron 2 and exon 15 of *PDGFRA*. Using this technique on the positive control EOL1, we confirmed an interstitial deletion on chromosome 4 which rearranges *FIP1L1* intron 12 to *PDGFRA* exon 12 (Figure 2B, top panel). The coverage pattern and sequence information obtained from Nalm6 and primary BCP-ALL samples with high *PDGFRA* expression did not indicate any genomic aberrations (Figure 2B).

Secondary genetic aberrations in *PDGFRA* expressing BCP-ALL cases

Next, we used MLPA and array CGH data to evaluate the incidence of other genetic aberrations that were previously shown to be recurrent in pediatric BCP-ALL (Table 2). The frequency of deletions in *IKZF1, EBF1, RB1, BTG1,* and *TCF3* did not differ significantly between B-other patients with high or low *PDGFRA* expression. *PAX5* and *CDKN2A* and/or *B* deletions were rare in patients with high *PDGFRA* ($p = 0.01$ and $p = 0.03$, respectively), and no loss of the entire chromosome-arm 9p was observed ($p = 0.02$). No *ETV6* deletion ($p = 0.003$), high *CRLF2* expression ($p = 0.04$), or chromosome 21 amplification ($p = 0.006$) was found in *PDGFRA*-high patients. In contrast, 63% of patients with high *PDGFRA* expression carried ERG deletions (10/16), compared to 0% in *PDGFRA* low B-other cases (0/71, $p<0.001$). Consequently, all ERG-deleted cases expressed high levels of *PDGFRA* (Figure S6).

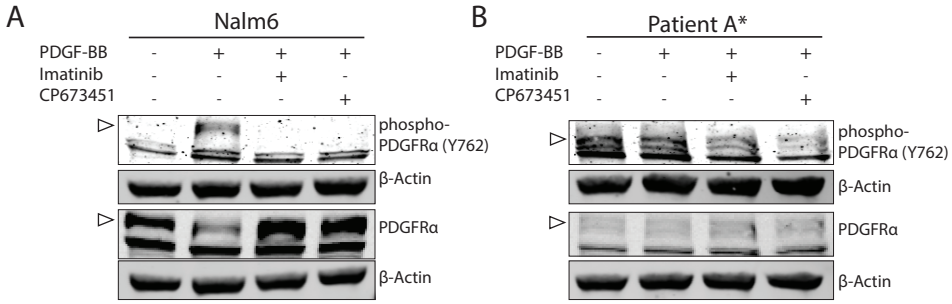

Figure 3: Western blot for PDGFRA activation.

Western blot for phosphorylated (Y762) and total PDGFRA protein in **(A)** the cell line Nalm-6 and **(B)** patient derived xenograft cells of patient A (labeled A*). Cells were treated with 10ng/mL recombinant human PDGF-BB for 10 minutes, either with or without 10μM Imatinib or 1μM CP673451. Arrow heads indicate the expected band. Total protein load was analyzed by staining for β-actin.

PDGFRα is actively signaling in BCP-ALL cells

Next, we confirmed protein expression and activation of PDGFRα by western blot, using Nalm6 and xenograft-derived material of a *PDGFRA*-high BCP-ALL case. Nalm6 cells were first starved and afterwards stimulated with recombinant PDGFR-ligand PDGF-BB. Western blot analysis revealed that the ligand activates the phosphorylation of *PDGFRA* and reduces the total *PDGFRA* levels (Figure 3). Exposure to the PDGFR inhibitors imatinib and CP673451 abrogated the ligand-induced activation of *PDGFRA*. High levels of phosphorylation were also detected in untreated and in ligand-treated primary BCP-ALL cells, which were not starved to avoid drastic reduction of cell viability. As in the Nalm6 cell line, PDGFR inhibitors clearly reduced phosphorylation of PDGFRα in primary BCP-ALL cells (Figure 3B). This effect persisted for at least 30 minutes (Figure S7).

PDGFRα signaling is not essential for the survival of *PDGFRA* expressing BCP-ALL cells

The sensitivity of BCP-ALL cells to PDGFRα inhibition was evaluated in an *ex vivo* co-culture model including bone marrow MSC. This model has been previously shown to improve the survival of primary BCP-ALL cells and also serves as a model of microenvironment-mediated drug resistance.(13, 14) In co-culture with MSC cell survival of *PDGFRA*-high cells was improved by about 3-fold compared to culture without MSC (Figure S8). A smaller benefit was observed for *PDGFRA*-low expressing cells.

The cell line EOL1 was highly sensitive to PDGFR inhibitors (imatinib and CP673451) in culture with and without MSC, while Nalm6 showed reduced viability only at the highest inhibitor concentration (Figure 4A). Primary BCP-ALL samples with high *PDGFRA* expression were marginally sensitive to imatinib, but not to CP673451, in mono-culture (Figure 4B, left side, red symbols) and in co-culture with MSC (Figure 4B, right side). No cytotoxic effect of PDGFR inhibitors was observed in cases with low *PDGFRA* expression (Figure 4B blue symbols). For Nalm6 and three BCP-ALL samples with sufficient material, the assay was repeated with recombinant human PDGF-BB included.

This ligand exposure did not sensitize to PDGFR inhibition (Figure S9). Therefore, the reduction in phosphorylated PDGFRα upon exposure to inhibitors (Figure 3) does not coincide with induction of cell death.

Discussion

Therapies targeting oncogenic signaling pathways in addition to standard chemotherapy may be a treatment strategy for children with BCP-ALL who respond poorly or relapse. It may also be able to replace highly toxic agents and reduce side effects. Here, we have identified a group of BCP-ALL cases with high expression of the receptor tyrosine kinase PDGFRα, which we subsequently evaluated as treatment target. Two thirds of the

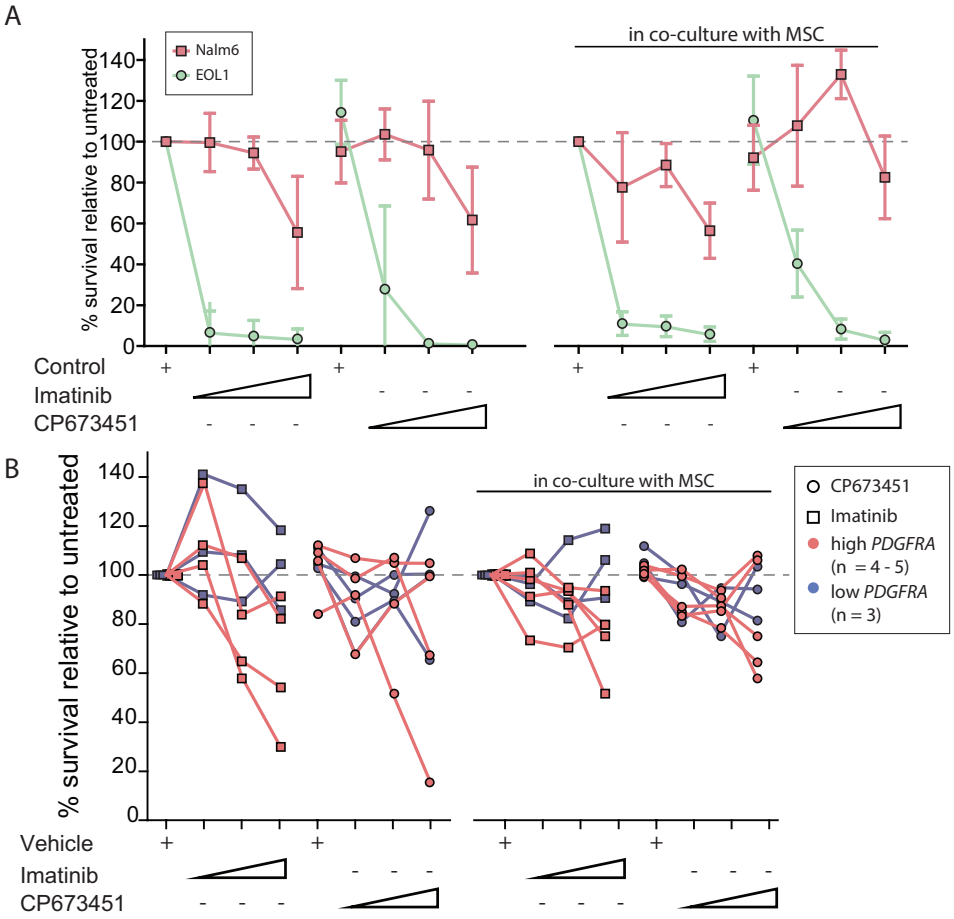

Figure 4: *Ex vivo* sensitivity of cell lines and primary leukemic cells to PDGFR inhibitors in an *in vitro* co-culture model.

(A) Cell lines and **(B)** primary leukemic cells were cultured with or without MSC and exposed to a range of Imatinib (0.2μM – 1.6μM – 12.5μM) or CP673451 (0.02μM – 0.16μM – 1.25μM) for four days. Cell survival was analyzed by flow cytometry and is depicted relative to the untreated control. Vehicle represents the respective vehicle control for imatinib (water) or CP673451 (DMSO) treated conditions.

cases carried ERG-deletions, and vice versa all ERG-deleted cases show high *PDGFRA* expression. Therefore, high *PDGFRA* expression likely characterizes the newly discovered DUX4-rearranged subtype with frequent ERG-deletions.[8-10]

Western blot experiments in cell line and primary BCP-ALL cells showed ligand-dependent activation of PDGFRα and inhibition by imatinib and CP673451. However, *ex vivo* drug testing by means of a previously established co-culture model showed that the activation of PDGFRα is not predictive for sensitivity to these inhibitors. Clinical baseline characteristics of *PDGFRA*-high cases were not significantly different from those of B-other cases with low *PDGFRA* expression, although the small group size may have limited the analysis. Nonetheless, we found a marked *ex vivo* sensitivity towards prednisolone in *PDGFRA*-high cases. This is in line with the good prognosis reported for *ERG*-deleted/*DUX4*-rearranged leukemia.[5, 8, 9]

Oncogenic fusions of tyrosine kinases other than *BCR-ABL1* fusions occur in about 3% of BCP-ALL cases and are currently being evaluated as treatment targets.[23, 24] Fusion genes involving *PDGFRA* have been described in different forms of myeloproliferative neoplasms, and fusion genes of the closely related *PDGFRB* are recurrently found in *BCR-ABL1*-like BCP-ALL.[18, 25-28] These cases are routinely and successfully treated with imatinib. Amplifications, rearrangements, and intragenic deletions of *PDGFRA* have been found in glioblastoma multiforme.[29] Amplification of *PDGFRA* in these cases results in overexpression, which is sufficient for constitutive activation.[30] Interestingly, imatinib is also not an effective therapy in these patients.[31] In the present study, we did not detect genomic aberrations that could explain high *PDGFRA* expression: Fusion-specific PCRs to all known translocations were negative, FISH to the genomic region around *FIP1L1* and *PDGFRA* showed no interstitial deletion or translocation affecting the *PDGFRA* locus, and targeted locus amplification revealed no structural aberrations affecting the *PDGFRA* gene. Furthermore, the validation of *PDGFRA* transcript levels by RT-qPCR showed consistent results for primer pairs designed to the 5', middle, and 3' located part of the transcript. This suggests that the *PDGFRA* transcript is intact and not shortened due to alternative splicing or gene fusions. The PDGFRα protein detected on western blot was detected at the expected molecular weight. Taken together, these results support the conclusion that the here characterized group of patients expresses wildtype *PDGFRA* transcript and protein.

BCP-ALL cases with high levels of *PDGFRA* showed few aberrations in *PAX5* and *CDKN2A/B*, no aberrations in the CRLF2 pathway, and no gains in chromosome 21. Rather, they are characterized by frequent *ERG*-deletions. *ERG*-deleted cases are known to be limited to a subgroup of BCP-ALL cases with a characteristic gene expression profiles.[7] This so-called R6 cluster, which includes but is not limited to ERG deleted cases, has recently been suggested to represent the newly identified *DUX4*-rearrangements.[8] The identification of *DUX4*-rearrangements on genomic level is challenging due to varying integration sites and many repeats in the genome. Transcript-directed assays are hindered by a high GC content and high homology, and our attempts to detect *DUX4* transcripts have failed. Therefore direct evidence linking *DUX4*-rearrangements and high *PDGFRA* expression is lacking, but several indications exist. Yasuda et al. have shown that Nalm6 carries a *DUX4*-rearrangement.[9] In addition, we evaluated the extensive dataset on *DUX4* *DUX4*-rearranged leukemia published by Zhang et al.[10] In their analysis, *PDGFRA* is

highly expressed in *DUX4* leukemia, and its transcription start site was directly bound by *DUX4* (see Supplemental Tables 3a and 14 of reference 10). We therefore regard it as highly likely that the *PDGFRA* high cases represent this novel *DUX4*-rearranged subtype.

In conclusion, high *PDGFRA* expression is found in a subgroup of B-other BCP-ALL patients with frequent *ERG*-deletions. The high gene expression does not seem to be caused by genetic aberrations of the *PDGFRA* locus, but results in a functional PDGFRα signaling pathway. These signals were not essential to BCP-ALL survival in vitro, which dismisses PDGFRα as therapeutic target in BCP-ALL.

Conflict of interest

The authors declare no conflict of interest.

Author contributions

I.S.J. and M.d.B. designed experiments, interpreted the data, and wrote the manuscript, I.S.J., D.C., and H.B.B. performed experiments and analyzed data, A.Q. and J.M.B. collected, analyzed, and interpreted genomics data, R.P. and M.d.B. conceptualized the study and interpreted the results. All authors read, revised, and approved the manuscript. Correspondence: Monique den Boer, m.l.denboer@erasmusmc.nl.

Acknowledgement

This work was supported by the NWO VICI program (grant 016.126.612), Dutch Cancer Society (grants AMC 2008-4265 and EMCR 2014-6998), KIKA Foundation (grant 132) and the Pediatric Oncology Foundation Rotterdam. We thank Cergentis BV (Utrecht) for collaboration on targeted locus amplification, and Judit Balog from Leiden University Medical Center for all efforts in detecting *DUX4*.

References

1. Pui CH, Yang JJ, Hunger SP, Pieters R, Schrappe M, Biondi A, et al. Childhood Acute Lymphoblastic Leukemia: Progress Through Collaboration. J Clin Oncol. 2015 Sep 20;33(27):2938-48.

2. Den Boer ML, van Slegtenhorst M, De Menezes RX, Cheok MH, Buijs-Gladdines JG, Peters ST, et al. A subtype of childhood acute lymphoblastic leukaemia with poor treatment outcome: a genome-wide classification study. Lancet Oncol. 2009 Feb;10(2):125-34.

3. Mullighan CG, Su X, Zhang J, Radtke I, Phillips LA, Miller CB, et al. Deletion of IKZF1 and prognosis in acute lymphoblastic leukemia. N Engl J Med. 2009 Jan 29;360(5):470-80.

4. van der Veer A, Waanders E, Pieters R, Willemse ME, Van Reijmersdal SV, Russell LJ, et al. Independent prognostic value of *BCR-ABL1*-like signature and IKZF1 deletion, but not high CRLF2 expression, in children with B-cell precursor ALL. Blood. 2013 Oct 10;122(15):2622-9.

5. Clappier E, Auclerc MF, Rapion J, Bakkus M, Caye A, Khemiri A, et al. An intragenic ERG deletion is a marker of an oncogenic subtype of B-cell precursor acute lymphoblastic leukemia with a favorable outcome despite frequent IKZF1 deletions. Leukemia : official journal of the Leukemia Society of America, Leukemia Research Fund, UK. 2014 Jan;28(1):70-7.

6. Zaliova M, Zimmermannova O, Dorge P, Eckert C, Moricke A, Zimmermann M, et al. ERG deletion is associated with CD2 and attenuates the negative impact of IKZF1 deletion in childhood acute lymphoblastic leukemia. Leukemia : official journal of the Leukemia Society of America, Leukemia Research Fund, UK. 2014 Jan;28(1):182-5.

7. Harvey RC, Mullighan CG, Wang X, Dobbin KK, Davidson GS, Bedrick EJ, et al. Identification of novel cluster groups in pediatric high-risk B-precursor acute lymphoblastic leukemia with gene expression profiling: correlation with genome-wide DNA copy number alterations, clinical characteristics, and outcome. Blood. 2010 Dec 2;116(23):4874-84.

8. Lilljebjorn H, Henningsson R, Hyrenius-Wittsten A, Olsson L, Orsmark-Pietras C, von Palffy S, et al. Identification of *ETV6-RUNX1*-like and DUX4-rearranged subtypes in paediatric B-cell precursor acute lymphoblastic leukaemia. Nat Commun. 2016 Jun 06;7:11790.

9. Yasuda T, Tsuzuki S, Kawazu M, Hayakawa F,

Kojima S, Ueno T, et al. Recurrent DUX4 fusions in B cell acute lymphoblastic leukemia of adolescents and young adults. Nature genetics. 2016 May;48(5):569-74.

10. Zhang J, McCastlain K, Yoshihara H, Xu B, Chang Y, Churchman ML, et al. Deregulation of DUX4 and ERG in acute lymphoblastic leukemia. Nature genetics. 2016 Oct 24.

11. Den Boer ML, Harms DO, Pieters R, Kazemier KM, Gobel U, Korholz D, et al. Patient stratification based on prednisolone-vincristine-asparaginase resistance profiles in children with acute lymphoblastic leukemia. J Clin Oncol. 2003 Sep 1;21(17):3262-8.

12. van den Berk LC, van der Veer A, Willemse ME, Theeuwes MJ, Luijendijk MW, Tong WH, et al. Disturbed CXCR4/CXCL12 axis in paediatric precursor B-cell acute lymphoblastic leukaemia. British journal of haematology. 2014 Jul;166(2):240-9.

13. Polak R, de Rooij B, Pieters R, den Boer ML. B-cell precursor acute lymphoblastic leukemia cells use tunneling nanotubes to orchestrate their microenvironment. Blood. 2015 Nov 19;126(21):2404-14.

14. Aries IM, Jerchel IS, van den Dungen RE, van den Berk LC, Boer JM, Horstmann MA, et al. EMP1, a novel poor prognostic factor in pediatric leukemia regulates prednisolone resistance, cell proliferation, migration and adhesion. Leukemia : official journal of the Leukemia Society of America, Leukemia Research Fund, UK. 2014 Sep;28(9):1828-37.

15. Kuiper RP, Waanders E, van der Velden VH, van Reijmersdal SV, Venkatachalam R, Scheijen B, et al. IKZF1 deletions predict relapse in uniformly treated pediatric precursor B-ALL. Leukemia : official journal of the Leukemia Society of America, Leukemia Research Fund, UK. 2010 Jul;24(7):1258-64.

16. Walz C, Curtis C, Schnittger S, Schultheis B, Metzgeroth G, Schoch C, et al. Transient response to imatinib in a chronic eosinophilic leukemia associated with ins(9;4)(q33;q12q25) and a CDK5RAP2-PDGFRA fusion gene. Genes, chromosomes & cancer. 2006 Oct;45(10):950-6.

17. Score J, Curtis C, Waghorn K, Stalder M, Jotterand M, Grand FH, et al. Identification of a novel imatinib responsive KIF5B-PDGFRA fusion gene following screening for PDGFRA overexpression in patients with hypereosinophilia. Leukemia : official journal of the Leukemia Society of America, Leukemia Research Fund, UK. 2006 May;20(5):827-32.

18. Cools J, DeAngelo DJ, Gotlib J, Stover EH, Legare RD, Cortes J, et al. A tyrosine kinase created by fusion of the PDGFRA and FIP1L1 genes as a therapeutic target of imatinib in idiopathic hypereosinophilic syndrome. N Engl J Med. 2003 Mar 27;348(13):1201-14.

19. Baxter EJ, Hochhaus A, Bolufer P, Reiter A, Fernandez JM, Senent L, et al. The t(4;22)(q12;q11) in atypical chronic myeloid leukaemia fuses BCR to PDGFRA. Hum Mol Genet. 2002 Jun 1;11(12):1391-7.

20. Curtis CE, Grand FH, Musto P, Clark A, Murphy J, Perla G, et al. Two novel imatinib-responsive PDGFRA fusion genes in chronic eosinophilic leukaemia. British journal of haematology. 2007 Jul;138(1):77-81.

21. de Vree PJ, de Wit E, Yilmaz M, van de Heijning M, Klous P, Verstegen MJ, et al. Targeted sequencing by proximity ligation for comprehensive variant detection and local haplotyping. Nat Biotechnol. 2014 Oct;32(10):1019-25.

22. Cools J, Quentmeier H, Huntly BJ, Marynen P, Griffin JD, Drexler HG, et al. The EOL-1 cell line as an in vitro model for the study of FIP1L1-PDGFRA-positive chronic eosinophilic leukemia. Blood. 2004 Apr 1;103(7):2802-5.

23. Roberts KG, Li Y, Payne-Turner D, Harvey RC, Yang YL, Pei D, et al. Targetable kinase-activating lesions in Ph-like acute lymphoblastic leukemia. N Engl J Med. 2014 Sep 11;371(11):1005-15.

24. Boer JM, Steeghs EM, Marchante JR, Boeree A, Beaudoin JJ, Beverloo HB, et al. Tyrosine kinase fusion genes in pediatric *BCR-ABL1*-like acute lymphoblastic leukemia. Oncotarget. 2016 Nov 22.

25. David M, Cross NC, Burgstaller S, Chase A, Curtis C, Dang R, et al. Durable responses to imatinib in patients with PDGFRB fusion gene-positive and BCR-ABL-negative chronic myeloproliferative disorders. Blood. 2007 Jan 1;109(1):61-4.

26. Gotlib J, Cools J. Five years since the discovery of FIP1L1-PDGFRA: what we have learned about the fusion and other molecularly defined eosinophilias. Leukemia : official journal of the Leukemia Society of America, Leukemia Research Fund, UK. 2008 Nov;22(11):1999-2010.

27. Lengline E, Beldjord K, Dombret H, Soulier J, Boissel N, Clappier E. Successful tyrosine kinase inhibitor therapy in a refractory B-cell precursor acute lymphoblastic leukemia with EBF1-PDGFRB fusion. Haematologica. 2013 Nov;98(11):e146-8.

28. Weston BW, Hayden MA, Roberts KG, Bowyer S, Hsu J, Fedoriw G, et al. Tyrosine kinase inhibitor therapy induces remission in a patient with refractory EBF1-PDGFRB-positive acute lymphoblastic leukemia. J Clin Oncol. 2013 Sep 1;31(25):e413-6.

29. Ozawa T, Brennan CW, Wang L, Squatrito M, Sasayama T, Nakada M, et al. PDGFRA gene rearrangements are frequent genetic events in PDGFRA-amplified glioblastomas. Genes & development. 2010 Oct 1;24(19):2205-18.

30. Demoulin JB, Essaghir A. PDGF receptor signaling networks in normal and cancer cells. Cytokine & growth factor reviews. 2014 Jun;25(3):273-83.

31. Reardon DA, Dresemann G, Taillibert S, Campone M, van den Bent M, Clement P, et al. Multicentre phase II studies evaluating imatinib plus hydroxyurea in patients with progressive glioblastoma. Br J Cancer. 2009 Dec 15;101(12):1995-2004.

Supplemental Data

Supplemental Table 1: Overview of fusion gene specific RT-PCRs for *PDGFRA*-rearrangement. Primer pairs used to detect previously reported rearrangements of *PDGRFA*.

Fusion partner	Forward primer	Reverse primer	Tested samples (n)
FIP1L1[1]	ACCTGGTGCTGATCTTTCTGAT	TGAGAGCTTGTTTTTCACTGGA	49
FIP1L1[1]	ACCTGGTGCTGATCTTTCTGAT	GCTCCCAGCAAGTTTACA	49
STRN[2]	TCTGAGTTAACAGATTCTGCCTC	GCTCCCAGCAAGTTTACA	49
BCR[3]	TACAAGCCTGTGGACCGTGT	GCTCCCAGCAAGTTTACA	49
CDK5RAP2[4]	CAAAGGAGACTGCACCATCCGT	GCTCCCAGCAAGTTTACA	49
ETV6[5]	ACTGTAGACTGCTTTGGGATTAC	GCTCCCAGCAAGTTTACA	49
KIF5B[6]	TGAACAGCAGATCCAGAGCCATA	GCTCCCAGCAAGTTTACA	49

Supplemental Figure S1: RT-qPCR for *PDGFRA*. RT-qPCR for *PDGFRA* mRNA levels in primary BCP-ALL samples, cell lines, and primary MSC with high (grey background) or low (white background) expression levels measured on gene expression arrays. *marks samples that showed high levels on gene expression arrays but not by RT-qPCR.

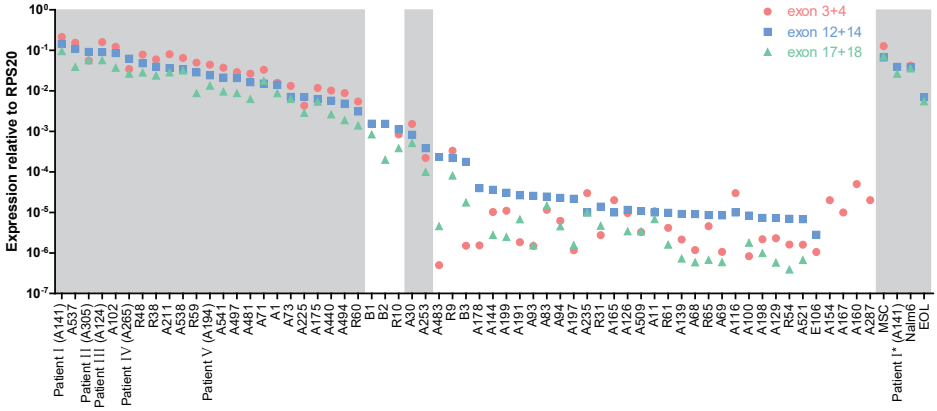

Supplemental Figure S2: *Ex vivo* drug sensitivity towards the 3 major therapeutic agents with prognostic relevance. LC50-values for prednisolone, vincristine, and L-asparaginase in primary B-other BCP-ALL cases with high or low *PDGFRA* expression. *Ex vivo* sensitivity was determined by means of an MTT assay as previously described and compared using a Mann-Whitney U test.[1] **: p<0.01

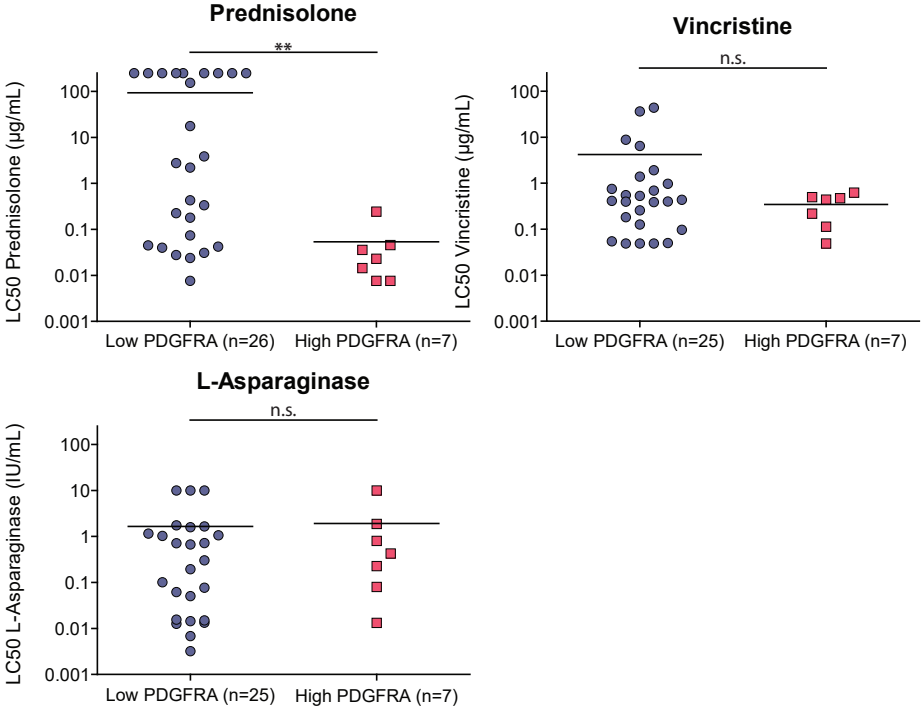

Supplemental Figure S3: Complete FISH results of tested BCP-ALL samples. (A) EOL-1 and Nalm-6 cell lines. **(B)** 25 of 26 patient samples with high *PDGFRA* expression. **(C)** 10 representative cases of BCP-ALL cases with low *PDGFRA* expression.

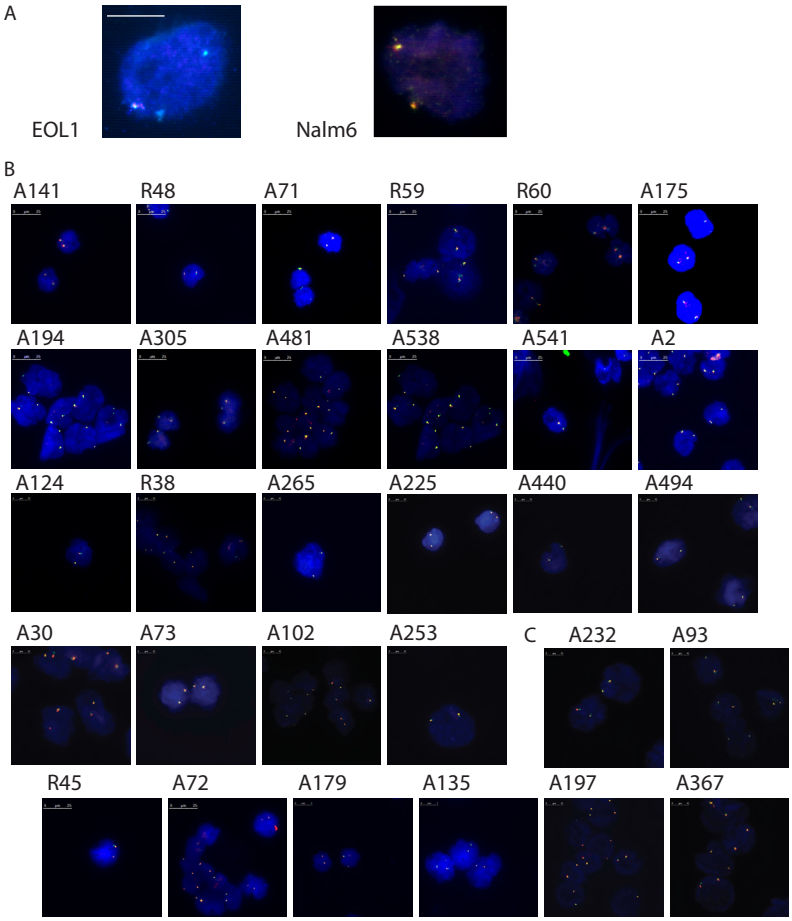

Supplemental Figure S4: *PDGFRA* gene expression in *ERG*-deleted B-other cases. *PDGFRA* gene expression was determined by the same probe sets as presented in Figure 1, and groups separated according to the deletion status of *ERG*.

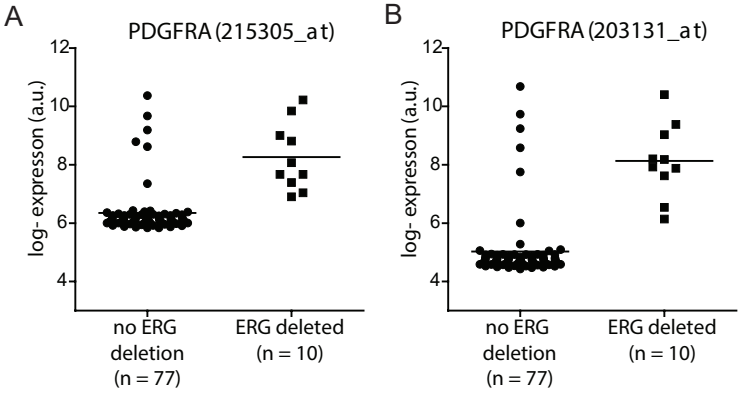

Supplemental Figure S5: Effect of PDGFR inhibition on primary BCP-ALL cells cultured with and without ligand. Nalm6 and three primary BCP-ALL samples with high *PDGFRA* expression (patients I, IV, and V) were tested in mono- and co-culture for sensitivity towards PDGFR inhibitors as in Figure 2C, but with or without recombinant ligand (50ng/mL PDGF-BB). Each dot represents one patient, matched samples with or without PDGF-BB are connected by lines. Dashed line indicates 100% survival relative to the untreated control, ‡ indicates PDX sample of patient I, which was used for western blot analysis in Figure 2A.

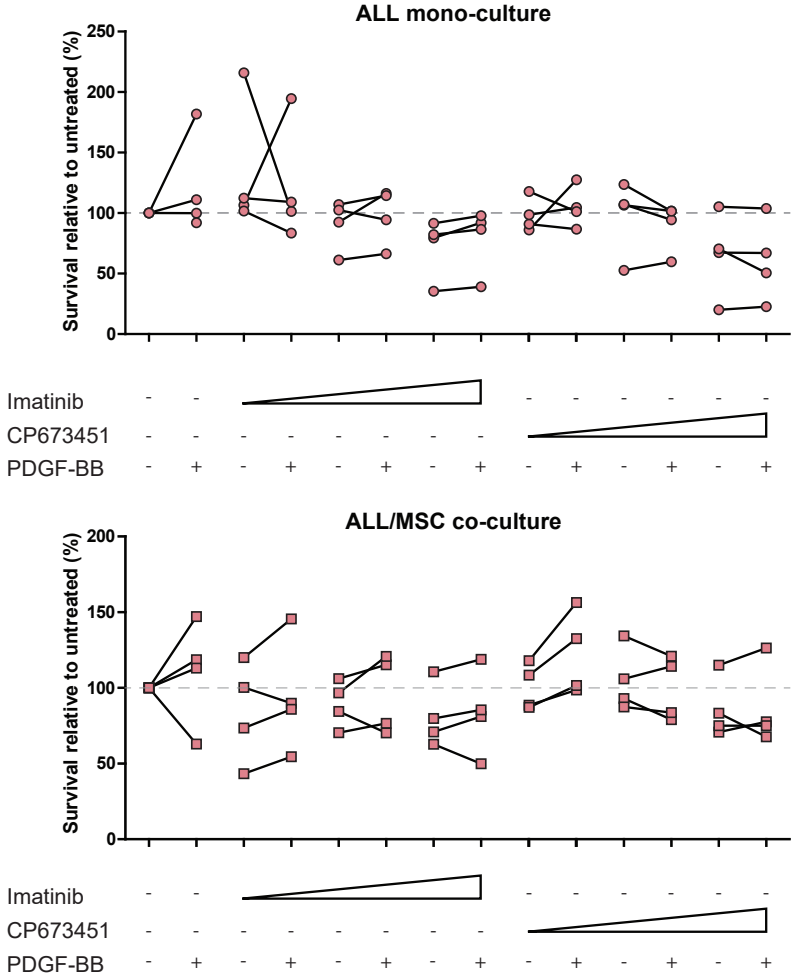

References

1. Cools J, DeAngelo DJ, Gotlib J, et al. A tyrosine kinase created by fusion of the PDGFRA and FIP1L1 genes as a therapeutic target of imatinib in idiopathic hypereosinophilic syndrome. N Engl J Med. 2003;348(13):1201-1214.

2. Curtis CE, Grand FH, Musto P, et al. Two novel imatinib-responsive PDGFRA fusion genes in chronic eosinophilic leukaemia. Br J Haematol. 2007;138(1):77-81.

3. Baxter EJ, Hochhaus A, Bolufer P, et al. The t(4;22)(q12;q11) in atypical chronic myeloid leukaemia fuses BCR to PDGFRA. Hum Mol Genet. 2002;11(12):1391-1397.

4. Walz C, Curtis C, Schnittger S, et al. Transient response to imatinib in a chronic eosinophilic leukemia associated with ins(9;4)(q33;q12q25) and a CDK5RAP2-PDGFRA fusion gene. Genes Chromosomes Cancer. 2006;45(10):950-956.

5. Score J, Curtis C, Waghorn K, et al. Identification of a novel imatinib responsive KIF5B-PDGFRA fusion gene following screening for PDGFRA overexpression in patients with hypereosinophilia. Leukemia. 2006;20(5):827-832.

Chapter 5

Fibroblast growth factor receptor signaling in pediatric B-cell precursor acute lymphoblastic leukemia

Isabel S. Jerchel, Alex Q. Hoogkamer, Ingrid M. Ariës, Judith M. Boer, Nicolle J.M. Besselink, Edwin Cuppen, Marco J. Koudijs, R. Pieters, and Monique L. den Boer

manuscript in preparation

Abstract

The FGF receptor signaling pathway is recurrently involved in leukemogenic processes. Oncogenic fusions of *FGFR1* with various fusion partners were described in myeloid proliferative neoplasms, and overexpression and *FGFR3* mutations are common in multiple myeloma. In addition, fibroblast growth factors are abundant in the bone marrow, and they were shown to enhance the survival of acute myeloid leukemia cells. Here we investigate the effect of FGFR stimulation on pediatric BCP-ALL cells in vitro, and search for mutations with targeted next-generation sequencing of mutational hotspots in *FGFR1*, *FGFR2*, and *FGFR3*. In 481 primary BCP-ALL cases, 28 samples from 19 unique relapsed BCP-ALL cases, and twelve BCP-ALL cell lines we found that mutations are rare (4/481 = 0.8%, 0/28 and 0/12) and do not affect codons which are frequently mutated in other malignancies. However, recombinant ligand FGF2 reduced the response to prednisolone in many BCP-ALL cell lines in vitro. We therefore conclude that FGFR signaling represents a possibly important signaling pathway by which the microenvironment protects BCP-ALL cells from chemotherapy, but that activating mutations in this receptor tyrosine kinase family are very rare.

Introduction

Despite generally excellent outcome for children with pediatric B-cell precursor acute lymphoblastic leukemia (BCP-ALL), therapeutic options are limited for refractory or relapsed cases. Small molecule inhibitors of oncogenic pathways, such as those targeting ABL-, MEK, and JAK kinase families, have shown (pre-)clinical efficacy and may be added to chemotherapy in the future. Here we studied the role of fibroblast growth factor receptor (FGFR) signaling in pediatric BCP-ALL.

FGFs are not only essential in hematopoietic development, but also influence bone formation by regulating expansion and stemness of mesenchymal stromal cells.[1,2] FGF2 is expressed in the hematopoietic and stromal compartments of the bone marrow.1 FGFR fusions have been described in atypical myeloproliferative disorders which may involve lymphoma or present as BCP-ALL.[3] High *FGFR3* expression is a hallmark of t(4;14)-positive multiple myeloma, and activating mutations are recurrently detected in this context.[4-6] Furthermore, FGFR signaling has been shown to contribute to drug resistance in chronic myeloid leukemia.[7] Thus, oncogenic FGFR signaling contributes to hematologic malignancies, but so far information on its role in pediatric BCP-ALL is limited. We therefore applied a customized targeted sequencing approach for mutational hotspots of *FGFR1*, *FGFR2*, and *FGFR3* and evaluated the effect of recombinant FGF2 on in vitro prednisolone sensitivity in BCP-ALL cell lines.

Methods

Patient material and cell lines

The study comprised children with BCP-ALL with age at diagnosis ranging from 0 to 18 years. Written informed consent was obtained from parents or guardians, and institutional review boards approved the use of excess diagnostic material for research purposes. Clinical characteristics were kindly provided by the Dutch Childhood

Oncology Group (the Hague, Netherlands). These studies were conducted in accordance with the Declaration of Helsinki. Mononuclear cells were isolated using density gradient centrifugation with Lymphoprep (Axis Shield, Norway) as previously described.8 All samples contained at least 90% leukemic blasts. Cytogenetic subtypes were determined by karyotype, fluorescence in-situ hybridization (FISH), and/or fusion-gene specific PCR. *BCR-ABL1*-like cases were identified using microarray gene expression profiling by the means of a 110 probeset classifier.[9] Leukemic cell lines were obtained from the German Collection of Microorganisms and Cell Cultures (DSMZ, Germany) and routinely validated by DNA fingerprinting. Unless indicated otherwise, all cell lines were cultured in RPMI-1640 supplemented with 10 to 20% fetal calf serum and penicillin, streptomycin and fungizone (all Life technologies).

In vitro cytotoxicity assays

The IC50 of prednisolone was determined in an MTS assay based on a six-step range from 250 to 0.08 μg/mL (Nalm6, 697, RCH-ACV, MHH-CALL3) or 1 to 0.003μg/mL (MHH-CALL2, MHH-CALL4, SupB15, Tom1). For these assays, cells were tested for viability in the prednisolone concentration range with or without 50ng/mL recombinant human FGF2 (Bio-Rad) and with or without 1μM AZD4547 (Selleckchem). After four days incubation at 37°C and 5% CO2, cell viability was evaluated using MTS. LC50-values were calculated as the prednisolone concentration at which 50% of cells survived relative to the respective prednisolone-free control of each condition. To avoid redundancies with abundant cytokines in fetal calf serum (FCS), these assays were performed under reduced serum conditions (2% FCS for cells usually cultured in 10% FCS, and 4% FCS for those usually cultured with 20% FCS). Sensitivity towards AZD4547 was measured similarly, but at normal serum concentrations (10μM-0.3nM).

Sequencing and code availability

DNA was isolated using Trizol reagent (Life Technologies), or in case of three cell lines using the DNeasy Kit (Qiagen). For TruSeq Custom Amplicon sequencing (Illumina, USA), sequencing libraries were prepared from 100-250ng genomic DNA. Successful library preparation was confirmed using the Labchip GX genomic analyzer (Caliper Life Sciences Benelux N.V., the Netherlands). Samples were then pooled equimolarly and sequenced on an Illumina MiSeq in paired-end reads of 250bp each. Targeted regions and the analysis script can be provided upon request. Next, sequence reads were aligned to the 1000 genomes human reference sequences (version b37, GATK resource bundle, Broad Institute, USA) using BWA v0.7.10[10] and GATK indel realigner v.3.3-0. Single nucleotide variants were called with Freebayes v0.9.18-24[11], Varscan v.2.3.7[12], Bcftools v1.0[13], and GATK v3.3-0[14]. The resulting variant call format files were annotated using snpEff and snpSift v.4.1a15 and dbNSFP v.2.7[16]. For reliable detection of high-confidence mutations, variants were filtered based on several criteria: For each sample, variants were excluded if they were reported by only one caller, coverage was <100 reads, or <20 reads supported the variant allele. Overall, recurrent variants (n≥10) were excluded if variant allele frequency (VAF) never exceeded 2% or if the distribution was unequal between runs. Furthermore, variants were only considered if they were non-synonymous, unlikely to be germline variants and not known SNPs. Mutational hotspots are indicated in Figure 1A and were obtained from literature and the COSMIC database (v79, released 14th

November 2016).[6]

Results

Using the TruSeq Custom Amplicon technique we screened for mutations in 481 primary BCP-ALL cases at initial diagnosis, in 28 relapse BCP-ALL samples (representing 19 unique patients) and in twelve BCP-ALL cell lines. The regions covered by the custom amplicons are indicated in Figure 1A, and were selected to cover previously reported mutational hotspots of *FGFR1*, *FGFR2*, and *FGFR3* (indicated as black bar above each gene). In 481 unique patients we only found 4 non-synonymous *FGFR* variants (0.8%). These variants were detected in samples taken at initial diagnosis, one FGFR1 (D129A) mutation, two FGFR2 mutations (V274I and D522N), and one FGFR3 (F384I) mutation (Figure 1A, above gene schematics). No mutations were detected in the B-cell precursor ALL cell line panel or in the 28 relapse samples of 19 unique patients. Only the FGFR1 D129A and FGFR2 V274I mutations were predicted to be deleterious to the protein function by the SIFT, Polyphen, LRT, and MutationTaster tools.17 Variant allele frequencies (VAF) varied between 8.4% (FGFR2 D522N) and 52.9% (FGFR3 F384I). None of these mutations represents a frequently observed pathogenic mutation, such as those reported in multiple myeloma, according to literature and the COSMIC database (v79, indicated below each gene in Figure 1A).

FGFR variants occurred in two *ETV6-RUNX1*-rearranged cases, one *BCR-ABL1*-like with a *JAK2* translocation, and one high hyperdiploid, and high white blood cell count (≥50 cells/nL) was found in 2/4, high minimal residual disease (percentage blasts in bone marrow on day 33 of therapy ≥0.1% relative to level at diagnosis) in 1/3 (1 without data available). The JAK2 translocated case with the FGFR1 D129A mutation experienced a relapse 1 year after diagnosis. In conclusion, *FGFR* variants occurred in various subtypes and patients did not consistently present with poor or good prognostic factors.

FGFR signaling has been previously implicated in therapy resistance.[7] To evaluate the effect of FGF receptor stimulation on BCP-ALL cells, we evaluated the effect of recombinant FGF2 on the cytotoxicity of the spearhead drug prednisolone in vitro. In four of the eight tested cell lines exposure to 50ng/mL recombinant human FGF2 resulted in two- to three-fold higher IC50-values for prednisolone (Figure 1B). The resistance induced by the ligand FGF2 was reversed by exposure to 1 μM of FGFR inhibitor AZD4547. AZD4547 as single agent reduced viability in BCP-ALL cell lines at higher concentrations (5 to 20μM, Figure 1C), except for Nalm6 and RCH-ACV cell line (20-40% cell death induced at 1 μM AZD4547). Therefore, the prednisolone IC50-values were corrected for cell viability of prednisolone-free conditions to account for possible effects of FGF2 and/or AZD4547 on cell proliferation and survival. Notably, the FGFR inhibitor was not effective in primary leukemic cells carrying a D129A point mutation in FGFR1 (Figure 1D). Unfortunately no viable leukemic cells were available for other mutated BCP-ALL cases.

Discussion

Here we screened 481 pediatric BCP-ALL cases at initial diagnosis, 19 relapse BCP-ALL cases, and 12 BCP-ALL cell lines for variants in *FGFR1*, *FGFR2*, and *FGFR3*. We found

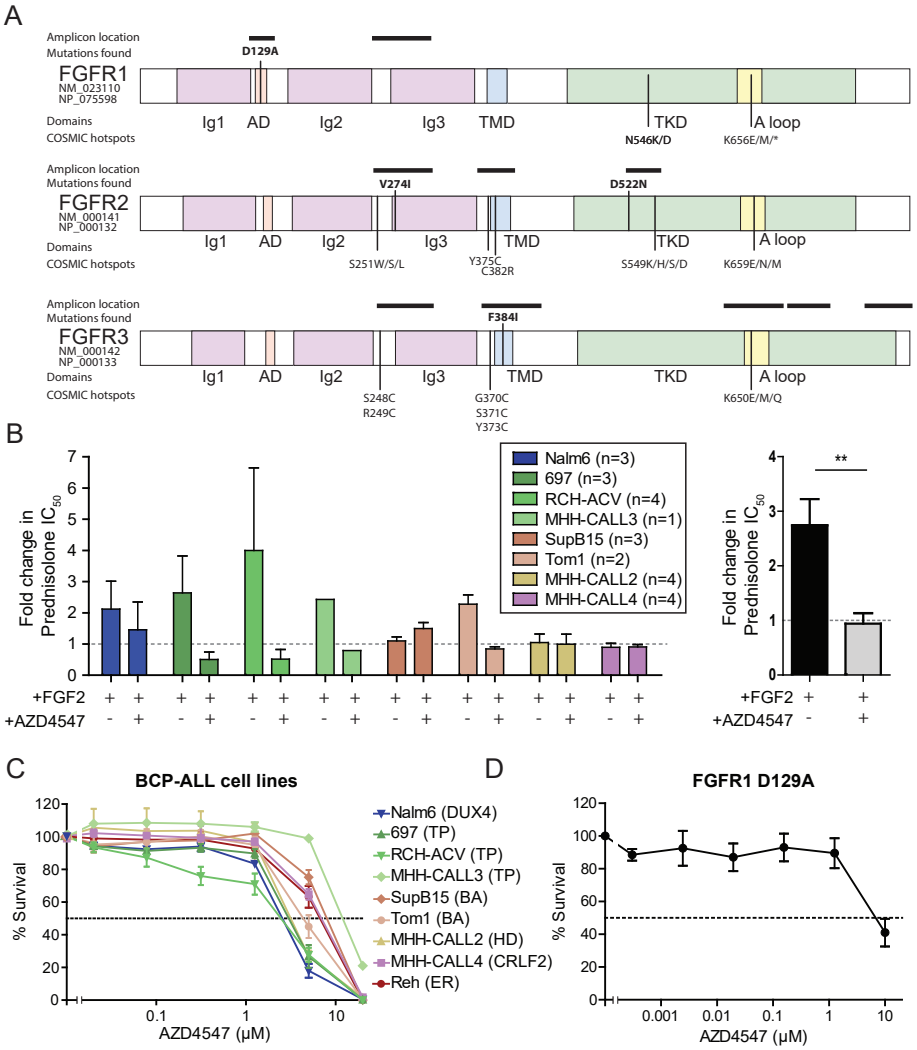

Figure 1: FGFR signaling is not essential to in pediatric BCP-ALL cells, but can reduce prednisolone sensitivity.

(A) Schematic protein structure of the *FGFR* genes and the observed variants. Black bars indicate the regions covered by targeted amplicon sequencing. Variants printed in bold above the scheme represent variants observed in this study, variants below represent those frequently reported in the COSMIC database. Ig: Immunoglobulin-like domain, AD: acidic domain, TMD: transmembrane domain, TKD: tyrosine-kinase domain, A-loop: activation loop. **(B)** Effect of 50ng/mL recombinant human FGF2 on prednisolone sensitivity (IC50-values) in BCP ALL cell lines and reversal by the FGFR-inhibitor AZD4547 (1µM). Fold-change in prednisolone IC50 is depicted on the y-axis. Left: all evaluated cell lines in detail, right: mean fold changes of Nalm6, 697, RCH-ACV, Tom1, and MHH-CALL3 combined, ** p= 0.0012 by Wilcoxon matched pairs test.**(C)** *In vitro* response of BCP-ALL cell lines to the FGFR-inhibitor AZD4547. Dashed line: 50% survival; Cytogenetic subtypes are indicated in brackets: DUX4: *DUX4*-rearranged leukemia, TP: *TCF3-PBX1*-rearranged, BA: *BCR-ABL1*-rearranged, HD: high hyperdiploid karyotype, CRLF2: high CRLF2 expression, ER: *ETV6-RUNX1*-rearranged. **(D)** Ex vivo response of primary BCP-ALL cells carrying an FGFR1 D129A mutation.

a low frequency of variants among patients at initial diagnosis, and no variants in the relapse cohort or in cell lines. These data indicate that *FGFR* mutations are very rare in pediatric BCP-ALL. Due to the low incidence and a small relapse cohort, it remains to be determined whether these rare mutations have an effect on the clinical prognosis. With the limited data available, we conclude that this does not seem to be the case.

The phenotypic effect of the described mutations is yet unclear, however, all mutations locate within functional domains of the FGFR proteins (Figure 1A, colored boxes). The FGFR1 D129A mutation affects the so-called acid box of the receptor, which has been shown to be essential for auto-inhibition and interaction with adhesion molecules.[18,19] The FGFR2 mutations V274I and D522N locate in the ligand-binding immunoglobulin-like (Ig) domain and the tyrosine kinase domain (TKD), respectively. They might therefore alter ligand-binding and kinase activation. Last, the FGFR3 F384I mutation is located in the transmembrane domain (TMD), which is frequently affected by mutations that cause aberrant receptor dimerization (e.g. by insertion of a cysteine). Of note, a rare F384L SNP at the same location has been reported and was also found in our screen. No functional consequences have been reported for this SNP, and the high similarity between leucine and isoleucine suggests no effect of the F384I variant on FGFR3 function.[20]

Given the previous implications of FGFR signaling in resistance, we evaluated its effect on the efficacy of prednisolone in vitro.[7] Our data indicate that the ligand FGF2 induced resistance to glucocorticoids which could be reversed by inhibition of FGFR. Traer et al. suggested that reactivation of the MAPK pathway by FGFR3 accounts for FGF-mediated resistance of *BCR-ABL1*-rearranged chronic myeloid leukemia cells to imatinib. In line with this observation, we and others have previously shown that MAPK pathway mediated signaling can also increase resistance towards prednisolone.[21-23] Downstream-located MAPK signaling may therefore be the mediator of FGF-induced glucocorticoid resistance, which could provide an alternative target for sensitization towards prednisolone in otherwise resistant cases.

Together, our data demonstrates that FGFR-activating lesions are rare in newly diagnosed pediatric BCP-ALL, and were not enriched at the time of relapse. Activating mutations which are frequently observed in multiple myeloma or solid cancers were not observed in 481 newly diagnosed nor in 19 relapsed BCP-ALL cases.[24] As such *FGFR* activating mutations were virtually absent, FGF2 ligand-mediated activation of FGFR-signaling may be more relevant for the sensitivity of leukemic cells to prednisolone.

Acknowledgements

This work was supported by the NWO VICI program (grant 016.126.612), the Dutch Cancer Society (grants AMC 2008-4265 and EMCR 2014-6998), and the KIKA Foundation (grants 132 and 161) and the Pediatric Oncology Foundation Rotterdam. The Center for Personalized Cancer Treatment is supported by the NutsOhra Foundation (grant 1102-062). We thank Ies Nijman and Annelies Smouters of the UMC Utrecht for their help in setting up the analysis pipeline and the Erasmus MC Cancer Computational Biology Center for giving access to their IT-infrastructure and software that was used for the computations and data analysis in this study. We also thank the Dutch Childhood Oncology Group (DCOG) and the German Cooperative Study Group for Childhood

Acute Lymphoblastic Leukemia (COALL) for contributing primary leukemic cells and clinical information.

Authorship contributions

I.S.J, M.L.d.B. designed and performed experiments, analyzed and interpreted the data, and wrote the manuscript, A.Q.H and J.M.B. analyzed and interpreted the data, I.M.A., M.J.K., and E.C. designed sequencing experiments, N.J.M.B. assisted in performing sequencing experiments, M.L.d.B. and R.P. conceptualized the study and interpreted the results. All authors read, revised, and approved the manuscript. Correspondence: Monique den Boer, Department of Pediatric Oncology, Erasmus Medical Center – Sophia Children's Hospital, Rotterdam, the Netherlands; E-Mail: m.l.denboer@erasmusmc.nl.

Conflict of interest

The authors declare no conflict of interest.

References

1. Moroni E, Dell'Era P, Rusnati M, Presta M. Fibroblast growth factors and their receptors in hematopoiesis and hematological tumors. J Hematother Stem Cell Res. 2002;11(1):19-32.

2. Coutu DL, Francois M, Galipeau J. Inhibition of cellular senescence by developmentally regulated FGF receptors in mesenchymal stem cells. Blood. 2011;117(25):6801-6812.

3. Wakim JJ, Tirado CA, Chen W, Collins R. t(8;22)/BCR-FGFR1 myeloproliferative disorder presenting as B-acute lymphoblastic leukemia: report of a case treated with sorafenib and review of the literature. Leuk Res. 2011;35(9):e151-153.

4. Richelda R, Ronchetti D, Baldini L, et al. A novel chromosomal translocation t(4; 14)(p16.3; q32) in multiple myeloma involves the fibroblast growth-factor receptor 3 gene. Blood. 1997;90(10):4062-4070.

5. Chesi M, Nardini E, Brents LA, et al. Frequent translocation t(4;14)(p16.3;q32.3) in multiple myeloma is associated with increased expression and activating mutations of fibroblast growth factor receptor 3. Nat Genet. 1997;16(3):260-264.

6. Chesi M, Brents LA, Ely SA, et al. Activated fibroblast growth factor receptor 3 is an oncogene that contributes to tumor progression in multiple myeloma. Blood. 2001;97(3):729-736.

7. Traer E, Martinez J, Javidi-Sharifi N, et al. FGF2 from Marrow Microenvironment Promotes Resistance to FLT3 Inhibitors in Acute Myeloid Leukemia. Cancer Res. 2016.

8. Den Boer ML, Harms DO, Pieters R, et al. Patient stratification based on prednisolone-vincristine-asparaginase resistance profiles in children with acute lymphoblastic leukemia. J Clin Oncol. 2003;21(17):3262-3268.

9. van der Veer A, Waanders E, Pieters R, et al. Independent prognostic value of BCR-ABL1-like signature and IKZF1 deletion, but not high CRLF2 expression, in children with B-cell precursor ALL. Blood. 2013;122(15):2622-2629.

10. Li H. Aligning sequence reads, clone sequences and assembly contigs with BWA-MEM. arXiv preprint arXiv:13033997. 2013.

11. Garrison E, Marth G. Haplotype-based variant detection from short-read sequencing. arXiv preprint arXiv:12073907. 2012.

12. Koboldt DC, Zhang Q, Larson DE, et al. VarScan 2: somatic mutation and copy number alteration discovery in cancer by exome sequencing. Genome Res. 2012;22(3):568-576.

13. Li H. A statistical framework for SNP calling, mutation discovery, association mapping and population genetical parameter estimation from sequencing data. Bioinformatics. 2011;27(21):2987-2993.

14. DePristo MA, Banks E, Poplin R, et al. A framework for variation discovery and genotyping using next-generation DNA sequencing data. Nat Genet. 2011;43(5):491-498.

15. Cingolani P, Platts A, Wang le L, et al. A program for annotating and predicting the effects of single nucleotide polymorphisms, SnpEff: SNPs in the genome of Drosophila melanogaster strain w1118; iso-2; iso-3. Fly (Austin). 2012;6(2):80-92.

16. Liu X, Wu C, Li C, Boerwinkle E. dbNSFP v3.0: A One-Stop Database of Functional Predictions and Annotations for Human Nonsynonymous and Splice-Site SNVs. Hum Mutat. 2016;37(3):235-241.

17. Liu X, Jian X, Boerwinkle E. dbNSFP: a lightweight database of human nonsynonymous SNPs and their functional predictions. Hum Mutat. 2011;32(8):894-899.

18. Den Boer ML, van Slegtenhorst M, De Menezes RX, et al. A subtype of childhood acute lymphoblastic leukaemia with poor treatment outcome: a genome-wide classification study. Lancet Oncol. 2009;10(2):125-134.

19. Mullighan CG, Su X, Zhang J, et al. Deletion

of IKZF1 and prognosis in acute lymphoblastic leukemia. N Engl J Med. 2009;360(5):470-480.

20. Kalinina J, Dutta K, Ilghari D, et al. The alternatively spliced acid box region plays a key role in FGF receptor autoinhibition. Structure. 2012;20(1):77-88.

21. Sanchez-Heras E, Howell FV, Williams G, Doherty P. The fibroblast growth factor receptor acid box is essential for interactions with N-cadherin and all of the major isoforms of neural cell adhesion molecule. J Biol Chem. 2006;281(46):35208-35216.

22. Kant SG, Cervenkova I, Balek L, et al. A novel variant of FGFR3 causes proportionate short stature. Eur J Endocrinol. 2015;172(6):763-770.

23. Rambal AA, Panaguiton ZL, Kramer L, Grant S, Harada H. MEK inhibitors potentiate dexamethasone lethality in acute lymphoblastic leukemia cells through the pro-apoptotic molecule BIM. Leukemia. 2009;23(10):1744-1754.

24. Aries IM, van den Dungen RE, Koudijs MJ, et al. Towards personalized therapy in pediatric acute lymphoblastic leukemia: RAS mutations and prednisolone resistance. Haematologica. 2015;100(4):e132-136.

25. Jones CL, Gearheart CM, Fosmire S, et al. MAPK signaling cascades mediate distinct glucocorticoid resistance mechanisms in pediatric leukemia. Blood. 2015;126(19):2202-2212.

26. Greulich H, Pollock PM. Targeting mutant fibroblast growth factor receptors in cancer. Trends Mol Med. 2011;17(5):283-292.

Supplementary Data

Supplementary Table 1 Characteristics of *FGFR* mutated cases. VAF: variant allele frequency. WBC: white blood cell count. MRD d33: minimal residual disease after induction therapy including high dose glucocorticoid treatment, high MRD is defined as blast percentage in bone marrow >0.1%. EFS: follow-up time for event-free survival estimation. BAL: *BCR-ABL1*-like, ER: *ETV6-RUNX1*-positive, HD: High Hyperdiploid. Polyphen abbreviations: B: benign, D: probably damaging P: possibly damaging.

Cytogenetic subtype	Mutated *FGFR* gene	Exact variant (GRCh37)	aa change	Coverage	Variant reads	VAF (%)	dbNSFP SIFT prediction	Age at diagnosis	WBC (/nL)	MRD d33	Event	EFS (years)
BAL	*FGFR1*	8:38285926 T/G	D129A	441	126	28.5	D	5	204	<0.1%	relapse	1.08
ER	*FGFR2*	10:123258117 C/T	D522N	1494	125	8.4	T	3	13	0	-	8.32
HD	*FGFR2*	10:123279612 C/T	V274I	864	352	40.8	D	5	10.5	>0.1%	-	6.35
ER	*FGFR3*	4:1806131 T/A	F384I	136	72	52.9	T	3	254.3	NA	-	8.49

Chapter 6

EMP1, a novel poor prognostic factor in pediatric leukemia regulates prednisolone resistance, cell proliferation, migration and adhesion

Ingrid M. Ariës, Isabel S Jerchel, E.S. Rosanna van den Dungen, Lieke C.J. van den Berk, Judith M. Boer, Martin A Horstmann, Gabriele Escherich, Rob Pieters and Monique L den Boer

Leukemia. 2014 Sep;28(9):1828-37

Abstract

Still 20% of pediatric acute lymphoblastic leukemia (ALL) patients relapse on or after current treatment strategies. Treatment failure is associated with resistance to prednisolone. We aimed to find new druggable targets that modulate prednisolone resistance. We generated microarray gene expression profiles of 256 pediatric ALL patient samples and identified a 3.4-fold increase in epithelial membrane protein 1 (*EMP1*) expression in in vitro prednisolone-resistant compared with -sensitive patients (p=0.003). *EMP1* silencing in six precursor-B ALL (BCP-ALL) and T-ALL cell lines induced apoptosis and cell-cycle arrest leading to 84.1±4.5% reduction in survival compared with non-silencing control transduced cells (non-silencing control short hairpin, shNSC) (p=0.014). Moreover, *EMP1* silencing sensitized to prednisolone up to 18.8-fold (p<0.001). *EMP1* silencing also abrogated migration and adhesion to mesenchymal stromal cells (MSCs) by 78.3±9.0 and 29.3±4.1% compared with shNSC (p<0.05). We discovered that EMP1 contributes to MSC-mediated prednisolone resistance. Pathway analysis indicated that EMP1 signals through the Src kinase family. *EMP1*-high BCP-ALL patients showed a poorer 5-year event-free survival compared with *EMP1*-low patients (77±2% vs. 89±2%, p=0.003). Multivariate analysis taking along white blood cell count, age, prednisolone resistance and subtype identified EMP1 as an independent predictor for poor outcome in BCP-ALL (p=0.004, hazard ratio: 2.36 (1.31–4.25). This study provides preclinical evidence that EMP1 is an interesting candidate for drug development to optimize treatment of BCP-ALL.

Introduction

Survival rates of pediatric acute lymphoblastic leukemia (ALL), the most common pediatric cancer, have improved enormously over the past decades. However, still 20% of B-cell precursor ALL (BCP-ALL) and 25% of T-ALL patients relapse during or shortly after completion of contemporary treatment protocols for newly diagnosed pediatric ALL.[1] Prednisolone is the spearhead drug used in multi-drug treatment of pediatric ALL and *in vivo* and *in vitro* response to prednisolone predicts long-term clinical outcome.[2] Moreover, relapsed ALL patients acquire prednisolone resistance disproportional to other anti-leukemic agents.[3] It is therefore necessary to find new druggable targets to reverse prednisolone resistance. Prednisolone, a glucocorticoid, diffuses passively into the cell, where it binds the glucocorticoid receptor. Consequently, glucocorticoid receptor chaperone proteins are released whereafter glucocorticoid receptor dimers can be formed. Dimerized glucocorticoid receptor acts as a transcription factor by either binding to positive or negative glucocorticoid response elements in the DNA, or by binding to other transcription factors, such as NF-κB or AP-1.[4] As a result, a large number of genes are either turned on or off. Due to this complexity, still little is known about the exact cause of resistance to glucocorticoids. To examine the gene expression pattern that might cause prednisolone resistance in more detail, we performed microarray analysis of 256 children with newly diagnosed ALL that were tested *in vitro* to be prednisolone sensitive, intermediate resistant or resistant. We identified epithelial membrane protein 1 (*EMP1*) as one of the most discriminative genes. EMP1 is a small hydrophobic four-transmembrane glycoprotein of 160 amino acids.[5] EMP1 has been implicated as a cell junction protein at

the plasma membrane;[6,7] however, little is known about the exact function. It has been shown to be involved in cell proliferation, is identified as a c-Myc target,[8] is correlated with brain[9] and breast carcinogenesis,[10] and was demonstrated to be a biomarker of gefitinib resistance in non-small lung carcinoma.[11] We are the first to identify a significant role for EMP1 in pediatric ALL. We have discovered that silencing of *EMP1* inhibited leukemic survival, sensitized leukemic cells to prednisolone and abrogated migration and adhesion to mesenchymal stromal cells (MSCs). Moreover, we identified *EMP1* as an independent predictor for poor outcome in BCP-ALL. Taken together, these results point to EMP1 as a potential new druggable target to tackle leukemia and potentially increase current survival rates.

Materials and Methods

Cell culture and primary cells

Bone marrow and peripheral blood samples were collected from children alleged to suffer from newly diagnosed ALL and before start of initial therapy. Normal bone marrow samples were obtained from children who were suspected for a malignancy but turned out to be negative for a hematological disorder. Informed consent was given by patients or parents/guidance to use excess of diagnostic material for research purposes as approved by the local institutional review board. Mononuclear cells were isolated by lymphoprep density gradient centrifugation, as previously described.12,13 Only samples with ≥90% leukemic blasts upon processing were used in the present study. The genetic subtype of each patient, that is, hyperdiploid (>50 chromosomes), *ETV6-RUNX1*+, *TCF3-PBX1*+, *MLL*- rearrangement, *BCR-ABL1*+, *BCR-ABL1*-like, or B-other (negative for aforementioned genomic lesions) was determined by means of fluorescent in situ hybridization, PCR and by utilizing the 110-probeset classifier.[14] An MTT (3-(4,5-dimethylthiazol-2-yl)-2,5-diphenyltetrazolium bromide) assay (see below for details) was used to select cases being in vitro highly sensitive, intermediate resistant or highly resistant to prednisolone; 74, 60 and 42 of BCP-ALL cases and 27, 34 and 19 T-ALL respectively, overall 256 samples. In total, data obtained from 373 BCP-ALL and 116 T-ALL cases were included to study the prognostic value of *EMP1* expression levels. All leukemic cell lines and HEK293T cells were obtained from DSMZ (Braunschweig, Germany). Reh, 697, NALM6 and SEM are BCP-ALL cell lines with an *ETV6-RUNX1*, *TCF3-PBX1*, t(5;12) and an *MLL-AF4* rearrangement, respectively. Jurkat is a tetraploid T-ALL and SupT1 is a T-lymphoblast cell line. All cell lines were resistant to prednisolone as determined by an MTS ((3-(4,5-dimethylthiazol-2-yl)-5-(3-carboxymethoxyphenyl)-2-(4-sulfophenyl)- 2H-tetrazolium) assay (Supplementary Table S2). HEK293T, a human embryonal kidney cell line, was used for the production of viral particles. hMSC-TERT cells are human MSCs modified with an increased telomerase activity and were a gift of Dr D Campana, St. Jude Childrens' Research Hospital, Memphis, USA.[15] Cell viability and cell count were determined by a trypan blue exclusion staining assay and analyzed by MACSQuant flow cytometer (Miltenyi Biotec, Leiden, Netherlands).

Microarrays

RNA was extracted by means of Trizol isolation (Invitrogen, Bleiswijk, Netherlands) according to the manufacturer's protocol and RNA quality and integrity determined with

the 2100 bioanalyzer (Agilent, Amstelveen, Netherlands). The Affymetrix One-Cycle cDNA Synthesis kit (Santa Clara, CA, USA) and the GeneChip IVT Labeling kit (Santa Clara, CA, USA) were used to synthesize cRNA. RNA processing and hybridization to the Affymetrix U133 Plus 2.0 GeneChip oligonucleotide microarray were performed according to the manufacturer's protocol. Gene-expression values were calculated with Affymetrix Microarray Suite version 5.0. Expression signals were scaled to the target intensity of 500 and log transformed. Only arrays with scaling factor <10 and GAPDH cRNA integrity (3'/5') <3 were used for subsequent analysis. All arrays were Robust Multichip Average and variance stabilization and normalization 2 (VSN2) normalized[16] and differentially expressed genes between in vitro prednisolone-resistant and prednisolone-sensitive patients were identified with Limma R Package taking along prednisolone intermediate patients and using subtype as a confounder in the statistical environment R, version 2.15.0. Correction for multiple tests was performed according to the false discovery rate method.[17] All *EMP1* probe sets were statistically differentially expressed between in vitro prednisolone-sensitive and -resistant patients. Probeset 201324_at was used for further analysis, as this probeset showed the most reliable differential expression between in vitro prednisolonesensitive and -resistant BCP-ALL patients.

Lentiviral production and infection

pLKO.1 Mission short-hairpin RNA vectors were purchased from Sigma- Aldrich (Zwijndrecht, Netherlands), that is, a non-silencing control SHC002 (shNSC) and TRCN0000117944 against *EMP1* (shEMP1). Lentiviral helper pMD2.G (Addgene plasmid 12259) and psPAX2 (Addgene plasmid 12260) were provided by Prof. D Trono (Geneva, Switzerland). Infection occurred during 45 min 1800 r.p.m. spin-oculation of 0.5×10^6 cells/ml with 2.5 transducing units/cell (Sigma, Zwijndrecht, Netherlands). After 24 h, infected cells were positively selected for puromycin resistance. Quantitative RT-PCR RNA was extracted using a Rneasy minikit (Qiagen, Venlo, Netherlands) according to the manufacturer's protocol, whereafter cDNA was synthesized. EMP1 mRNA levels were quantified by incorporation of SYBR Green (Thermo Scientific, Breda, Netherlands) by quantitative real-time PCR (Applied Biosystems 7900HT, Life Technologies, Bleiswijk, Netherlands). Primers for *EMP1* were 50-TTGCTGGCTGGTATCTTT-30 (forward) and 50-TTGAGGGCATCTTCACTG-30 (reverse). Primers used for the reference gene *RPS20* were 50-AAGGGCTGAGGATTTTTG-30 (forward) and 50-CGTTGCG GCTTGTTAG-30 (reverse). Protein isolation and western blot analysis Proteins were isolated with protein lysis buffer, details see Supplementary information. Subsequently, the supernatant was used for the luminex (see below) and the remaining pellet harboring membrane proteins was sonicated on ice (Branson Sonifier 250) in Laemmli Sample Buffer. Protein concentrations were quantified with the 2-D Quant Assay (Amersham Biosciences, Piscataway, NJ, USA). Protein (25 mg) was loaded on Bio-Rad Mini-Protean gels (TGX pre-cast anyKD) and transferred onto nitrocellulose membranes (Bio-Rad, Veenendaal, Netherlands). Membranes were blocked with 5% bovine serum albumin and probed with 1:200 anti-EMP1 (Santa Cruz, Heidelberg, Germany; sc-50467) and anti-b-actin 1:20 000 (Abcam, Cambridge, UK; ab6276) in 5% bovine serum albumin, followed by IRDye 800CW- and IRDye 680CW-labeled secondary antibody (Li-COR, Leusden, Netherlands), respectively. Protein levels were quantified using the Odyssey 3.0 application software (Li-COR).

Luminex

Protein phosphorylation was determined with the 9-plex Multi-Pathway Magnetic Bead Panel (Millipore #46-680MAG, Amsterdam, Netherlands) and Milliplex 8-plex Human Src Family kinase kit (Millipore #48-650MAG) following the manufacturer's protocol. To both kits, b-Tubulin beads (Millipore #64-713MAG) and GAPDH beads (Millipore #46-667MAG) were added to correct for protein load. See Supplementary information for detailed information. Apoptosis measurement Cell viability was assessed with an Annexin V/Propidium iodide staining. Fractions of Annexin V/Propidium iodide double-positive and Annexin V single-positive cells were quantified on a MACSQuant flow cytometer (Miltenyi Biotec).

Cell-cycle distribution assay

Cell-cycle distribution was analyzed using the FITC BrdU Flow Kit (B&D Pharmingen, Breda, Netherlands) following the manufacturer's instructions. See Supplementary information for detailed information.

In vitro drug-resistance assay

Cellular cytotoxicity of prednisolone (Bufa Pharmaceutical Products, Uitgeest, Netherlands) was determined by the in vitro MTT assay for patients' samples and the MTS assay for cell lines.[2,13] See Supplementary information for detailed information.

Cell adhesion assay

Subconfluent (80%) hMSC-TERT cells were irradiated with 30 Gy and co-cultured either in a 6-well plate with 2×10^6 Maroon-labeled (Cellvue, eBiosciences, Vienna, Austria) Reh cells in plain AIMV (Gibco, Life Technologies, Bleiswijk, Netherlands) for 24 h in the case of flowsort experiments, or overnight in a 24-well plate with 0.4×10^6 leukemic cells in plain AIMV (Gibco) in the case of adhesion experiments of *EMP1*-silenced cells. Hereafter, non-adherent leukemic cells were harvested from the supernatant (suspension cells), and adherent leukemic cells were harvested by trypsinizing the supernatant-depleted hMSC-TERT layer with Trypsin-EDTA (Gibco) for 5 min at 37°C, 5% CO2. Suspension and adherent cells were quantified both by trypan blue exclusion assays and by the MACSQuant flow cytometer. In the case of the flowsort experiment, the adherent Maroonlabeled leukemic cells were separated from unlabeled hMSC-TERT cells by fluorescence activated cell sorting (BD Biosciences FACSAria cell sorter, Breda, Netherlands) and total RNA of the suspension and adherent cells was isolated.

Transwell migration assay

Subconfluent hMSC-TERT layers were cultured in a 24-well plate at 37°C, 5% CO_2, whereafter they were irradiated with 30 Gy and placed on plain AIMV (Gibco) 48 h before migration assay. In indicated experiments, medium was collected from hMSC-TERT layers after 48 h of culture and was subsequently used as a conditioned medium. Maroon-labeled leukemic cells (0.4×10^5) were transferred on top of a 3-µm pore polycarbonate membrane insert. In this transwell assay, leukemic cells were allowed to migrate overnight at 37°C in 5% CO_2 to the bottom compartment that contained either an hMSC-TERT layer, or conditioned medium collected from hMSC-TERT after 48 h

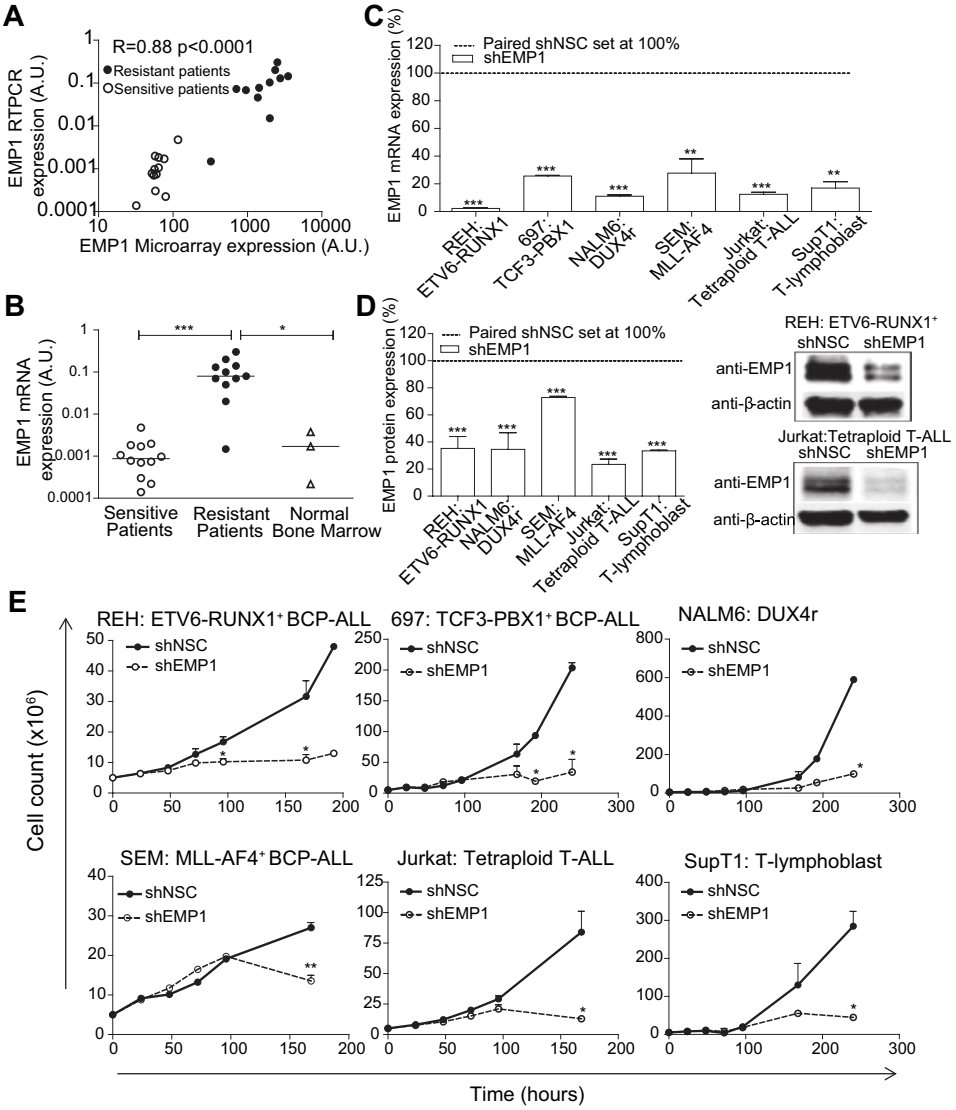

Figure 1. *EMP1* expression is increased in prednisolone-resistant leukemic cells. shEMP1 efficiently silences the expression of *EMP1* and reduces cell proliferation. **(A)** Microarray expression (x axis) was confirmed with qRT-PCR (y axis). qRT-PCR and microarray RNA expression correlated significantly (Spearman R=0.88, P<0.01). **(B)** *EMP1* mRNA levels in 12 prednisolone-sensitive and 11 prednisolone-resistant BCPALL patients and 3 normal bone marrow samples were analyzed by means of qRT-PCR. **(C)** *EMP1* mRNA levels were measured 168 h after infection with shEMP1 or an shNSC in six leukemic cell lines. Values were adjusted for expression of the housekeeping gene *RPS20* and are relative to the levels seen in shNSC-transduced cells of each cell line (set to 100%). **(D)** Protein levels of EMP1 were assessed by western blotting at 168 h after shEMP1 and shNSC transduction. EMP1 protein levels were corrected for b-actin and are relative to shNSC-transduced cells of each cell line (set to 100%). A representative western blot for a BCP-ALL cell line, that is, *ETV6-RUNX+* and a T-ALL cell line, that is, tetraploid T-ALL, is shown. **(E)** Cell proliferation of *EMP1*-silenced cells and shNSC control cells was monitored over time by MACSQuant flow. Data are presented as mean plus s.e.m. of three independent experiments (*p<0.05, **p<0.01, ***p<0.001).

or plain AIMV medium. Subsequently, the amount of leukemic cells in the bottom compartment was quantified by both trypan blue exclusion assays and the MACSQuant flow cytometer (Miltenyi Biotec).

MSCs AND LEUKEMIC CELLS CO-CULTURE EXPERIMENTS

Leukemic cells (0.4×10^5) alone (condition 1) or co-cultured on top of an 80% subconfluent 30 Gy irradiated hMSC-TERT layer (condition 2) were cultured in 24-well plates in RPMI 10% fetal calf serum with or without 0.488 mg/ml prednisolone for 3 days. Hereafter, leukemic cells in condition 1 were directly harvested from the culture medium. In condition 2, the non-adherent leukemic cells were collected from the supernatant, whereafter the adherent leukemic cells were harvested by trypsinizing the supernatant-

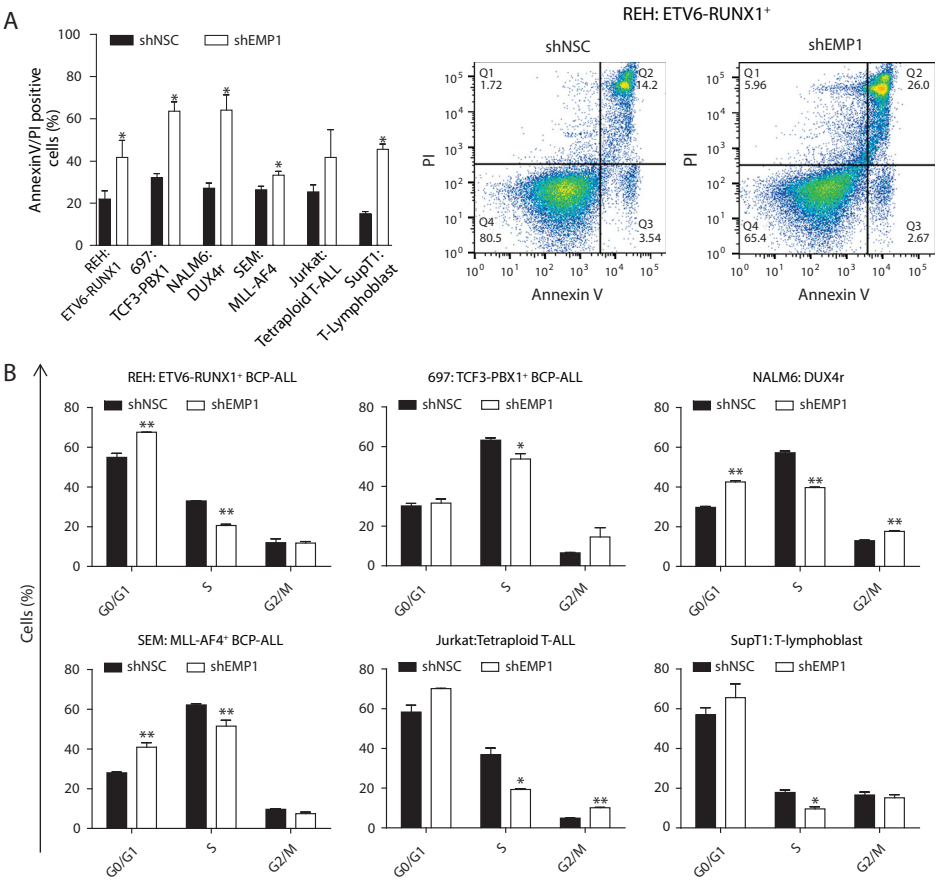

Figure 2. *EMP1* silencing increases apoptosis and induces cell-cycle arrest.

(A) *EMP1* knockdown-induced apoptosis was assessed in six leukemic cell lines 168 h after transduction with the MACSQuant using an Annexin V/Propidium iodide (PI) staining. The percentage of apoptotic cells was calculated using the quadrant method. A representative fluorescence activated cell sorting plot is shown for REH. **(B)** Cell-cycle distribution of *EMP1*-silenced cells and non-silencing control cells was analyzed after 1 h BrdU incorporation, followed by BrdU-FITC and 7-AAD staining. The percent of cells in G0/G1, S and G2/M is presented as means plus s.e.m. of three independent experiments (*P<0.05, **P<0.01).

depleted hMSC-TERT layer. Suspension and adherent cells were counted by trypan blue exclusion assays and the MACSQuant flow cytometer. To determine whether hMSC-TERT cells consume prednisolone, and thereby lower the available prednisolone concentration in leukemia co-culture experiments, the hMSC-TERT layer was cultured with 0.488 mg/ml prednisolone at 37°C, 5% CO_2. After 3 days, this MSC-derived prednisolone medium was collected and transferred to leukemic cells. In parallel, leukemic cells were exposed to prednisolone exposed to 37°C, 5% CO_2 for 3 days (similar to the MSC medium), and to a freshly made dilution of prednisolone. After 3 days, the cytotoxic effect of prednisolone in these three media conditions was compared by an MTS assay.

Statistical analysis

Spearman's rank correlation coefficient was calculated to compare microarray gene expression results with qRT-PCR results. Data from other experiments were compared in unpaired T tests and Mann–Whitney U tests, p=0.05 was considered as statistically significant. The dose–response curves of prednisolone in combination with shNSC compared with shEMP1 were analyzed by repeated measurement one-way ANOVA, testing the interaction between short-hairpin RNA*prednisolone. Cumulative incidence of relapse (CIR) was calculated as time to relapse and nonresponse with death as a competing event in the statistical environment R version 2.15.0 using the method of Fine and Gray[18] with the software packages mstate 0.2.6[19] and cmprsk 2.2-2.[20] Event-free survival (EFS) was calculated as time to relapse, non-response, secondary malignancy and death in IBM SPPS Statistics 20 using Kaplan–Meier analysis and Cox proportional hazard analyses. Univariate and multivariate analysis on EFS were performed in IBM SPPS Statistics 20 using Cox proportional hazard analyses that were stratified for treatment protocol. More detailed information regarding materials and methods can be found in the Supplementary Information.

Results

EMP1 expression is increased in prednisolone-resistant leukemic cells

Gene expression profiling revealed that the mRNA levels of EMP1 were median 3.4-fold higher in leukemic cells of 74 prednisolone resistant compared with 42 sensitive BCP-ALL patients calculated with limma taking along 60 prednisolone intermediate resistant patients and subtype as confounder (p=0.003, Supplementary Table S1). We verified this with qRT-PCR in 23 BCP-ALL patients (Figure 1a). qRT-PCR and microarray mRNA expression levels correlated significantly (Spearman R=0.88 p<0.0001, Figure 1a) and qRT-PCR confirmed that EMP1 was higher expressed in prednisolone-resistant patients compared with sensitive patients (Figure 1b, p<0.0001). Moreover, *EMP1* expression was higher in BCP-ALL compared with normal bone marrow-derived mononuclear cells (p<0.03, Figure 1b). *EMP1* was most differentially expressed in prednisolone-resistant B-other cases (23.5-fold, p=0.003), followed by *BCR-ABL1*-like cases (2.2-fold, p=0.04), *ETV6-RUNX1*$^{+}$-rearranged cases (2.1-fold, p=0.05), and hyperdiploid cases (1.9-fold, p=0.1, Supplementary Figure S1). In T-ALL patients. EMP1 expression levels differed median 2.0-fold between 27 prednisolone-resistant and 19 sensitive cases (p=0.04, Supplementary Figure S1). Basal *EMP1* expression levels in prednisolone- sensitive BCP-

ALL patients were highest in hyperdiploid patients followed by *BCR-ABL1*-like cases (Supplementary Figure S1)

EMP1 SILENCING INCREASES APOPTOSIS AND INDUCES PARTIAL CELL-CYCLE ARREST

To assess the role of EMP1 in prednisolone-resistant ALL, we silenced EMP1 in six different prednisolone-resistant leukemic cell lines, that is, an *ETV6-RUNX1*$^+$ BCP-ALL, a *TCF3-PBX1*$^+$ BCP-ALL, an t(5;12) BCP-ALL, an *MLL-AF4*$^+$ BCP-ALL, a tetraploid T-ALL and a T-lymphoblast cell line. Robust *EMP1* knockdown was achieved following lentiviral transduction to levels varying between 2.3±0.5 and 27.7±20% of those observed in cells transduced with shNSC ($p<0.001$ Figure 1c). Protein levels in *EMP1*-silenced cells were reduced up to 20.2±3.7% ($p<0.05$) of those observed in shNSC-transduced cells after 168 h (Figure 1d; Supplementary Figure S2). Silencing of *EMP1* decreased cell proliferation in all six cell lines, resulting in a proliferation rate down to 16% of that seen for shNSC-transduced cells ($p<0.05$; Figure 1e). Annexin V/Propidium iodide staining revealed a significant increase in apoptosis in five out of six cell lines, with a maximum increase of 2.4-fold ($p<0.05$, Figure 2a, a representative fluorescence activated cell sorting plot is shown for *TEL-AML*$^+$ BCP-ALL). BrdU incorporation assays showed a significant reduction in *EMP1*-silenced cells in S phase in all six cell lines up to 1.7-fold ($p<0.05$, Figure 2b). Four out of six cell lines demonstrated an increase in *EMP1*-silenced cells in G0/G1 phase and/or G2/M phase, with a maximum increase of 1.5-fold and 2.1-fold, respectively ($p<0.01$, Figure 2b). Available shEMP1 constructs present in the Sigma-Aldrich short-hairpin RNA library were tested and only one construct provided sufficient knockdown of *EMP1* (Supplementary Figure S3). As independent validation experiment, we performed siRNA-mediated knockdown experiments of *EMP1* and confirmed a significant inhibition of proliferation similar to shEMP1 results (Supplementary Figure S4). We were unable to study shEMP1- mediated knockdown in primary patients' ALL cells, since these primary cells only survive for 96 h in *ex vivo* cultures and EMP1 protein knockdown only becomes evident after 168 h (Supplementary Figure S2). For similar reasons, we were not able to reach sufficient knockdown of *EMP1* using siRNA-mediated knockdown in primary patients' ALL cells. Knockdown of *EMP1* sensitizes to prednisolone We next evaluated whether inhibiting *EMP1* expression sensitized leukemic cells toward prednisolone-induced apoptosis. Silencing of *EMP1* expression rendered three out of six cell lines more sensitive toward prednisolone-induced apoptosis. (Figure 3; Supplementary Table S2, Of note: The cytotoxic effect of prednisolone was corrected for death caused by silencing of *EMP1* or shNSC.) The cytotoxicity of prednisolone in the other three cell lines did not change nor did the cells become more resistant to prednisolone (Figure 3). Silencing of EMP1 resulted in a fold-change reduction in LC50 values for prednisolone of 4.3-fold in the *TCF3-PBX1*$^+$ BCP-ALL, 1.6-fold in Tetraploid T-ALL and 18.7-fold in the T-lymphoblast cell lines (Supplementary Table S2, all $p<0.001$). siRNA-mediated knockdown of *EMP1* also showed significant sensitization toward prednisolone of *TCF3-PBX1*$^+$ BCP-ALL cells (Supplementary Figure S4).

EMP1 IS IMPORTANT FOR LEUKEMIC CELL MIGRATION AND CELL ADHESION

Recently, the bone marrow microenvironment was demonstrated to contribute to

resistance of leukemic cells to drugs.[21,22] When we co-cultured leukemic cells with a human MSC layer (hMSC-TERT) (Figure 4a), we observed a 4.1-fold increase in *EMP1* mRNA levels in the fraction of leukemic cells that adhered to hMSC-TERT compared with the fraction that remained in suspension (Figure 4b). *EMP1* expressions levels returned to normal after the adhered ALL fraction was cultured without hMSC-TERT for 72 h (Figure 4b). In five out of six cell lines viable *EMP1*-silenced cells adhered less to hMSC-TERT, up to 29.3±4.1% reduction, compared with shNSC-transduced control cells ($p<0.01$, Figure 4c). Next, we evaluated migration of *EMP1*-silenced cells placed in an upper compartment of a transwell assay (Figures 4d and e). The bottom compartment contained either an hMSC-TERT layer that was pre-incubated with AIMV for 48 h or did not contain an hMSC-TERT layer but only the preconditioned AIMV medium which had been collected from hMSC-TERT after 48 h of incubation. A bottom compartment with only plain AIMV was used as a negative control. Viable *EMP1*-silenced cells migrated less to the bottom compartment containing the hMSC-TERT layer or the preconditioned medium in all six cell line models, with a maximal reduction in migration by 78.3±9.0% in *EMP1*-silenced cells compared with shNSC-transduced control cells ($p<0.05$, Figure 4d). To rule out that apoptosis induced by *EMP1* knockdown is the explanation for the observed reduction in migration and adhesion, we analyzed the effect of *MCL1* (anti-apoptotic gene) knockdown and found that this also decreased cell proliferation, but in contrast to *EMP1*, did not hamper migration and adhesion of viable cells (Supplementary Figure S5).

Role of EMP1 in bone marrow microenvironment-mediated prednisolone resistance

Our preliminary observation that EMP1 is not only important in prednisolone resistance, but might be important in leukemic cell migration and adherence to hMSC-TERT

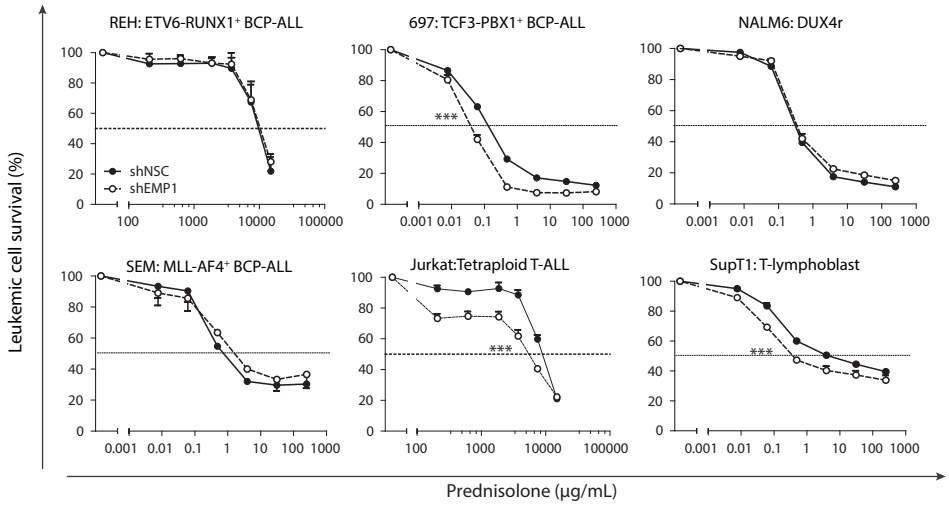

Figure 3. Knockdown of *EMP1* sensitizes to prednisolone.

Sensitivity to prednisolone after *EMP1* knockdown was measured in a 3-day MTS assay. Sensitivity was corrected for cell death induced by *EMP1* knockdown itself in the absence of prednisolone. Data are presented as mean plus s.e.m of three or more independent experiments (repeated measurement one-way ANOVA, ***P<0.001).

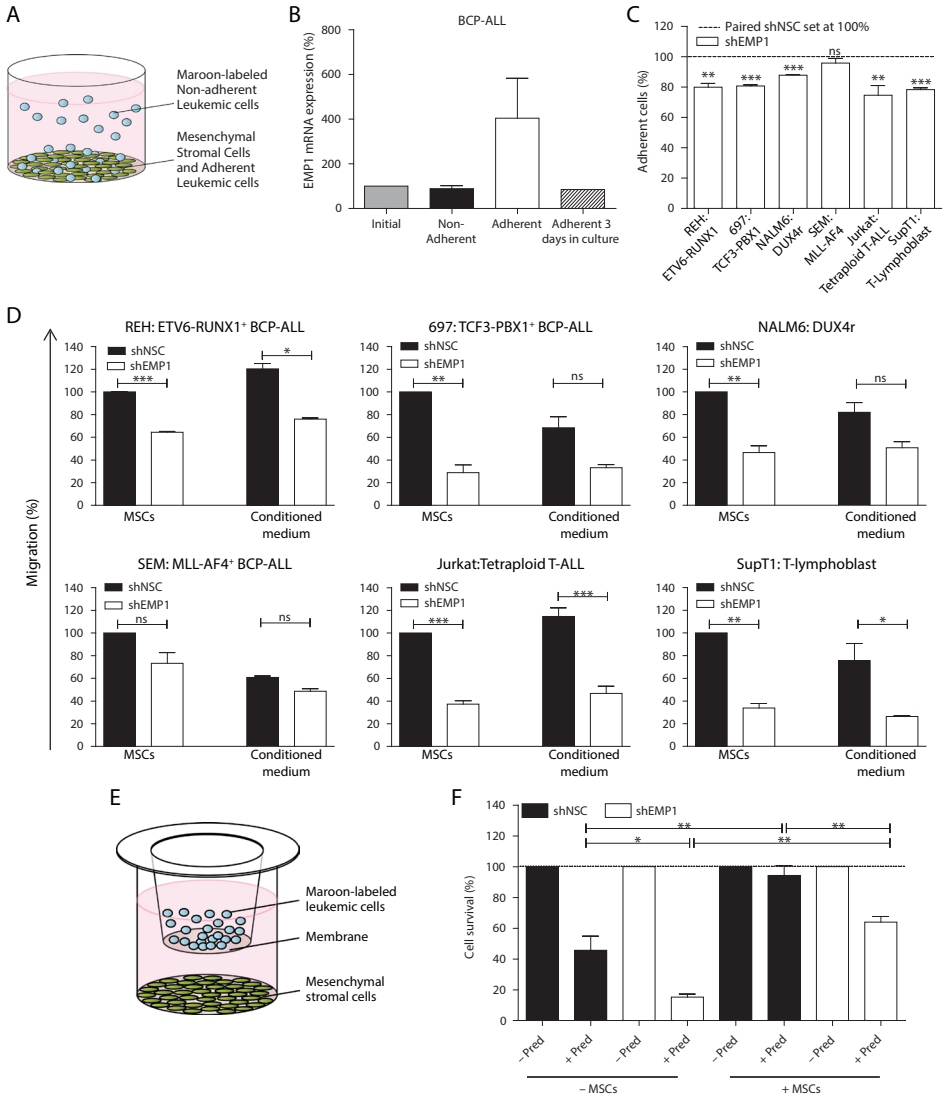

Figure 4. EMP1 is important in leukemic cell migration, adhesion to MSCs and might be important in bone marrow microenvironmentmediated prednisolone resistance (opposite page).

(A, B) Maroon-labeled *ETV6-RUNX1*+ leukemic cells were co-cultured with hMSC-TERT for 24 h. EMP1 mRNA levels were measured in non-adherent leukemic cells and adherent leukemic cells that were separated from hMSC-TERT by fluorescence activated cell sorting. Separated adherent leukemic cells were subsequently cultured without hMSC-TERT for 72 h. **(C)** Leukemic cells were cocultured on an MSC layer overnight, whereafter only viable non-adherent and adherent cells were quantified by means of the trypan blue exclusion assay and MACSQuant flow cytometer. **(D, E)** Non-silencing control leukemic cells or *EMP1*-silenced leukemic cells were placed in AIMV medium into an upper compartment of a transwell assay and allowed to migrate to a lower compartment containing hMSC-TERT preconditioned for 48 h in AIMV or to a lower compartment with only preconditioned AIMV medium taken from MSCs. Migration of viable cells was assessed by trypan blue exclusion assay and MACSQuant flow cytometer.

prompted us to investigate the role of EMP1 in bone marrow microenvironmentmediated prednisolone resistance. We cultured *EMP1*-silenced cells with or without hMSC-TERT layer and with or without 0.488 mg/ml prednisolone for 3 days. We discovered that an hMSCTERT layer can rescue shNSC-transduced control cells from prednisolone-induced apoptosis (Figure 4f). This was not caused by prednisolone-induced apoptosis of the MSCs, since hMSC-TERT cells are prednisolone resistant, nor by reduced availability of prednisolone in the medium due to consumption by hMSC-TERT (Supplementary Figures S6A and B). Most importantly, *EMP1* knockdown partly prevented hMSC-TERT-mediated prednisolone resistance (Figure 4f, $p< 0.01$). EMP1 signals through the Src kinase family and further downstream to JNK, STAT3, STAT5, CREB and NF-kB We next determined which signaling pathways are affected by EMP1. We demonstrate that EMP1 silencing in *ETV6-RUNX1*$^+$ and *MLL-AF4*$^+$ BCP-ALL, and Tetraploid T-ALL cell lines decreased phosphorylation of several Src kinases, that is, Src, Yes, Fgr, Blk and Hck, up to 55% ($p<0.05$, Figures 5a and b). Further downstream, EMP1 silencing resulted in decreased phosphorylation of JNK, STAT3, STAT5, CREB and NF-kB, up to 80% reduction ($p< 0.05$, Figures 5a and b). p38 and ERK1/2 phosphorylation levels were below detection level in BCP-ALL cell lines (ND = not detectable).

EMP1 status is an independent prognostic factor for clinical outcome in BCP-ALL

EMP1 mRNA levels were determined by Affymetrix microarrays for 134 BCP-ALL and 60 T-ALL patients treated on the German COALL97-03-protocol, and 239 BCP-ALL and 56 T-ALL patients treated on the Dutch ALL10 (DCOG) protocol. EMP1 expression status (that is, low or high expression levels) was based on the median cutoff value of mRNA levels detected by microarrays among a batch of BCP-ALL and a batch of T-ALL cases. In the combined analysis of the COALL and DCOG patients stratified for treatment protocol, *EMP1*-high BCP-ALL (n=187) patients had a significantly poorer EFS compared with *EMP1*-low BCP-ALL (n=186) patients with 5-year EFS rates of 77±3 and 89±2%, respectively ($p<0.004$, Figure 6a; Table 1). CIR analysis demonstrated a significant higher relapse and non-response risk for *EMP1*-high than *EMP1*-low cases in BCP-ALL (5-year CIR: 17±3 vs 9±2% P=0.02, Figure 6b). EFS and CIR curves per treatment protocol are depicted in Supplementary Figure S7. To evaluate the independent prognostic value of EMP1, we performed Cox's multivariate regression analysis on all 373 BCP-ALL patients stratified according to treatment protocol using white blood cell count, age and EMP1 expression status as covariates. We identified *EMP1*-high expression levels at diagnosis as an independent predictor ($p<0.01$) for poor outcome in BCP-ALL with a hazard ratio of 2.36 (95% confidence interval: 1.31–4.25, Table 1). The poor prognosis of *EMP1*-high expressing BCP-ALL patients at diagnosis is independent of in vitro and in vivo prednisolone response (Supplementary Table S3) and subtype of ALL (Supplementary Table S4). Although we found a similar functional role for EMP1 in T-ALL cell line models and a trend for poorer outcome of *EMP1*-high cases in the T-ALL cohort, this

Figure 4 continued: (F) Non-silencing control leukemic cells and (*EMP1*-silenced leukemic cells were cultured for 3 days with or without MSCs and with or without 0.488 mg/ml prednisolone. Hereafter, leukemic cells were harvested and cell survival was assessed by trypan blue exclusion assay and MACSQuant flow. Data are presented as mean plus s.e.m. of three or more independent experiments (*P<0.05, **P<0.01, ***P<0.001).

was not statistically significant neither in a treatment-protocol stratified analysis (Figures 6c and d; Table 1B) nor in each of the protocols separately (Supplementary Figure S7; Supplementary Table S3).

Discussion

Prednisolone, a glucocorticoid, regulates transcription of numerous genes eventually leading to cell-cycle arrest and apoptosis in lymphocytes. These properties make glucocorticoids pivotal in the treatment of hematologic malignancies and have led to their inclusion in all chemotherapy protocols for lymphoid malignancies.[23] Prednisolone resistance is a major driver of therapeutic failure.[2] Children with T-ALL are more often in vitro resistant to prednisolone compared with children with the more favorable prognostic BCP-ALL immunophentoype.[24] Elucidating causes of resistance to prednisolone remains

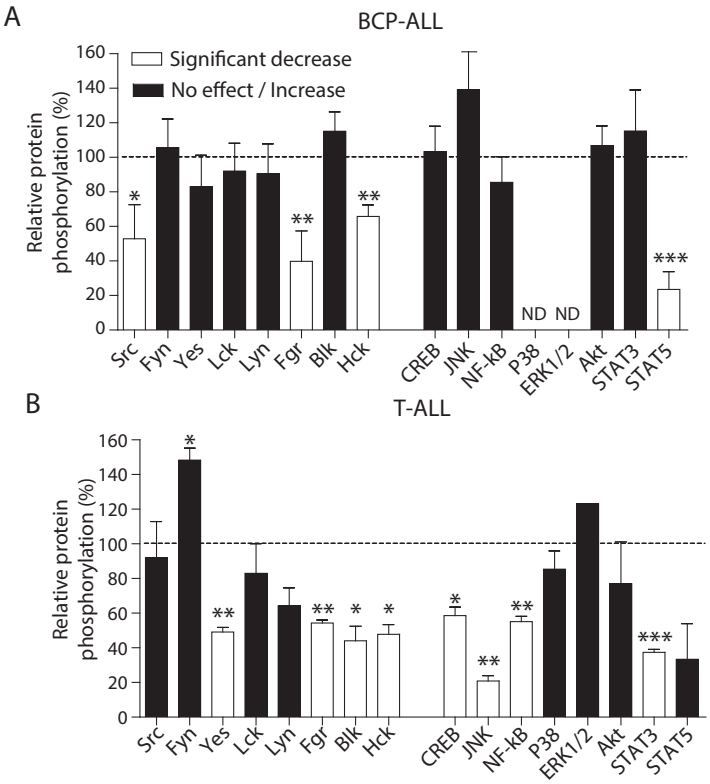

Figure 5. EMP1 signals through the Src kinase family to activate JNK, STAT3, STAT5, CREB and NF-kB.

(A, B) Phosphorylation levels of Src kinase family members and several key members of important cellular pathways were determined by means of a luminex assay in protein harvested from non-silencing control cells and *EMP1*-silenced cells at 168 h after infection. Phosphorylation levels in shNSC-transduced control cells were put to 100% (dashed line). Phosphorylation levels were corrected for protein load by GAPDH and b-tubulin levels in the same sample. Data are presented as mean plus s.e.m. of REH and SEM BCP-ALL cell lines (n = 4) (A) and Jurkat T-ALL cell line experiments (n = 2) (B) (*P<0.05, **P<0.01, ***P<0.001). ND: not detectable, p38 and ERK1/2 measurements in BCP-ALL were below the background level.

challenging due to the multifactorial processes in which these glucocorticoids are involved. In this study, we identified a significant overexpression of *EMP1* mRNA in leukemic cells taken from prednisolone-resistant ALL patients. We show that knockdown of *EMP1* moderately sensitized leukemic cells to prednisolone. Interestingly, a link between glucocorticoids and EMP1 family members has been shown before, as glucocorticoids can regulate the promoter activity of the homologous family members PMP22 and EMP2.[25,26] We show that EMP1 is important for leukemic cell survival, as silencing of *EMP1* results in cell-cycle arrest and apoptosis. In line with this are several studies associating *EMP1* expression levels with cell cycle and cell survival.[5,27,28] The potential observed role of EMP1 in migration and adhesion of leukemic cells might be supported by the notion that EMP1 regulates cell–cell contact,[6,7] and contributes to integrin-mediated leukocyte migration and adhesion.[11] These findings are important in relation to the tumor microenvironment, as this has a significant role in leukemic cell survival and in chemotherapy resistance. Chemokines secreted by MSCs, such as stem cell factor 1 and CXCL12, stimulate leukemic cell homing and survival.[29,30] MSCs can also induce leukemic drug resistance through upregulation of the voltage-dependent channel hERG1[21], or rescue cells from

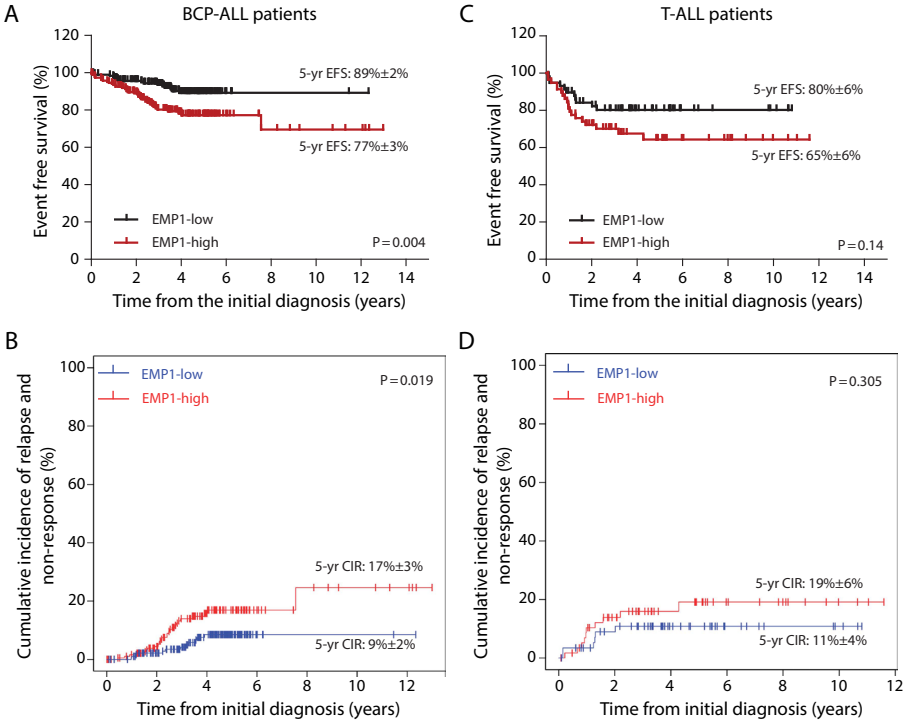

Figure 6. EMP1 status is an independent prognostic factor in BCP-ALL.

EMP1 status was based on the median cutoff value of microarray mRNA expression levels seen in 373 BCP-ALL **(A, B)** and 116 T-ALL **(C, D)**. EFS (upper panels) and cumulative incidence of relapse and non-response (CIR) (lower panels) were calculated. EFS was calculated as time to relapse, non-response, secondary malignancy and death using Kaplan– Meier analysis and Cox proportional hazard analyses. CIR was calculated as time to relapse and non-response with death as a competing event using the method of Fine and Gray.[18]

Table 1. Univariate and multivariate analysis of EMP1 status and event-free survival.

A						
BCP-ALL						
			Univariate analysis		Multivariate analysis	
	Patients	Events	HR (95%-CI)	p-value	HR (95%-CI)	p-value
EMP1 expression (mRNA)						
<Median	186	16				
≥Median	187	37	2.42 (1.34–4.35)	<0.01	2.36 (1.31–4.25)	<0.01
Age at diagnosis (years)						
Low <10	255	35				
High ≥10	118	18	1.50 (0.84–2.67)	0.17	1.44 (0.80–2.56)	0.22
WBC count (x 10^9/l)						
Low <50	288	37				
High≥50	85	16	1.58 (0.88–2.83)	0.13	1.46 (0.81–2.63	0.21
B						
T-ALL						
			Univariate analysis		Multivariate analysis	
	Patients	Events	HR (95%-CI)	p-value	HR (95%-CI)	p-value
EMP1 expression (mRNA)						
<Median	58	11				
≥Median	58	19	1.75 (0.83-3.68)	0.14	1.76 (0.83-3.71)	0.14
Age at diagnosis (years)						
Low <10	63	16				
High ≥10	53	14	1.09 (0.53-2.25)	0.81	1.10 (0.53-2.25)	0.80
WBC count (x 10^9/l)						
Low <50	36	8				
High≥50	79	22	1.17 (0.52-2.64)	0.71	1.09 (0.48-2.48)	0.83

Abbreviations: BCP-ALL, B-cell precursor ALL; CI, confidence interval; EMP1, epithelial membrane protein 1; HR, hazard ratio; T-ALL, T acute lymphoblastic leukemia; WBC, white blood cell. Univariate and multivariate analysis of the indicated prognostic factors stratified according to treatment protocol (DCOG: Dutch, COALL: German) were performed by a Cox regression model in BCP-ALL (A) and T-ALL (B).

L-asparaginase by secreting asparagine.[22] Furthermore, sequestration of ALL cells by MSCs may provide a physical barrier for chemotherapeutics. We show here that MSCs can protect leukemic cells against prednisolone-induced apoptosis and, moreover, that silencing of *EMP1* reduces the protection by MSCs. These data suggest that EMP1 contributes to microenvironment-induced prednisolone resistance. We furthermore determined which signaling pathways underlie EMP1-mediated effects. Recent studies in non-small lung carcinoma suggest that EMP1 increases EGFR signaling,[11] and showed that EMP1 activates the PI3K/AKT pathway.[31] We did, however, not find an association between EMP1 and EGFR signaling (Ariës et al., unpublished data), nor could we demonstrate an effect on AKT phosphorylation after EMP1 silencing in ALL (Figure 5). In contrast, we demonstrated that EMP1 mediates its effect through the Src kinase family, including Src, Fgr, Hck, Yes and Blk. This is in line with data showing that the family member EMP2 promotes Src and FAK phosphorylation.[32] Src kinase family members are oncogenes that are essential in B-cell and T-cell receptor signaling.[33,34] Silencing of EMP1 also decreased the phosphorylation of CREB, NF-kB, JNK, STAT3 and STAT5 in our study. Src kinase activation was previously shown to affect the proliferation and migration of cells via these proteins.[35] Furthermore, JNK and STAT pathways have proven to be important in cell survival of both BCP-ALL and T-ALL.[36–38] We propose the following model; EMP1 most likely serves together with integrines[11] as an anchor molecule essential

for proper function of receptor tyrosine kinases. Knockdown of *EMP1* probably results in destabilized receptor tyrosine kinases, impairing Src kinase phosphorylation and context-dependent downstream signaling to STAT5 in BCP-ALL and JNK, STAT3, CREB and NF-kB in T-ALL, leading to decreased proliferation, potentially also migration and adhesion, and a modest decrease in prednisolone resistance. Most importantly, in addition to our functional studies, we identified that *EMP1* expression status is an independent prognostic factor for clinical outcome in BCP-ALL. Although we showed that EMP1 has a functional role in T-ALL cell line models, the EMP1 expression status was not a strong prognostic indicator in T-ALL patients. Taken together, this study substantiates an important pathobiological role for EMP1 in ALL. The membrane protein property of EMP1 potentiates it as an interesting candidate for drug targeting since problems of drug penetration and partitioning in the cytoplasm or elimination of the drug by drug-efflux pumps can be avoided.[39] Currently, no drugs are available to target EMP1 and the development of an EMP1 inhibitory small compound or antibody is desirable and may serve as a potential new therapeutic option for ALL.

Conflict of Interest

The authors declare no conflict of interest.

Acknowledgements

Dr D Campana, St. Jude Childrens' Research Hospital, Memphis, USA, is highly acknowledged for supplying of MSC-hTERT cell line. This work was supported by the Dutch Cancer Society (MLDB, RP, EMCR 2005-3313 and AMC 2008-4265). The funding source had no role in the collection, analysis and interpretation of data; in the writing of the report; and in the decision to submit the paper for publication.

Author contributions

IMA designed and performed experiments, analyzed and interpreted data, and wrote the paper; ISJ and ERD assisted in part of the experiments; LCJVDB performed and analyzed flowsort experiment; JMB assisted with the statistical analysis of microarray data; MH and GE provided COALL survival data; RP and MLDB designed research, interpreted data and revised the paper.

References

1. Pui CH, Carroll WL, Meshinchi S, Arceci RJ. Biology, risk stratification, and therapy of pediatric acute leukemias: an update. J Clin Oncol 2011; 29: 551–565.

2 Kaspers GJ, Pieters R, Van Zantwijk CH, VanWering ER, Van DerDoes-Van Den Berg A,Veerman AJ. Prednisolone resistance in childhood acute lymphoblastic leukemia:vitro-vivo correlations and cross-resistance to other drugs. Blood 1998; 92: 259–266.

3 Klumper E, Pieters R, Veerman AJ, Huismans DR, Loonen AH, Ha¨hlen K et al. In vitro cellular drug resistance in children with relapsed/refractory acute lymphoblastic leukemia. Blood 1995; 86: 3861–3868.

4 Kfir-Erenfeld S, Sionov RV, Spokoini R, Cohen O, Yefenof E. Protein kinase networks regulating glucocorticoid-induced apoptosis of hematopoietic cancer cells: fundamental aspects and practical considerations. Leuk Lymphoma 2010; 51: 1968–2005.

5 Taylor V, Welcher AA, Program AE, Suter U. Epithelial membrane protein-1, peripheral myelin protein 22, and lens membrane protein 20 define a novel gene family. J Biol Chem 1995; 270: 28824–28833.

6 Bangsow T, Baumann E, Bangsow C, Jaeger MH, Pelzer B, Gruhn P et al The epithelial membrane protein 1 is a novel tight junction protein of the bloodbrain barrier. J Cereb Blood Flow Metab 2008; 28: 1249–1260

7 Lee H-S, Sherley JL, Chen JJW, Chiu C-C, Chiou

L-L, Liang J-D et al. EMP-1 is a junctional protein in a liver stem cell line and in the liver. Biochem Biophys Res Commun 2005; 334: 996–1003

8 Ben-Porath I, Yanuka O, Benvenisty N. The tmp gene, encoding a membrane protein, is a c-Myc target with a tumorigenic activity. Mol Cell Biol 1999; 19: 3529–3539

9 Bredel M, Bredel C, Juric D, Harsh GR, Vogel H, Recht LD et al. Functional network analysis reveals extended gliomagenesis pathway maps and three novel MYC-interacting genes in human gliomas. Cancer Res 2005; 65: 8679–8689

10 Turashvili G, Bouchal J, Ehrmann J, Fridman E, Skarda J, Kolar Z. Novel immunohistochemical markers for the differentiation of lobular and ductal invasive breast carcinomas. Biomed Papers 2007; 151: 59–64

11 Jain A, Tindell CA, Laux I, Hunter JB, Curran J, Galkin A et al. Epithelial membrane protein-1 is a biomarker of gefitinib resistance. Proc Natl Acad Sci USA 2005; 102: 11858–11863

12 Holleman A, Cheok MH, den Boer ML, Yang W, Veerman AJP, Kazemier KM et al Gene-expression patterns in drug-resistant acute lymphoblastic leukemia cells and response to treatment. N Engl J Med 2004; 351: 533–542

13 Den Boer ML, Harms DO, Pieters R, Kazemier KM, Gobel U, Ko¨ rholz D et al. Patient stratification based on prednisolone-vincristine-asparaginase resistance profiles in children with acute lymphoblastic leukemia. J Clin Oncol 2003; 21: 3262–3268

14 Den Boer ML, van Slegtenhorst M, De Menezes RX, Cheok MH, JGCAM Buijs-Gladdines, STCJM Peters et al. A subtype of childhood acute lymphoblastic leukaemia with poor treatment outcome: a genome-wide classification study. Lancet Oncol 2009; 10: 125–134

15 Mihara K, Imai C, Coustan-Smith E, Dome JS, Dominici M, Vanin E et al. Development and functional characterization of human bone marrow mesenchymal cells immortalized by enforced expression of telomerase. Br J Haematol 2003; 120: 846–849

16 Huber W, von Heydebreck A, Su¨ ltmann H, Poustka A, Vingron M. Variance stabilization applied to microarray data calibration and to the quantification of differential expression. Bioinformatics 2002; 18(Suppl 1): S96–S104

17 Benjamini Y, Hochberg Y. Controlling the false discovery rate: a practical and powerful approach to multiple testing. J R Stat Soc 1995; 57: 289–300

18 Fine JP, Gray RJ. A proportional hazards model for the subdistribution of a competing risk. J Am Stat Assoc 1999; 94: 496–509

19 de Wreede LC, Fiocco M, Putter H. mstate: an R package for the analysis of competing risks and multi-state models. J Stat Softw 2011; 38

20 Gray R. Cmprsk: Subdistribution Analysis of Competing Risks. R package version 2.2-2 2011

21 Pillozzi S, Masselli M, De Lorenzo E, Accordi B, Cilia E, Crociani O et alChemotherapy resistance in acute lymphoblastic leukemia requires hERG1 channels and is overcome by hERG1 blockers. Blood 2011; 117: 902–914

22 Iwamoto S, Mihara K, Downing JR, Pui C-H, Campana D. Mesenchymal cells regulate the response of acute lymphoblastic leukemia cells to asparaginase. J Clin Investig 2007; 117: 1049–1057

23 Sionov RV, Spokoini R, Kfir-Erenfeld S, Cohen O, Yefenof E. Mechanisms regulating the susceptibility of hematopoietic malignancies to glucocorticoid-induced apoptosis. Adv Cancer Res 2008; 101: 127–248

24 Pieters R, Kaspers GJ, van Wering ER, Huismans DR, Loonen AH, Ha¨hlen K et al

Cellular drug resistance profiles that might explain the prognostic value of immunophenotype and age in childhood acute lymphoblastic leukemia Leukemia 1993; 7: 392–397

25 Désarnaud F, Bidichandani S, Patel PI, Baulieu E-E, Schumacher M. Glucocorticosteroids stimulate the activity of the promoters of peripheral myelin protein-22 and protein zero genes in Schwann cells. Brain Res 2000; 865: 12–16

26 Wadehra M, Mainigi M, Morales SA, Rao RG, Gordon LK, Williams CJ et al. Steroid hormone regulation of EMP2 expression and localization in the endometrium

Reprod Biol Endocrinol 2008; 6: 15

27 Li Z-Y, Xiong S-H, Hu M, Zhang C-S. Epithelial membrane protein 1 inhibits human spinal chondrocyte differentiation. Anat Record 2011; 294: 1015–1024

28 Ben-Porath I, Benvenisty N. Characterization of a tumor-associated gene, a member of a novel family of genes encoding membrane glycoproteins. Gene 1996; 183: 69–75

29 Sison EAR, Brown P. The bone marrow microenvironment and leukemia: biology and therapeutic targeting. Expert Rev Hematol 2011; 4: 271–283

30 Masson K, Ro¨ nnstrand L. Oncogenic signaling from the hematopoietic growth factor receptors c-Kit and Flt3. Cell Signal 2009; 21: 1717–1726

31 Lai S, Wang G, Cao X, Li Z, Hu J, Wang J. EMP-1 promotes tumorigenesis of NSCLC through PI3K/AKT pathway. J Huazhong Univ Sci Technol Med Sci 2012; 32: 834–838

32 Morales SA, Mareninov S, Coulam P, Wadehra M, Goodglick L, Braun J et al

Functional consequences of interactions between FAK and epithelial membrane protein 2 (EMP2). Investig Ophthalmol Vis Sci 2009; 50: 4949–4956

33 Gauld SB, Cambier JC. Src-family kinases in B-cell development and signaling Oncogene 2004; 23: 8001–8006

34 Palacios EH, Weiss A. Function of the Src-family kinases, Lck and Fyn, in T-cell development and activation. Oncogene 2004; 23: 7990–8000

35 Silva CM. Role of STATs as downstream signal transducers in Src family kinase-mediated tumorigenesis. Oncogene 2004; 23: 8017–8023

36 Quintas-Cardama A, Verstovsek S. Molecular pathways: JAK/STAT pathway: mutations, inhibitors, and resistance. Clin Cancer Res. 2013; 19: 1933–1940

37 Malin S, McManus S, Busslinger M. STAT5 in B

cell development and leukemia Curr Opin Immunol 2010; 22: 168–176

38 Mangolini M, de Boer J, Walf-Vorderwu¨ lbecke V, Pieters R, den Boer ML, Williams O STAT3 mediates oncogenic addiction to TEL-AML1 in t(12;21) acute lymphoblastic leukemia. Blood 2013; 122: 542–549

39 Pignatello R, Musumeci T, Basile L, Carbone C, Puglisi G. Biomembrane models and drug-biomembrane interaction studies: Involvement in drug design and development. J Pharm Bioallied Sci 2011; 3: 4–14

Supplementa Data

Supplemental Table S1 This table is available on the Leukemia website

https://images-nature-com.eur.idm.oclc.org/full/nature-assets/leu/journal/v28/n9/extref/leu201480x2.pdf

Supplemental Table S2. Prednisolone resistance IC50 values of cell lines after shNSC or shEMP1 transfection.

Cell lineL	Sensitive/Resistant*	C50 shNSC (µg/ml)	LC50 shEMP1 (µg/ml)	Significant decrease
REH	Resistant	10487+/- 672	10170+/- 722	
6970	Intermediate Resistant	.222+/- 0.022	0.050+/- 0.003	***
NALM60	Intermediate Resistant	.396+/- 0.005	0.421+/- 0.022	
SEM1	Intermediate Resistant	.175+/- 0.117	1.980+/- 0.270	
Jurkat	Resistant	9352+/- 422	5914+/- 389	***
SupT1	Intermediate Resistant	8.138+/- 0.3250	.435+/- 0.007	***

* in vitro prednisolone resistance compated to IC50-values of primary ALL cells as described in reference 13. *** $p < 0.001$

Table S3. Univariate and multivariate analysis of EMP1 status, age, white blood cell count, and in vitro and in vivo prednisolone resistance and prognosis. Univariate and multivariate analysis of the inidcated prognostic factors were performed by a Cox regression model based on event-free survival and with riskgroup as stratum. In vitro prednisolone response data are only available of COALL-97/03 patients, in contrast in vivo prednisolone response data are only available of DCOG-ALL10 patients.

BCP-ALL						
COALL-97/03 protocol						
			Univariate Analysis		Multivariate Analysis	
	Patients	Events	HR (95%-CI)	*p*-value	HR (95%-CI)	*p*-value
EMP1 expression (mRNA)						
<Median	67	9	1		1	
≥Median	67	19	2.09(0.94-4.64)	0.07	1.81(0.77-4.25)	0.17
Age at diagnosis (years)						
Low <10	103	20	1		1	
High ≥10	31	8	1.23(0.54-2.79)	0.62	1.22(0.51-2.95)	0.66
WBC count (x 10^9/ L)						
Low <50	100	16	1		1	
High ≥50	34	12	2.64(1.25-5.57)	0.01	2.66(1.12-6.35)	0.03
In vitro Prednisolone response						
Good	54	8	1		1	
Intermediate	47	12	1.95(0.80-4.78)	0.14	1.57(0.62-3.94)	0.34
Poor	33	8	1.61(0.60-4.30)	0.34	1.38(0.47-4.05)	0.56

Supplementary Table S3 (continued):

DCOG-ALL10 protocol						
			Univariate Analysis		Multivariate Analysis	
	Patients	Events	HR (95%-CI)	*p*-value	HR (95%-CI)	*p*-value
***EMP1* expression (mRNA)**						
<Median	119	7	1		1	
≥Median	120	18	2.84(1.19-6.81)	0.02	3.17(1.12-8.96)	0.03
Age at diagnosis (years)						
Low <10	152	15	1		1	
High ≥10	87	10	1.86(0.81-4.24)	0.14	1.40(0.50-3.92)	0.52
WBC count (x 10^9/ L)						
Low < 50	188	21	1		1	
High ≥50	51	4	0.72(0.25-2.11)	0.55	0.56(0.18-1.80)	0.33
***In vivo* Prednisolone response**						
Good	223	23	1		1	
Poor	7	2	2.75(0.65-11.69)	0.17	0.86(0.16-4.65)	0.87

T-ALL						
COALL-97/03 protocol						
			Univariate Analysis		Multivariate Analysis	
	Patients	Events	HR (95%-CI)	*p*-value	HR (95%-CI)	*p*-value
***EMP1* expression (mRNA)**						
<Median	30	9	1		1	
≥Median	30	11	1.19(0.49-2.86)	0.70	1.39(0.54-3.53)	0.49
Age at diagnosis (years)						
Low <10	34	11	1		1	
High ≥10	26	9	1.09(0.45-2.64)	0.85	1.13(0.46-2.80)	0.79
WBC count (x 10^9/ L)						
Low < 50	15	4	1		1	
High≥50	45	16	1.45(0.49-4.34)	0.51	1.17(0.35-3.87)	0.80
***In vitro* Prednisolone response**						
Good	21	7	1		1	
Intermediate	22	9	1.37(0.51-3.68)	0.533	1.36(0.48-3.85)	0.56
Poor	17	4	0.72(0.21-2.48)	0.61	0.66(0.19-2.37)	0.53

DCOG-ALL10 protocol						
			Univariate Analysis		Multivariate Analysis	
	Patients	Events	HR (95%-CI)	*p*-value	HR (95%-CI)	*p*-value
***EMP1* expression (mRNA)**						
<Median	28	2	1		1	
≥Median	28	8	4.40(0.93-20.73)	0.06	6.27(1.18-3.29)	0.03
Age at diagnosis (years)						
Low <10	29	5	1		1	
High ≥10	27	5	1.10(0.32-3.80)	0.88	1.80(0.43-7.45)	0.42
WBC count (x 10^9/ L)						
Low < 50	21	4	1		1	
High≥50	34	6	0.85(0.24-3.01)	0.80	0.44(0.11-1.74)	0.24
***In vivo* Prednisolone response**						
Good	39	5	1		1	
Poor	16	5	2.54(0.74-8.79)	0.14	3.23(0.80-13.01)	0.10

Table S4. Univariate and multivariate analysis of EMP1 status, age, white blood cell count and subtypes in BCP-ALL.

Univariate and multivariate analysis of the indicated prognostic factors were performed by a Cox regression model stratified for treatment protocol (COALL/DCOG) based on event-free survival. The percent of 5-year event-free survival was analyzed using Kaplan-Meier statistics. WBC=white blood cell count; ER=ETV6-RUNX1+, HD=hyperdiploid, E2A=TCF3-PBX1+, BO=B-other, BA=BCR-ABL1+, BAL=BCR-ABL1-like, MLL=MLL-rearranged. ER and HD belong to the low-risk group, E2A and BO to intermediate-risk group and BA, BAL and MLL to high-risk group.

BCP-ALL						
COALL-97/03 protocol and DCOG-ALL10 cohort						
			Univariate Analysis		Multivariate Analysis	
	Patients	Events	HR (95%-CI)	*p*-value	HR (95%-CI)	*p*-value
EMP1 **expression (mRNA)**						
< Median	186	16	1		1	
≥Median	187	37	2.42(1.34-4.35)	<0.01	2.41(1.32-4.39)	<0.01
Age at diagnosis (years)						
Low <10	255	35	1		1	
High ≥10	118	18	1.50(0.84-2.67)	0.17	0.89(0.485-1.635)	0.71
WBC count (x 10^9/ L)						
Low < 50	288	37	1		1	
High ≥ 50	85	16	1.58(0.88-2.83)	0.13	1.22(0.665-2.249	0.52
Subtype (risk)						
ER HD	227	17	1		1	
E2A BO	66	16	3.25(1.69-6.28)	<0.01	3.69(1.86-7.31)	<0.01
BA BAL MLL	67	20	3.84(1.96-7.54)	<0.01	3.35(1.61-6.98)	<0.01

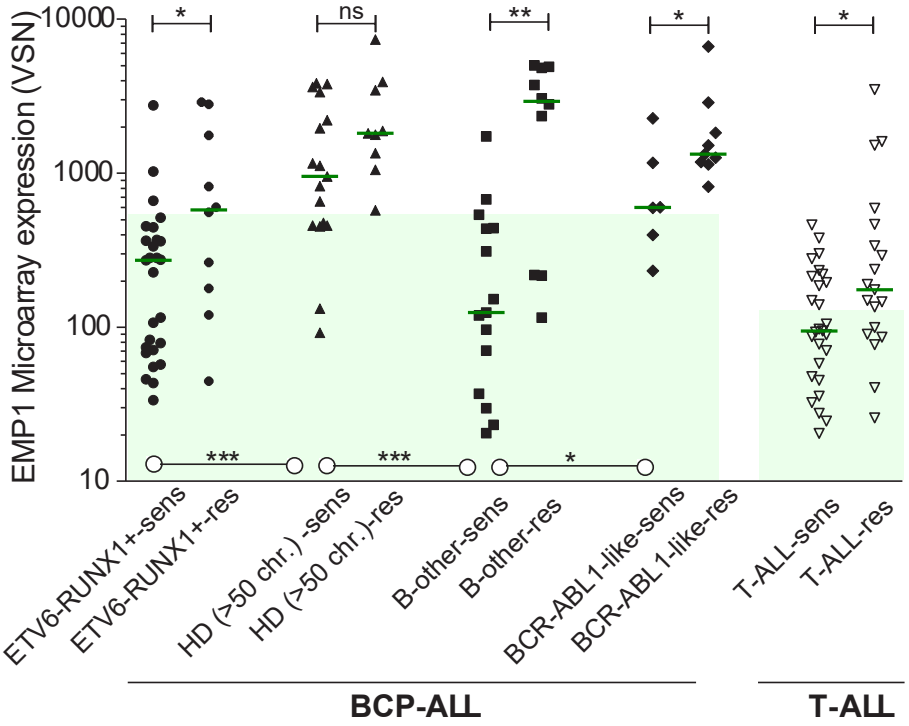

Figure S1. Differential expression of EMP1 between prednisolone resistant and sensitive patients per subtype of ALL.

Microarray expression levels of EMP1 probeset 201324_at are compared between in vitro prednisolone sensitive (sens) and resistant (res) ETV6-RUNX1+, hyperdiploid (HD) (>50 chromosomes), BCR-ABL1-like, B-other BCP-ALL patients and T-ALL patients indicated by |--|. Green block indicates patients with an EMP1 expression below the median. The median expression level differed between BCP and T-ALL cases because these patients were tested in two different batches of microarrays. Mann-Whitney comparison of basal EMP1 expression levels between prednisolone sensitive subtypes are indicated by O—O, all sensitive groups were compared and only the statistical significant ones are indicated.

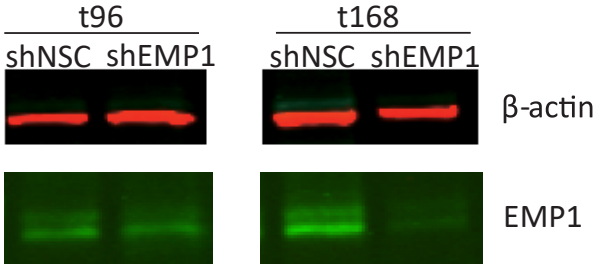

Figure S2. Knockdown of EMP1 protein expression became apparent after 168h.

EMP1 protien expression in NALM6 was assessed after 96h and 168h. Knockdown of EMP1 protein expression became apparent after 168h. We were therefore not able to achieve EMP1 knockdown in primary ALL cells, since these cells are viable for up to 96h.

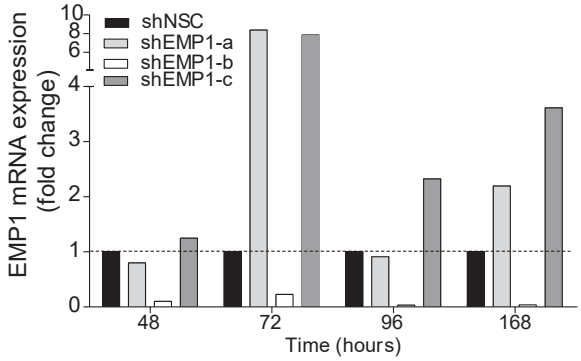

Figure S3. Only shEMP1-b yields sufficient EMP1 mRNA knockdown.

EMP1 mRNA expression was assessed at three different timepoints after transfection with three different shEMP1 constructs available TRCN 0000117943 (shEMP1-a), TRCN 0000117944 (shEMP1-b) and TRCN 0000117945 (shEMP1-c). Only shEMP1-b yielded sufficient knockdown.

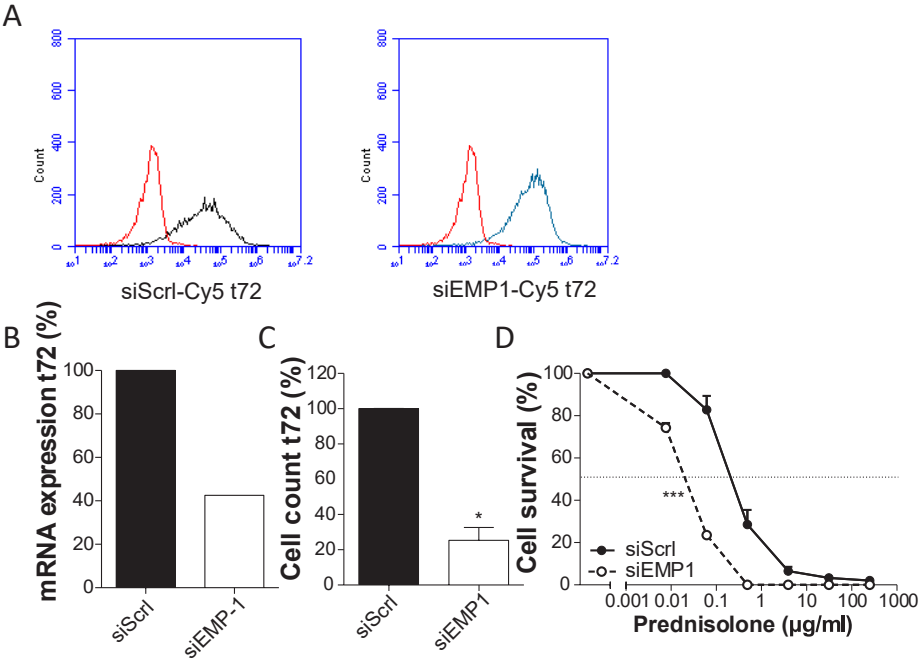

Figure S4. EMP1 knockdown using siEMP1 inhibits leukemic cell proliferation and sensitizes cells towards prednisolone.

The leukemic cell line 697, E2A-PBX1+, was transfected with siEMP1-Cy5 or with siScrl-Cy5. (A) Transfection efficiency at 72 hours after transfection was assessed by means of flow cytometry. (Mock; red line, siScrl; black line, siEMP1; blue line) (B) EMP1 mRNA levels were determined 72 hours after transfection by qRT-PCR and calculated relative to siScrl after correcting for the housekeeping gene RPS20. (C) Leukemic cell survival 72 hours after transfection was evaluated with a trypan blue exclusion assay (*p<0.05). (D) Response to prednisolone was assessed in a three day MTT assay directly after transfection with either siScrl or siEMP1. Sensitivity was corrected for cell death induced by EMP1 knockdown without co-exposure to prednisolone. Data are presented as mean plus SEM of two experiments (*p<0.001).

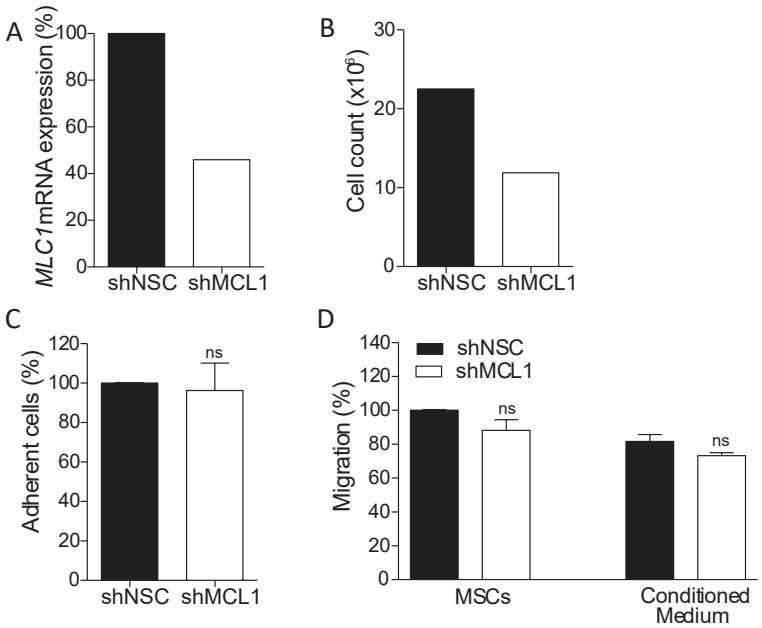

Figure S5. MCL1 knockdown decreases proliferation, but not adhesion and migration.

(A) : MCL1 mRNA levels were measured after treatment with shMCL1 or shNSC in REH: ETV6-RUNX1+ leukemic cells. Values were adjusted for expression of the housekeeping gene RPS20 and are relative to shNSC-transduced cells (NSC). (B) Cell proliferation of MCL1 silenced cells and shNSC-transduced cells was monitored over time on the MACSQuant. (C) Leukemic cells were cocultured with mesenchymal stromal cells (hMSC-TERT) overnight, whereafter viable non-adherent and adherent cells were quantified by means of trypan blue exclusion assay and/or MACSQuant flow. (D) Non-silencing control or MCL1-silenced ETV6-RUNX1+ leukemic cells were placed in AIMV into an upper compartment of a transwell assay and allowed to migrate either to hMSC-TERT preconditioned for 48h in AIMV or to 48h preconditioned AIMV that was collected from hMSC-TERT. Migration of viable cells was assessed by trypan blue exclusion assay and MACSQuant flow. Data are presented as mean plus SEM of a triplicate experiment.

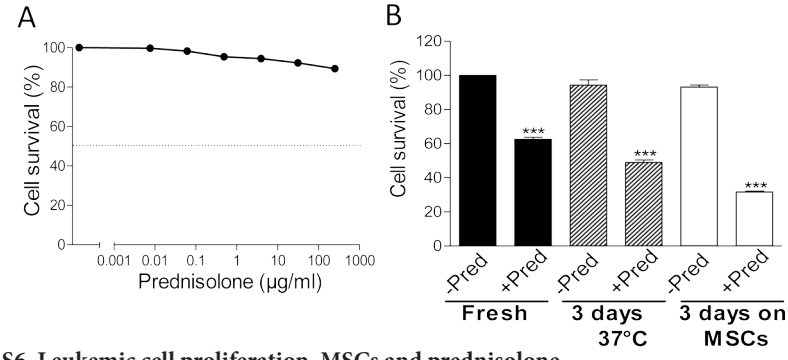

Figure S6. Leukemic cell proliferation, MSCs and prednisolone.

(A) Cell survival of hMSC-TERT after 3-day prednisolone exposure determined by an MTS assay. (B) Leukemic cell survival determined by a 3-day MTS assay with either fresh prednisolone in RPMI medium, prednisolone that was incubated for three days at 37 °C in RPMI medium, and prednisolone in RPMI medium that was harvested from hMSC-TERT after three days of incubation at 37 °C . Data are presented as mean plus SEM of three independent experiments (***p<0.001).

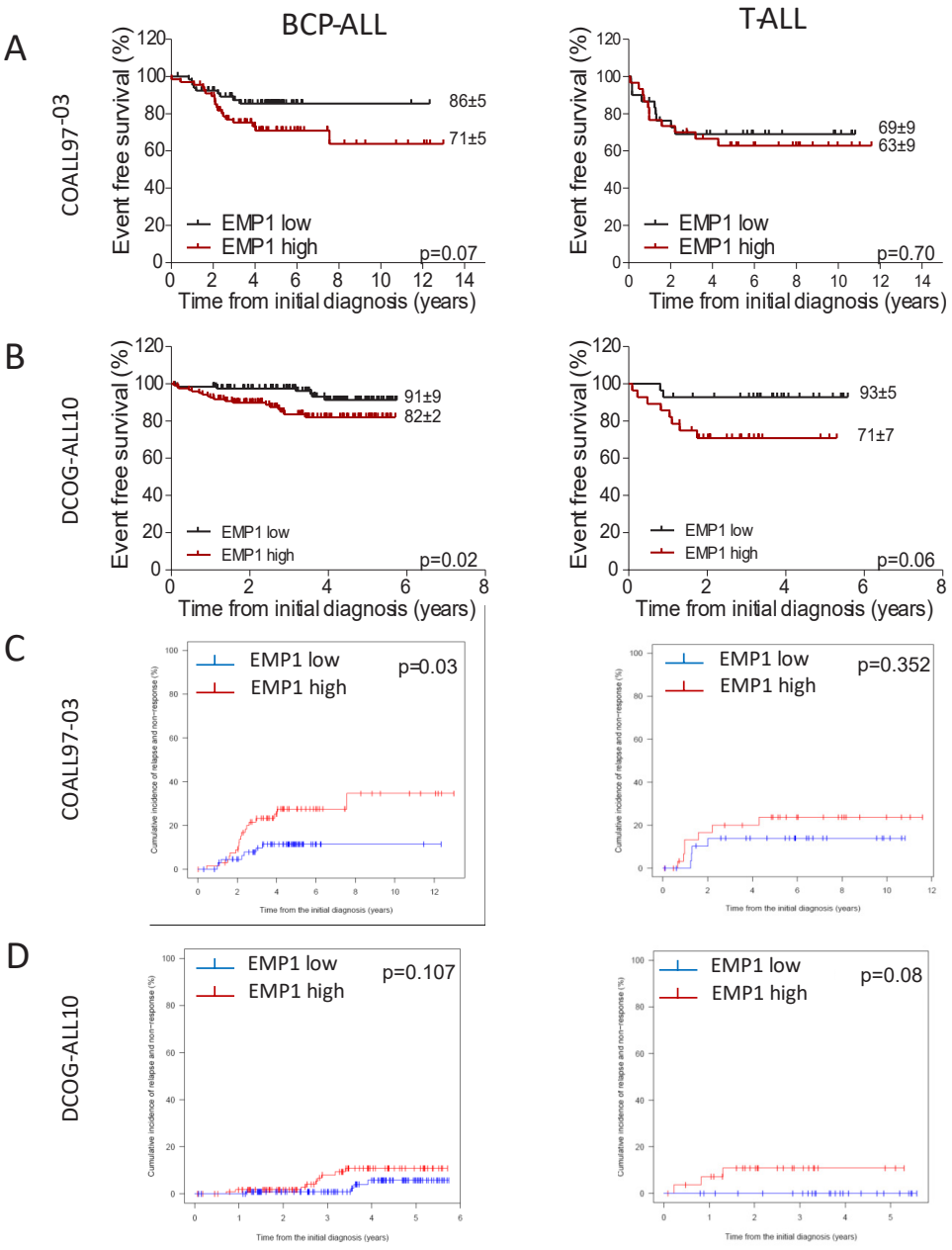

Figure S7. EFS and CIR of EMP1 high versus EMP1 low patients per treatment protocol.

EMP1 status was determined by the median value of microarray mRNA expression for 134 BCP-ALL (left) and 60 T-ALL patients (right) treated on the German COALL97-03-protocol (A and C panel), and 249 BCP-ALL (left) and 56 T-ALL (right) patients treated on the Dutch ALL10 protocol (B and D panel). 5-year event-free survival were analyzed using Kaplan-Meier statistics. Cumulative incidence of relapse was calculated with the method of Fine and Gray.

Chapter 7

General Discussion and Perspective

General Discussion and Perspective

Decades of clinical and pre-clinical research have achieved high rates of cure in children diagnosed with acute lymphoblastic leukemia (ALL). However, therapy is intense and has serious side effects. This changes the priorities and goals of therapy adaptations. With this context in mind, we evaluated several signaling pathways as therapeutic targets in pediatric BCP-ALL. Genetic aberrations often indicate relevant molecular pathways, because they constitutively activate or inactivate signaling pathways

The advent of next-generation sequencing has facilitated the identification of oncogenic drivers and led us to search for mutations and structural aberrations in four potential treatment targets. Secondly, we evaluated the in vitro response to drugs against these pathways, which also revealed resistance mechanisms. Ultimately, this work aimed to give suggestions for the clinical implementation of therapies targeting signaling pathways.

Targeting oncogenic signaling pathways in pediatric BCP-ALL

Kinases play a major role in sustained proliferation and anti-apoptotic signaling. The characteristic ATP-binding pockets of kinases offer many possibilities for small molecule-binding, which initiated the development of specific inhibitors. This biological and clinical relevance is the basis for a large part of the work presented in this thesis.

JAK2 aberrant leukemia comprises two distinct entities: in some cases chimeric fusion genes are generated by translocations, in others *JAK2* mutations are thought to cause constitutive activation (Chapter 2). In general, tyrosine kinase fusions are primary oncogenic events and therefore excellent treatment targets. Discovery of the *BCR-ABL1* fusion gene as leukemic driver has led to implementation of ABL inhibitors as standard of care, which now serve as the prime example for targeted therapy in hemato-oncology. In our study, fusions involving *JAK2* were, as expected, restricted to the *BCR-ABL1*-like subtype. These *JAK2* fusions, as well as other kinase fusions discovered in recent years, may serve as therapy targets similarly to *BCR-ABL1* but their suitability as therapeutic target has not been proven.[1-4] Cellular context and additional mutations likely affect the vulnerability to targeted inhibition. Previous studies support the hypothesis that JAK2 inhibitors are most effective in combination therapies.[4,5]

JAK2 mutations occurred in *BCR-ABL1*-like and B-other cases and sporadically in high hyperdiploid leukemia. Importantly, all JAK2 mutations in R683 occurred in the background of high CRLF2 expression (chapter 2). While *JAK2* fusions are known to be primary, leukemia-initiating lesions, *JAK2* mutations were detected at a range of variant allele frequencies (VAF) and could be lost in patient-derived xenografts. They therefore represent secondary genetic aberrations. This is likely to affect the dependence of leukemic cells on JAK2-mediated signals. Although some of our data disagrees, it is generally thought that JAK2 mutations provide TSLP-independent growth signals by constitutively activating the JAK STAT pathway.[6,7] Our data and previously published reports suggest that this indeed creates a dependency on JAK signaling.[8-10] However, we also found that signaling rebound after inhibitor release, activation of alternative pathways, as well as microenvironment-mediated resistance could hinder the effect of JAK inhibitors in pediatric BCP-ALL. While these points do not generally contest JAK

inhibitor treatment, thorough genomic characterization at therapy initiation and close disease monitoring may be required.

The RAS family genes were some of the first oncogenes to be described. Germline RAS mutations increase the risk for malignancies, proving that RAS pathway activation is oncogenic, but insufficient on its own.[11,12] However, these cases are rare, and frequent subclonal mutations show that RAS pathway mutations are usually secondary events in leukemia development.

As the RAS protein itself is so far "undruggable", targeting downstream effector pathways is so far the most promising approach.[13] In line with other reports, our pre-clinical data suggests that inhibition of the MAPK pathway (the RAF-MEK-ERK signaling axis) is a promising approach in BCP-ALL.[14] Carefully designed clinical studies are necessary to investigate whether these pre-clinical results can be replicated in patients.

The RAS GTPases relate extracellular growth signaling from different cytokine receptors into an intracellular response. Three major pathways are activated by RAS signaling, but many others are indirectly connected. In this central position, the mutational activation of RAS cooperates with different oncogenic mechanisms. It is therefore not surprising that RAS mutations are found in different genomic backgrounds (chapter 3) and tumor types (reviewed by Pylayeva-Gupta et al.[15]).

Deep sequencing allowed evaluation of tumor heterogeneity and detection of small subclones. As has been suggested by retrospective studies, we discovered that many children with BCP-ALL (20%) carry RAS pathway mutations only in a minor fraction of leukemic cells.[14,16,17] Our data showed that the prognostic relevance of clonal RAS pathway mutations was different from that of subclonal mutations. This suggests that other mechanisms are driving the leukemia in cases with subclonal mutations. These may represent better treatment targets and should therefore be investigated. Despite this likely difference at diagnosis, cases with subclonal mutations recurrently relapsed with clonal RAS pathway mutations. Re-evaluating RAS pathway mutation status at relapse is therefore necessary to determine which patients are eligible to MEK inhibitor treatment.

It is noticeable that the RAS pathway and JAK2 have a similar role within the cancer cell: Both are intracellular effectors which relate external signals into a cellular response. In *JAK2* mutant BCP-ALL, these signals are derived from TSLP-bound CRLF2, but in other diseases mutant JAK2 mimics activation of single chain receptors such as EPOR or MPL.[18] In addition, JAK2 is known to transmit signals of many other receptors, e.g. the interferon receptor family, GCSF receptor family, and IL6 receptor.[18] The RAS-mediated MAPK signaling transmits signals of many different receptors, such as growth factor receptors (e.g. FGFR, PDGFR, FLT3, CSF1R), G-protein coupled receptors, or cytokine receptors.[19,20] Environmental signals likely play an important role during the early development, and genetic aberrations that constitutively activate growth and survival signaling can circumvent negative feedback regulation and dependence on external sources of the signal.

However, the tumor microenvironment continues to play an important role also in JAK2 and RAS mutant leukemia. For example, we and others have shown that CRLF2 activation strongly enhances signaling through mutant JAK2 (chapter 2). Regarding RAS activation,

it is important to keep in mind that RAS mutations actually inactivate its enzymatic function, which results in the failure to turn down signal generation. External signaling activation in the mutated background may also activate other components of the pathway which are not activated by the activating mutation alone. The partial dependence on environmental cues becomes obvious in in vitro culture systems. ALL cell survival is largely enhanced by co-culture with mesenchymal stromal cells (chapter 2, chapter 4, and ref.21)

Indirect effects of the leukemic microenvironment have been described through CXCL12 and ITGA4-mediated adhesion.[22-26] Recently, additional effects have been shown to be mediated by tunneling nano-tubes, which are formed between ALL cells and the mesenchymal stromal cells.[21,27] Tunneling nanotubes serve as transport structures for the transmission of autophagosomes, mitochondria, and the adhesion molecule ICAM, and disruption of tunneling nanotube formation reduces the cell survival benefit mediated by mesenchymal stromal cells in vitro. Such novel mechanisms are currently being discovered and will lead to a better understanding of the leukemic bone marrow environment, also with regard to cellular drug resistance (see below).

Looking for novel targets, we investigated the tyrosine kinases PDGFRα and FGFR1-3 (chapters 4 and 5). FGFR signaling had been previously implicated in other hematologic malignancies, as well as fusions of PDGFRA.[28-30] However, our investigations did not reveal recurrent genetic aberrations in these genes.

Despite being highly expressed in a distinct subgroup of BCP-ALL patients, inhibition of PDGFRα signaling had no effect on the survival of these leukemic cells. PDGFRA high cases were also sensitive to prednisolone, and not more resistant towards other chemotherapeutic drugs than other BCP-ALL cases. Combining PDGFRα inhibition with other therapeutics is therefore not likely to yield a benefit.

Oncogenic FGFR signaling was previously demonstrated in multiple myeloma and CML, but in pediatric BCP-ALL virtually no mutations are present at initial diagnosis.[28,30] In vitro drug testing with specific inhibitors showed no sensitivity towards inhibition of FGFR signaling in BCP-ALL cells. Receptor tyrosine kinases with high expression (e.g. PDGFRα) or relevance in other hematological subclasses (FGFR1-3) may be actively signaling, but those are not necessarily essential survival signals.

With molecular characterization still ongoing, novel mediators of signaling pathways may still be discovered. We have found that the poorly studied EMP1 is a biomarker and mediator of prednisolone resistance (chapter 6). The structure of this molecule indicates a function in cell adhesion, and our studies assessing migration and adhesion of leukemic cells in vitro support this. In addition, we found that Src signaling is downregulated upon *EMP1* knockdown. This example points out that not only classic growth factors, but also other cellular mechanisms such as cell adhesion affect cellular signaling pathways. Factors such as EMP1 should therefore also be included in a wider search for possible drug targets within signaling pathways.

For the future of signaling-directed therapies, the experience of the past years has shown that resistance, e.g. caused by the microenvironment or tumor evolution, is almost inevitable. Managing resistance will be essential to achieve lasting treatment effects with

signaling-directed therapies.

Anticipating and overcoming cellular drug resistance

After the first successes in clinical application, several mechanisms for resistance towards kinase inhibitors were discovered. Although they are often specific to the inhibitors and targets, common principles can be identified that aid drug development.

First of all, efficacy can often be improved by compound optimization. As discussed in chapter 2, type-I inhibitors, which bind kinases in active conformation, are eventually less effective drugs than type-II inhibitors, which keep kinases in an inactive conformation. We and others observed rebound activation of JAK2 after inhibitor release, in cases with both mutations and fusions. Although the precise consequences have not been studied, it is possible that the reactivation after inhibitor release hinders the therapeutic efficacy of type I-JAK inhibitors. Recently, two novel type-II inhibitors were reported, which showed greater anti-tumor efficiency in myeloid and lymphoid leukemia with JAK2 aberrations.[5] Clinical studies are yet required to reveal superiority of these inhibitors.

Lower target specificity may be a vice as well as a virtue: As shown in chapter 2, at least part of the difference observed between the efficiency of momelotinib and ruxolitinib may be due to inhibition of other targets, such as the kinase TBK1 and the BMP receptor ACVR1/ALK2 by momelotinib.[31,32] Similarly, suppression of FGFR3 signaling was shown to be part of the anti-leukemic effect of the ABL1 inhibitor ponatinib.[30] However, such reduced selectivity is also likely to cause an increased amount of side effects and, for example, requires additional safety measures for ponatinib therapy.[33]

Even in molecules targeting the same kinases, differences in the chemical interaction may lead to variations in their efficacy. For example, the MEK inhibitor trametinib binds MEK1 as well as MEK2, while other candidates, such as cobimetinib or selumetinib, show higher selectivity towards MEK1 (FDA Memorandum on Cobimetinib Oct. 2015 and references 34 and 35). As MEK1 and MEK2 are thought to act redundantly, this selectivity may affect efficacy and facilitate development of drug resistance. In addition, Lito et al. and Hatzivassiliou et al. have shown that disrupting the interaction between MEK and RAF kinases by the inhibitor is essential for its effectiveness in RAS-mutant cancers.[36,37] In contrast, these MEK inhibitors were less effective towards BRAF mutant cancers.[37] The various genotypes that activate identical oncogenic pathways may therefore require tailored inhibitors.

In addition to the chemical compounds, therapy schedules can be optimized to anticipate the development of resistance. For example, reactivating mutations are common in relapsed, imatinib-treated *BCR-ABL1*-rearranged leukemia in adults, and will very likely develop in other kinase fusion cases as well.[38] In this type of leukemia, the aberrant kinase is central to the disease and only reactivation can restore the oncogenic effect of the aberrant kinase. The gatekeeper residue in the ATP binding pocket is crucial for binding of many kinase inhibitors, and mutations that block this interaction (e.g. ABL1 T315I) are selected for by therapy. As these mutations can be relatively easily anticipated, second generation drugs can be developed which bypass the resistance induced by specific mutations. Several generations and mutant-selective inhibitors are already available for the some kinases, such as BTK and ABL1.[39,40] Notably, kinase domain mutations seem to

be rare in children with *BCR-ABL1*-rearranged BCP-ALL, where imatinib is integrated into an intense combination chemotherapy and often followed by hematopoietic stem cell transplantation.[38,41,42]

Pathway crosstalk and plasticity within signaling networks may also limit the efficacy of drugs targeting signaling molecules. So-called redundancy is the major way of resistance towards drugs targeting secondary aberrations. Our data and previously published reports suggest that secondary mutations in alternative pathways (e.g. RAS pathway) could bypass the therapeutic effects of JAK inhibition.[17,43] This could also explain the varying degree of sensitivity towards MEK and JAK inhibitors observed in vitro (e.g. chapters 2 and 3). Further support for the hypothesis comes from xenograft studies: CRLF2-driven leukemia grows in mice, despite mouse TSLP being unable to activate human CRLF2 (own observation and reference 44). In one xenograft, we observed a KRAS-mutant clone outgrowing the *JAK2*-mutant clone. This suggests that CRLF2 signaling may be less relevant for leukemia propagation than for initiation, at least in some cases. Revealing the relevant downstream effects of secondary aberrations will improve therapy through combination approaches (see below).

In addition to these intracellular mechanisms of resistance, we and others have shown that also the micro-environment contributes to resistance to targeted therapy, e.g. through cytokine secretion and cell-cell contact (chapters 2, 5 and 6).[45-48] Inhibiting the effects of cytokines secreted in the leukemic niche, e.g. FGF2 or CXCL12, can overcome environment-mediated therapy resistance.[30,49-51] It is important to note that chemokines, such as CXCL12 or CX3CL1, may indirectly affect therapy response by changing migration towards and egress from the leukemic bone marrow.[23,52,53] Furthermore, the newly described tunneling nanotubes were shown to mediate cellular resistance towards prednisolone.[21] Further investigations, especially utilizing in vivo models, are warranted to identify new potential targets in the leukemic niche.

Clonal diversity allows selection for therapy resistance in all cancers. Therapy represents a selective pressure, which will select for those cells that a capable to adapt to the effects of therapy. With regard to secondary aberrations, we made an interesting observation in RAS mutant ALL after relapse: In more than half of all cases several RAS mutant clones co-existed at initial diagnosis. In the small cohort of relapsed cases we investigated, this clonal diversity seemed to be reduced to single, clonal mutations driving the relapsed leukemia. It is tempting to speculate that these relapses may be more susceptible to MEK inhibitor therapy because they were derived from a single, MEK-dependent leukemic cell.

In conclusion, all therapeutic strategies and targeted therapy in particular, need to embrace tumor evolution. The logical consequence is combination therapy, which changes the selective pressures to eradicate all leukemic cells. In the future, it may be tailored to the molecular aberrations found in individual cases.

Combination therapies

With a quickly growing number of drugs and targets, a vast amount of combination therapies is conceivable. Some data is already available to pre-select combinations that should be evaluated in further studies, and more detailed knowledge on the mode of

action of old and new drugs will allow more informed decisions and designs.

Molecular explanations and evidence-based suggestions for combination strategies are not yet fully revealed. Unfortunately, only few pre-clinical studies address the interaction of targeted therapeutics with standard of care drugs so far.[4,5,54] Especially with regard to development of resistance, however, combining targeted therapy with broadly acting cytotoxic drugs could be valuable. By using optimal combinations and enhancing efficacy of some standard therapeutics, other drugs with severe side effects might become obsolete. We and others showed that MEK inhibitors synergize with glucocorticoids in vitro (chapter 2).[55-59] Interestingly, many RAS pathway mutant cases were resistant to chemotherapy, indicating that inhibitors such as trametinib may be beneficial when applied in combination with glucocorticoids as the spearhead drug in the treatment of ALL.

Identification of redundant pathways may also yield more effective therapies. For example, JAK inhibitors have been shown to be more effective in combination with PI3K/mTOR inhibition in *JAK2* mutant *BCR-ABL1*-like ALL.[8,10] The previously mentioned link between RAS and *JAK2* mutations provides a rationale to also asses a combination of JAK and MEK inhibition in *JAK2* mutant leukemia. Additionally, combination of two drugs targeting the same pathway has proven beneficial in RAS- or RAF-mutant melanoma and lung cancer, most likely through more effective signaling inhibition as compared with single-agent therapy.[60-62]

Especially for cases where current therapies often fail, e.g. *TCF3-LF*- or *MLL*-rearranged ALL, radically new therapies are needed. Immunotherapy has shown great successes to eradicate cancer cells and is quickly becoming available to more patients. However, resistance or non-response will likely arise as well, and the combination with small molecule inhibitors could boost treatment success.[63-65]

Clinical implementation: The importance of biomarkers and clinical studies

Unfortunately, most targeted therapy approaches have stayed behind the expectations, and criticism is rising.[66,67] It should be noted that these conclusions are derived from trials in adult patients, very often with carcinomas. Comparable studies evaluating the benefit of targeted therapy in children with cancer are still limited, mainly due to the rarity of different cancer types in children and the relatively low frequency of (relapsed) cases. International collaborative studies are essential to enroll sufficient numbers of patients in early clinical trials.[68]

Many targeted therapeutics have disappointed because the effect size observed in pre-clinical models was not replicated in clinical settings. Responses were often of short duration and remain difficult to predict. Biomarkers for patient selection will therefore become increasingly important in pre-clinical and clinical studies. In addition, the combination approaches require carefully controlled studies that also delineate the risks of possible drug interactions in combination therapy.

The vast majority of children with BCP-ALL achieve a complete remission with standard chemotherapy, and refractory disease is rare (represented in Figure 1A). This raises the

question whether targeted therapy should be aimed at preventing or at treating relapses. As a result, two main possibilities for treatment adaptation exist: Identification of actionable lesions could be performed at diagnosis and trigger inclusion of targeted therapy up-front (Figure 1B). Alternatively, targeted therapy could be initiated after relapse as part of treatment intensification (Figure 1C).

The data presented in this thesis suggests that MEK inhibitors could be applied in the latter setting. While RAS pathway mutations were common at diagnosis and certainly affect a significant number of patients, only a minority of these children are at risk for relapse. While children with RAS mutations had a poorer prognosis in certain therapy settings, the effect size was relatively small and requires confirmation. In contrast, RAS pathway mutations are poor prognostic at relapse, and survival chances were considerably lower.[14,69]

JAK2 inhibitors may be promising adjuvant therapy for *BCR-ABL1*-like BCP-ALL with *JAK2*-rearrangements and mutations. Both *JAK2*-rearranged and -mutant leukemia

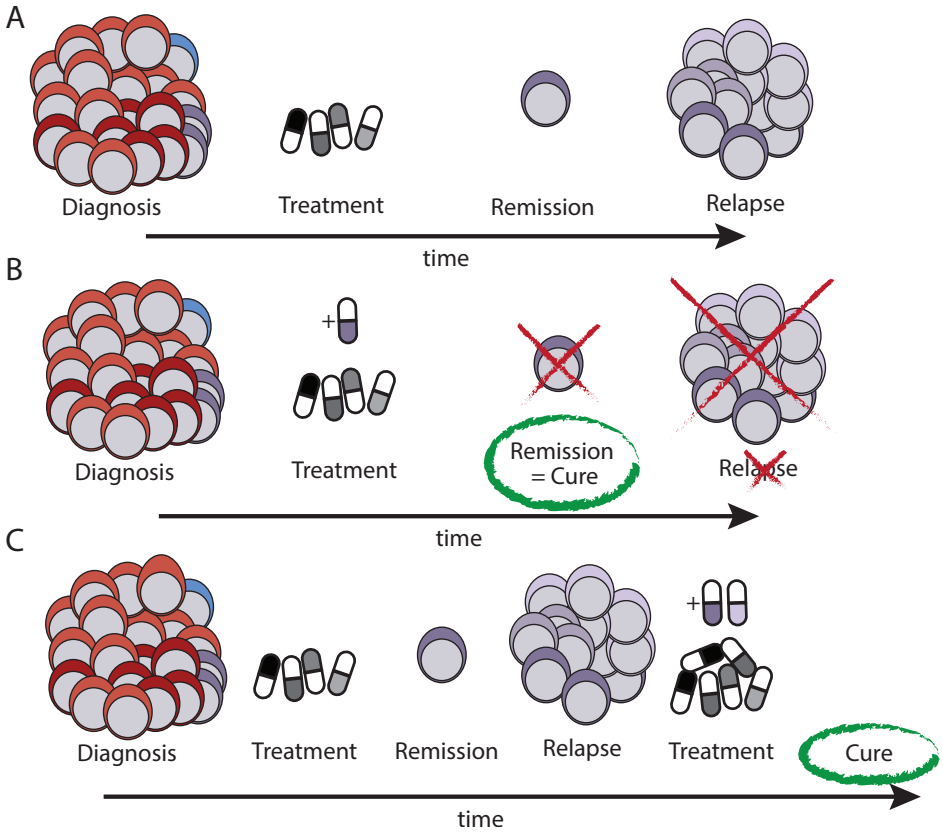

Figure 1: Possible therapeutic strategies for targeted therapy in pediatric BCP-ALL.

Currently, treatment failure (relapse) in pediatric BCP-ALL usually appears after a temporary remission **(A)**. Targeted therapy might be included upfront for cases with high risk of treatment failure **(B)**, or at relapse for those cases where upfront inclusion is not justified e.g. due to good prognostic features or risk of toxic side effects **(C)**.

represents a high risk disease, which calls for a clinical study evaluating the additional benefit of JAK2 inhibitors.[1,70] Nonetheless, they represent two biologically distinct patient groups, and mutations and rearrangements should be evaluated as separate biomarkers. The findings presented in this thesis and elsewhere furthermore suggest to conduct further investigations with type II JAK inhibitor.[5,71]

Conclusion

In this thesis we found several actionable lesions in pediatric BCP-ALL. Targeted therapy is applicable, but it is so far restricted to a low number of cases that have a targetable lesion and are high risk, refractory, or relapsed cases. Establishment of good biomarkers for drug targets during disease and rationally designed (early) clinical trials driven by target presence instead of disease subtype will allow a more rapid implementation of new precision medicines in clinical practice. In the end, these new drugs need to be implemented more upfront at time of diagnosis, thereby preventing occurrence of relapse and avoiding side-effects of chemotherapy by allowing dose-reduction of currently used chemotherapeutic agents.

References

1. Roberts, K.G. et al. Genetic alterations activating kinase and cytokine receptor signaling in high-risk acute lymphoblastic leukemia. Cancer Cell 22, 153-66 (2012).

2. Izraeli, S. Beyond Philadelphia: 'Ph-like' B cell precursor acute lymphoblastic leukemias - diagnostic challenges and therapeutic promises. Curr Opin Hematol 21, 289-96 (2014).

3. Boer, J.M. et al. Tyrosine kinase fusion genes in pediatric *BCR-ABL1*-like acute lymphoblastic leukemia. Oncotarget (2016).

4. Iacobucci, I. et al. Truncating Erythropoietin Receptor Rearrangements in Acute Lymphoblastic Leukemia. Cancer Cell 29, 186-200 (2016).

5. Wu, S.C. et al. Activity of the Type II JAK2 Inhibitor CHZ868 in B Cell Acute Lymphoblastic Leukemia. Cancer Cell 28, 29-41 (2015).

6. Bercovich, D. et al. Mutations of JAK2 in acute lymphoblastic leukaemias associated with Down's syndrome. Lancet 372, 1484-92 (2008).

7. Hertzberg, L. et al. Down syndrome acute lymphoblastic leukemia, a highly heterogeneous disease in which aberrant expression of CRLF2 is associated with mutated JAK2: a report from the International BFM Study Group. Blood 115, 1006-17 (2010).

8. Maude, S.L. et al. Targeting JAK1/2 and mTOR in murine xenograft models of Ph-like acute lymphoblastic leukemia. Blood 120, 3510-8 (2012).

9. Tasian, S.K. et al. Aberrant STAT5 and PI3K/mTOR pathway signaling occurs in human CRLF2-rearranged B-precursor acute lymphoblastic leukemia. Blood 120, 833-42 (2012).

10. Tasian, S.K. et al. Potent efficacy of combined PI3K/mTOR and JAK or ABL inhibition in murine xenograft models of Ph-like acute lymphoblastic leukemia. Blood 129, 177-187 (2017).

11. Kratz, C.P. et al. Cancer spectrum and frequency among children with Noonan, Costello, and cardio-facio-cutaneous syndromes. Br J Cancer 112, 1392-7 (2015).

12. Cave, H. et al. Acute lymphoblastic leukemia in the context of RASopathies. Eur J Med Genet (2016).

13. Cox, A.D., Fesik, S.W., Kimmelman, A.C., Luo, J. & Der, C.J. Drugging the undruggable RAS: Mission possible? Nat Rev Drug Discov 13, 828-51 (2014).

14. Irving, J. et al. Ras pathway mutations are prevalent in relapsed childhood acute lymphoblastic leukemia and confer sensitivity to MEK inhibition. Blood 124, 3420-30 (2014).

15. Pylayeva-Gupta, Y., Grabocka, E. & Bar-Sagi, D. RAS oncogenes: weaving a tumorigenic web. Nat Rev Cancer 11, 761-74 (2011).

16. Malinowska-Ozdowy, K. et al. KRAS and CREBBP mutations: a relapse-linked malicious liaison in childhood high hyperdiploid acute lymphoblastic leukemia. Leukemia 29, 1656-67 (2015).

17. Nikolaev, S.I. et al. Frequent cases of RAS-mutated Down syndrome acute lymphoblastic leukaemia lack JAK2 mutations. Nat Commun 5, 4654 (2014).

18. Vainchenker, W. & Constantinescu, S.N. JAK/STAT signaling in hematological malignancies. Oncogene 32, 2601-13 (2013).

19. Lemmon, M.A. & Schlessinger, J. Cell signaling by receptor tyrosine kinases. Cell 141, 1117-34 (2010).

20. Caunt, C.J., Sale, M.J., Smith, P.D. & Cook, S.J. MEK1 and MEK2 inhibitors and cancer therapy: the long and winding road. Nat Rev Cancer 15, 577-92 (2015).

21. Polak, R., de Rooij, B., Pieters, R. & den Boer, M.L. B-cell precursor acute lymphoblastic leukemia cells use tunneling nanotubes to orchestrate their microenvironment. Blood 126, 2404-14 (2015).

22. Greenbaum, A. et al. CXCL12 in early mesenchymal progenitors is required for haematopoietic stem-cell maintenance. Nature 495, 227-30 (2013).

23. van den Berk, L.C. et al. Disturbed CXCR4/CXCL12 axis in paediatric precursor B-cell acute lymphoblastic leukaemia. Br J Haematol 166, 240-9 (2014).

24. Juarez, J. et al. CXCR4 antagonists mobilize childhood acute lymphoblastic leukemia cells into the peripheral blood and inhibit engraftment. Leukemia 21, 1249-57 (2007).

25. Randhawa, S. et al. Effects of pharmacological and genetic disruption of CXCR4 chemokine receptor function in B-cell acute lymphoblastic leukaemia. Br J Haematol 174, 425-36 (2016).

26. Hsieh, Y.T. et al. Integrin alpha4 blockade sensitizes drug resistant pre-B acute lymphoblastic leukemia to chemotherapy. Blood 121, 1814-8 (2013).

27. de Rooij, B., Polak, R., Stalpers, F., Pieters, R. & Boer, M.L.D. Tunneling nanotubes facilitate autophagosome transfer in the leukemic niche. Leukemia 31, 1651-1654 (2017).

28. Chesi, M. et al. Activated fibroblast growth factor receptor 3 is an oncogene that contributes to tumor progression in multiple myeloma. Blood 97, 729-36 (2001).

29. Moroni, E., Dell'Era, P., Rusnati, M. & Presta, M. Fibroblast growth factors and their receptors in hematopoiesis and hematological tumors. J Hematother Stem Cell Res 11, 19-32 (2002).

30. Traer, E. et al. Ponatinib overcomes FGF2-mediated resistance in CML patients without kinase domain mutations. Blood 123, 1516-24 (2014).

31. Zhu, Z. et al. Inhibition of KRAS-driven tumorigenicity by interruption of an autocrine cytokine circuit. Cancer Discov 4, 452-65 (2014).

32. Asshoff, M. et al. Momelotinib inhibits ACVR1/ALK2, decreases hepcidin production and ameliorates anemia of chronic disease in rodents. Blood (2017).

33. Jain, P. et al. Ponatinib as first-line treatment for patients with chronic myeloid leukaemia in chronic phase: a phase 2 study. Lancet Haematol 2, e376-83 (2015).

34. Yoshida, T. et al. Identification and characterization of a novel chemotype MEK inhibitor able to alter the phosphorylation state of MEK1/2. Oncotarget 3, 1533-45 (2012).

35. Davis, M.I. et al. Comprehensive analysis of kinase inhibitor selectivity. Nat Biotechnol 29, 1046-51 (2011).

36. Lito, P. et al. Disruption of CRAF-mediated MEK activation is required for effective MEK inhibition in KRAS mutant tumors. Cancer Cell 25, 697-710 (2014).

37. Hatzivassiliou, G. et al. Mechanism of MEK inhibition determines efficacy in mutant KRAS- versus BRAF-driven cancers. Nature 501, 232-6 (2013).

38. Soverini, S. et al. Drug resistance and BCR-ABL kinase domain mutations in Philadelphia chromosome-positive acute lymphoblastic leukemia from the imatinib to the second-generation tyrosine kinase inhibitor era: The main changes are in the type of mutations, but not in the frequency of mutation involvement. Cancer 120, 1002-9 (2014).

39. Zhou, W. et al. Novel mutant-selective EGFR kinase inhibitors against EGFR T790M. Nature 462, 1070-4 (2009).

40. Burger, J.A. Bruton's tyrosine kinase (BTK) inhibitors in clinical trials. Curr Hematol Malig Rep 9, 44-9 (2014).

41. Chang, B.H. et al. Imatinib resistant *BCR-ABL1* mutations at relapse in children with Ph+ ALL: a Children's Oncology Group (COG) study. Br J Haematol 157, 507-10 (2012).

42. Bernt, K.M. & Hunger, S.P. Current concepts in pediatric Philadelphia chromosome-positive acute lymphoblastic leukemia. Front Oncol 4, 54 (2014).

43. Ma, X. et al. Rise and fall of subclones from diagnosis to relapse in pediatric B-acute lymphoblastic leukaemia. Nat Commun 6, 6604 (2015).

44. Quentmeier, H. et al. Cloning of human thymic stromal lymphopoietin (TSLP) and signaling mechanisms leading to proliferation. Leukemia 15, 1286-92 (2001).

45. Feldhahn, N. et al. Environment-mediated drug resistance in Bcr/Abl-positive acute lymphoblastic leukemia. Oncoimmunology 1, 618-629 (2012).

46. Frolova, O. et al. Regulation of HIF-1alpha signaling and chemoresistance in acute lymphocytic leukemia under hypoxic conditions of the bone marrow microenvironment. Cancer Biol Ther 13, 858-70 (2012).

47. Mallampati, S. et al. Tyrosine kinase inhibitors induce mesenchymal stem cell-mediated resistance in BCR-ABL+ acute lymphoblastic leukemia. Blood 125, 2968-73 (2015).

48. Meads, M.B., Hazlehurst, L.A. & Dalton, W.S. The bone marrow microenvironment as a tumor sanctuary and contributor to drug resistance. Clin Cancer Res 14, 2519-26 (2008).

49. Sugimoto, K. et al. Fibroblast Growth Factor-2 facilitates the growth and chemo-resistance of leukemia cells in the bone marrow by modulating osteoblast functions. Sci Rep 6, 30779 (2016).

50. Traer, E. et al. FGF2 from Marrow Microenvironment Promotes Resistance to FLT3 Inhibitors in Acute Myeloid Leukemia. Cancer Res (2016).

51. Zeng, Z. et al. Inhibition of CXCR4 with the novel RCP168 peptide overcomes stroma-mediated chemoresistance in chronic and acute leukemias. Mol Cancer Ther 5, 3113-21 (2006).

52. Welschinger, R. et al. Plerixafor (AMD3100) induces prolonged mobilization of acute lymphoblastic leukemia cells and increases the proportion of cycling cells in the blood in mice. Exp Hematol (2012).

53. Corcione, A., Ferretti, E. & Pistoia, V. CX3CL1/fractalkine is a novel regulator of normal and malignant human B cell function. J Leukoc Biol 92, 51-8 (2012).

54. Li, Y. et al. IL-7 Receptor Mutations and Steroid Resistance in Pediatric T cell Acute Lymphoblastic Leukemia: A Genome Sequencing Study. PLoS Med 13, e1002200 (2016).

55. Aries, I.M. et al. Towards personalized therapy in pediatric acute lymphoblastic leukemia: RAS mutations and prednisolone resistance. Haematologica 100, e132-6 (2015).

56. Rambal, A.A., Panaguiton, Z.L., Kramer, L., Grant, S. & Harada, H. MEK inhibitors potentiate dexamethasone lethality in acute lymphoblastic leukemia cells through the pro-apoptotic molecule BIM. Leukemia 23, 1744-54 (2009).

57. Jones, C.L. et al. MAPK signaling cascades mediate distinct glucocorticoid resistance mechanisms in pediatric leukemia. Blood 126, 2202-12 (2015).

58. Driessen, E.M. et al. Frequencies and prognostic impact of RAS mutations in MLL-rearranged acute lymphoblastic leukemia in infants. Haematologica 98, 937-44 (2013).

59. Jing, D. et al. Opposing regulation of BIM and BCL2 controls glucocorticoid-induced apoptosis of pediatric acute lymphoblastic leukemia cells. Blood 125, 273-83 (2015).

60. Long, G.V. et al. Combined BRAF and MEK inhibition versus BRAF inhibition alone in melanoma. N Engl J Med 371, 1877-88 (2014).

61. Robert, C. et al. Improved overall survival in melanoma with combined dabrafenib and trametinib. N Engl J Med 372, 30-9 (2015).

62. Dhawan, N.S., Scopton, A.P. & Dar, A.C. Small molecule stabilization of the KSR inactive state antagonizes oncogenic Ras signalling. Nature (2016).

63. Sharma, P., Hu-Lieskovan, S., Wargo, J.A. & Ribas, A. Primary, Adaptive, and Acquired Resistance to Cancer Immunotherapy. Cell 168, 707-723 (2017).

64. Vanneman, M. & Dranoff, G. Combining immunotherapy and targeted therapies in cancer treatment. Nat Rev Cancer 12, 237-51 (2012).

65. Ali, K. et al. Inactivation of PI(3)K p110delta breaks regulatory T-cell-mediated immune tolerance to cancer. Nature 510, 407-11 (2014).

66. Le Tourneau, C. et al. Molecularly targeted therapy based on tumour molecular profiling versus conventional therapy for advanced cancer (SHIVA): a multicentre, open-label, proof-of-concept, randomised, controlled phase 2 trial. Lancet Oncol 16, 1324-34 (2015).

67. Tannock, I.F. & Hickman, J.A. Limits to Personalized Cancer Medicine. N Engl J Med 375, 1289-94 (2016).

68. Harris, M.H. et al. Multicenter Feasibility Study of Tumor Molecular Profiling to Inform Therapeutic Decisions in Advanced Pediatric Solid Tumors: The Individualized Cancer Therapy (iCat) Study. JAMA Oncol (2016).

69. Irving, J.A. et al. Integration of genetic and clinical risk factors improves prognostication in relapsed childhood B-cell precursor acute lymphoblastic leukemia. Blood 128, 911-22 (2016).

70. van der Veer, A. et al. Independent prognostic value of *BCR-ABL1*-like signature and IKZF1 deletion, but not high CRLF2 expression, in children with B-cell precursor ALL. Blood 122, 2622-9 (2013).

71. Meyer, S.C. et al. CHZ868, a Type II JAK2 Inhibitor, Reverses Type I JAK Inhibitor Persistence and Demonstrates Efficacy in Myeloproliferative Neoplasms. Cancer Cell 28, 15-28 (2015).

Chapter 8

Summary

Summary

Despite large improvements, therapy success for children with BCP-ALL currently stagnates at an event-free survival rate of 85%. After therapy, children frequently suffer from life-long side effects of therapy, and patients who relapse have a far worse prognosis. Several oncogenic signaling pathways have been identified that are activated by genetic aberrations and contribute to leukemogenesis. In this thesis we evaluated different signaling pathways and their potential implication in therapeutic strategy.

In chapter 2 we searched for mutations and gene fusions of the kinase JAK2 among a large cohort of BCP-ALL patients. They mostly occur among BCP-ALL patients lacking the classical cytogenetic aberrations (therefore termed B-other) and in BCP-ALL patients whose gene expression profile resembles that of *BCR-ABL1*-rearranged leukemia (*BCR-ABL1*-like). The cytotoxic effects of JAK inhibitors in vitro varied: While cells with JAK2 fusion genes were effectively killed by ruxolitinib and momelotinib, cells carrying JAK2 mutations responded best in presence of the cytokine TSLP. We further discovered potential limits to JAK inhibitor therapy due to biochemical properties of the inhibitor, activation of alternative signaling pathways, and microenvironment-mediated drug resistance. Based on our results we conclude that JAK inhibitor therapy may be of benefit for patients with JAK2 aberrations, but cases with *JAK2* mutations should be monitored closely for disease progression.

In chapter 3 we evaluated the clinical and therapeutic significance of RAS pathway mutations. We discovered that these mutations were largely restricted to 4 genes central to the pathway, and that they frequently occurred in a small fraction of leukemic cells (subclonal mutations). Clonal mutations associated with in vitro drug resistance and a higher chance of relapse in certain settings, while subclonal mutations had no significant effect on poor prognostic characteristics or on prognosis itself. We further show that the MEK-inhibitor was highly effective in killing RAS mutant BCP-ALL cells and could sensitize them to prednisolone. We conclude that these MEK inhibitors could potentially be tested in patients at high risk for relapse or after relapse if the leukemic cells carry a RAS pathway mutation.

In chapter 4 we investigate the phenomenon of high *PDGFRA* expression in a group of pediatric BCP-ALL patients. We show that many of these cases carry ERG-deletions on chromosome 21, and that there is no evidence for genetic aberrations affecting the *PDGFRA* gene locus on chromosome 4. Despite detectable PDGFRα activation, the PDGFR inhibitors imatinib and CP673451 had no cytotoxic effect in vitro. Targeting PDGFRα is therefore unlikely to be of therapeutic relevance in pediatric BCP-ALL.

In chapter 5 of this thesis we investigated the fibroblast growth factor receptor in pediatric BCP-ALL. We found that the fibroblast-growth factor FGF2 can decrease the sensitivity of leukemic cell lines towards prednisolone. With targeted next-generation sequencing we searched for somatic mutations in the *FGFR1, 2* and *3* genes, and found that there are few mutations and that these are usually outside the known mutational hotspot regions. While the link with therapy resistance warrants further investigation, FGFR signaling likely plays a less important role in BCP-ALL than, for example, the RAS pathway.

A completely novel therapeutic target for pediatric ALL was suggested in chapter 6 of this

thesis. We showed that *EMP1* expression is increased in in vitro prednisolone-resistant BCP-ALL, and is a poor prognostic marker. Knock-down of *EMP1* increased sensitivity to prednisolone and decreased migration towards and adhesion to mesenchymal stromal cells. Pathway analysis revealed that *EMP1*-silencing reduced the phosphorylation of Src-family kinases in ALL cell lines. Downstream targets included STAT proteins as well as JNK and CREB. We conclude that EMP1 is integrating micro-environmental signals via the Src kinase pathway and serves as prognostic biomarker and potential therapeutic target in pediatric ALL.

Overall, the results of this thesis show that several signaling pathways may be relevant to the development and progression of pediatric BCP-ALL. However, not all represent valuable treatment targets because the inhibitory effects are transient, reversible, or can be circumvented by activation of alternative pathways. Future investigations should be aimed at finding accurate biomarkers for efficacy, generating combination strategies of pathway inhibitors and chemotherapeutic drugs, and overcoming cellular resistance, especially with respect to the leukemic micro-environment.

Nederlandse samenvatting

Ondanks grote vooruitgang in de lange termijn prognose van kinderen met acute lymfatische leukemie (ALL) door steeds betere behandelprotocollen, stagneert het genezingspercentage nu rond de 85%. Behalve het feit dat 15% van de kinderen met ALL niet geneest, is de andere keerzijde van de intensieve, 2 tot 3 jaar durende behandeling het optreden van ongewenste bij-effecten op zowel korte als lange termijn. Er zijn verschillende signaalpaden ontdekt die vaak over-reactief zijn in leukemiecellen. Deze activatie wordt vaak veroorzaakt door mutaties in genen die betrokken zijn bij het doorgeven van signalen van buiten de cel naar binnenin de cel en die dan aanzetten tot overmatig delen van de witte bloedcellen, met als gevolg leukemie. In dit proefschrift hebben we het optreden van mutaties in verschillende signaalpaden onderzocht en getest of deze mutaties doelwit voor nieuwe meer doelgerichte medicijnen (precision medicines) kunnen zijn waardoor de leukemiecellen selectiever gedood kunnen worden en er mogelijk minder kans is op bijwerkingen van de (chemo)therapie.

In hoofdstuk 2 onderzochten we de frequentie van afwijkingen in het DNA coderend voor het JAK2 kinase, een gen betrokken bij het activeren van een celdelingsprogramma. In het DNA kunnen zowel kleine mutaties (puntmutaties) als grote versmeltingen van 2 genen (zogenaamde fusiegenen) optreden die beide leiden tot een hyperactivatie van JAK2. Deze afwijkingen werden onderzocht in B-cel acute lymfatische leukemie, een vorm die bij 85% van de kinderen met ALL voorkomt. De meeste mutaties in *JAK2* komen voor in de groep waar klassieke cytogenetische afwijkingen ontbreken (daarom B-others genoemd) en in patiënten waarvan het genexpressieprofiel lijkt op *BCR-ABL1*-positieve leukemie (*BCR-ABL1*-like genoemd). De celdodende effecten van JAK-remmers varieerden in onze laboratoriumstudies: cellen met *JAK2*-fusiegenen werden effectief gedood door ruxolitinib en momelotinib, terwijl cellen met alleen puntmutaties in *JAK2* minder snel dood gingen en afhankelijk waren van het cytokine TSLP dat de JAK eiwitten indirect kan aanschakelen. We ontdekten verder potentiële beperkingen van JAK-remmers zoals het feit dat deze remmers juist tot activering van alternatieve signaalpaden kunnen leiden waarvan bekend is dat deze het overleven en delen van leukemiecellen stimuleren. Bovendien ontdekten we dat mesenchymale cellen die in het beenmerg belangrijk zijn voor de overleving van gezonde witte bloedcellen, ook de leukemiecellen ongevoeliger maakten voor de JAK remmers. Op basis van deze resultaten concluderen we dat JAK remmers effectief kunnen zijn voor patiënten met *JAK2* fusiegenen, maar veel minder voor patienten met een JAK2 puntmutatie. In de klinische praktijk moet hierbij het effect op het aantal leukemiecellen maar vooral ook het optreden van (nieuwe) mutaties gemonitored worden.

In hoofdstuk 3 hebben we het belang van mutaties in het RAS signaalpad geëvalueerd. We ontdekten dat deze mutaties grotendeels beperkt zijn tot 4 sleutelgenen, en dat mutaties vaak in een klein percentage van de leukemiecellen (subklonale mutaties) gevonden wordt. Klonale mutaties waren geassocieerd met resistentie voor cytostatica in het laboratorium en met een hogere kans op het terugkomen van de leukemie in de patient(recidief genoemd). Daarentegen waren subklonale mutaties niet voorspellend voor de prognose van de patient. We zagen dat RAS gemuteerde cellen heel gevoelig waren voor de remmer trametinib, en bovendien maakte deze remmer de leukemiecellen

ook gevoeliger voor prednisone. Een combinatie van beide medicijnen ligt daarom voor de hand om te gaan gebruiken in de klinische praktijk.

In hoofdstuk 4 onderzochten we het fenomeen van hoge *PDGFRA* expressie in een groep kinderen met B-other en BCR-ABL-like leukemie. Dit gen is belangrijk voor het delen maar ook uitrijpen (differentieren) van witte bloedcellen. We ontdekten dat veel patienten met hoge *PDGFRA* expressie deleties hebben van het *ERG* gen, maar dat er geen aanwijzingen zijn voor genetische afwijkingen in het *PDGFRA* gen zelf. Ondanks dat PDGFRα geactiveerd was in deze patienten, hadden de PDGFR-remmers imatinib en CP673451 geen effect in onze laboratoriumstudies. We concludeerden dat *PDGFRA* geen goed doelwit is in de behandeling van kinderen met ALL.

In hoofdstuk 5 van dit proefschrift onderzochten we de mutatiefrequentie in *FGFR1*, *2*, en *3* de fibroblast growth factor receptor, welke betrokken is bij celdelingen. We waren geinteresseerd in deze receptor omdat we ook vonden dat stimulatie van deze receptor (met het zogenaamde FGF2 ligand) tot minder gevoeligheid voor prednisolone leidde van de leukemiecellen. Ons mutatie-onderzoek leverde echter weinig afwijkingen op in de 3 *FGFR*-familie genen. Verder onderzoek naar de link met prednisolone resistentie is nodig, maar vermoedelijk speelt FGFR signalering geen prominente rol in kinderleukemie omdat er weinig tot geen mutaties voorkomen in deze genen.

Een volledig nieuw therapeutisch doelwit voor kinderleukemie staat beschreven in hoofdstuk 6, namelijk het membraan-gebonden eiwit EMP1. We hebben aangetoond dat *EMP1* expressie verhoogd is in prednisolon resistente ALL, en dat deze verhoogde expressie vooral voorkomt bij patienten met een slechte prognose. Het uitzetten van dit *EMP1* gen in het laboratorium, verhoogde de gevoeligheid voor prednisolon en verminderde de migratie van leukemiecellen naar mesenchymale beenmerg cellen. We toonden aan dat de Src-familie van kinases een belangrijke rol speelt bij het doorgeven van signalen opgepikt door EMP1 naar het binnenste van de cel toe. Onze studie suggereert dat EMP1 de potentie heeft om als target te dienen voor nieuw te ontwikkelen medicijnen in de behandeling van kinder ALL.

Samenvattend beschrijven we in dit proefschrift welke signaalpaden geactiveerd zijn in kinderen met ALL. Echter, niet alle signaalpaden zijn geschikt als therapeutisch doelwit omdat de remmende effecten kortdurend, omkeerbaar of omzeild kunnen worden door activering van alternatieve signaalpaden in de leukemiecellen en/of omzeild kunnen worden door de ondersteunende werking van mesenchymale cellen in het beenmerg. Het vervolgonderzoek zal zich dan ook richten op het vinden van goede combinaties van precision medicines en traditionele cytostatica (zoals prednisolon) en het doorbreken van de leukemisch beenmerg (micromilieu) gemedieerde medicijn-resistentie.

Chapter 9

About the Author

Biography

Isabel Sophie Jerchel was born in Helmstedt, Germany on the 21st of January 1989. After growing up as the middle child on a beautiful farm in Ingeleben, she graduated with her university entry diploma (Abitur) from the Gymnasium Anna-Sophianeum Schöningen in July 2007. Following her curiosity for how the human body works and how chemical molecules can be used to influence it, she chose to study for a Bachelor of Science in Molecular Medicine at the Georg-August University of Göttingen, Germany. She obtained the degree in September 2010, and one long train ride later she continued for a Master of Science degree at the Erasmus Medical Center in Rotterdam, the Netherlands. For her Master thesis internship she became a member of the group of Prof. Dr. Monique den Boer under supervision of Dr. Ingrid Ariës. In 2012, she decided to continue her postgraduate education under supervision of Prof. Dr. Monique den Boer and Prof. Dr. Rob Pieters. Results of the work performed in these 5 years are presented in this thesis. Isabel currently works as a Postdoc at Bayer in Berlin, Germany, where she investigates mechanisms of resistance to kinase inhibitors in various oncologic indications.

List of publications

Fibroblast growth factor receptor signaling in pediatric B-cell precursor acute lymphoblastic leukemia.
Jerchel IS, Hoogkamer AQ, Ariës IM, Boer JM, Besselink NJM, Koudijs MJ, Pieters R, den Boer ML. Manuscript in preparation

High PDGFRA expression does not serve as effective therapeutic target in ERG-deleted B-cell precursor acute lymphoblastic leukemia.
Jerchel IS; Chatzivasileiou D; Hoogkamer AQ, Boer JM, Beverloo HB, Pieters R, and den Boer ML. *Haematoligica,* 2017. PMID: 29170250

RAS pathway mutations as predictive biomarker for treatment adaptation in pediatric B-cell precursor acute lymphoblastic leukemia.
Jerchel IS, Hoogkamer AQ, Ariës IM, Steeghs EMP, Boer JM, Besselink NJM, Boeree A, van de Ven C, de Groot-Kruseman HA, de Haas V, Horstmann MA, Escherich G, Zwaan CM, Cuppen E, Koudijs MJ, Pieters R, den Boer ML. *Leukemia,* 2017. PMID: 28972594

JAK2 aberrations in childhood B-cell precursor acute lymphoblastic leukemia.
Steeghs EMP*, **Jerchel IS***, de Goffeau-Nobel W, Hoodkamer AQ, Boer JM, Boeree A, van de Ven C, Koudijs MC, Besselink NJM, de Groot-Kruseman HA, Zwaan CM, Horstmann MA, Pieters R, den Boer ML. *these authors contributed equally to this work. *Oncotarget*, 2017. PMID: 29163799

XLF deficiency results in reduced N-nucleotide addition during V(D)J recombination.
IJspeert H, Rozmus J, Schwarz K, Warren RL, van Zessen D, Holt RA, Pico-Knijnenburg I, Simons E, **Jerchel I**, Wawer A, Lorenz M, Patıroğlu T, Akar HH, Leite R, Verkaik NS, Stubbs AP, van Gent DC, van Dongen JJ, van der Burg M. *Blood*, 2016. PMID: 27281794.

Inflammation and Organ Failure Severely Affect Midazolam Clearance in Critically Ill Children.
Vet NJ, Brussee JM, de Hoog M, Mooij MG, Verlaat CW, **Jerchel IS**, van Schaik RH, Koch BC, Tibboel D, Knibbe CA, de Wildt SN; SKIC (Dutch collaborative PICU research network). *American Journal of Respiratory and Critical Care Medicine*, 2016. PMID: 26796541.

EMP1, a novel poor prognostic factor in pediatric leukemia regulates prednisolone resistance, cell proliferation, migration and adhesion.
Ariës IM, **Jerchel IS**, van den Dungen RE, van den Berk LC, Boer JM, Horstmann MA, Escherich G, Pieters R, den Boer ML. *Leukemia*, 2014. PMID:24625531

Leptin-dependent and leptin-independent paracrine effects of perivascular adipose tissue on neointima formation.
Schroeter MR, Eschholz N, Herzberg S, **Jerchel I**, Leifheit-Nestler M, Czepluch FS, Chalikias G, Konstantinides S, Schäfer K. *Arteriosclerosis, Thrombosis, and Vascular Biology,* 2013. PMID:23520165

PhD portfolio

Name PhD candidate	Isabel Sophie Jerchel
Erasmus MC department	Pediatric Oncology
Research school	Molecular Medicine
PhD period	September 2012 - September 2016
Promotors	Prof. dr. M. L. den Boer
	Prof. dr. R. Pieters

		ECTS
Courses, seminars, and workshops		
Research management for PhDs and Postdocs	2012	1
Ensembl Gene Browsing workshop	2013	0.6
SPSS	2012	0.8
Microarray and gene expression analysis using R	2013	2
Galaxy course	2015	0.6
Course on R	2016	1.4
Molecular aspects of hematological disorders	2013, 2014, 2015, 2016	2,8
NIHES Biostatistical Methods I: Basic Principles	2015	4
Bio-Business Summer School	2016	1
Research integrity course	2016	0.3
National and international conference attendance and presentations		
MolMed Day, attendance	2013	0.3
KiKa Princess Maxíma Research retraîte	2012, 2015	1.2
KiKa day and Tom Voûte award	2012, 2014, 2016	1
Daniel den Hoed Day	2013	0.3
EHA annual meeting Milano, Italy; attendance	2014	1.6
59th ASH annual meeting San Diego, USA; poster presentation	2016	2
Research Meetings in the laboratory of pediatrics & Journal Clubs	2012-2016	9
Teaching and supervision		
Supervision of Gerdo Evertsen, M. Sc. internship and report (6 months)	2015	10
Supervision of Danai Chatzivasileiou, M. Sc. internship and thesis (12 months)	2015-2016	20
Total sum of ECTS		**60**

Curriculum vitae

Education	
Since February 2017	Postdoc Oncogenic Signaling, Therapeutic Research Group Bayer AG, Berlin, Germany
September 2012 – September 2016	PhD at the Department of Pediatric Oncology/ Hematology at the Erasmus Medical Center Rotterdam, the Netherlands.
September 2010 – August 2012	Master of Science degree in Molecular Medicine at the Erasmus University Rotterdam, the Netherlands.
October 2007 - August 2010	Bachelor of Science degree Molecular Medicine at the University of Göttingen, Germany
June – October 2007	Application period for study programs in the field of life sciences
June 2007	Graduation from secondary school with the university entrance diploma (Abitur) at the Anna-Sophianeum Schöningen, Germany

Working Experience	
PhD project (4 years)	*Signaling Pathways as Therapeutic Targets in Pediatric B-cell precursor Acute Lymphoblastic Leukemia* Promoter: Prof. Dr. Monique den Boer, PhD, and Prof. Dr. Rob Pieters, MD, PhD Results: 1. Determined the impact of RAS pathway mutations on outcome, and chemotherapy response, and evaluated the in vitro efficacy of Mitogen-activated protein kinase kinase-inhibitors. 2. Evaluate the receptor tyrosine kinase PDGFRA as a treatment target in a subset of patients characterized by high PDGFRA gene expression 3. Evaluate the efficacy of Janus kinase inhibitors and identify possible drug resistance mechanisms to guide therapy adaptation. 4. Determine frequency and nature of fibroblast growth factor receptor mutations in pediatric BCP-ALL. Key techniques: Next-generation sequencing, *ex vivo* culture assays with primary leukemic and mesenchymal cells, patient-derived xenograft cells, and cell lines; lentivirus-mediated expression of shRNAs, flow cytometry, *ex vivo* drug sensitivity testing, multiplex protein assays (Luminex platform), clinical outcome analysis (Kaplan-Meier and cumulative incidence methods)

Master thesis project (1 year)	*Unraveling Glucocorticoid Resistance in Pediatric B-cell Precursor Acute Lymphoblastic Leukemia*
	Supervisor: Dr. Ingrid Ariës, PhD, and Prof. Dr. Monique den Boer, PhD
	Results: We identified EMP1 as a novel biomarker for glucocorticoid resistance and provided insight into the functional mechanism.
Master internship (7 months)	*Interaction of XLF and pol μ polymerases in the non-homologous end joining complex.*
	Supervisor: Dr. Hanna IJspeert, PhD, Dr. Mirjam van der Burg, PhD, and Prof. Dr. Dik van Gent, PhD
	Results: We generated fluorescent-protein tagged constructs of pol μ polymerases and set up PCR- and microscopy-based assays to study the polymerase recruitment and functionality in XLF-deficient cells.
Bachelor thesis project (3 months)	*Role of Leptin in Immune Cell Recruitment and Perivascular Inflammation*
	Supervisor: Prof. Dr. med. Katrin Schäfer, MD, PhD
	Results: We studied leptin gene and protein expression in obese mice, and quantified the integrin α4 expression on leukocytes of obese subjects. An in vitro adipocyte differentiation protocol was established
Part-time Assistant (4 months)	Blood donation service at the Department of Transfusion Medicine, University Hospital Göttingen
Teaching	Supervision of two Master of Science students during project-based practical internships (6 months and 1 year, respectively)

Skills

Languages	German (native), English (fluent), Dutch (good command), French (basic communication), Spanish (basic, currently learning)
Computer skills	Adobe Photoshop, Illustrator, InDesign, SPSS, LaTeX, FlowJo, EndNote, GraphPad Prism, basic command of R
Special Courses	Radiation Protection Course at the Central Radionuclide Laboratory, University Göttingen
	Quality Management and Good Manufacturing Practice at the Department of Transfusion Medicine, University Medical Hospital Göttingen
	Science Based Business Ventures at the Leiden University Medical Center, the Netherlands
	Bio Business Summer School in Amsterdam, organized by Hyphen Projects

Dankwoord

Writing this acknowledgement was a great pleasure, which I have on purpose saved for the end. Right now I am on a train (where else?), 30 minutes from Schiphol. This part of my thesis made me realize and shall illustrate how many people have contributed to this work directly or indirectly. Before I begin, I would like to point out that the order in which people are mentioned is not an indicator of relevance, that the list is very likely incomplete, and that words are hardly enough to express how grateful I am for the support I received.

My first thank you goes out to Monique, who has been a great supervisor and leader through these 5+ years. You were impressive from the first encounter, but I got to know many more sides of you through all these years. Your empathic, (usually) calm, whole-hearted, and truly (sometimes too) honest nature will always be an example to me. I am very grateful to call you my Doktormutter! Secondly, I want to thank Rob for his guidance through the PhD period. Your accurate analysis of our research during meetings and discussions has been very helpful, and your clinical experience often put the facts into a context. Your clear guidelines have steered this work even when you moved to Utrecht. I am impressed to see the Princess Máxima Center for Childhood Oncology shaping from your work.

Of course we could not do our research without the people and organizations that support our day-to-day work. I would especially like to thank the parents and children that participate in our studies, the lab specieel of the Sophia Children's Hospital, the Dutch Childhod Oncology Group (DCOG), the Cooperative Study Group for Children with ALL (COALL), Stichting Kinderonkologisch Centrum Rotterdam (KOCR), the laboratory of pediatrics, and the Erasmus University Rotterdam. I would also like to thank our collaborators Nicolle Besselink, Marco Koudijs, and Edwin Cuppen from the University Medical Center Utrecht, the team of Cergentis BV in Utrecht, and Judit Balog from the Leiden University Medical Center for their help in our projects. Furthermore I am grateful to the members of the Doctoral Committee, prof. dr. Frank Holstege, prof. dr. Ivo Touw, and prof. dr. Michel Zwaan, for reading and commenting on this thesis, and for participation in our "gedachtewisseling".

Many people in the laboratory have become very dear to me, and their support for writing this thesis has been tremendous. The first to introduce me into the proceedings of lab KGK was Ingrid. It is no exaggeration if I say you have laid a (very big) corner stone for this thesis, and you were, and will continue to be, an example to me. Thank you so much for everything. In addition, I would like to thank my fellow PhD candidates for their helpful discussions, tips & tricks, gentle worlds, strong shoulders, and just for silent working along: Lieneke, you are a tough nut! I am so grateful to be working with you, to go mountain-biking and to learn about korfball from you. Mark, we have virtually and literally walked a long and winding road together, where we erred and feared for wolves, but have eventually made it home safely (albeit later than we hoped

for). Thanks for having my back during the last years! Roel & Bob, whom even a full stop cannot separate, your helpful discussion and pep-talks were well appreciated. As well as those brain gymnastics and good laughs we had –even if sometimes they were about me. Priscilla, you had a habit of surprising me in a good way, thank you especially for getting us in and out of those escape rooms! The Portuguese: Rui, you have been a great support in the beginning of my PhD, and I would like to thank you for that. João, your social and welcoming nature has made life in Rotterdam different, and introduced me to many friends and special people. Diana Sà da Bandeira, it was a short but great pleasure to have you as a colleague, and now you are a friend. Sandralein, you are a great friend and colleague, and I wish you the best in Utrecht. Obrigada a todos vocês! Iris, am so happy to have you as my friend – I knew it when you answered the music question during your interview! En misschien kunnen wij ooit in drie taalen met elkaar praten! Other PhD candidates I am happy to have shared this path with are Arian, Daria, Farhad, Jasmijn, Jill, Jordy, Linda, Patrick, Ruben, and Stefanie.

Judith and Alex you were not only great roomies, but also your computing-power was of tremendous help. Judith, there are so many things I have learned from you, and so many more that I have tried but failed. You are patient and helpful and this book would not exist without your efforts. Thank you so much! Alex, your coding skills R legendary, and I cannot thank you enough. In addition, your listening skills and wisdom helped me to eat this elephant – one bite at a time.

Special thanks also go out to Aurelie, Femke, and Willemieke. Your magic hands, organizing skills, flexibility, and your endless eagerness to help until the very end have impressed and also spoiled me. You were a dream team, and I'm happy to see that you have added Marjolein to your team. Rosanna, I had a great time working side-by-side with you during the Master thesis project, I have enjoyed our honest discussions, and Abba now has a special spot in my heart. Also many thanks to the other technicians who have helped and accompanied me on the way: Ad, Dicky, Ellen, Jessica, Lisette, Lonneke, Merel, Myrte, Rolien, Susann, Sylvia, Theo, Wilco, Ytje. Special thanks go to the brilliant mind and big heart behind the Onco lab: Pauline. Your ability to organize, negotiate, and translate between all of us is unique, and I am sure it will also get you a long way in your PhD. I wish you the best of luck! Speaking of organizing: Marcel, thank you so much for all your efforts to help order primers, refund milk powder, and for being such a great lunch buddy.

During the years I was lucky to supervise two wonderful people in their Master of Science internships: Gerdo, it was so much fun working with you! I admire your spirits to run up steep mountains for fundraising and your positive energy which you give so generously to everyone around you. I wish you all the best for the future, and hope to hear many more of your mix tapes and radio shows! Danai, I am so happy that life has connected us twice, and that the second time I was smart enough to let you in! You were a great student, and your constant curiosity, your patience, and your positive thinking has made the PDGFRA story so much more than just a paper I wrote. Thank you so

much for repeating blots over and over and for getting the FISH to work. I am happy that as a friend I now don't have to grade you anymore.

Wisdom, experience, and good friends I have also found among the postdocs: Lieke, thank you so much for setting up and introducing me to the MSC world. Eddy, thanks for good mood you brought with you. Patricia, Celia, and Yunlei the three of you have been amazing friends these years. You enjoyed the good parts with me, and you helped me through the rough times. I am looking up to your beautiful souls, your kind hearts and your strong minds, and knowing you there makes me want to come back to visit Rotterdam many times. Thank you also to the postdocs and former roomies Cesca, Eva and Mahban. Cesca, thank you for the nice time in our office upstairs, and for the many things you have taught me.

Janneke, Ronald, Jules, Maarten, Kees, and Wendy, thanks a lot for shaping this laboratory and for your scientific and non-scientific life lessons. I would also like to thank the physicians of the pediatric oncology department, especially Marry and Max for organizing the patient meetings during the Biology of Disease classes of my Molecular Medicine Masters. The children and parents we met have been an inspiration to me ever since.

Many more people have turned life in- and outside the lab into a great time in Rotterdam. My Colombians David, Alejo, and especially Diana: you have a very special place in my heart. I admire your strength and positivity, and your passion for the beautiful ideals you have. You are also VERY convincing, for which I am especially grateful because it has not only cheered me up but also often been the start of our shared adventures. I am betraying my 11th proposition a little, because I sincerely hope we will be living more close to another at some point again. Thank you also to the other fellow Rotterdamers from Master times, with special thanks to Anna for awesome nights out, the occasionally necessary "Kopfwäsche", and relaxing trips to the beach. Many flat mates I have had, but special thanks goes out to Adna, Ari, and Vera: It was so nice to share a home with you, and you all have very special spots in my heart.

Isa, it feels like I've known you for so long, but actually it was relatively recent that you introduced yourself with creepy white eyes to me in your Halloween party. You have become one of my closest friends in Rotterdam, and someone I don't need to tell much to know what I'm thinking. Thank you for so many unique memories, and especially for your organ box inspired prophecy last December. Together with Isa and Isa, we will be connected in our heart (though unfortunately not by a gang tattoo). The hermano who connected us is the amazing Rodrigo. Thank you for being in our lab and becoming a true friend!

Meanwhile, my train has arrived to Schiphol, I boarded a plane, another train, and arrived to my home in Berlin, where I am now sitting at my desk, embraced by sunshine. It is my new home, where I am close again to my family. Die sechseinhalb Jahre in der Ferne haben mich einiges gelehrt, und uns letztlich doch dichter zusammen gebracht.

Mama und Papa, ich bin euch endlos dankbar für alles was ihr mir mitgegeben habt. Diese Fähigkeiten und Prinzipien geben mir eine offene und rationale Denkweise, Geduld, Kampfgeist, das Selbstvertrauen für Streitbarkeit, und die Bescheidenheit andere Meinungen zu akzeptieren. Katha und Heni, mit und zwischen euch durfte ich diese Fähigkeiten ausprobieren. Dass ich mich auf euch vier blind verlassen kann weiß ich nicht nur durch zig mal geänderte Planungen, selbstgebaute Küchenmöbel, individualisierte Badspiegel oder Kilo-weise Erdbeeren. Dass Berlin sich so schnell wie zuhause anfühlt ist größtenteils euch zu verdanken. But also to you, Calin. In a relatively short time you have already contributed so much to the finalization of this thesis and the recovery from its side effects. It is impossible to imagine what the last months would have been like without you. Mulţumesc for being in the right spot at the right time.

With the best wishes for everyone's future,

Yours,

Appendix

List of Abbreviations

aCGH	array comparative genomic hybridization
ALL	acute lymphoblastic leukemia
AML	Acute myeloblastic leukemia
ASP	L-asparaginase
BA	BCR-ABL1-positive
BAL	BCR-ABL1-like
BCP-ALL	B-cell precursor acute lymphoblastic leukemia
BO	B-other
CI	confidence interval
CIR	cumulative incidence of relapse and non-response
CLL	chronic acute lymphoblastic leukemia
CML	chronic myeloblastic leukemia
COALL	Cooperative study group for childhood acute lymphoblastic leukemia
COG	Childhood oncology group
DCOG	Dutch Childhood Oncology Group
DLSO	downstream located specific oligo
EFS	Event-free survival
ER	ETV6-RUNX1
FISH	fluorescence in-situ hybridization
HD	High hyperdiploid
HR	high risk
HR-S	high risk standard
HSC	hematopoietic stem cell
iAMP21	intrachromosomal amplification of chromosome 21
IQR	inter-quartile range
JMML	Juvenile myelomonocytic leukemia
LC50	50% lethal concentration
LR-R	low risk reduced
LR-S	low risk standard
MAPK	mitogen-activated protein kinases
MLL	mixed lineage leukemia
MLPA	Multiplex ligation-dependent probe amplification
MR	medium risk
MRD	minimal residual disease
MSC	mesenchymal stromal cell

MTT	3-(4,5-dimethylthiazol-2-yl)-2,5-diphenyltetrazolium bromide
NHR	non-high risk
NSG	NOD.Cg-PrkdcscidIl2rgtm1Wjl/SzJ (NSG)
OR	odds ratio
PDX	patient-derived xenograft
PPR	prednisone poor response
PRED	prednisolone
SEM	standard error of the mean
shEMP1	short-hairpin agains EMP1
shNSC	short-hairpin non-silencing control
SNP	single-nucleotide polymorphism
SNV	single-nucleotide variant
SR	standard risk
T-ALL	T-cell acute lymphoblastic leukemia
TCF3r	TCF3-rearranged
TKD	tyrosine kinase domain
TKI	tyrosine kinase inhibitor
TLA	targeted locus amplification
TMD	transmembrane domain
ULSO	upstream located specific oligo
VAF	Variant allele frequency
VCR	vincristine
WBC	white blood cell count
wt	wildtype